

CHEMISTRY AND BIOLOGY OF TRICARBONYL COMPLEXES
OF TECHNETIUM AND RHENIUM

by

Daniel Joshua Kramer

B.A. Chemistry, Brandeis University (1998)

SUBMITTED TO THE DEPARTMENT OF CHEMISTRY IN
PARTIAL FULFILLMENT OF THE REQUIREMENTS
FOR THE DEGREE OF DOCTOR OF PHILOSOPHY
at the
MASSACHUSETTS INSTITUTE OF TECHNOLOGY

JUNE 2003

© 2003 Massachusetts Institute of Technology. All rights reserved.

Signature of Author: _____

Department of Chemistry
May 2, 2003

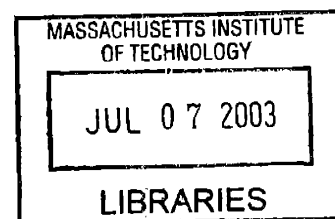
Certified by: _____

Alan Davison
Professor of Chemistry
Thesis Supervisor

Accepted by: _____

Robert Field
Professor of Chemistry
Chairman, Committee for Graduate Students

ARCHIVES



This doctoral thesis has been examined by a committee of the

Department of Chemistry as follows:

Professor Joseph P. Sadighi



Committee Chairman

Professor Alan Davison



Thesis Supervisor

Professor Christopher C. Cummins



Committee Member

Dedicated
to

my grandmother, Mildred Berger, whose memory is always in my thoughts.

CHEMISTRY AND BIOLOGY OF TRICARBONYL COMPLEXES OF TECHNETIUM AND RHENIUM

by

Daniel Joshua Kramer

Submitted to the Department of Chemistry on May 2, 2003, in partial fulfillment of the requirements for the Degree of Doctor of Philosophy.

Abstract

Chapter One: Two of the most famous tripodal ligands, Kläui's cyclopentadienyltris(dialkylphosphito)cobaltate(III) and Trofimenko's hydrotris(1-pyrazolyl)borate, were studied with respect to their reactivity towards Alberto's tris(solvento)tricarbonyltechnetium(I) and tris(solvento)tricarbonylrhenium(I) cations.

The reaction of $[M(H_2O)_3(CO)_3]^+$ ($M = Tc, Re$) with $Na[CpCo[PO(OR)_2]_3]$ (NaL_{OR} ; $R = Me, Et$) in water produced the compounds $M(CO)_3(L_{OR})$. The two compounds $M(CO)_3(L_{OEt})$ were structurally characterized by single crystal X-ray crystallography. In both cases, the ligand L_{OEt} was bound to the metal center in a tridentate fashion utilizing an {OOO} donor set. The ligands L_{OR} can be used as models for facially coordinated triaqua groups owing to their position in the spectrochemical series. Therefore, these four compounds, $M(CO)_3(L_{OR})$, can be considered structural models for $[M(H_2O)_3(CO)_3]^+$.

The reaction of $[Re(CO)_3(sol)_3]^+$ ($sol = H_2O, MeOH, MeCN$) with $K[HB(pz)_3]$ (KTp) has yielded a variety of products depending on the solvent used. For the two protic solvents, mixtures of $TpRe(CO)_3$ and a byproduct $(NEt_4)[Re_2(CO)_6(\mu-pz)_2(\mu-OR)]$ ($R = H$ or Me) were obtained. The methoxy-bridged species has been isolated and fully characterized, and the crystal structure has been determined. While a chemical separation of the analogous hydroxy-bridged species from $TpRe(CO)_3$ was not accomplished, a crystal of the compound was selected from the mixture, and a partial crystal structure was solved. When an aprotic solvent such as acetonitrile was used, only $TpRe(CO)_3$ was obtained and was recovered in high yield.

Chapter Two: *N*-(2-mercaptoethyl)picolyamine (MEPAH) was studied as a potentially biologically relevant ligand for the "*fac*-[M(CO)₃]⁺" core (M = Re, ⁹⁹Tc, ^{99m}Tc). To this end, the complex Re(CO)₃(MEPA) was synthesized. The reaction of MEPAH with *fac*-[Re(CO)₃(MeCN)₃]⁺ took place over the course of seconds, showing the high affinity possessed by this ligand for the "*fac*-[Re(CO)₃]⁺" core. A single crystal X-ray diffraction study was performed, confirming the nature of Re(CO)₃(MEPA), a rare mononuclear rhenium(I) thiolate complex. Exploration into derivatization of the ligand backbone has afforded the analogous *N*-ethyl complex, Re(CO)₃(MEPA-NEt). Further work has given rhenium complexes of bioconjugated ligands, whereby biologically active molecules have been tethered to the ligand framework. The high affinity of the ligand for the metal, coupled with the ease of its derivatization, implies that this ligand system is promising for the purposes of ^{99m}Tc radiopharmaceutical development.

Chapter Three: The bioevaluation of ^{99m}Tc complexes of derivatives of MEPAH is described. Complexes analogous to the tricarbonylrhenium(I) complexes described in Chapter 2 were synthesized and characterized by HPLC. After confirmation of the composition of these ^{99m}Tc complexes, *in vitro* and *in vivo* studies were performed. These compounds of the "*fac*-[^{99m}Tc(CO)₃]⁺" core, containing the biologically active molecules morpholine and normicotine, were evaluated for uptake by melanoma and brain tissue, respectively, in mice.

Thesis Supervisor: Alan Davison

Title: Professor of Chemistry

Table of Contents

Dedication.....	3
Abstract.....	4
Preface.....	14
Chapter One: Reactivity of Tris(solvento)tricarbonyltechnetium(I) and Tris(solvento)- tricarbonylrhenium(I) Cations with Tripodal Ligands	
Introduction.....	16
Experimental.....	20
Discussion.....	30
Conclusions.....	44
References.....	54
Chapter Two: Chemistry of <i>N</i> -(2-mercaptoethyl)picolyamine and its Derivatives as Ligands for the " <i>fac</i> -[Re(CO) ₃] ⁺ " Core	
Introduction.....	59
Experimental.....	65
Results and Discussion.....	84
Conclusions.....	103
References.....	117
Chapter Three: Radiopharmaceutical Application of Derivatives of <i>N</i> -(2-Mercapto- ethyl)picolyamine as Ligands for the " <i>fac</i> -[^{99m} Tc(CO) ₃] ⁺ " Core	
Introduction.....	121
Experimental.....	125
Results and Discussion.....	131
Conclusions.....	137
References.....	138
Appendix A: Synthesis of Tricarbonylrhenium Complexes of Aminocarboxylate Ligands	
Introduction.....	141
Experimental.....	143
Results and Discussion.....	147
Conclusions.....	150
References.....	151

Appendix B: Synthesis and Bioevaluation of Rhenium and Technetium Complexes of
a Nicotinic Conjugate

Introduction.....	153
Experimental.....	154
Results and Discussion.....	159
Conclusions.....	162
References.....	163
Appendix C: X-ray Crystallographic Data.....	164
Acknowledgments.....	217
Biographical Note.....	219
Curriculum Vitae.....	220

List of Figures

Chapter 1

1.1	Tripodal ligands cyclopentadienyltris(dialkylphosphito)cobaltate(III) (R = Me, Et) and hydrotris(1-pyrazolyl)borate.	18
1.2	Thermal ellipsoid plots (35% ellipsoids) of $\text{Re}(\text{CO})_3(\text{L}_{\text{OEt}})$ and $\text{Tc}(\text{CO})_3(\text{L}_{\text{OEt}})$ (ethoxy groups omitted for clarity).	33
1.3	ESI(-)MS of $[\text{Re}_2(\text{CO})_6(\mu\text{-pz})_2(\mu\text{-OMe})]^-$ showing Re_2 isotope pattern.	36
1.4	Thermal ellipsoid plot (35% ellipsoids) of $[\text{Re}_2(\text{CO})_6(\mu\text{-pz})_2(\mu\text{-OMe})]^-$.	37
1.5	$\nu(\text{CO})$ region of IR spectrum (KBr) of $(\text{NEt}_4)[\text{Re}_2(\text{CO})_6(\mu\text{-pz})_2(\mu\text{-OMe})]$.	39
1.6	Thermal ellipsoid plot (35% probability) of $[\text{Re}_2(\text{CO})_6(\mu\text{-pz})_2(\mu\text{-OH})]^-$.	41

Chapter 2

2.1	Three philosophies of design of $^{99\text{m}}\text{Tc}$ radiopharmaceuticals: Tc-essential, conjugate design, and integrated design.	59
2.2	Schematic of conjugate design.	60
2.3	The two principal labeling approaches for $^{99\text{m}}\text{Tc}$ radiopharmaceuticals.	61
2.4	<i>N</i> -(2-mercaptoethyl)picolylamine (MEPAH).	63
2.5	UV (280 nm) chromatogram of crystals of $\text{Re}(\text{CO})_3(\text{MEPA})$ on RP-18 HPLC with pH 2.25 TEAP buffer (A) and methanol (B) linear gradient as follows (t/%B): 0/0, 5/0, 20/100, 30/100, 40/0.	85
2.6	Thermal ellipsoid plot (35% probability) of $\text{Re}(\text{CO})_3(\text{MEPA})$.	87
2.7	Thermal ellipsoid plot (35% probability) of $\text{Re}(\text{CO})_3(\text{MEPA-NEt})$.	91
2.8	Thermal ellipsoid plot (35% probability) of <i>N</i> -propionic acid derivative of MEPAH-STr.	93
2.9	HRESI(+)-MS of NHS ester.	94
2.10	Amines whose conjugates were utilized in biological studies: morpholine and nornicotine.	96
2.11	HRESI(+)-MS of $\text{Re}(\text{CO})_3(\text{MEPA-C}_2\text{C}_2\text{Omorph})$.	97
2.12	Thermal ellipsoid plot (35% probability) of $\text{Re}(\text{CO})_3(\text{MEPA-C}_2\text{C}_2\text{Omorph}) \cdot 2\text{H}_2\text{O}$ (water molecules omitted for clarity).	98
2.13	Synthesis and HRESI(+)-MS of $\text{Re}(\text{CO})_3(\text{MEPA-C}_2\text{C}_2\text{Oornic})$.	100
2.14	Synthesis and HRESI(+)-MS of $\text{Re}(\text{CO})_3(\text{MEPA-C}_3\text{morph})$.	102

Chapter 3

3.1	Examples of radiopharmaceuticals targeting melanoma.	123
3.2	The bioactive molecule, nicotine, and its analogue, nornicotine.	124
3.3	HPLC chromatogram of co-injected $^{99m}\text{Tc}/\text{Re}(\text{CO})_3(\text{MEPA}-\text{C}_2\text{COmorph})$.	132
3.4	HPLC chromatogram of co-injected $^{99m}\text{Tc}/\text{Re}(\text{CO})_3(\text{MEPA}-\text{C}_3\text{morph})$.	133
3.5	HPLC chromatogram of co-injected $^{99m}\text{Tc}/\text{Re}(\text{CO})_3(\text{MEPA}-\text{C}_2\text{CONornic})$.	133

Appendix A

A.1	The ligands ethylenediamine- <i>N,N'</i> -diacetic acid and L-methionine.	141
A.2	$\text{Tc}(\text{CO})_3(\text{PADA})$ (PADAH = picolylamine- <i>N,N'</i> -diacetic acid).	142
A.3	Thermal ellipsoid plot (35% probability) of $\text{Re}(\text{CO})_3(\text{EDDA})\cdot\text{H}_2\text{O}$ (water molecule omitted for clarity).	148

Appendix B

B.1	Synthesis and HRESI(+)-MS of $\text{Re}(\text{CO})_3(\text{MEPA}-\text{C}_3\text{nornic})$.	159
B.2	HPLC chromatogram of co-injected $^{99m}\text{Tc}/\text{Re}(\text{CO})_3(\text{MEPA}-\text{C}_3\text{nornic})$.	161

List of Schemes

Chapter 1

- 1.1 The behavior of *fac*-[MX₃(CO)₃]²⁻ (M = Tc, Re) in coordinating solvents. 17
- 1.2 The synthesis of technetium and rhenium tricarbonyl complexes of the Kläui ligand. 30
- 1.3 Effect of solvent on products of reaction of [ReBr₃(CO)₃]²⁻ with KTp. 35

Chapter 2

- 2.1 The reaction of [MX₃(CO)₃]²⁻ (M = Tc, X = Cl; M = Re, X = Br) with a variety of ligands in the presence of coordinating solvents. 62
- 2.2 Synthesis of Re(CO)₃(MEPA) including synthetic variations. 84
- 2.3 Synthesis, protection, and derivatization of MEPAH. 89
- 2.4 Synthesis of Re(CO)₃(MEPA-NEt). 90
- 2.5 Conjugation of MEPAH-based ligand to amines to form amides. 95
- 2.6 Synthesis of Re(CO)₃(MEPA-C₂COMorph). 97

Chapter 3

- 3.1 Synthesis of [^{99m}Tc(CO)₃(H₂O)₃]⁺. 121
- 3.2 Synthesis of ^{99m}Tc radiopharmaceuticals based on MEPAH. 131

Appendix A

- A.1 Synthesis of Re(CO)₃(EDDA) and Re(CO)₃(L-met). 147

List of Tables

Chapter 1

1.1	Crystal data and structure refinement for $\text{Re}(\text{CO})_3(\text{L}_{\text{OEt}})$ and $\text{Tc}(\text{CO})_3(\text{L}_{\text{OEt}})$.	27
1.2	Crystal data and structure refinement for $(\text{NEt}_4)[\text{Re}_2(\text{CO})_6(\mu\text{-pz})_2(\mu\text{-OMe})]$.	28
1.3	Crystal data and structure refinement for $(\text{NEt}_4)[\text{Re}_2(\text{CO})_6(\mu\text{-pz})_2(\mu\text{-OH})] \cdot (\text{CH}_3)_2\text{CO} \cdot 0.5\text{H}_2\text{O}$.	29
1.4	Selected bond lengths (Å) and angles (°) for $\text{Re}(\text{CO})_3(\text{L}_{\text{OEt}})$ and $\text{Tc}(\text{CO})_3(\text{L}_{\text{OEt}})$.	34
1.5	Selected bond lengths (Å) and angles (°) for $(\text{NEt}_4)[\text{Re}_2(\text{CO})_6(\mu\text{-pz})_2(\mu\text{-OMe})]$.	38

Chapter 2

2.1	Crystal data and structure refinement for $\text{Re}(\text{CO})_3(\text{MEPA})$.	80
2.2	Crystal data and structure refinement for $\text{Re}(\text{CO})_3(\text{MEPA-NEt})$.	81
2.3	Crystal data and structure refinement for $\text{MEPAH-C}_2\text{CO}_2\text{H-STr}$.	82
2.4	Crystal data and structure refinement for $\text{Re}(\text{CO})_3(\text{MEPA-C}_2\text{COMorph}) \cdot 2\text{H}_2\text{O}$.	83
2.5	Selected bond distances (Å) and angles (°) for $\text{Re}(\text{CO})_3(\text{MEPA})$.	88
2.6	Selected bond distances (Å) and angles (°) for $\text{Re}(\text{CO})_3(\text{MEPA-NEt})$.	91
2.7	Selected bond distances (Å) and angles (°) for <i>N</i> -propionic acid derivative of MEPAH-STr .	93
2.8	Selected bond distances (Å) and angles (°) for $\text{Re}(\text{CO})_3(\text{MEPA-C}_2\text{COMorph}) \cdot 2\text{H}_2\text{O}$.	99

Chapter 3

3.1	Biodistribution of $^{99\text{m}}\text{Tc}(\text{CO})_3(\text{MEPA-C}_2\text{COMorph})$ and $^{99\text{m}}\text{Tc}(\text{CO})_3(\text{MEPA-C}_3\text{morph})$.	128
3.2	Biodistribution of $^{99\text{m}}\text{Tc}(\text{CO})_3(\text{MEPA-C}_2\text{CONomic})$.	129
3.3	Serum stability of selected $^{99\text{m}}\text{Tc}$ complexes.	129

Appendix A

A.1	Crystal data and structure refinement for $\text{Re}(\text{CO})_3(\text{EDDA})\cdot\text{H}_2\text{O}$.	146
-----	--	-----

Appendix B

B.1	Biodistribution of $^{99\text{m}}\text{Tc}(\text{CO})_3(\text{MEPA}-\text{C}_3\text{normic})$.	158
-----	---	-----

List of Spectra

Chapter 1

1.1	IR spectrum of $\text{Tc}(\text{CO})_3(\text{L}_{\text{OMe}})$.	45
1.2	IR spectrum of $\text{Re}(\text{CO})_3(\text{L}_{\text{OMe}})$.	46
1.3	IR spectrum of $\text{Tc}(\text{CO})_3(\text{L}_{\text{OEt}})$.	47
1.4	IR spectrum of $\text{Re}(\text{CO})_3(\text{L}_{\text{OEt}})$.	48
1.5	^1H NMR spectrum (CDCl_3) of $\text{Tc}(\text{CO})_3(\text{L}_{\text{OMe}})$.	49
1.6	^1H NMR spectrum (CDCl_3) of $\text{Re}(\text{CO})_3(\text{L}_{\text{OMe}})$.	50
1.7	^1H NMR spectrum (CDCl_3) of $\text{Tc}(\text{CO})_3(\text{L}_{\text{OEt}})$.	51
1.8	^1H NMR spectrum (CDCl_3) of $\text{Re}(\text{CO})_3(\text{L}_{\text{OEt}})$.	52
1.9	^1H NMR spectrum (CD_3COCD_3) of $(\text{NEt}_4)[\text{Re}_2(\text{CO})_6(\mu\text{-pz})_2(\mu\text{-OMe})]$.	53

Chapter 2

2.1	IR spectrum of $\text{Re}(\text{CO})_3(\text{MEPA})$.	104
2.2	^1H NMR spectrum (wet CD_2Cl_2) of $\text{Re}(\text{CO})_3(\text{MEPA})$.	105
2.3	^1H NMR spectrum (CDCl_3) of MEPAH-STr.	106
2.4	^1H NMR spectrum (CD_2Cl_2) of MEPAH-NEt-STr.	107
2.5	IR spectrum of $\text{Re}(\text{CO})_3(\text{MEPA-NEt})$.	108
2.6	^1H NMR spectrum (CD_3COCD_3) of $\text{Re}(\text{CO})_3(\text{MEPA-NEt})$.	109
2.7	^1H NMR spectrum (CD_2Cl_2) of MEPAH- $\text{C}_2\text{CO}_2\text{H}$ -STr.	110
2.8	^1H NMR spectrum (CD_2Cl_2 , traces EtOAc) of <i>N</i> -propionyl-NHS-MEPAH-STr.	111
2.9	^1H NMR spectrum (CD_2Cl_2) of MEPAH- $\text{C}_2\text{COmorph}$ -STr.	112
2.10	^1H NMR spectrum (CD_2Cl_2) of MEPAH- $\text{C}_2\text{CONornic}$ -STr.	113
2.11	^1H NMR spectrum (CD_3COCD_3) of $\text{Re}(\text{CO})_3(\text{MEPA-}\text{C}_2\text{COmorph})$.	114
2.12	^1H NMR spectrum (CDCl_3) of MEPAH- C_3Cl -STr.	115
2.13	^1H NMR spectrum (CD_2Cl_2) of MEPAH- C_3morph -STr.	116

Preface

The research presented in this thesis is focused on the synthesis of new compounds of the "*fac*-[M(CO)₃]⁺" core (M = Tc, Re). While Chapter 1 deals with fundamental coordination chemistry of technetium and rhenium, the main focus of the research presented here is the synthesis of new potential radiopharmaceuticals. This effort is detailed in Chapters 2 and 3. Given the importance of technetium to this work, and to our group as a whole over the last 25 years, perhaps it is appropriate to make a few introductory comments about the lightest solely artificially produced element.

Mendeleev first predicted the existence of the element *ekamanganese* (Z=43) in 1869. This element, which was later named technetium, after the Greek word *technetos* meaning artificial, was first discovered by Segrè and Perrier in 1937 by the bombardment of molybdenum by deuterons.¹ All known isotopes of technetium are radioactive, and their atomic masses range from 91 to 110.

The most commonly used isotopes of technetium today are ⁹⁹Tc and ^{99m}Tc. The long-lived isotope, ⁹⁹Tc (t_{1/2} = 2.15 × 10⁵ y, β⁻ emitter), is obtained in 6% yield from the neutron-induced fission of ²³⁵U. We obtain ⁹⁹Tc in gram quantities, and normal chemical transformations can be investigated and characterized (with proper precautions). The medically relevant isotope, ^{99m}Tc (E_γ = 141 KeV, t_{1/2} = 6 h), is obtained from the β-decay of ⁹⁹Mo (t_{1/2} = 66 h), and is available as a tracer (<10⁻⁸ M) from the cost-effective ⁹⁹Mo/^{99m}Tc generator developed at the Brookhaven National Laboratory in 1958.² A combination of low cost and favorable physical characteristics (discussed in more depth in the thesis) has led to ^{99m}Tc being the most widely used radionuclide in all of nuclear medicine.³

(1) Perrier, C.; Segrè, E. *Nature* **1937**, *140*, 193.

(2) Tucker, W. D.; Greene, M. W.; Weiss, A. J.; Murrenhoff, A. P. *USAEC Report BNL-3746* **1958**.

(3) Mahmood, A.; Jones, A. G. *Handbook of Radiopharmaceuticals: Radiochemistry and Applications*; Welch, M. J. and Redvanly, C., Ed.; John Wiley and Sons: Chichester, 2003, p. 323.

Chapter One

Reactivity of Tris(solvento)tricarbonyltechnetium(I) and Tris(solvento)tricarbonylrhenium(I) Cations with Tripodal Ligands

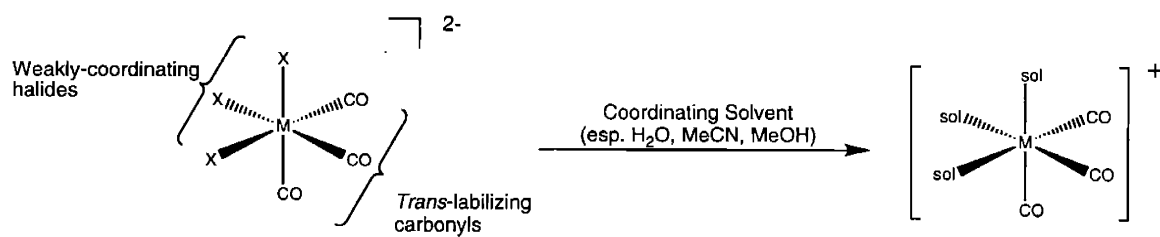
Introduction

The chemistry of the "[Re(CO)₃]⁺" core has been extensively studied for nearly fifty years, and it has found use in many fields.¹⁻³ Compounds of the "[Re(CO)₃]⁺" core traditionally have been prepared from ReX(CO)₅ (X = halide) under rather harsh conditions. In addition, chromatographic purification has often been necessary to isolate the desired compounds. Recently, Alberto has developed the chemistry of a newly explored synthon⁴ that avoids the use of ReX(CO)₅ altogether. This discovery has led to much improved syntheses of tricarbonylrhenium(I) compounds.

Though the "[Re(CO)₃]⁺" core has been well-explored, there is considerably less known about the analogous core with rhenium's second-row congener, technetium. Tricarbonyltechnetium(I) species have, in the past, only been accessible *via* Tc₂(CO)₁₀, which is a volatile radioactive compound. Thus, practical concerns have precluded much work into tricarbonyltechnetium(I) compounds. Recently, however, work by Alberto⁵⁻⁸ has afforded technetium analogues of the aforementioned rhenium synthon *via* low-pressure carbonylation of the ubiquitous starting material of all of technetium chemistry, [TcO₄]. This procedure avoids the use of TcX(CO)₅, and therefore Tc₂(CO)₁₀, as a starting material.

This recently explored synthon is *fac*-(NEt₄)₂[MX₃(CO)₃] (M = Tc, X = Cl; M = Re, X = Br), which is extremely versatile due to the behavior of the complex in coordinating solvents.^{4,5,9} The halides are replaced by solvent molecules to give complexes of the type [MX_n(sol)_{3-n}(CO)₃]⁽ⁿ⁻¹⁾⁻, where n is 0, 1, or 2 depending upon the

coordinating ability of the solvent. This substitution occurs due to the coupled effects of weakly coordinated halides and the *trans* labilization of said halides by the mutually *cis* carbonyls (Scheme 1.1). Though they are air- and water-stable, the resulting complexes are reactive towards substitution of various monodentate, bidentate, and tridentate ligands, yielding compounds containing the "[Re(CO)₃]⁺" or "[Tc(CO)₃]⁺" core.^{5,7,9-18} For some solvents, such as THF (n = 1) and CH₂Cl₂ (n = 2), only partial halide replacement occurs (the *tris*-THF species may be obtained by precipitation of halides with silver salts of weakly-coordinating anions). In the case of sol = H₂O, MeOH, and MeCN, the tris(solvento)tricarbonyl cations *fac*-[M(sol)₃(CO)₃]⁺ (M = Tc, Re) are formed upon dissolution of the trihalo species in the appropriate solvent.^{4,5,7,13,19} The reactivity of [M(sol)₃(CO)₃]⁺ has enabled the development of new, facile routes into low-valent carbonyl compounds of rhenium and technetium.



Scheme 1.1. The behavior of *fac*-[MX₃(CO)₃]²⁻ (M = Tc, Re) in coordinating solvents.

While convincing evidence for the existence of [M(CO)₃(H₂O)₃]⁺ (M = Tc, Re) in aqueous solutions of [MX₃(CO)₃]²⁻ has been presented through various solution spectra,^{4,7} neither the technetium nor the rhenium aqua complex has been isolated in the solid state. Since it is often difficult to isolate transition metal complexes containing aqua ligands, Kläui's tripodal oxygen donor ligands, {CpCo[PO(OR)₂]₃}⁻ (L_{OR}; R = Me, Et; Figure

1.1a), have been used to synthesize and isolate the model complexes $M(\text{CO})_3(\text{L}_{\text{OR}})$ ($M = \text{Tc, Re; R = Me, Et}$).

The Kläui ligand^{20,21} possesses characteristics similar to those of three facially coordinated water molecules as are found in $[\text{M}(\text{CO})_3(\text{H}_2\text{O})_3]^+$. It is a weak field ligand and has a nephelauxetic parameter similar to that of three water molecules. The Kläui ligand is often used to replace three facially coordinated water molecules because the resultant 'Kläui complexes' are typically easier to isolate than the corresponding triaqua species.^{22,23}

The syntheses of the compounds $M(\text{CO})_3(\text{L}_{\text{OR}})$ ($M = \text{Tc, Re; R = Me, Et}$) not only provide model complexes for $[\text{M}(\text{CO})_3(\text{H}_2\text{O})_3]^+$; they provide low-valent Tc and Re complexes analogous to the Tc(VII) complexes reported by Thomas and Davison,²⁴ and to the Re(VII) complexes reported by Banbery *et al.*²⁵ In addition, the ability to synthesize compounds $M(\text{CO})_3(\text{L}_{\text{OR}})$ further shows the versatility of $[\text{M}(\text{CO})_3(\text{H}_2\text{O})_3]^+$ in expanding the aqueous chemistry of the " $[\text{M}(\text{CO})_3]^+$ " core ($M = \text{Tc, Re}$).

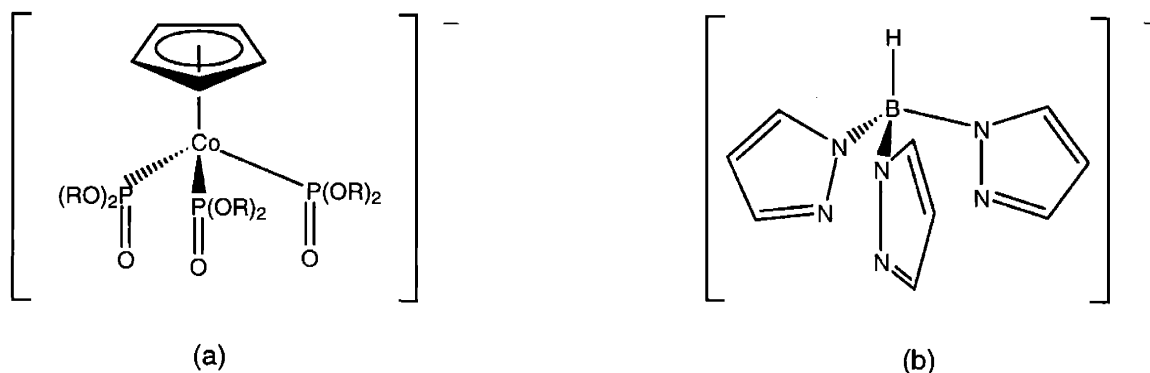


Figure 1.1. Tripodal ligands (a) cyclopentadienyltris(dialkylphosphito)cobaltate(III) ($R = \text{Me, Et}$), and (b) hydrotris(1-pyrazolyl)borate.

We continued our examination of the synthesis of rhenium tricarbonyl complexes containing tripodal ligands by employing one of the most widely used ligands, namely Trofimenko's hydrotris(1-pyrazolyl)borate (Tp⁻; Figure 1.1b).²⁶⁻³¹ This study was undertaken to see if TpRe(CO)₃ could be synthesized in a more facile fashion from [Re(CO)₃(sol)₃]⁺ rather than from ReX(CO)₅. Particular focus was placed on carrying out reactions in water as part of an attempt to expand the small, but increasingly important field of aqueous organometallic chemistry.²²

Experimental

General Considerations

All manipulations were carried out in air. All solvents, KTp and NaL_{OMe} were obtained commercially and used as received. Starting materials (NEt₄)₂[TcCl₃(CO)₃]^{5,9} and (NEt₄)₂[ReBr₃(CO)₃],⁴ were prepared as described in the literature. Dr. Evan Freiberg prepared NaL_{OEt}²¹ according to literature procedure. Elemental analyses were performed by Atlantic Microlab, Inc., Norcross, GA.

Caution! ⁹⁹Tc is a weak β⁻ emitter ($E = 0.292$ MeV; $t_{1/2} = 2.12 \times 10^5$ y) and may only be handled in laboratories approved for use of low-level radioactivity. Precautions for handling ⁹⁹Tc have been described elsewhere.³²

Physical Measurements

Proton NMR spectra were recorded on a Varian Unity-300 or Varian Mercury-300 300 MHz spectrometer. Chemical shifts were referenced to residual protons in the specified deuterated solvent. Infrared spectra were obtained on a Perkin-Elmer 1600-FTIR or Perkin-Elmer 2000-FTIR spectrometer. The fast atom bombardment mass spectra (FABMS) were recorded in a 3-nitrobenzyl alcohol matrix with a MAT 731 mass spectrometer equipped with an Ion Tech B11N FAB gun, operating at an accelerating voltage of 8 keV. The FAB gun produced a beam of 6-8 keV xenon neutrals. The electrospray ionization mass spectra (ESIMS) were recorded on a Bruker 3T FT-MS. Mass spectra were recorded by Ms. Li Li of the MIT Department of Chemistry Instrumentation Facility (DCIF). Two masses are reported for rhenium-containing

fragments to indicate the significant isotopic abundances of both ^{185}Re and ^{187}Re . Each peak was observed to have the proper relative abundances.

Synthesis of [Cyclopentadienyltris(dimethylphosphito)cobaltato]tricarbonyltechnetium(I), $\text{Tc}(\text{CO})_3(\text{L}_{\text{OMe}})$

In 3 mL deionized water was dissolved $(\text{NEt}_4)_2[\text{TcCl}_3(\text{CO})_3]$ (43 mg, 0.078 mmol). A solution of NaL_{OMe} (36 mg, 0.076 mmol) in 1 mL deionized water was added to the aqueous solution of $[\text{Tc}(\text{CO})_3(\text{H}_2\text{O})_3]^+$. Within 2 minutes, the solution became turbid, and a precipitate was observed within 20 minutes. The solution was stirred for 4 hours to allow complete precipitation. The reaction mixture was filtered, washed with deionized water, ice-cold methanol, and hexanes, and dried *in vacuo* to give a yellow powder. Yield: 38 mg (79%). ^1H NMR (CDCl_3): δ 3.70 (virt. q, 18H, $-\text{CH}_3$), 5.03 (s, 5H, Cp-H). IR (KBr): $\nu(\text{CH})$ 2949, 2844; $\nu(\text{CO})$ 2030, 1885; $\nu(\text{PO})$ 1137 cm^{-1} . FAB(+)-MS: m/z 635 $[\text{M}+\text{H}]^+$, 634 M^+ , 606 $[\text{M}-\text{CO}]^+$, 603 $[\text{M}-2\text{O}+\text{H}]^+$, 550 $[\text{M}-3\text{CO}]^+$, 547 $[\text{M}-2\text{CO}-2\text{O}+\text{H}]^+$, 519 $[\text{M}-3\text{CO}-2\text{O}+\text{H}]^+$, 497 $[\text{M}-\text{PO}(\text{OCH}_3)_2+\text{H}]^+$, 472 $[\text{M}-3\text{CO}-3\text{O}-\text{OCH}_3+\text{H}]^+$, 469 $[\text{M}-\text{CO}-\text{PO}(\text{OCH}_3)_2+\text{H}]^+$. *Anal.* Calc. for $\text{C}_{14}\text{H}_{23}\text{CoO}_{12}\text{P}_3\text{Tc}$: C, 26.52; H, 3.56. Found: C, 26.78; H, 3.49%.

Synthesis of [Cyclopentadienyltris(dimethylphosphito)cobaltato]tricarbonylrhenium(I), $\text{Re}(\text{CO})_3(\text{L}_{\text{OMe}})$

The preparation of the Re analogue was accomplished using the method above but substituting $(\text{NEt}_4)_2[\text{ReBr}_3(\text{CO})_3]$ (77 mg, 0.10 mmol) for $(\text{NEt}_4)_2[\text{TcCl}_3(\text{CO})_3]$ and adding the appropriate molar amount of NaL_{OMe} . A precipitate was observed within 20

minutes. The solution was stirred overnight, filtered, washed, and dried as described above to give a yellow powder. Yield: 40 mg (55%). $^1\text{H NMR}$ (CDCl_3): δ 3.72 (virt. q, 18H, $-\text{CH}_3$), 5.05 (s, 5H, Cp-H). IR (KBr): $\nu(\text{CH})$ 2955; $\nu(\text{CO})$ 2015, 1878, 1864; $\nu(\text{PO})$ 1124 cm^{-1} . FAB(+)-MS: m/z 720/722 M^+ , 692/694 $[\text{M}-\text{CO}]^+$, 689/691 $[\text{M}-2\text{O}+\text{H}]^+$, 661/663 $[\text{M}-2\text{O}-\text{CO}+\text{H}]^+$, 633/635 $[\text{M}-2\text{O}-2\text{CO}+\text{H}]^+$, 605/607 $[\text{M}-2\text{O}-3\text{CO}+\text{H}]^+$. *Anal.* Calc. for $\text{C}_{14}\text{H}_{23}\text{CoO}_{12}\text{P}_3\text{Re}$: C, 23.31; H, 3.21. Found: C, 23.39; H, 3.19%.

Synthesis of [Cyclopentadienyltris(diethylphosphito)cobaltato]tricarbonyltechnetium(I), $\text{Tc}(\text{CO})_3(\text{L}_{\text{OEt}})$

A solution of $(\text{NEt}_4)_2[\text{TcCl}_3(\text{CO})_3]$ (51 mg, 0.092 mmol) in 2 mL deionized water was prepared. To this was added NaL_{OEt} (55 mg, 0.099 mmol) dissolved in 1 mL deionized water. The solution immediately became turbid, and within 2 minutes, a yellow precipitate was observed. The solution was stirred for 4 hours. The reaction mixture was filtered, washed with deionized water, and dried in air. Yield: 59 mg (89%). Pale yellow needles suitable for a single crystal X-ray diffraction study were grown by slow evaporation of a saturated acetone-water solution of $\text{Tc}(\text{CO})_3(\text{L}_{\text{OEt}})$. $^1\text{H NMR}$ (CDCl_3): δ 1.30 (t, 18H, $-\text{CH}_2\text{CH}_3$), 4.09 (m, 12H, $-\text{CH}_2\text{CH}_3$), 4.98 (s, 5H, Cp-H). IR (KBr): $\nu(\text{CH})$ 2981, 2901; $\nu(\text{CO})$ 2026, 1908, 1895; $\nu(\text{PO})$ 1122 cm^{-1} . FAB(+)-MS: m/z 718 M^+ , 690 $[\text{M}-\text{CO}]^+$, 673 $[\text{M}-\text{OEt}]^+$, 634 $[\text{M}-3\text{CO}]^+$, 617 $[\text{M}-2\text{CO}-\text{OEt}]^+$, 589 $[\text{M}-3\text{CO}-\text{OEt}]^+$, 560 $[\text{M}-3\text{CO}-2\text{OEt}]^+$, 525 $[\text{M}-2\text{CO}-\text{PO}(\text{OEt})_2]^+$, 498 $[\text{M}-3\text{CO}-\text{PO}(\text{OEt})_2+\text{H}]^+$. *Anal.* Calc. for $\text{C}_{20}\text{H}_{35}\text{CoO}_{12}\text{P}_3\text{Tc}$: C, 33.45; H, 4.91. Found: C, 33.60; H, 4.94%.

Synthesis of [Cyclopentadienyltris(diethylphosphito)cobaltato]tricarbonylrhenium(I), $\text{Re}(\text{CO})_3(\text{L}_{\text{OEt}})$

The Re analogue was prepared according to the same procedure using $(\text{NEt}_4)_2[\text{ReBr}_3(\text{CO})_3]$ (77 mg, 0.10 mmol) and the appropriate molar amount of NaL_{OEt} (62 mg, 0.11 mmol). Precipitation was observed immediately. The reaction mixture was stirred overnight, filtered, washed with deionized water, and dried in air. Yield: 59 mg (73%). Pale yellow needles suitable for a single crystal X-ray diffraction study were grown by slow evaporation of a saturated acetone-water solution of $\text{Re}(\text{CO})_3(\text{L}_{\text{OEt}})$. ^1H NMR (CDCl_3): δ 1.30 (t, 18H, $-\text{CH}_2\text{CH}_3$), 4.10 (m, 12H, $-\text{CH}_2\text{CH}_3$), 5.00 (Cp-H). IR (KBr): $\nu(\text{CH})$ 2984, 2902; $\nu(\text{CO})$ 2013, 1872; $\nu(\text{PO})$ 1117 cm^{-1} . FAB(+)-MS: m/z 805/807 $[\text{M}+\text{H}]^+$, 804/806 M^+ , 776/778 $[\text{M}-\text{CO}]^+$, 759/761 $[\text{M}-\text{CO}-\text{O}-\text{H}]^+$. Anal. Calc. for $\text{C}_{20}\text{H}_{35}\text{CoO}_{12}\text{P}_3\text{Re}$: C, 29.82; H, 4.38. Found: C, 29.91; H, 4.48%.

Synthesis of Tetraethylammonium bis(μ -pyrazolyl)(μ -methoxy)hexacarbonyldirhenate(I,I), $(\text{NEt}_4)[\text{Re}_2(\text{CO})_6(\mu\text{-pz})_2(\mu\text{-OMe})]$

To a vial containing a solution of 77 mg (0.10 mmol) $(\text{NEt}_4)_2[\text{ReBr}_3(\text{CO})_3]$ in 3 mL methanol was added a methanolic solution of 25 mg (0.10 mmol) KTp. The solution was stirred for 3 hours, during which time a white precipitate formed. The precipitate was filtered, washed with ice-cold methanol, and dried *in vacuo* for a short time. To the solid was added 15 mL chloroform to dissolve the major product ($\text{TpRe}(\text{CO})_3$), and the resulting suspension was stirred for 1 hour. The suspension was filtered and washed with chloroform (3 mL). The title compound is also slightly soluble in chloroform so that a small portion was lost in this step. The remaining solid was dissolved in acetone; the

acetone was then removed *in vacuo* to give the title compound as an analytically pure white solid. Yield: 4 mg (10% based on initial Re). A colorless crystal suitable for a single crystal X-ray diffraction study was obtained by slow evaporation of a saturated acetone solution of $(\text{NEt}_4)[\text{Re}_2(\text{CO})_6(\mu\text{-pz})_2(\mu\text{-OMe})]$. $^1\text{H NMR}$ ($(\text{CD}_3)_2\text{CO}$): δ 1.39 (tt, 12H, NCH_2CH_3), 3.49 (q, 8H, NCH_2CH_3), 4.42 (s, 3H, OCH_3), 6.03 (t, 2H, $\text{pz-H}_{\text{inner}}$), 7.64 (d, 4H, $\text{pz-H}_{\text{outer}}$). IR (KBr): $\nu(\text{CO})$ 1996, 1897, 1871, 1857 cm^{-1} . ESI(-)MS: m/z 703/705/707 M. *Anal.* Calc. for $\text{C}_{21}\text{H}_{29}\text{N}_5\text{O}_7\text{Re}_2$: C, 30.18; H, 3.50; N, 8.38. Found: C, 30.15; H, 3.54; N, 8.32%.

Synthesis of (Hydrotris(1-pyrazolyl)borato)tricarbonylrhenium(I), $\text{TpRe}(\text{CO})_3$

To a solution of 77 mg (0.10 mmol) $(\text{NEt}_4)_2[\text{ReBr}_3(\text{CO})_3]$ in 1 mL acetonitrile was added a solution of 26 mg (0.10 mmol) KTp in 0.25 mL acetonitrile. A white precipitate formed immediately. The solution was stirred for 1 h at which time 10 mL deionized water was added to precipitate more white powder. The solution was filtered, and the solid was washed with deionized water (2.5 mL) and *n*-pentane (3 x 2 mL). The solid was then dried in air. Yield: 35 mg (79%). $^1\text{H NMR}$ ($(\text{CD}_3)_2\text{CO}$): δ 8.05 (d, 3H), 7.94 (d, 3H), 6.37 (t, 3H). *Anal.* Calc. for $\text{C}_{12}\text{H}_{10}\text{BN}_6\text{O}_3\text{Re}$: C, 29.82; H, 2.09; N, 17.39. Found: C, 29.63; H, 2.07; N, 17.11%. Spectroscopic and analytical data agree with previously reported literature values.³⁰

Reaction of the triaquatricarbonylrhenium(I) cation with potassium hydrotris(1-pyrazolyl)borate

To a solution of 77 mg (0.10 mmol) $(\text{NEt}_4)_2[\text{ReBr}_3(\text{CO})_3]$ in 2 mL deionized water was added a solution of 26 mg (0.10 mmol) KTp in 0.75 mL water. A white precipitate formed immediately. After stirring for 30 minutes, the suspension was filtered, washed with deionized water (3 mL) and hexanes (3 x 2 mL) and dried in air. Yield: 32 mg of a product mixture. A crystal suitable for an X-ray diffraction study was obtained from the mixture from wet acetone-pentane. FAB(+)MS: m/z 482/484 $[\text{TpRe}(\text{CO})_3]^+$, 454/456 $[\text{M} - \text{CO}]^+$, 415/417 $[\text{M} - \text{pz}]^+$. FAB(-)MS m/z 689/691/693 $[\text{Re}_2(\text{CO})_6(\text{pz})_2(\text{OH})]^-$.

X-ray Crystallography

Crystals of $\text{Tc}(\text{CO})_3(\text{L}_{\text{OEt}})$, $\text{Re}(\text{CO})_3(\text{L}_{\text{OEt}})$, $(\text{NEt}_4)[\text{Re}_2(\text{CO})_6(\mu\text{-pz})_2(\mu\text{-OMe})]$, and $(\text{NEt}_4)[\text{Re}_2(\text{CO})_6(\mu\text{-pz})_2(\mu\text{-OH})] \cdot (\text{CH}_3)_2\text{CO} \cdot 0.5\text{H}_2\text{O}$ were transferred onto a microscope slide from a scintillation vial and coated with STP[®]. A crystal of each compound was selected, mounted on a glass fiber, and optically centered. The data were collected on a Siemens platform goniometer with a CCD detector. Crystal data and structure refinement are shown in Tables 1.1 - 1.3. The structures of $\text{Tc}(\text{CO})_3(\text{L}_{\text{OEt}})$, $(\text{NEt}_4)[\text{Re}_2(\text{CO})_6(\mu\text{-pz})_2(\mu\text{-OMe})]$, and $(\text{NEt}_4)[\text{Re}_2(\text{CO})_6(\mu\text{-pz})_2(\mu\text{-OH})] \cdot (\text{CH}_3)_2\text{CO} \cdot 0.5\text{H}_2\text{O}$ were solved by direct methods in conjunction with standard difference Fourier techniques, and the rhenium in $\text{Re}(\text{CO})_3(\text{L}_{\text{OEt}})$ was located by the Patterson method before using standard difference Fourier techniques to complete the solution of the structure (SHELXTL v5.0, Sheldrick, G. M. and Siemens Industrial Automation, 1995, and SHELXTL v5.1, Sheldrick, G. M. and Siemens Industrial Automation, 1997). Non-hydrogen atoms were

treated anisotropically, and hydrogen atoms were placed in calculated positions ($d_{\text{C-H}} = 0.96 \text{ \AA}$). For $\text{Tc}(\text{CO})_3(\text{L}_{\text{OEt}})$ and $(\text{NEt}_4)[\text{Re}_2(\text{CO})_6(\mu\text{-pz})_2(\mu\text{-OMe})]$, a semi-empirical absorption correction from ψ scans was applied. Refinement of all structures was carried out by full-matrix least-squares on F^2 .

Two carbon atoms in $\text{Tc}(\text{CO})_3(\text{L}_{\text{OEt}})$, C(12) and C(20), were found to have split positions. The atoms C(12A) and C(12B) were each refined with an occupancy of 0.5, and C(20A) and C(20B) were refined with occupancies of 0.67 and 0.33, respectively.

Table 1.1. Crystal data and structure refinement for $\text{Re}(\text{CO})_3(\text{L}_{\text{OEt}})$ and $\text{Tc}(\text{CO})_3(\text{L}_{\text{OEt}})$.

Compound	$\text{Re}(\text{CO})_3(\text{L}_{\text{OEt}})$	$\text{Tc}(\text{CO})_3(\text{L}_{\text{OEt}})$
Empirical formula	$\text{C}_{20}\text{H}_{35}\text{CoO}_{12}\text{P}_3\text{Re}$	$\text{C}_{20}\text{H}_{35}\text{CoO}_{12}\text{P}_3\text{Tc}$
Formula weight	805.52	717.32
Temperature	183(2) K	183(2) K
Wavelength	0.71073 Å	0.71073 Å
Crystal system	Monoclinic	Monoclinic
Space group	$\text{P}2_1/\text{n}$	$\text{P}2_1/\text{n}$
a/Å	11.5113(7)	11.5661(11)
b/Å	18.6022(12)	18.671(2)
c/Å	13.7397(8)	13.7852(13)
$\beta/^\circ$	92.7580(10)	92.770(2)
Volume/Å ³	2938.7(3)	2973.5(5)
Z	4	4
ρ_{calc} , Mg/m ³	1.821	1.602
μ , mm ⁻¹	4.898	1.238
F(000)	1592	1464
Crystal dimensions, mm	0.31 x 0.07 x 0.07	0.38 x 0.09 x 0.09
θ range for data collection	2.19 to 23.29	2.07 to 20.00
Limiting indices	$-12 \leq h \leq 12, -20 \leq k \leq 17, -10 \leq l \leq 15$	$-12 \leq h \leq 12, -20 \leq k \leq 20, -12 \leq l \leq 15$
Reflections collected	11728	8605
Independent reflections	4224 ($R_{\text{int}} = 0.0685$)	2775 ($R_{\text{int}} = 0.0750$)
Max. and min. transmission	None	0.6456 and 0.4481
Data / restraints / parameters	4224 / 0 / 335	2743 / 0 / 353
Goodness-of-fit on F^2	1.081	1.173
Final R indices [$I > 2\sigma(I)$]	$R_1 = 0.0384, wR_2 = 0.0760$	$R_1 = 0.0669, wR_2 = 0.1361$
R indices (all data)	$R_1 = 0.0502, wR_2 = 0.0792$	$R_1 = 0.0824, wR_2 = 0.1427$
Extinction coefficient	0.00000(7)	0.0002(2)
Largest diff. peak and hole, eÅ ⁻³	0.791 and -0.963	0.521 and -0.559

Table 1.2. Crystal data and structure refinement for (NEt₄)[Re₂(CO)₆(μ-pz)₂(μ-OMe)].

Empirical formula	C ₂₁ H ₂₉ N ₅ O ₇ Re ₂
Formula weight	835.89
Temperature (K)	183(2) K
Wavelength (Å)	0.71073 Å
Crystal system	Monoclinic
Space group	P2(1)/c
a (Å)	10.023(3)
b (Å)	14.010(2)
c (Å)	37.701(6)
β (°)	95.388(18)
Volume (Å ³)	5270.4(19)
Z	8
ρ _{calc} (Mg m ⁻³)	2.107
μ (mm ⁻¹)	9.227
F(000)	3168
Crystal dimensions (mm ³)	0.16 x 0.06 x 0.02
Theta range for data collection (°)	2.04 to 23.25
Limiting Indices	-9 ≤ h ≤ 11, -14 ≤ k ≤ 15, -41 ≤ l ≤ 40
Reflections collected	21055
Independent reflections (R _{int})	7539 (0.0880)
Completeness to theta	99.8 %
Max. and min. transmission	0.2045 and 0.1034
Data / restraints / parameters	7539 / 0 / 632
Goodness-of-fit on F ²	0.936
Final R indices [I > 2σ(I)]	R ₁ = 0.0422, wR ₂ = 0.0716
R indices (all data)	R ₁ = 0.0781, wR ₂ = 0.0794
Extinction coefficient	0.000000(11)
Largest diff. peak and hole (eÅ ⁻³)	0.971 and -0.924

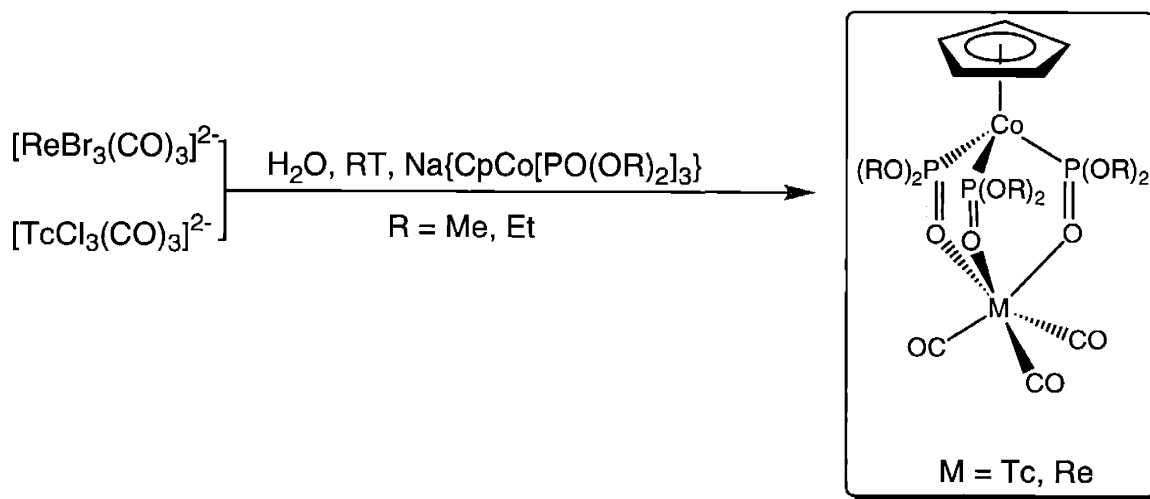
Table 1.3. Crystal data and structure refinement for $(\text{NEt}_4)[\text{Re}_2(\text{CO})_6(\mu\text{-pz})_2(\mu\text{-OH})]\cdot(\text{CH}_3)_2\text{CO}\cdot 0.5\text{H}_2\text{O}$.

Empirical formula	$\text{C}_{22}\text{H}_{32}\text{N}_5\text{O}_{8.5}\text{Re}_2$
Formula weight	886.94
Temperature (K)	183(2) K
Wavelength (\AA)	0.71073 \AA
Crystal system	Orthorhombic
Space group	Pnma
a (\AA)	20.368(4)
b (\AA)	12.843(2)
c (\AA)	11.211(2)
Volume (\AA^3)	2932.7(9)
Z	4
ρ_{calc} (Mg m^{-3})	2.008
μ (mm^{-1})	4.150
F(000)	846
Crystal dimensions (mm^3)	0.34 x 0.06 x 0.04
Theta range for data collection ($^\circ$)	2.04 to 23.27
Limiting Indices	$-22 \leq h \leq 22, -14 \leq k \leq 10, -12 \leq l \leq 12$
Reflections collected	11527
Independent reflections (R_{int})	2221 (0.1141)
Completeness to theta	99.9 %
Max. and min. transmission	None
Data / restraints / parameters	2221 / 0 / 198
Goodness-of-fit on F^2	1.131
Final R indices [$I > 2\sigma(I)$]	$R_1 = 0.0463, wR_2 = 0.1132$
R indices (all data)	$R_1 = 0.0497, wR_2 = 0.1157$
Extinction coefficient	0.00130(15)
Largest diff. peak and hole ($\text{e}\text{\AA}^{-3}$)	2.212 and -1.460

Discussion

Kläui Complexes of Technetium and Rhenium:

The complexes $\text{Tc}(\text{CO})_3(\text{L}_{\text{OMe}})$, $\text{Tc}(\text{CO})_3(\text{L}_{\text{OEt}})$, $\text{Re}(\text{CO})_3(\text{L}_{\text{OMe}})$, and $\text{Re}(\text{CO})_3(\text{L}_{\text{OEt}})$ (Scheme 1.2) were synthesized by reaction of the corresponding triqua tricarbonyl cation with NaL_{OMe} or NaL_{OEt} in water. Since the resulting metal complexes are neutral and the ligands L_{OR} are rather lipophilic, it was hypothesized that the complexes would be relatively insoluble in water. The higher yields obtained in the case of $\text{R} = \text{Et}$ may, in part, be due to the higher lipophilicity of L_{OEt} as opposed to L_{OMe} , leading to poorer solubility of the metal complexes in aqueous solution.



Scheme 1.2. The synthesis of technetium and rhenium tricarbonyl complexes of the Kläui ligand.

The rhenium tricarbonyl complexes of L_{OR} have been reported,³³ however, a more facile method is reported here (*i.e.* reaction occurs at room temperature in air and requires no column chromatography). The Kläui ligand replaces the three aqua ligands of [Re(CO)₃(H₂O)₃]⁺ in aqueous solution under ambient conditions, and neutral Re(CO)₃(L_{OMe}) and Re(CO)₃(L_{OEt}) precipitate as analytically pure powders in good yield. No technetium tricarbonyl complex of the Kläui ligand has been previously reported. The syntheses reported herein are straightforward; the desired products precipitate from aqueous solutions of [Tc(CO)₃(H₂O)₃]⁺ as analytically pure powders in high yield.

The IR and NMR spectra of the Tc and Re complexes of the Kläui ligands are similar. All compounds contain the expected A₁ + E pattern for *fac*-M(CO)₃ species in the infrared spectra (Spectra 1.1 - 1.4). The peak observed for Re(CO)₃(L_{OMe}) at 1878 cm⁻¹ and for Tc(CO)₃(L_{OEt}) at 1908 cm⁻¹ is a split of the E peak and likely corresponds to a slight distortion from idealized C_{3v} symmetry due to the presence of the cyclopentadienyl group. The ν(PO) peak observed in each complex spans the range of 1117 - 1137 cm⁻¹, similar to observed values in other Group 7 complexes of the Kläui ligand.^{24,33} The proton NMR spectra (Spectra 1.5 - 1.8) all show a singlet due to the cyclopentadienyl protons. For the M(CO)₃(L_{OMe}) complexes, a virtual quartet is observed for the methyl protons which are coupled to the phosphorus of each phosphite group. In addition to the expected triplet for the methyl group, a multiplet is observed for the methylene group in M(CO)₃(L_{OEt}) due to more complex coupling.

Each of the four compounds exhibits a parent ion in the FAB(+) mass spectrum, as well as extensive and assignable fragmentation patterns. The carbonyl ligands were observed to be the most easily lost fragments in the mass spectrometer. In fact, the $[(L_{OR})M(CO)_2]^+$ fragment was observed in the mass spectra of each of the four compounds. In addition, the oxo groups of the phosphite ligands were often lost, which is consistent with previously observed fragmentation patterns in other complexes of the Kläui ligand.²⁴

The crystal structures of $Re(CO)_3(L_{OEt})$ and $Tc(CO)_3(L_{OEt})$ have been determined. The two structures are isomorphous. Both crystallize in the monoclinic space group $P2_1/n$. These are the first crystal structures of either rhenium or technetium tricarbonyl complexes of this genre of tripodal ligands. In fact, this is only the second reported crystal structure of any compound containing technetium and the Kläui ligand.³⁴ Selected bond lengths and angles are presented in Table 1.4, and the thermal ellipsoid plots of the two structures are given in Figure 1.2 (with the ethoxy groups omitted for clarity). The geometry about the metal centers is only slightly distorted from octahedral. The greatest deviation from 90° is $83.6(3)^\circ$ in $Tc(CO)_3(L_{OEt})$ [O(10) - Tc(1) - O(12)] and $82.5(2)^\circ$ in $Re(CO)_3(L_{OEt})$ [O(10) - Re(1) - O(11)]. The mean Re-O bond distance is $2.158(4) \text{ \AA}$, which is quite similar to Re-O bond distances in the high valent $(L_{OMe})ReO_3$ (mean $d(Re-O) = 2.13(2)$).²⁵ This is in the normal range for Re-O(=P) bond distances when the P=O moiety stands *trans* to an oxo or a carbonyl ($2.08 - 2.18 \text{ \AA}$). This range of distances does not vary much on changing oxidation state.³⁵⁻⁴⁰ No Tc-O bond distances were reported in the other example of a crystallographically characterized technetium Kläui complex.³⁴

Other Tc-O(=P) bond distances have been reported in a Tc(II) example⁴¹ (2.097(4) Å) and two cationic Tc(III) examples⁴² (2.107(3) Å and 2.109(6) Å). Given the lower oxidation state of the technetium and the strong *trans* effect of the carbonyl ligands, the longer mean Tc-O bond length of 2.172(7) Å is not surprising.

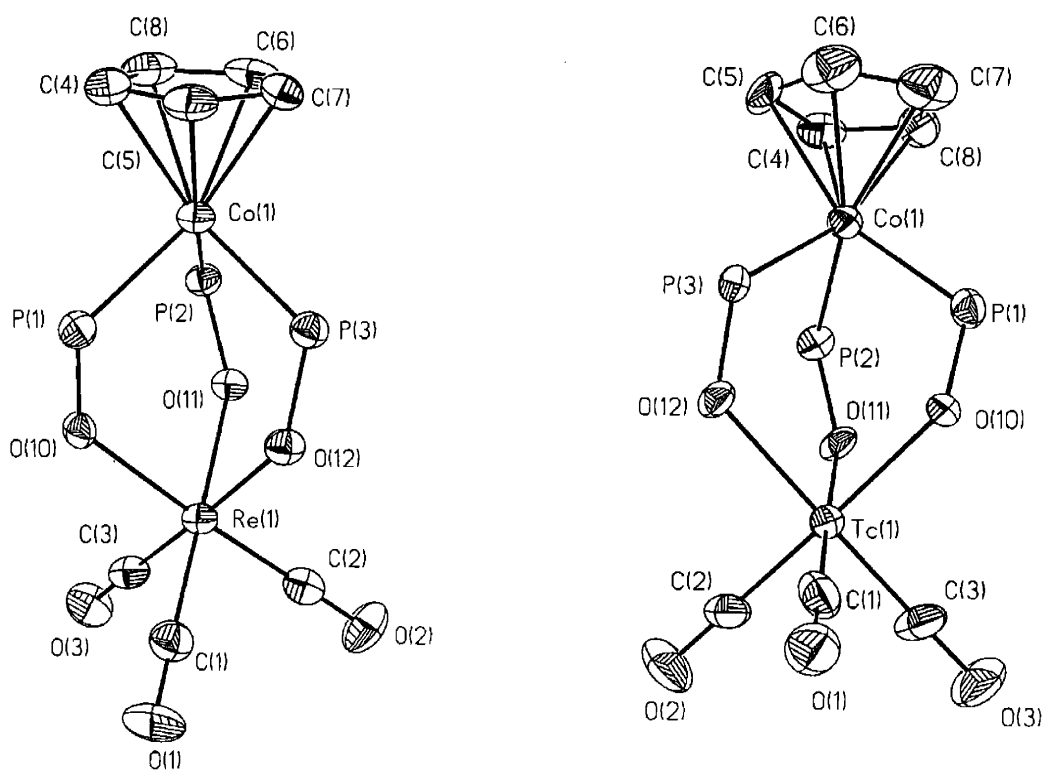


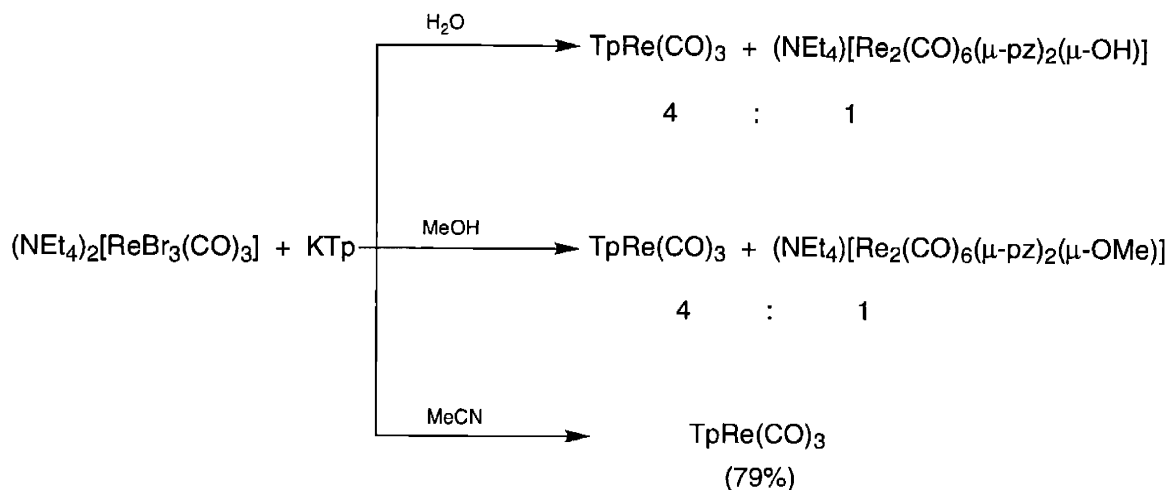
Figure 1.2. Thermal ellipsoid plots (35% ellipsoids) of $\text{Re}(\text{CO})_3(\text{L}_{\text{OEt}})$ and $\text{Tc}(\text{CO})_3(\text{L}_{\text{OEt}})$ (ethoxy groups omitted for clarity).

Table 1.4. Selected bond lengths (Å) and angles (°) for $\text{Re}(\text{CO})_3(\text{L}_{\text{OEt}})$ and $\text{Tc}(\text{CO})_3(\text{L}_{\text{OEt}})$.

$\text{Re}(\text{CO})_3(\text{L}_{\text{OEt}})$		$\text{Tc}(\text{CO})_3(\text{L}_{\text{OEt}})$	
Re(1)-C(1)	1.889(8)	Tc(1)-C(1)	1.84(2)
Re(1)-C(2)	1.887(8)	Tc(1)-C(2)	1.869(14)
Re(1)-C(3)	1.893(8)	Tc(1)-C(3)	1.877(14)
Re(1)-O(10)	2.157(4)	Tc(1)-O(10)	2.170(6)
Re(1)-O(11)	2.162(4)	Tc(1)-O(11)	2.168(7)
Re(1)-O(12)	2.155(4)	Tc(1)-O(12)	2.178(6)
C(1)-Re(1)-C(2)	87.3(3)	C(1)-Tc(1)-C(2)	87.3(5)
C(1)-Re(1)-C(3)	87.3(3)	C(1)-Tc(1)-C(3)	87.1(5)
C(2)-Re(1)-C(3)	87.5(3)	C(2)-Tc(1)-C(3)	85.8(6)
C(1)-Re(1)-O(10)	95.2(3)	C(1)-Tc(1)-O(10)	94.0(4)
C(2)-Re(1)-O(10)	176.8(2)	C(2)-Tc(1)-O(10)	177.8(4)
C(3)-Re(1)-O(10)	94.6(2)	C(3)-Tc(1)-O(10)	96.1(4)
C(1)-Re(1)-O(11)	176.4(2)	C(1)-Tc(1)-O(11)	178.1(4)
C(2)-Re(1)-O(11)	94.8(2)	C(2)-Tc(1)-O(11)	94.6(4)
C(3)-Re(1)-O(11)	95.7(2)	C(3)-Tc(1)-O(11)	93.1(4)
C(1)-Re(1)-O(12)	93.7(3)	C(1)-Tc(1)-O(12)	95.9(4)
C(2)-Re(1)-O(12)	94.5(2)	C(2)-Tc(1)-O(12)	94.4(4)
C(3)-Re(1)-O(12)	177.8(2)	C(3)-Tc(1)-O(12)	177.0(4)
O(10)-Re(1)-O(11)	82.5(2)	O(10)-Tc(1)-O(11)	84.2(3)
O(10)-Re(1)-O(12)	83.4(2)	O(10)-Tc(1)-O(12)	83.6(3)
O(11)-Re(1)-O(12)	83.3(2)	O(11)-Tc(1)-O(12)	83.9(2)

Reactions of $[\text{Re}(\text{sol})_3(\text{CO})_3]^+$ with KTp:

The reaction of $[\text{Re}(\text{CO})_3(\text{sol})_3]^+$ with KTp (Tp⁻ = hydrotris(1-pyrazolyl)borate) gave a variety of products depending on the solvent used (Scheme 1.3). In the case of methanol, the proton NMR spectrum of the crude reaction mixture indicated the existence of two products, in roughly a 4:1 ratio. As expected, the most abundant product was $\text{TpRe}(\text{CO})_3$, which is formed by the simple replacement of the three weakly-bound methanol ligands by the hydrotris(1-pyrazolyl)borate monoanionic tridentate ligand. The proton NMR spectrum also exhibited signals due to $(\text{NEt}_4)^+$, which indicated the presence of a second, anionic product. In fact, upon obtaining an ESI(-)MS, it was clear that an



Scheme 1.3. Effect of solvent on products of reaction of $[\text{ReBr}_3(\text{CO})_3]^{2-}$ with KTp.

anionic species containing two rhenium centers was present (based on isotope pattern; Figure 1.3). The neutral, mononuclear compound is soluble in chloroform, but the anionic, dinuclear complex is only slightly soluble. Slurrying the mixture with chloroform, followed by filtration, enabled the isolation a pure sample of the ionic compound. Recrystallization from acetone yielded crystals suitable for a single crystal X-ray diffraction study.

The crystal structure showed that the hydrotris(1-pyrazolyl)borate ligand had decomposed.⁴³⁻⁴⁵ The resulting metal complex consisted of two rhenium tricarbonyl units, two bridging pyrazolyl groups, and a bridging methoxide. Such coordination resulting from a reaction involving a tris(pyrazolyl)borate ligand has only been reported one other time.⁴⁶

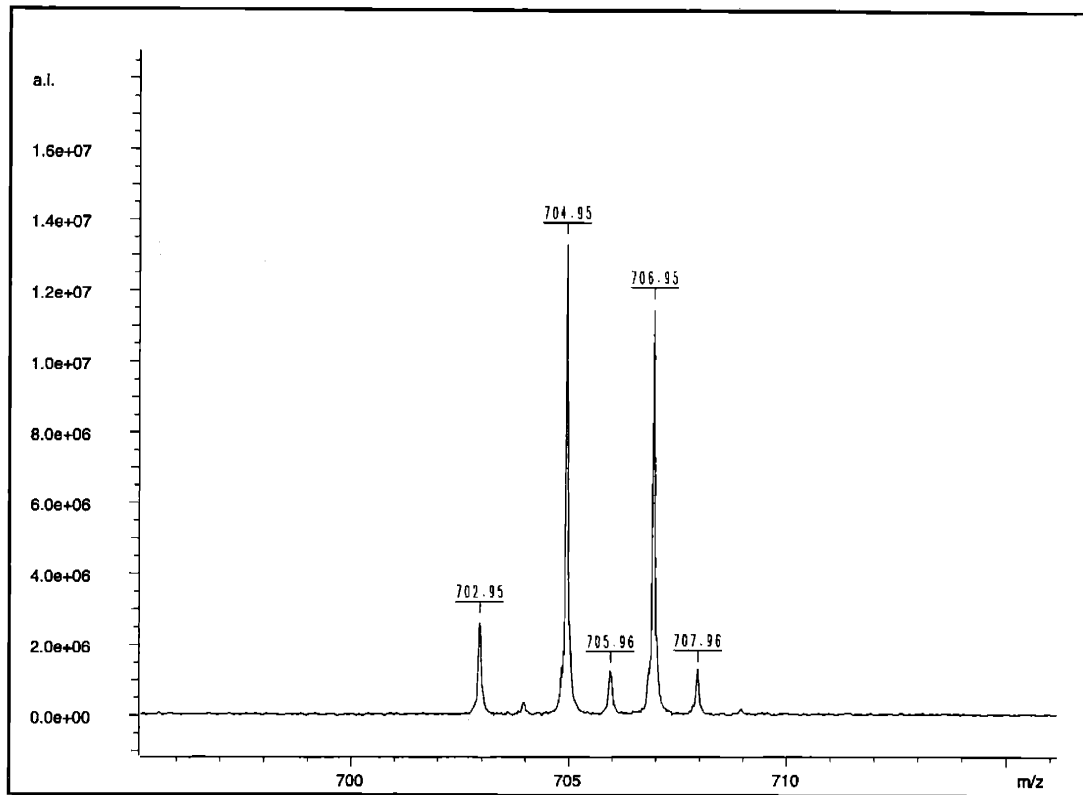


Figure 1.3. ESI(-)MS of $[\text{Re}_2(\text{CO})_6(\mu\text{-pz})_2(\mu\text{-OMe})]^-$ showing Re_2 isotope pattern.

Two molecules exist in the asymmetric unit of the crystal structure, but they are nearly identical. As a result, only one anion is shown (Figure 1.4). The geometry about each rhenium center is distorted octahedral, with two bridging pyrazolides and a bridging methoxide. The greatest deviation from ideal octahedral geometry is a small O(7) - Re(2) - N(2) angle of $79.5(3)^\circ$ (Table 1.5). The mean Re-O(Me) bond distance is $2.128(7) \text{ \AA}$, very similar to other Re-O(bridging methoxide) bond distances.⁴⁷ In $\text{Tp}^*\text{In}(\mu\text{-}3,5\text{-Me}_2\text{pz})_2(\mu\text{-OH})\text{InTp}^*$ ($\text{Tp}^* = \text{HB}(3,5\text{-Me}_2\text{pz})_3$), the other example of such coordination arising from a reaction involving a tris(pyrazolyl)borate ligand, direct comparison of M-

N(Tp) and M-N(μ -pz) bond lengths is possible as both types of bonds are present. Mean bond distance for In-N(Tp^{*}) was 2.267(8) Å, and that for In-N(μ -3,5-Me₂pz) was a slightly shorter 2.236(8) Å.⁴⁶ Similar direct comparison is not possible in the rhenium compound described here, but comparison with the previously synthesized and crystallographically characterized TpRe(CO)₃³⁰ is useful. As in the indium case, a small

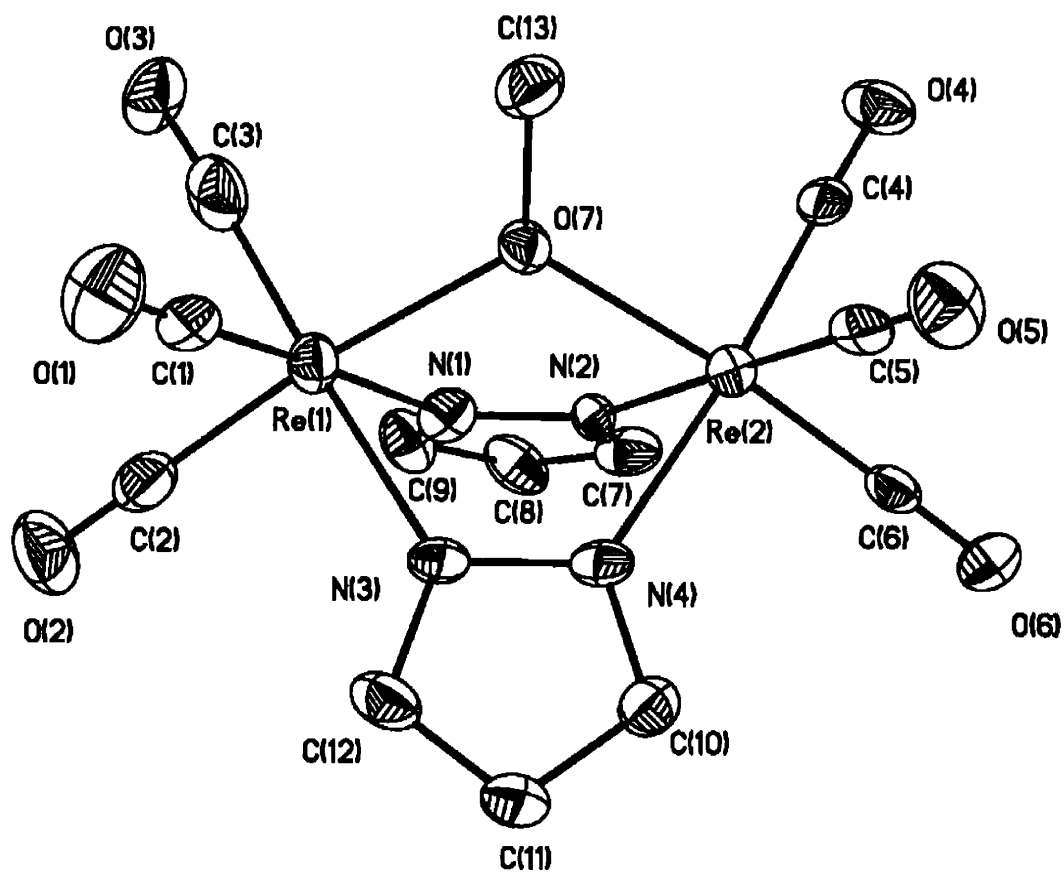


Figure 1.4. Thermal ellipsoid plot (35% ellipsoids) of [Re₂(CO)₆(μ -pz)₂(μ -OMe)].

Table 1.5. Selected bond lengths (Å) and angles(°) for (NEt₄)[Re₂(CO)₆(μ-pz)₂(μ-OMe)].

Re(1)-C(1)	1.930(14)	Re(2)-C(4)	1.911(13)
Re(1)-C(2)	1.899(16)	Re(2)-C(5)	1.921(15)
Re(1)-C(3)	1.912(15)	Re(2)-C(6)	1.881(13)
Re(1)-N(1)	2.182(9)	Re(2)-N(2)	2.158(9)
Re(1)-N(3)	2.159(8)	Re(2)-N(4)	2.160(9)
Re(1)-O(7)	2.121(7)	Re(2)-O(7)	2.134(7)
C(1)-Re(1)-C(2)	86.8(5)	C(4)-Re(2)-C(5)	89.2(5)
C(1)-Re(1)-C(3)	88.9(5)	C(4)-Re(2)-C(6)	88.4(4)
C(2)-Re(1)-C(3)	88.0(5)	C(5)-Re(2)-C(6)	87.4(5)
C(1)-Re(1)-N(1)	175.0(4)	C(4)-Re(2)-N(2)	94.2(4)
C(2)-Re(1)-N(1)	176.8(2)	C(5)-Re(2)-N(2)	176.1(4)
C(3)-Re(1)-N(1)	95.9(4)	C(6)-Re(2)-N(2)	94.5(4)
C(1)-Re(1)-N(3)	91.9(4)	C(4)-Re(2)-N(4)	175.1(4)
C(2)-Re(1)-N(3)	94.6(4)	C(5)-Re(2)-N(4)	92.8(4)
C(3)-Re(1)-N(3)	177.4(5)	C(6)-Re(2)-N(4)	96.0(4)
C(1)-Re(1)-O(7)	98.5(4)	C(4)-Re(2)-O(7)	94.5(4)
C(2)-Re(1)-O(7)	173.2(4)	C(5)-Re(2)-O(7)	98.4(4)
C(3)-Re(1)-O(7)	96.3(4)	C(6)-Re(2)-O(7)	173.5(4)
N(1)-Re(1)-N(3)	83.2(3)	N(2)-Re(2)-N(4)	83.6(3)
N(1)-Re(1)-O(7)	79.7(3)	N(2)-Re(2)-O(7)	79.5(3)
N(3)-Re(1)-O(7)	81.1(3)	N(4)-Re(2)-O(7)	80.9(3)

shortening of the M-N bond length is seen on going from Tp to bridging pyrazolide. The mean Re-N bond distance in TpRe(CO)₃ is 2.22(2) Å while that for (NEt₄)[Re₂(CO)₆(μ-pz)₂(μ-OMe)] is 2.170(9) Å. The Re-C bond length from the two carbonyl complexes can also be compared. The carbonyl ligands are not as strongly bound in (NEt₄)[Re₂(CO)₆(μ-pz)₂(μ-OMe)] (mean Re-C = 1.910(14) Å) as compared with TpRe(CO)₃ (mean Re-C = 1.82(2) Å), suggesting less π-backbonding in the dinuclear anionic compound. However, because of the lower ν(CO) of 1996 cm⁻¹ (A₁) in (NEt₄)[Re₂(CO)₆(μ-pz)₂(μ-OMe)] as compared to 2020 cm⁻¹ (A₁) in TpRe(CO)₃ (which contradicts the bond distance argument), little can be said of the backbonding differences between the two complexes.

The ^1H NMR spectrum of $(\text{NEt}_4)[\text{Re}_2(\text{CO})_6(\mu\text{-pz})_2(\mu\text{-OMe})]$ is consistent with identical solution and solid-state structures (Spectrum 1.9). Two signals for the pyrazolide protons are present at 7.64 and 6.03 ppm in a 2:1 ratio as well as a singlet at 4.42 ppm due to the bridging methoxide. The infrared spectrum shows four peaks in the $\nu(\text{CO})$ region, corresponding to a $2A_1 + 2B_1 + B_2$ pattern (Figure 1.5). Only four peaks are reported, but it is possible that the fifth peak is either buried in the broad 1900 - 1850 cm^{-1} peak or is the very slight shoulder at around 2000 cm^{-1} .

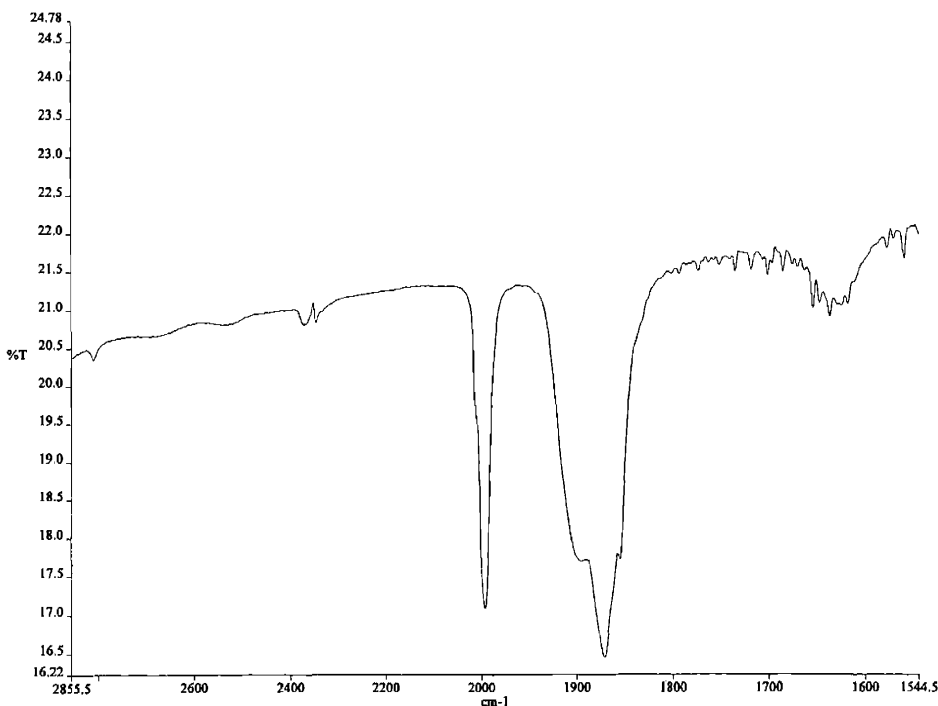


Figure 1.5. $\nu(\text{CO})$ region of IR spectrum (KBr) of $(\text{NEt}_4)[\text{Re}_2(\text{CO})_6(\mu\text{-pz})_2(\mu\text{-OMe})]$.

The analogous reaction was next carried out in water. Once again, a product mixture precipitated from solution, and the two most abundant products were formed in a

4:1 ratio according to the proton NMR spectrum, though other products were formed in small quantities as well. In contrast, the methanol reaction was clean. A FAB(-)MS determined that the product mixture was similar to that of the methanol reaction (*i.e.* anionic dinuclear product present). Unfortunately, the products could not be separated effectively, even by chromatography.

Recrystallization of the product mixture from wet acetone-pentane yielded crystals of two distinct morphologies: small prisms and long needles. A needle was selected for a single crystal X-ray diffraction study. Although a complete solution was not possible due to extended disorder in the tetraethylammonium cation and the solvated acetone molecule, the structure of the anion is unambiguous. The X-ray study clearly established the identity of the anion as the hydroxy analogue of the triply-bridged dinuclear compound previously discussed. A thermal ellipsoid plot for the hydroxy-bridged complex is presented in Figure 1.6. Only half of the anion is unique as a mirror plane generates the other half of the dinuclear complex. No statistically significant differences in geometry exist between $[\text{Re}_2(\text{CO})_6(\mu\text{-pz})_2(\mu\text{-OH})]^-$ and its methoxy analogue (*vide supra*). The assignment of the bridging oxygen as a hydroxide anion is based upon charge balance. Additionally, the Re(1)-O(4) distance of 2.126(4) Å is on the lower end of, though still within, the range of typical Re-O(bridging hydroxide) distances.^{4,48-50}

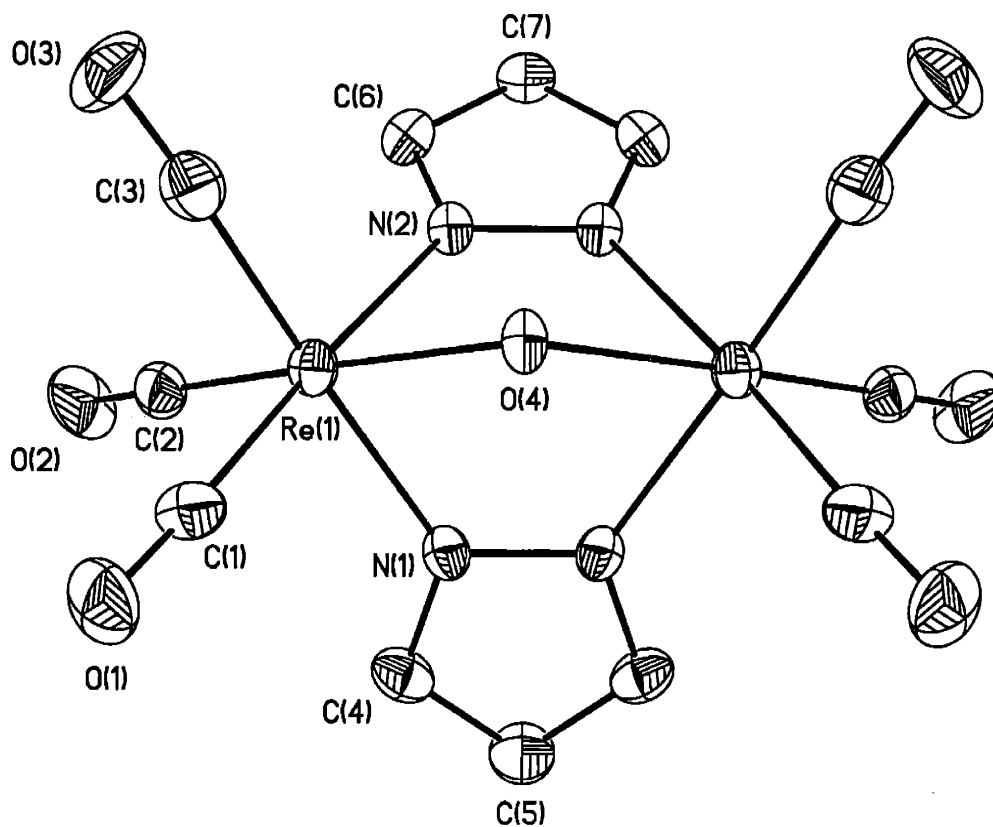


Figure 1.6. Thermal ellipsoid plot (35% probability) of $[\text{Re}_2(\text{CO})_6(\mu\text{-pz})_2(\mu\text{-OH})]^-$.

The anionic complex $[\text{Re}_2(\text{CO})_6(\mu\text{-pz})_2(\mu\text{-OH})]^-$ has been previously reported (prepared by addition of hydroxide to $[\text{Re}_2(\text{CO})_6(\mu\text{-pz})_2(\mu\text{-Br})]^-$); however, no experimental, spectroscopic, analytical, or crystallographic details are provided in the paper.⁵¹ A search of the Cambridge Structural Database⁵² does find the compound, but no atomic coordinates are available. No other information is available regarding this compound or the quality (or lack thereof) of the crystal.

When an aprotic solvent, namely acetonitrile, was employed, only $\text{TpRe}(\text{CO})_3$ was observed, and it was isolated in high yield (79%). The reaction took place in air at

room temperature, and analytically pure material precipitated from the reaction mixture upon addition of water. This shows that the lack of a protic solvent seems to suppress the formation of dinuclear species to give only the initially expected product.

The preparation of pyrazole-containing complexes from reactions involving KTp led to questions as to the purity of commercial KTp obtained from Alfa Aesar. A ^1H NMR spectrum of commercially obtained KTp in CDCl_3 showed the presence of pzH (KTp itself is virtually insoluble in CDCl_3). Separately, reaction of pzH with $[\text{Re}(\text{CO})_3(\text{H}_2\text{O})_3]^+$ gave a small yield of a product mixture, a component of which was $[\text{Re}_2(\text{CO})_6(\mu\text{-pz})_2(\mu\text{-OH})]^-$ (ESIMS and ^1H NMR). This led to investigation of the production of the dinuclear anion when a purer source of KTp was used. Recrystallization of KTp from acetone-hexanes yielded a white, microcrystalline sample of KTp. A ^1H NMR obtained in acetone- d_6 showed at least 98% molar purity. Examination of the reactions of $[\text{Re}(\text{sol})_3(\text{CO})_3]^+$ (sol = H_2O , MeOH) with recrystallized KTp showed very similar results as with commercial KTp. The ratio of products did not change significantly in the case of sol = H_2O or MeOH. In both cases, based on the purity of the recrystallized KTp, neither mixture is completely attributable to pyrazole in the KTp. In fact, upon examination of the ^1H NMR of the 'crude' KTp in acetone- d_6 , a better solvent for KTp (not just pzH), the purity is as high as in the recrystallized sample. Therefore, it is possible to state that the production of the product mixtures is likely due to *in situ* decomposition of Tp^- (perhaps resulting in the production of some pzH), not the existence of pzH in the initial reagent.

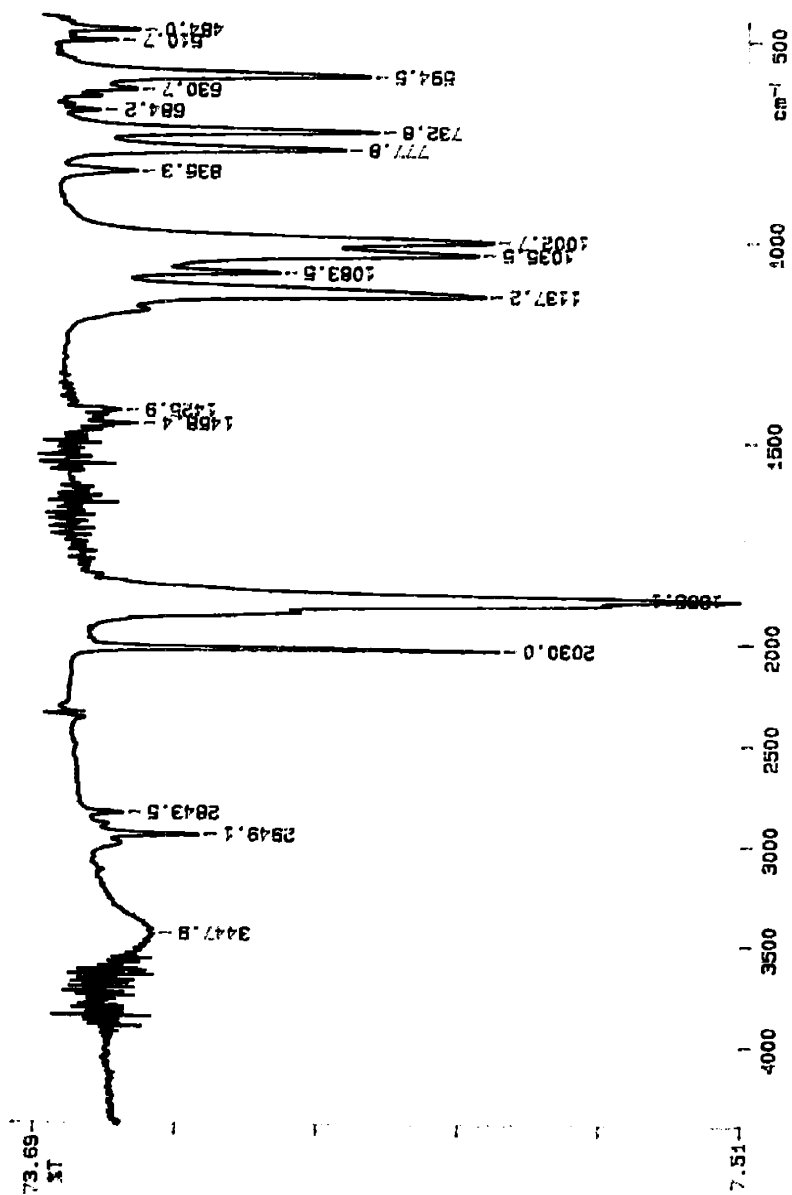
Since both water and methanol are protic solvents, the resulting tris(solvento)tricarbonylrhenium(I) cations are somewhat acidic. Coupled with the Lewis basic nature of borate anions, it was hypothesized that an acid-base reaction took place to give the dinuclear species.⁵³ To gain insight into whether or not this ligand decomposition took place prior to or after complexation, a sample of pure $\text{TpRe}(\text{CO})_3$ was dissolved in acetone- d_6 and exposed to acid (drops of $\text{D}_2\text{O}/\text{DCl}$). Besides a small change in the chemical shifts of the protons due to the DCl addition, no change in the spectrum was observed, even after one day of acid exposure. Further experiments in which $\text{TpRe}(\text{CO})_3$ was stirred for one hour with solutions of $[\text{Re}(\text{CO})_3(\text{sol})_3]^+$ ($\text{sol} = \text{H}_2\text{O}$, MeOH) also showed no decomposition. Given that the dinuclear complex was observed to form on the order of seconds or minutes, it is concluded that the ligand decomposition likely occurred prior to complexation.

Conclusions

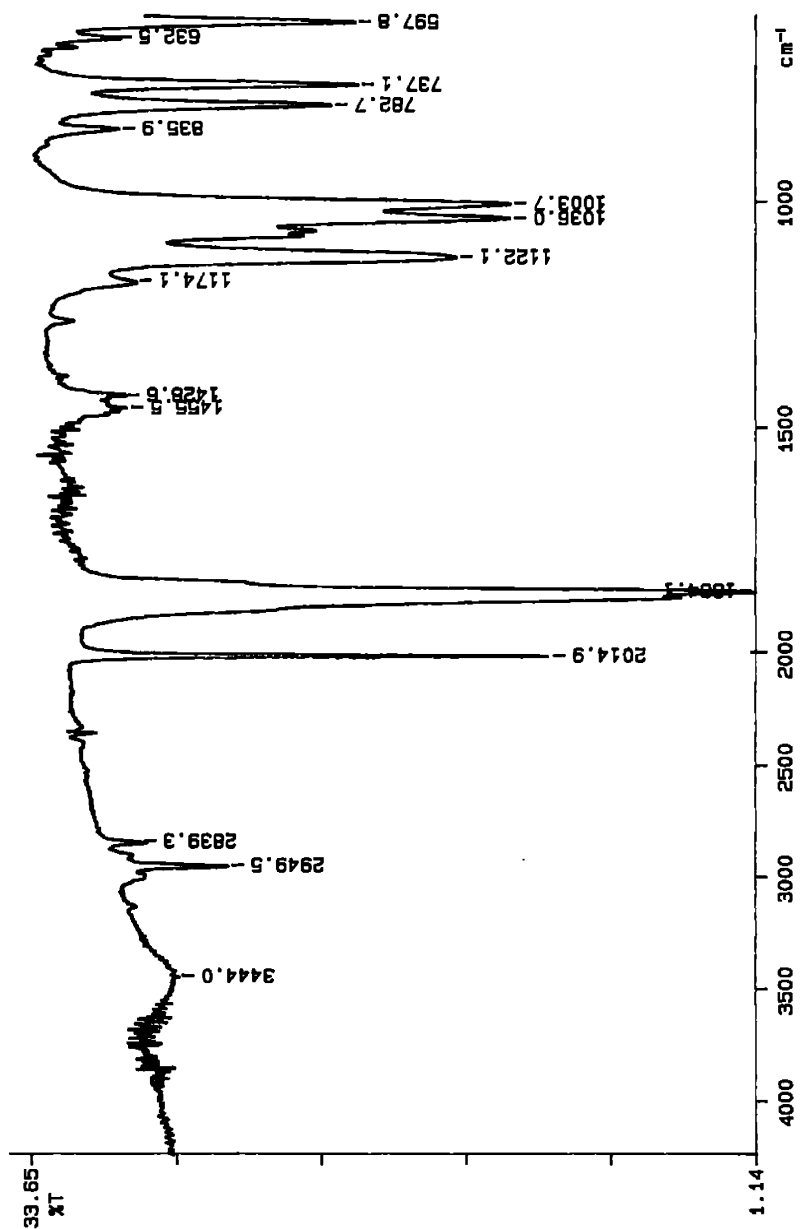
The reactivity of the tris(solvento)tricarbonylrhenium(I) and tris(solvento)tricarbonyltechnetium(I) cations towards two genres of tripodal ligands has been explored. Herein we described the facile synthesis and characterization of structural models for $[M(H_2O)_3(CO)_3]^+$ ($M = Tc, Re$), $M(CO)_3(L_{OR})$ ($M = Tc, Re$; $R = Me, Et$). In addition, the compounds $M(CO)_3(L_{OEt})$ have been crystallographically characterized and show the coordination of a triaqua-like weak-field ligand to the "*fac*- $[M(CO)_3]^+$ " core. Also, the reaction of the tris(solvento)tricarbonylrhenium(I) cations with potassium hydrotris(1-pyrazolyl)borate was investigated and displayed unexpected complexity. Though $TpRe(CO)_3$ was the major product of each reaction regardless of solvent (H_2O , $MeOH$, or $MeCN$), complexes resulting from the decomposition of the borate ligand, $(NEt_4)[Re_2(CO)_6(\mu-pz)_2(\mu-OR)]$ ($R = H, Me$), were identified.

The chemistry presented here illustrates the facility of the substitution of the solvent ligands of $[M(CO)_3(sol)_3]^+$. Though some unexpected results were encountered, it is clear that reaction of $[M(CO)_3(sol)_3]^+$ with monoanionic tridentate ligands proceeds under ambient conditions to yield complexes of the type $LM(CO)_3$. In the forthcoming chapters, studies of tridentate ligand systems which have potential application to radiopharmaceutical development will be detailed.

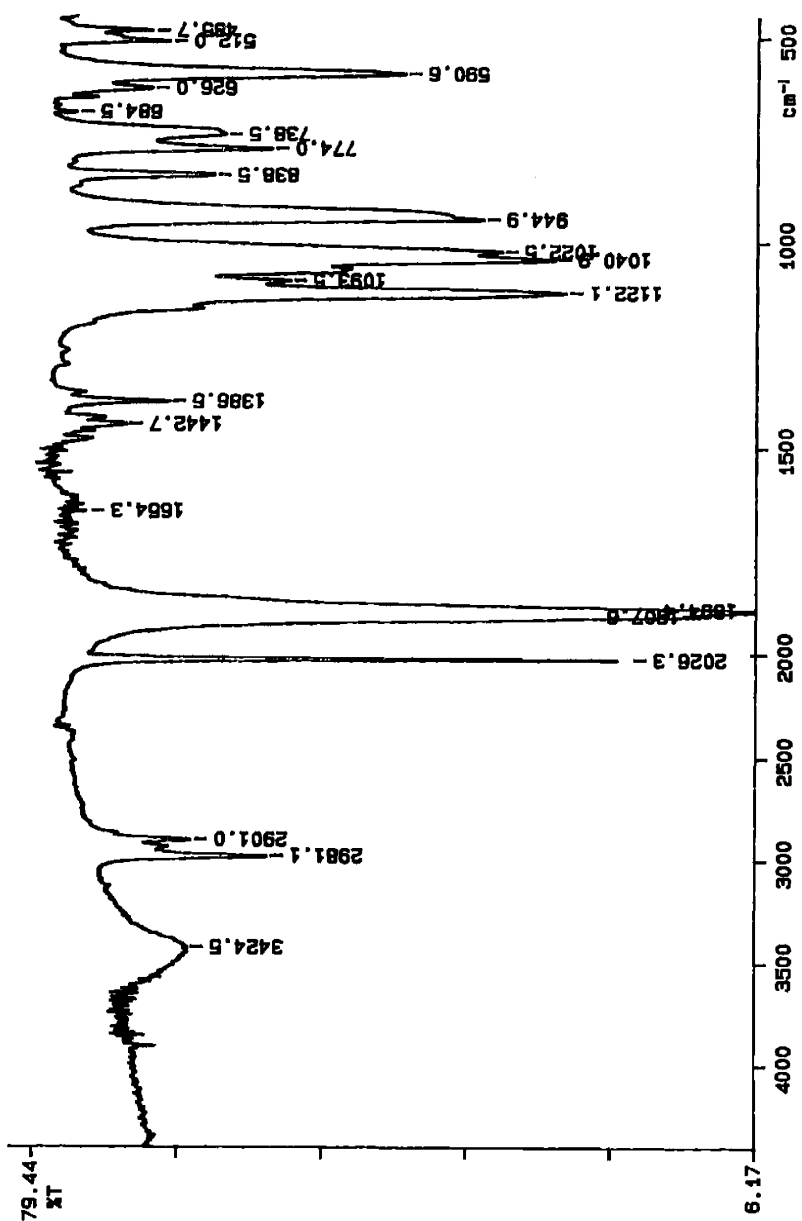
Spectrum 1.1. IR spectrum of $Tc(CO)_3(L_{OMe})_3$.



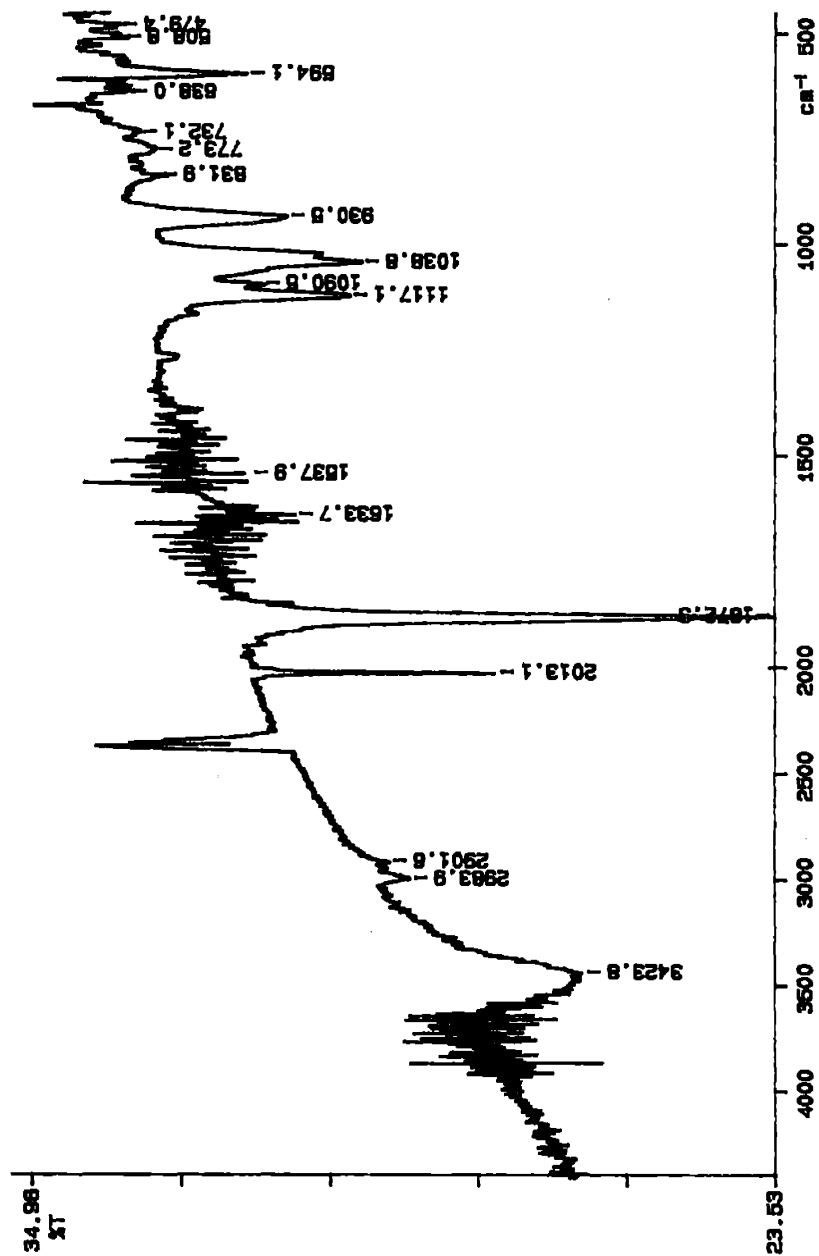
Spectrum 1.2. IR spectrum of $\text{Re}(\text{CO})_3(\text{L}_{\text{OMe}})$.



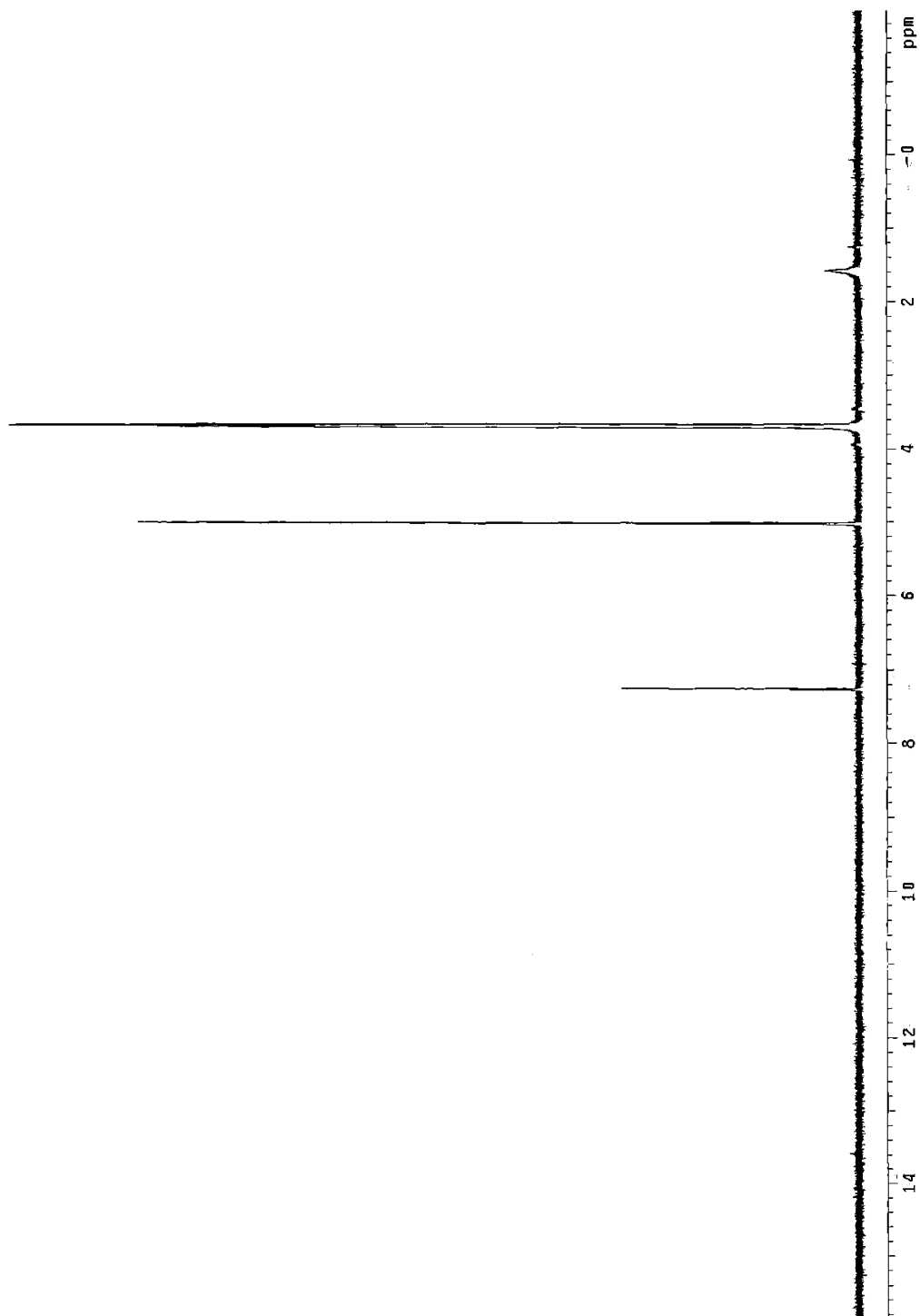
Spectrum 1.3. IR spectrum of $\text{Tc}(\text{CO})_3(\text{L}_{\text{OEt}})$.



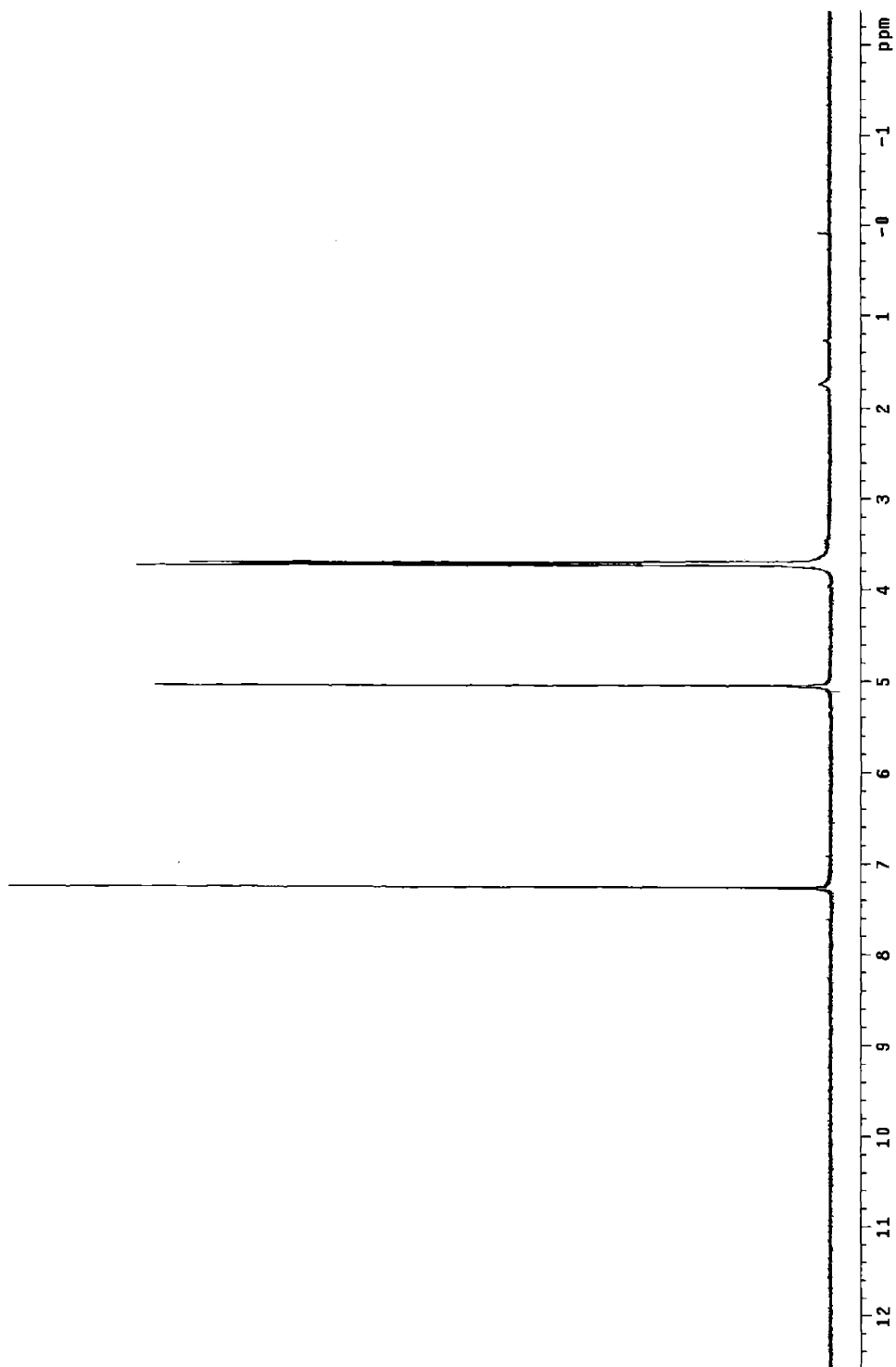
Spectrum 1.4. IR spectrum of $\text{Re}(\text{CO})_3(\text{L}_{\text{OEt}})$.



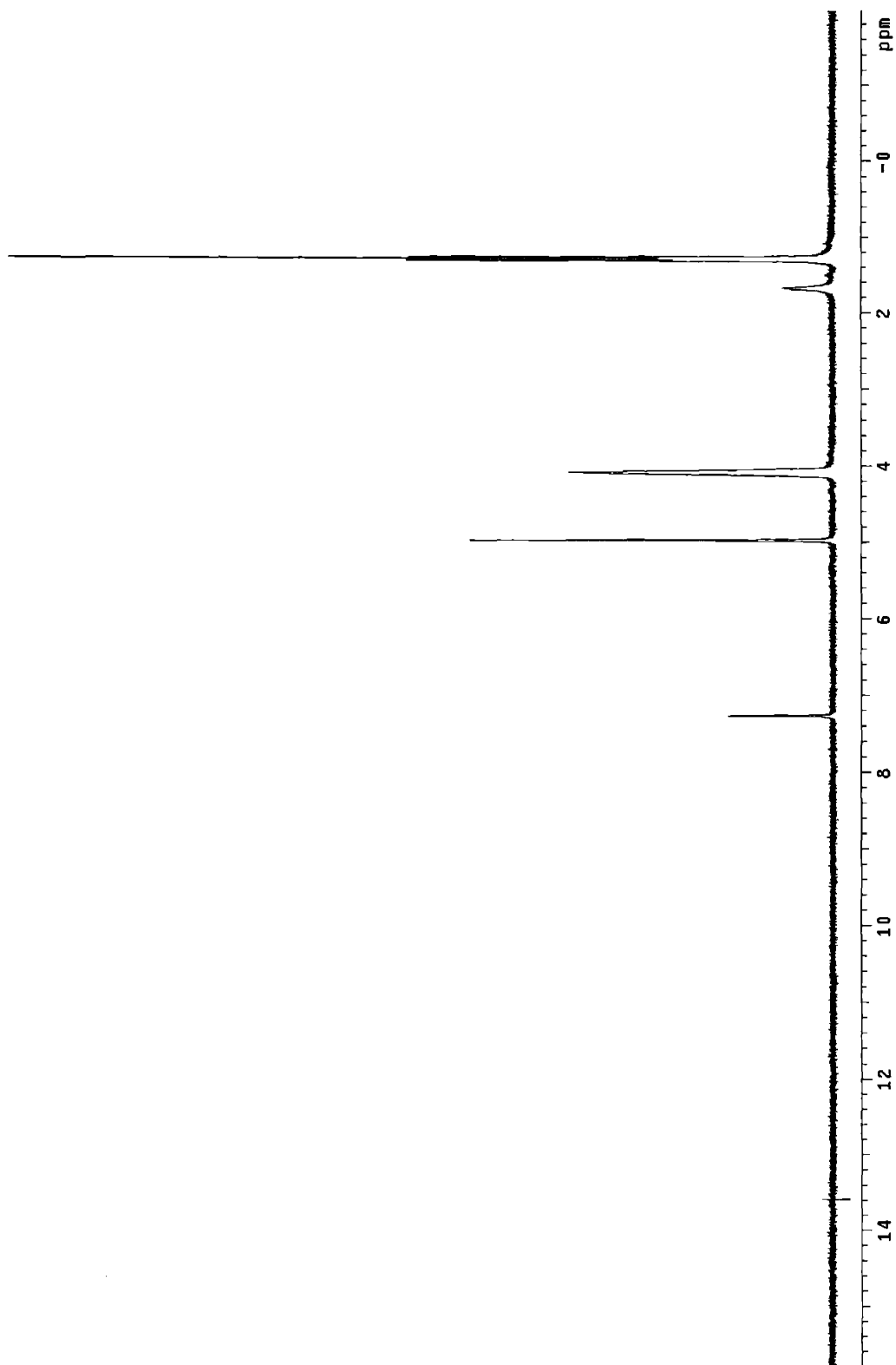
Spectrum 1.5. ^1H NMR spectrum (CDCl_3) of $\text{Tc}(\text{CO})_3(\text{L}_{\text{OMe}})$.



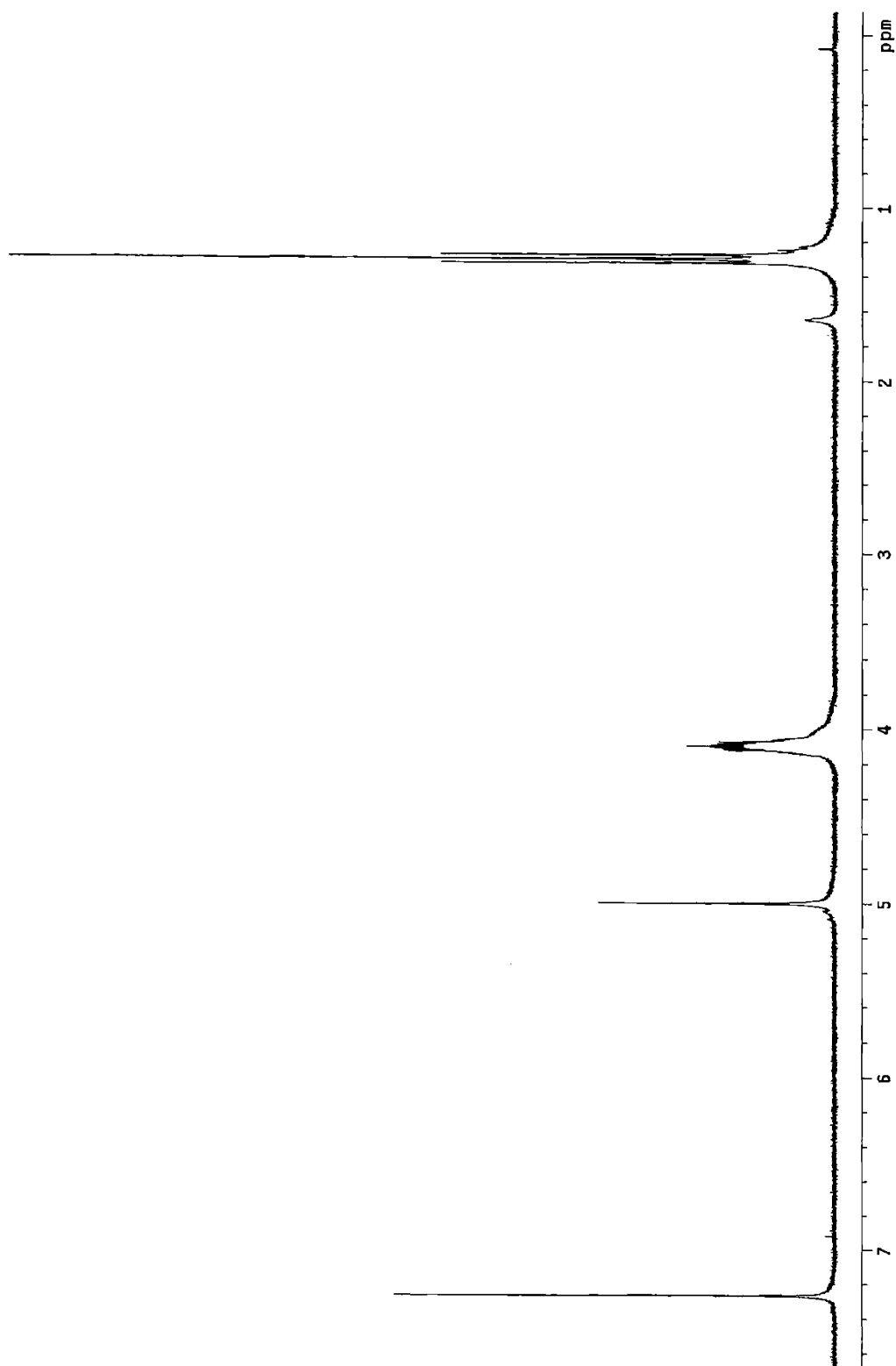
Spectrum 1.6. ^1H NMR spectrum (CDCl_3) of $\text{Re}(\text{CO})_3(\text{LOMe})$.



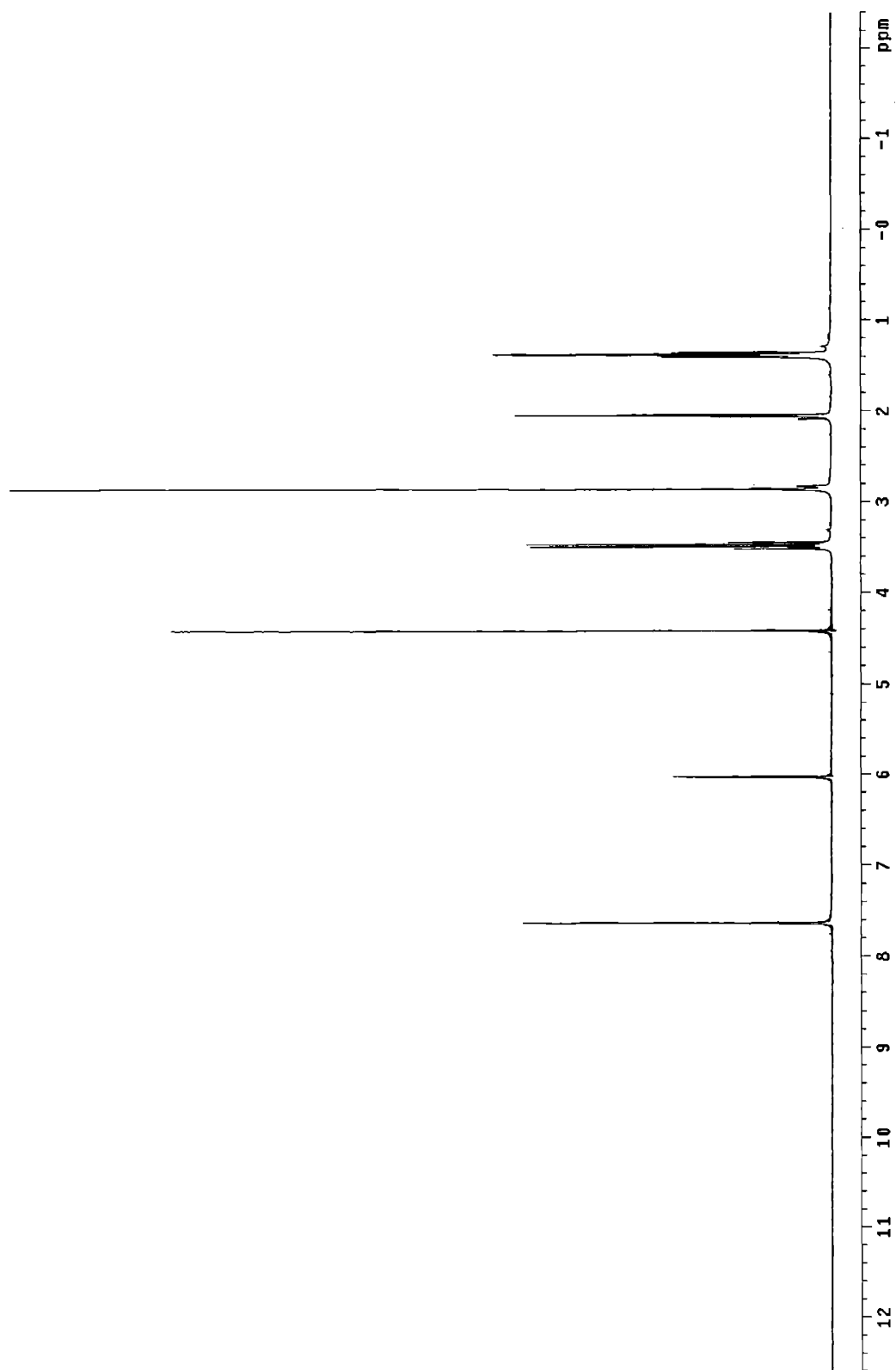
Spectrum 1.7. ^1H NMR spectrum (CDCl_3) of $\text{Tc}(\text{CO})_3(\text{L}_{\text{OEt}})$.



Spectrum 1.8. ^1H NMR spectrum (CDCl_3) of $\text{Re}(\text{CO})_3(\text{L}_{\text{OEt}})$.



Spectrum 1.9. ^1H NMR spectrum (CD_3COCD_3) of $(\text{NEt}_4)[\text{Re}_2(\text{CO})_6(\mu\text{-pz})_2(\mu\text{-OMe})]$.



References

- (1) Green, M. L. H.; Wilkinson, G. *J. Chem. Soc.* **1958**, 4314.
- (2) Striplin, D. R.; Crosby, G. A. *Coord. Chem. Rev.* **2001**, *211*, 163.
- (3) Sun, S. S.; Lees, A. J. *Coord. Chem. Rev.* **2002**, *230*, 171.
- (4) Alberto, R.; Egli, A.; Abram, U.; Hegetschweiler, K.; Gramlich, V.; Schubiger, P. A. *J. Chem. Soc. Dalton Trans.* **1994**, 2815.
- (5) Alberto, R.; Schibli, R.; Egli, A.; Schubiger, P. A.; Herrmann, W. A.; Artus, G.; Abram, U.; Kaden, T. A. *J. Organomet. Chem.* **1995**, *493*, 119.
- (6) Alberto, R. *Top. Curr. Chem.* **1996**, *176*, 149.
- (7) Alberto, R.; Schibli, R.; Egli, A.; Schubiger, A. P.; Abram, U.; Kaden, T. A. *J. Am. Chem. Soc.* **1998**, *120*, 7987.
- (8) Alberto, R. Personal communication; **1999**.
- (9) Alberto, R.; Schibli, R.; Egli, A.; Abram, U.; Abram, S.; Kaden, T. A.; Schubiger, P. A. *Polyhedron* **1998**, *17*, 1133.
- (10) Abram, U.; Abram, S.; Alberto, R.; Schibli, R. *Inorg. Chim. Acta* **1996**, *248*, 193.
- (11) Alberto, R.; Schibli, R.; Schubiger, P. A.; Abram, U.; Kaden, T. A. *Polyhedron* **1996**, *15*, 1079.
- (12) Hoepfing, A.; Reigys, M.; Brust, P.; Seifert, S.; Spies, H.; Alberto, R.; Johannsen, B. *J. Med. Chem.* **1998**, *41*, 4429.
- (13) Alberto, R.; Schibli, R.; Waibel, R.; Abram, U.; Schubiger, P. A. *Coord. Chem. Rev.* **1999**, *190-192*, 901.
- (14) Pietzsch, H.-J.; Gupta, A.; Reigys, M.; Drews, A.; Seifert, S.; Syhre, R.; Spies, H.; Alberto, R.; Abram, U.; Schubiger, P. A.; Johannsen, B. *Bioconjugate Chem.* **2000**, *11*, 414.
- (15) Schibli, R.; Bella, R. L.; Alberto, R.; Garcia-Garayoa, E.; Ortner, K.; Abram, U.; Schubiger, P. A. *Bioconjugate Chem.* **2000**, *11*, 345.
- (16) Kramer, D. J.; Davison, A.; Jones, A. G. *Inorg. Chim. Acta* **2001**, *312*, 215.

- (17) Kramer, D. J.; Davison, A.; Jones, A. G. In *Technetium and Rhenium in Chemistry and Nuclear Medicine 6*; Nicolini, M. and Mazzi, U., Ed.; SGEEditoriali: Padova, **2002**; p. 107.
- (18) Kramer, D. J.; Davison, A.; Davis, W. M.; Jones, A. G. *Inorg. Chem.* **2002**, *41*, 6181.
- (19) Schibli, R.; Alberto, R.; Abram, U.; Abram, S.; Egli, A.; Schubiger, P. A.; Kaden, T. A. *Inorg. Chem.* **1998**, *37*, 3509.
- (20) Kläui, W. *Angew. Chem. Int. Ed. Engl.* **1990**, *29*, 627.
- (21) Kläui, W. *Z. Naturforsch* **1979**, *B34*, 1403.
- (22) Koelle, U. *Coord. Chem. Rev.* **1994**, *135-136*, 623.
- (23) Kläui, W.; Müller, A.; Scotti, M. *J. Organomet. Chem.* **1983**, *253*, 45.
- (24) Thomas, J. A.; Davison, A. *Inorg. Chem.* **1992**, *31*, 1976.
- (25) Banbery, H. J.; Hussain, W.; Evans, I. G.; Hamor, T. A.; Jones, C. J.; McCleverty, J. A.; Schulte, H.-J.; Engles, B.; Kläui, W. *Polyhedron* **1990**, *9*, 2549.
- (26) Trofimenko, S. *J. Am. Chem. Soc.* **1967**, *89*, 3170.
- (27) Trofimenko, S. *Chem. Rev.* **1993**, *93*, 943.
- (28) Thomas, J. A.; Davison, A. *Inorg. Chim. Acta* **1991**, *190*, 231.
- (29) Reger, D. L.; Tarquini, M. E. *Inorg. Chem.* **1982**, *21*, 840.
- (30) Joachim, J. E.; Apostolidis, C.; Kanellakopoulos, B.; Maier, R.; Marques, N.; Meyer, D.; Müller, J.; Matos, A. P. d.; Nuber, B.; Rebizant, J.; Ziegler, M. L. *J. Organometal. Chem.* **1993**, *448*, 119.
- (31) Paulo, A.; Domingos, Â.; Garcia, R.; Santos, I. *Inorg. Chem.* **2000**, *39*, 5669.
- (32) Davison, A.; Orvig, C.; Trop, H. S.; Sohn, M.; DePamphilis, B. V.; Jones, A. G. *Inorg. Chem.* **1980**, *19*, 1988.
- (33) Kläui, W.; Okuda, J.; Scotti, M.; Valderrama, M. *J. Organomet. Chem.* **1985**, *280*, C26.

- (34) Simpson, R. D.; Thomas, J. A.; Davison, A.; Jones, A. G.; Davis, W. M. In *Technetium and Rhenium in Chemistry and Nuclear Medicine 4*; Nicolini, M., Bandoli, G. and Mazzi, U., Ed.; SGEEditoriali: Padova, **1995**; p. 39.
- (35) Battistuzzi, G.; Cannio, M.; Saladini, M.; Battistuzzi, R. *Inorg. Chim. Acta* **2001**, *320*, 178.
- (36) Hansen, L.; Alessio, E.; Iwamoto, M.; Marzilli, P. A.; Marzilli, L. G. *Inorg. Chim. Acta* **1995**, *240*, 413.
- (37) Mévellec, F.; Roucoux, A.; Noiret, N.; Patin, H. *J. Chem. Soc. Dalton Trans.* **2001**, 3603.
- (38) Perez-Lourido, P.; Romero, J.; Garcia-Vazquez, J.; Sousa, A.; Maresca, K. P.; Rose, D. J.; Zubieta, J. *Inorg. Chem.* **1998**, *37*, 3331.
- (39) Rose, D. J.; Maresca, K. P.; Kettler, P. B.; Chang, Y. D.; Soghomomian, V.; Chen, Q.; Abrams, M. J.; Larsen, S. K.; Zubieta, J. *Inorg. Chem.* **1996**, *35*, 3548.
- (40) Scotti, M.; Valderrama, M.; Moreno, R.; López, R.; Boys, D. *Inorg. Chim. Acta* **1994**, *219*, 67.
- (41) Kaden, L.; Lorenz, B.; Kirmse, R.; Stach, J.; Behm, H.; Beurskens, P. T.; Abram, U. *Inorg. Chim. Acta* **1990**, *169*, 43.
- (42) Freiberg, E.; Davis, W. M.; Nicholson, T.; Davison, A.; Jones, A. G. *Inorg. Chem.* **2002**, *41*, 5667.
- (43) Mohan, M.; Bond, M. R.; Otieno, T.; Carrano, C. J. *Inorg. Chem.* **1995**, *34*, 1233.
- (44) Kosugi, M.; Hikichi, S.; Akita, M.; Moro-oka, Y. *Inorg. Chem.* **1999**, *38*, 2567.
- (45) Kime-Hunt, E.; Spartalian, K.; DeRusha, M.; Nunn, C. M.; Carrano, C. J. *Inorg. Chem.* **1989**, *28*, 4392.
- (46) Fraser, A.; Piggott, B. *J. Chem. Soc. Dalton Trans.* **1999**, 3483.
- (47) Woessner, S. M.; Helms, J. B.; Shen, Y.; Sullivan, B. P. *Inorg. Chem.* **1998**, *37*, 5406.
- (48) Jiang, C.; Wen, Y.-S.; Liu, L.-K.; Hor, T. S. A.; Yan, Y. K. *Organometallics* **1998**, *17*, 173.

(49) Lee, K.-W.; Pennington, W. T.; Cordes, A. W.; Brown, T. L. *Organometallics* **1984**, *3*, 404.

(50) Wang, W.; Yan, Y. K.; Hor, T. S. A.; Vittal, J. J.; Wheaton, J. R.; Hall, I. H. *Polyhedron* **2002**, *21*, 1991.

(51) Ardizzoia, G. A.; LaMonica, G.; Maspero, A.; Moret, M.; Masciocchi, N. *Eur. J. Inorg. Chem.* **1998**, 1503.

(52) Allen, F. H.; Davies, J. F.; Galloy, J. J.; Johnson, O.; Kennard, O.; Macrae, C. F.; Mitchell, E. M.; Mitchell, G. F.; Smith, J. M.; Watson, D. G. *J. Chem. Info. Comp. Sci.* **1991**, *31*, 187.

(53) Bradley, D. C.; Hursthouse, M. B.; Newton, J.; Walker, N. P. C. *J. Chem. Soc. Chem. Commun.* **1984**, 188.

Chapter Two

Chemistry of *N*-(2-mercaptoethyl)picolyamine and its Derivatives as Ligands for the "*fac*-[Re(CO)₃]⁺" Core

Introduction

Since the early 1960's, ^{99m}Tc has been recognized as a useful isotope for diagnostic nuclear medicine due to its nearly ideal physical characteristics ($E_\gamma = 141$ KeV; $t_{1/2} = 6$ h). The strong, clean gamma ray is easily detectable with gamma cameras available in hospitals, and the short half-life of ^{99m}Tc minimizes the radiation dose incurred by the patient. Consequently, greater than 85% of all nuclear medicine scans performed today use ^{99m}Tc as the radiotracer. However, since their inception, ^{99m}Tc

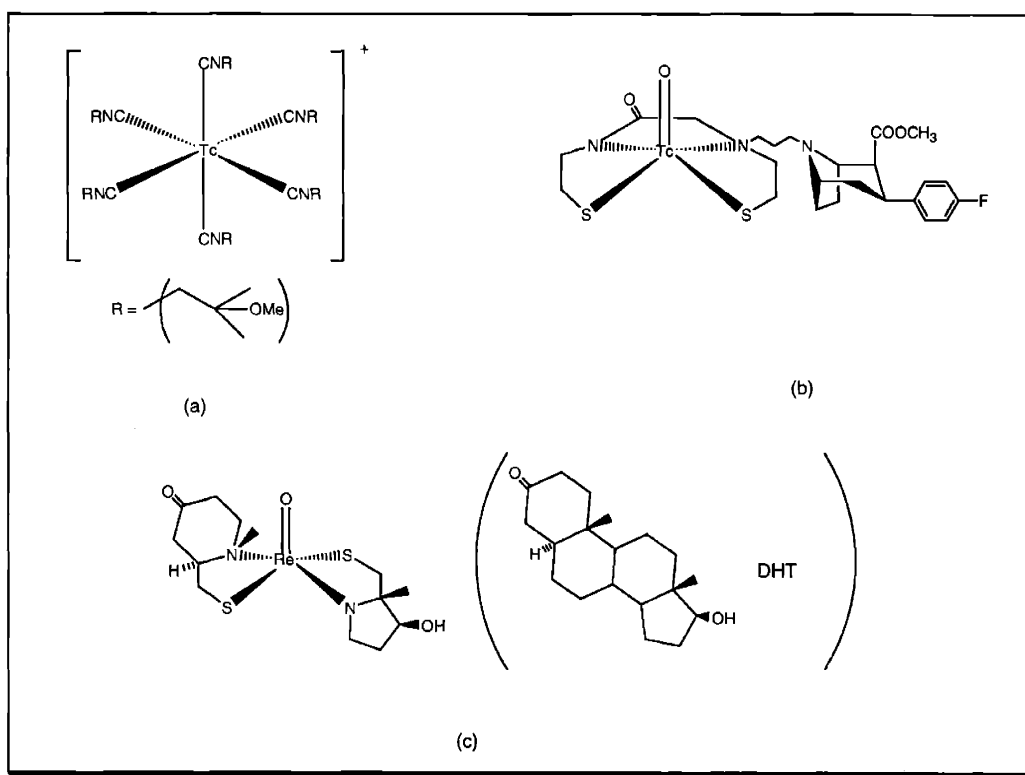


Figure 2.1. Three philosophies of design of ^{99m}Tc radiopharmaceuticals: (a) Tc-essential, (b) conjugate design, and (c) integrated design.

radiopharmaceuticals have gone through several distinct changes in philosophy of design, including (1) the Tc-essential imaging agents, which localize based on their size and charge (Figure 2.1a; Cardiolite[®]),¹ (2) agents of the conjugate design, which localize based on their pendant functionalities (Figure 2.1b, *vide infra*),² and (3) agents of the integrated design, which attempt to mimic the characteristics of a biomolecule (Figure 2.1c; dihydrotestosterone (DHT) is mimicked biomolecule).³⁻⁶

Approximately fifteen years ago, the approach used in our group, the conjugate design, was developed. This approach uses a rational drug design model whereby a ^{99m}Tc chelate is linked, *via* a covalent tether, to a biologically active molecule known to localize in a particular location in the body (Figure 2.2). Technepine, for instance, which contains a pendant phenyltropane analogue known to localize in the dopamine transporter in the brain (Figure 2.1b), penetrates the blood-brain barrier and was studied with potential relevance to Parkinson's Disease diagnosis.²

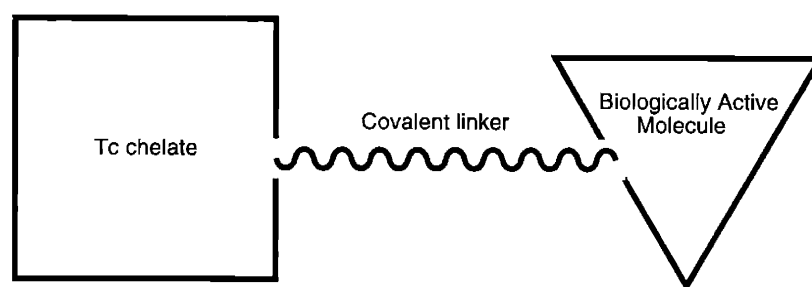


Figure 2.2. Schematic of conjugate design.

The conjugate approach can accommodate two ways of incorporating the ^{99m}Tc metal center: the pre-labeling approach and the post-labeling (preformed chelate)

approach (Figure 2.3). In the pre-labeling approach, a ^{99m}Tc complex is synthesized prior to bioconjugation, and in the post-labeling approach, the chelate is synthesized in its entirety prior to labeling with ^{99m}Tc . The latter method is more desirable as it reduces the number of steps that must take place at the tracer level (from two to one). It also limits the amount of time ^{99m}Tc is involved in the process, reducing the amount of radioactive material lost (due to the short half-life).

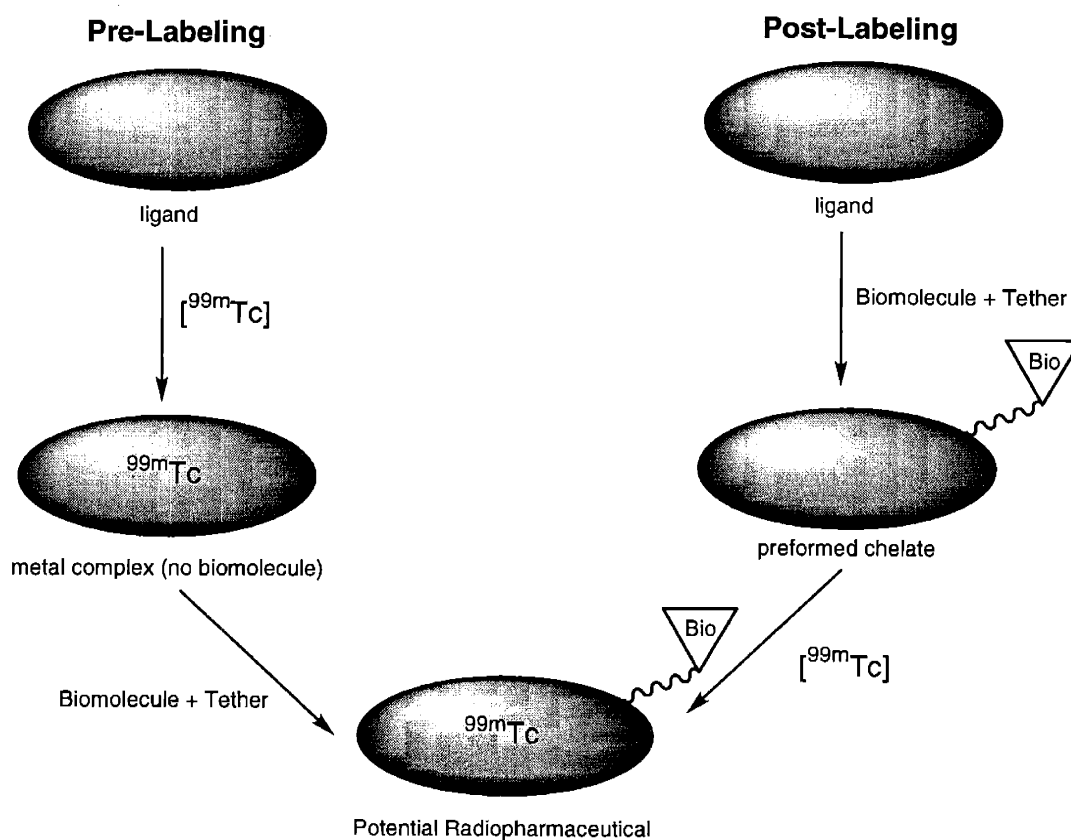
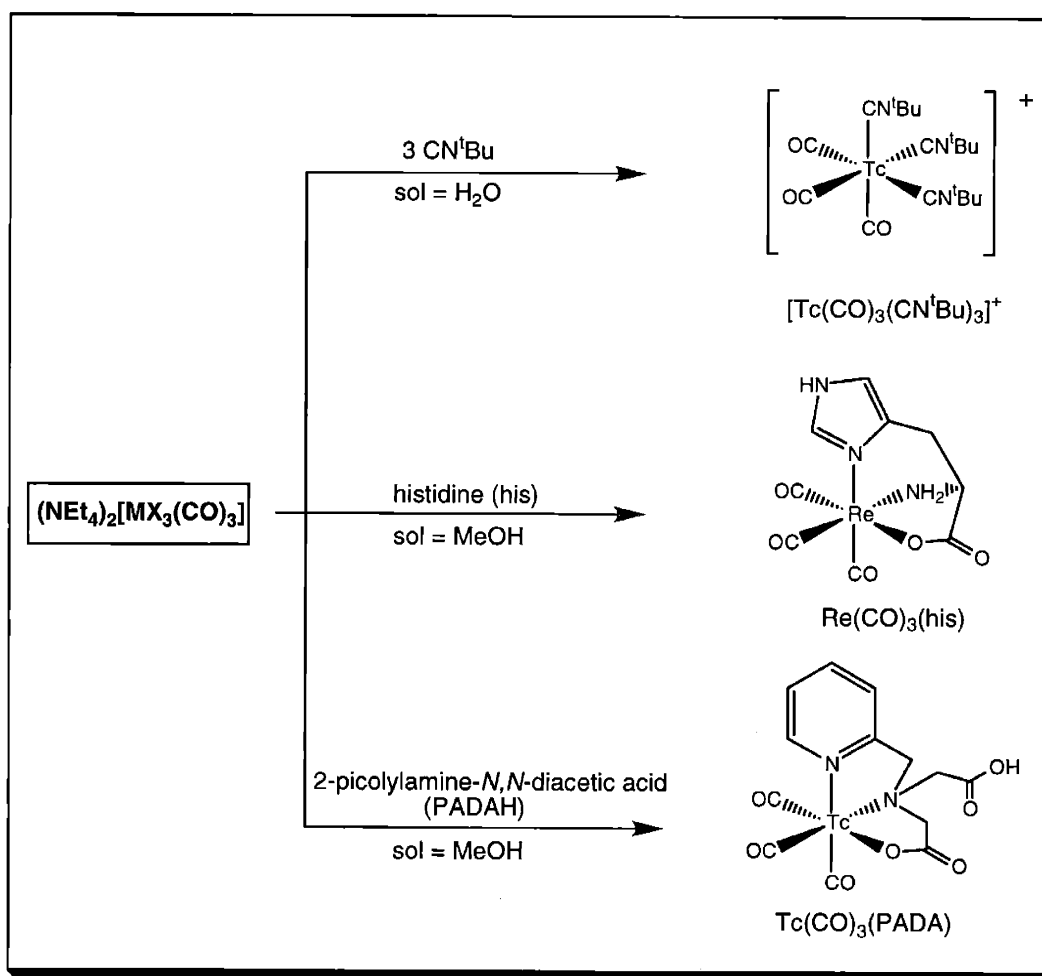


Figure 2.3. The two principal labeling approaches for ^{99m}Tc radiopharmaceuticals.

Over the last twenty years, much of the research focus in the area of ^{99m}Tc radiopharmaceutical development has been directed towards development of the

chemistry of the "[TcO]³⁺" core.⁷ As discussed in Chapter 1, Alberto has made accessible a new core, the "*fac*-[Tc(CO)₃]⁺" moiety, which is available as the reactive, but air-stable, *fac*-[TcCl₃(CO)₃]²⁻.⁸⁻¹⁵ Analogous rhenium complexes have been synthesized¹⁶ and are used widely as non-radioactive mimics of the corresponding technetium complexes (Scheme 2.1). The similarity in chemistry of technetium and rhenium complexes is well-documented, provided that redox chemistry is not a concern.¹⁷⁻²¹



Scheme 2.1. The reaction of $[\text{MX}_3(\text{CO})_3]^{2-}$ ($\text{M} = \text{Tc}$, $\text{X} = \text{Cl}$; $\text{M} = \text{Re}$, $\text{X} = \text{Br}$) with a variety of ligands in the presence of coordinating solvents.

Although technetium is more kinetically labile than Re, this difference is negligible in the case of the tricarbonyl chemistry, since both metals have a low-spin d^6 configuration.²² The reactivity of technetium and rhenium tris(solvento)tricarbonyl cations has enabled the development of a very rich chemistry and the potential application to radiodiagnostic (^{99m}Tc) and radiotherapeutic ($^{186/188}\text{Re}$; β^- emitters) medicine.^{9-12,18,23-27} Additionally, the starting material $(\text{NEt}_4)_2[\text{ReBr}_3(\text{CO})_3]$ has been suggested recently as a potentially selective chemotherapeutic agent and has shown significant activity against breast carcinoma.²⁸

Given that $[\text{M}(\text{CO})_3(\text{sol})_3]^+$ ($\text{M} = \text{Tc}, \text{Re}$) is a cation with three available coordination sites, it became desirable to develop a monoanionic tridentate ligand system. This would allow for maximum stability due to the chelate effect along with neutrality of the overall complex. A ligand which has been used in the study of zinc enzyme active sites, *N*-(2-mercaptoethyl)picolyamine²⁹ (MEPAH; Figure 2.4), was chosen as a good fit for these requirements. Studies conducted aimed at ascertaining what types of ligands are considered to have a high affinity for the "*fac*- $[\text{M}(\text{CO})_3]^+$ " core have shown that those

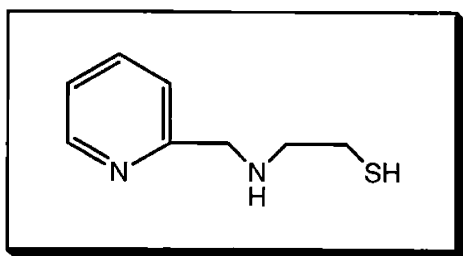


Figure 2.4. *N*-(2-mercaptoethyl)picolyamine (MEPAH).

possessing an amine-containing aromatic heterocycle tend to show the fastest coordination.^{23,24} Additionally, mononuclear thiolate complexes of this core had not yet been studied in great detail, and the one proton-bearing nitrogen appeared to be well-suited for potential derivatization. In this chapter, the chemistry of the ligand with respect to the "*fac*-[Re(CO)₃]" core is presented as a precursor to work involving ^{99m}Tc and potential radiopharmaceutical synthesis.

Experimental

General Considerations. All manipulations were carried out in air unless otherwise noted. All solvents and reagents were obtained commercially and used as received unless otherwise noted. $(\text{NEt}_4)_2[\text{ReBr}_3(\text{CO})_3]^{16}$ and MEPAH^{29} were prepared as described in the literature. Elemental analyses were performed by Atlantic Microlab, Inc., Norcross, GA. Normal phase preparative scale silica TLC plates were purchased from Analtech (20 cm x 20 cm x 1000 μ), and C_{18} reversed-phase silica TLC plates were purchased from Whatman (20 cm x 20 cm x 1000 μ).

Physical Measurements. Proton NMR spectra were recorded on a Varian Unity-300 (300 MHz), a Varian Mercury-300 (300 MHz), or a Varian Unity-Inova 500 (500 MHz) spectrometer. Chemical shifts were referenced to residual protons in the specified deuterated solvent. Infrared spectra were obtained on a Perkin-Elmer 2000-FTIR or Perkin-Elmer 1600-FTIR spectrometer. The fast atom bombardment mass spectra (FABMS) were recorded in a 3-nitrobenzyl alcohol matrix with a MAT 731 mass spectrometer, and the electrospray ionization mass spectra (ESIMS) were recorded on a Bruker 3T FT-MS. Mass spectra were obtained by Ms. Li Li of the MIT DCIF. Multiple masses are reported for rhenium-containing fragments to indicate the significant isotopic abundances of both ^{185}Re and ^{187}Re . Each peak was observed to have the proper relative abundances.

Synthesis of (*N*-(2-Mercaptoethyl)picolylamino)tricarbonylrhenium(I), $\text{Re}(\text{CO})_3(\text{MEPA})$

To a solution of 75 mg (0.097 mmol) $(\text{NEt}_3)_2[\text{ReBr}_3(\text{CO})_3]$ in 2 mL acetonitrile was added 0.1 mL (~2 equivalents) of a 2:1 (v/v) solution of triethylamine-MEPAH. The resulting solution turned yellow within seconds and was stirred at room temperature for 45 minutes. At that time, 10 mL deionized water was added, and a fine yellow precipitate formed. This solution was filtered, and the precipitate was washed with deionized water and *n*-pentane (4 x 1 mL), and dried in air to give a yellow powder. Yield: 27 mg (63% based on Re). Pale yellow needles suitable for a single crystal X-ray diffraction study were grown by the slow evaporation of a saturated acetone-water solution. $^1\text{H NMR}$ (CD_2Cl_2): δ 1.27 (m, 1H, $\text{NCH}_2\text{CH}_2\text{S}$), 2.33 (m, 1H, $\text{NCH}_2\text{CH}_2\text{S}$), 2.85 (m, 1H, $\text{NCH}_2\text{CH}_2\text{S}$), 3.27 (m, 1H, $\text{NCH}_2\text{CH}_2\text{S}$), 4.33 (A of ABX, 1H, $J_{\text{AX}} = 0 \text{ Hz}$, $J_{\text{AB}} = 16.2 \text{ Hz}$, py- CH_2), 4.64 (B of ABX, 1H, $J_{\text{BX}} = 6.9 \text{ Hz}$, py- CH_2), 4.90 (br s, 1H, NH), 7.34 (m, 2H, py- H_β and py- H_δ), 7.82 (dt, 1H, py- H_γ), 8.74 (dd, 1H, py- H_α). IR (KBr): $\nu(\text{CH})$ 3072, 2919; $\nu(\text{CO})$ 2006, 1874 cm^{-1} . FAB(+)-MS: m/z 437/439 $[\text{M}+\text{H}]^+$, 436/438 M^+ , 408/410 $[\text{M}-\text{CO}]^+$. *Anal. Calc.* for $\text{C}_{11}\text{H}_{11}\text{N}_2\text{O}_3\text{ReS}$: C, 30.20; H, 2.53; N, 6.40; S, 7.33. Found: C, 29.97; H, 2.53; N, 6.39; S, 7.22%.

Synthesis of *N*-[2-[(Triphenylmethyl)thio]ethyl]picolylamine, MEPAH-STr

To a flask previously purged with Ar was added MEPAH (2.47 g, 14.7 mmol), Ph_3COH (3.85 g, 14.8 mmol), and CF_3COOH (16.5 mL, 222 mmol). Upon addition of trifluoroacetic acid (TFA), the solution became reddish-brown and the triphenylmethanol (TrOH) dissolved to form a homogeneous solution which was stirred at room temperature

for 90 minutes. The TFA was then removed *in vacuo* to yield a brownish, extremely viscous oil. Trituration with 100 mL diethyl ether gave complete color discharge and a white precipitate, which was filtered, washed with diethyl ether, and dried *in vacuo*. The white TFA salt of the trityl-protected thiol was partitioned between 1 M NaOH and diethyl ether. The ether layer was dried over MgSO₄ and evaporated *in vacuo* to give the TFA-free protected thiol as a white powder. Yield: 3.80 g (63%). ¹H NMR (CDCl₃): δ 1.66 (br s, 1H, NH), 2.41 (t, 2H, NCH₂CH₂S), 2.61 (t, 2H, NCH₂CH₂S), 3.78 (s, 2H, py-CH₂), 7.14-7.44 (m, 17H, Tr-H and py-H), 7.62 (dt, 1H, py-H_γ), 8.54 (d, 1H, py-H_α). IR (KBr): ν(NH) 3353; ν(CH) 3054, 3019, 2955, 2861 cm⁻¹. Anal. Calc. for C₂₇H₂₆N₂S: C, 78.99; H, 6.38; N, 6.82; S, 7.81. Found: C, 78.70; H, 6.37; N, 6.74; S, 7.74%

Synthesis of *N*-(Ethyl)-*N*-[2-[(triphenylmethyl)thio]ethyl]picolylamine, MEPAH-NEt-STr

To MEPAH-STr (299 mg, 0.728 mmol), dissolved in 20 mL acetonitrile, was added KHCO₃ (373 mg, 3.73 mmol) and bromoethane (398 mg, 0.27 mL, 3.65 mmol). The solution was refluxed for 7 h, while monitoring the reaction progress by TLC (1:1 EtOAc/hexanes). The reaction was cooled to room temperature and stirred overnight. Acetonitrile was then removed *in vacuo*, and the resulting dark orange oil was chromatographed on silica with 1:1 EtOAc/hexanes as eluent to yield an off-white oil (hygroscopic). Yield: 194 mg (61%). ¹H NMR (CD₂Cl₂, 500 MHz): δ 0.98 (t, 3H, -CH₂CH₃), 2.37 (t, 2H, NCH₂CH₂S), 2.46 (q, 2H, -CH₂CH₃), 2.56 (t, 2H, NCH₂CH₂S), 3.64 (s, 2H, py-CH₂), 7.14-7.50 (m, 17H, py-H and Tr-H), 7.65 (dt, 1H, py-H_γ), 8.51 (dd, 1H, py-H_α). HRESI(+)-MS: *m/z* Calc. for [M+H]⁺: 439.2202. Found: 439.2197. Anal.

Calc. for $C_{29}H_{30}N_2S \cdot 0.5H_2O$: C, 77.81; H, 6.98; N, 6.26; S, 7.16. Found: C, 77.67; H, 6.74; N, 6.18; S, 7.12%.

Synthesis of *N*-(Ethyl)-*N*-(2-mercaptoethyl)picolyamine, MEPAH-NEt

To a vial containing 80 mg (0.18 mmol) MEPAH-NEt-STr was added 5 mL TFA. Triethylsilane was added dropwise to the resulting orange solution until color discharge was observed. A white precipitate (triphenylmethane) formed. The TFA solution was washed with 3 x 5 mL hexanes to remove the triphenylmethane. A drop of water was added to aid in separation of the layers. The resulting solution was concentrated to a pale yellow oil. This was used immediately in the next step with no further purification.

Synthesis of (*N*-(Ethyl)-*N*-(2-mercaptoethyl)picolyamino)tricarbonylrhenium(I), $Re(CO)_3(MEPA-NEt)$

To a solution of 77 mg (0.10 mmol) $(NEt_4)_2[ReBr_3(CO)_3]$ in 1 mL acetonitrile was added a solution of 0.25 mL NEt_3 and the deprotected ligand, MEPAH-NEt. The resulting solution turned yellow within seconds and was stirred at room temperature for 45 minutes. At that time, 10 mL deionized water was added, and a fine yellow precipitate formed. This solution was filtered, and the precipitate was washed with deionized water (3 x 1 mL), hexanes (4 x 2 mL), and *n*-pentane (3 x 2 mL), and dried in air to give a yellow powder. Yield: 30 mg (68% based on Re). 1H NMR ($(CD_3)_2CO$): δ 1.39 (t, 3H, $-CH_2CH_3$), 1.59 (m, 1H, NCH_2CH_2S), 2.42 (m, 1H, NCH_2CH_2S), 2.71 (m, 1H, NCH_2CH_2S), 3.18 (m, 1H, NCH_2CH_2S), 3.55 - 3.90 (m, 2H, NCH_2CH_3), 4.66 (AB pattern, $J_{AB} = 16.2$ Hz, 2H, $py-CH_2$), 7.51 (t, 1H, $py-H_\beta$), 7.60 (d, 1H, $py-H_\delta$), 8.02 (dt,

1H, py- H_γ), 8.69 (dd, 1H, py- H_α). IR (KBr): $\nu(\text{CO})$ 2001, 1888, 1860 cm^{-1} . HRESI(+)-MS: m/z Calc. for $[\text{M}+\text{H}]^+$: 467.0434, Found: 467.0430. Anal. Calc. for $\text{C}_{13}\text{H}_{15}\text{N}_2\text{O}_3\text{ReS}$: C, 33.54; H, 3.25; N, 6.02; S, 6.89. Found: C, 33.71; H, 3.35; N, 6.06; S, 6.68%.

Synthesis of *N*-(3'-Propionic acid)-*N*-[2-[(triphenylmethyl)thio]ethyl]picolyamine, MEPAH- $\text{C}_2\text{CO}_2\text{H}$ -STr

To MEPAH-STr (158 mg, 0.385 mmol), dissolved in 11 mL acetonitrile, was added KHCO_3 (192 mg, 1.92 mmol) and 3-bromopropionic acid (293 mg, 1.92 mmol). The solution was refluxed for 2.5 h, while monitoring the reaction progress by TLC (10% MeOH in EtOAc). The acetonitrile was removed *in vacuo*, and 20 mL dichloromethane was added. This yellow solution was stirred for 10 minutes. The KHCO_3 and any resulting salts were removed by filtration. The dichloromethane was removed *in vacuo*. Approximately 1 mL methanol was added to the resulting oil, and the solution was stirred overnight at room temperature during which time a white precipitate formed. This precipitate was removed by filtration, washed with a few drops of methanol, and dried *in vacuo* to give a white powder. Yield: 115 mg (62%). An analytically pure sample was obtained by allowing a saturated 10% MeOH in EtOAc solution of the compound to slowly evaporate and mechanically removing the crystals. These crystals were suitable for an X-ray diffraction study. ^1H NMR (CD_2Cl_2): δ 2.32 (t, 2H, $\text{NCH}_2\text{CH}_2\text{COOH}$), 2.41 (m, 4H, $\text{NCH}_2\text{CH}_2\text{S}$ and $\text{NCH}_2\text{CH}_2\text{COOH}$), 2.65 (t, 2H, $\text{NCH}_2\text{CH}_2\text{S}$), 3.64 (s, 2H, py- CH_2), 7.1-7.4 (m, 17H, Tr- H and py- H), 7.66 (dt, 1H, py- H_γ), 8.54 (d, 1H, py- H_α). IR (KBr): $\nu(\text{CH})$ 3060, 2966, 2796; $\nu(\text{CO})$ 1705 cm^{-1} . FAB(+)-MS: m/z 483 $[\text{M}+\text{H}]^+$, 243

$[\text{Ph}_3\text{C}]^+$. *Anal.* Calc. for $\text{C}_{30}\text{H}_{30}\text{N}_2\text{O}_2\text{S}$: C, 74.66; H, 6.26; N, 5.80. Found: C, 74.34; H, 6.34; N, 5.82%.

**S y n t h e s i s o f *N*-(3'-Propionyl-*N*-hydroxysuccinimidato)-*N*-[2-
[(triphenylmethyl)thio]ethyl]picolylamine**

In a dry 50 mL Schlenk flask was charged 161 mg (0.780 mmol) 1,3-dicyclohexylcarbodiimide, 189 mg (0.392 mmol) *N*-(3'-propionic acid)-*N*-[2-[(triphenylmethyl)thio]ethyl]picolylamine, and 72 mg (0.626 mmol) *N*-hydroxysuccinimide. Under argon, 20 mL anhydrous THF was transferred *via* cannula to the flask, and the reactants dissolved. The reaction was stirred at room temperature. Within 48 hours, a white precipitate had formed, and the reaction was complete (TLC). After filtration, the filtrate was concentrated *in vacuo* and chromatographed on silica (EtOAc eluent). The appropriate fractions were combined and concentrated *in vacuo* to give a white foam (hygroscopic). Yield: 139 mg (61%). ^1H NMR (CD_2Cl_2): δ 2.33 (t, 2H), 2.43 (t, 2H), 2.61 (t, 2H), 2.74 - 2.85 (m, 6H), 3.61 (s, 2H, py- CH_2), 7.1 - 7.4 (m, 17H, py-*H* and Tr-*H*), 7.63 (dt, 1H, py- H_α), 8.45 (d, 1H, py- H_α). IR (KBr): $\nu(\text{CO})$ 1739, 1735, 1653, 1636. ESI(+)*MS*: m/z 580 $[\text{M}+\text{H}]^+$, 243 $[\text{Ph}_3\text{C}]^+$. HRESI(+)*MS*: m/z Calc. for $[\text{M}+\text{H}]^+$: 580.2265. Found: 580.2263. *Anal.* Calc. for $\text{C}_{34}\text{H}_{33}\text{N}_3\text{O}_3\text{S}\cdot 1.5 \text{H}_2\text{O}$: C, 67.31; H, 5.98; N, 6.93; S, 5.28. Found: C, 67.27; H, 5.88; N, 7.26; S, 4.84%.

Synthesis of *N*-(3'-Propionylisopropylamido)-*N*-[2-[(triphenylmethyl)thio]ethyl]picolyamine

Under argon, 69 mg (0.12 mmol) *N*-(3'-propionyl-*N*-hydroxysuccinimidato)-*N*-[2-[(triphenylmethyl)thio]ethyl]picolyamine were dissolved in 10 mL anhydrous THF. To this solution was added 71 mg (0.10 mL, 1.2 mmol) isopropylamine. Within thirty seconds, a white precipitate formed. The reaction completed within 70 minutes (TLC), and the white precipitate was removed by filtration. The solvent was removed *in vacuo*, and the residue redissolved in dichloromethane. This solution was shaken with 3 x 10 mL water to remove NHS-containing byproducts. The organic layer was dried over MgSO₄ and concentrated *in vacuo* to give an off-white residue. Yield: 54 mg (87%). ¹H NMR (CD₂Cl₂): δ 1.02 (d, 6H, -CH-(CH₃)₂), 2.18 (t, 2H), 2.35 (m, 2H), 2.43 (t, 2H), 2.57 (t, 2H), 3.56 (s, 2H, py-CH₂), 3.89 (m, 1H, CH-(CH₃)₂), 7.18 - 7.40 (m, 17H, py-*H* and Tr-*H*), 7.63 (dt, 1H, py-H_γ), 8.49 (dd, 1H, py-H_α). ESI(+)-MS: *m/z* 524 [M+H]⁺, 243 [Ph₃C]⁺.

Synthesis of *N*-(3'-Propionylmorpholinamido)-*N*-[2-[(triphenylmethyl)thio]ethyl]picolyamine, MEPAH-C₂COMorph-STr

In a 50 mL round bottomed flask were placed 150 mg (1.8 mmol) NaHCO₃, 150 μL (150 mg, 1.7 mmol) morpholine, and 25 mL of a 1:1 MeCN-H₂O solution. Then, 98 mg (0.17 mmol) *N*-(3'-propionyl-*N*-hydroxysuccinimidato)-*N*-[2-[(triphenylmethyl)thio]ethyl]picolyamine, dissolved in ~4 mL MeCN was added to the reaction solution. The colorless, homogeneous solution was stirred for 1 h and monitored by TLC (appears complete within 20 minutes). The MeCN (and a little H₂O) was removed *in vacuo*, and a cloudy solution with an amorphous precipitate resulted. Water

(5 mL) was added, and the water-insoluble product was extracted into 5 x 15 mL CH₂Cl₂. The organic fractions were combined and washed with 6 x 50 mL H₂O. The organic layer was dried over MgSO₄ and concentrated *in vacuo* to give an off-white residue (hygroscopic). Crude yield: 73 mg (78%). An analytically pure sample was obtained by chromatographing the crude material on a 20 cm x 20 cm x 1000 μ silica plate with 10% MeOH in EtOAc as eluent. The proper fraction was scraped from the plate, washed off the silica with MeOH and concentrated *in vacuo*. Yield: 50 mg (53% overall). ¹H NMR (CD₂Cl₂, 500 MHz): δ 2.31 (t, 2H), 2.35 (t, 2H), 2.49 (t, 2H), 2.66 (m, 2H), 3.31 (t, 2H, morph-*H*), 3.49 (t, 2H, morph-*H*), 3.53 (t, 2H, morph-*H*), 3.57 (m, 4H, py-CH₂ and morph-*H*), 7.15 - 7.40 (m, 17H, py-*H* and Tr-*H*), 7.63 (dt, 1H, py-H_γ), 8.45 (dd, 1H, py-H_α). ESI(+)-MS: *m/z* 552 [M+H]⁺, 243 [Ph₃C]⁺. *Anal.* Calc. for C₃₄H₃₇N₃O₂S·1.5 H₂O: C, 70.56; H, 6.97; N, 7.26; S, 5.54. Found: C, 70.34; H, 6.51; N, 7.12; S, 5.39%.

Synthesis of *N*-(3'-Propionylmorpholinamido)-*N*-(2-mercaptoethyl)picolyamine, MEPAH-C₂COmorph

To a vial containing 23 mg (0.042 mmol) *N*-(3'-propionylmorpholinamido)-*N*-[2-[(triphenylmethyl)thio]ethyl]picolyamine was added 5 mL TFA. Triethylsilane was added dropwise to the resulting yellow solution until color discharge was observed. A white precipitate (triphenylmethane) formed. The TFA solution was washed with 3 x 5 mL hexanes to remove the triphenylmethane. A drop of water was added to aid in separation of the layers. The resulting solution was concentrated to a pale yellow oil. This was used immediately in the next step with no further purification.

Synthesis of (*N*-(3'-Propionylmorpholinamido)-*N*-(2-mercaptoethyl)picolylamino)-tricarboxylrhenium(I), $\text{Re}(\text{CO})_3(\text{MEPA-C}_2\text{COMorph})$

To a solution of 30 mg (0.039 mmol) $(\text{NEt}_3)_2[\text{ReBr}_3(\text{CO})_3]$ in 1 mL acetonitrile was added a solution of 0.25 mL NEt_3 and the deprotected ligand, MEPAH-C₂COMorph. The resulting solution turned yellow within seconds and was stirred at room temperature for 45 minutes. The MeCN and NEt_3 were then removed *in vacuo*. The resulting residue was triturated with 2 mL deionized water to give a yellow powder. The solution was filtered, and the solid was washed with deionized water (1 mL) and *n*-hexanes (3 x 2 mL). The powder was dried in air for a short while. The precipitate was dissolved in MeCN and chromatographed on a C₁₈ reversed-phase silica plate with 2:1 MeOH:H₂O as the eluent. A yellow band coincident with a UV active band was scraped off of the plate. The material was washed off of the silica with MeOH, and the solution was concentrated to dryness *in vacuo* to give a solid, yellow residue. Yield: 7 mg (30%). ¹H NMR (CD_3COCD_3 , 500 MHz): δ 1.59 (m, 1H, $\text{NCH}_2\text{CH}_2\text{S}$), 2.42 (m, 1H, $\text{NCH}_2\text{CH}_2\text{S}$), 2.76 (m, 1H, $\text{NCH}_2\text{CH}_2\text{S}$), 3.06 (dt, 2H, $-\text{NCH}_2\text{CH}_2\text{CO}-$), 3.22 (m, 1H, $\text{NCH}_2\text{CH}_2\text{S}$), 3.53 (t, 2H, morph-*H*), 3.60 (m, 4H, morph-*H*), 3.65 (t, 2H, morph-*H*), 3.81 - 4.16 (m, 2H, $-\text{NCH}_2\text{CH}_2\text{CO}-$), 4.63 (AB pattern, $J_{\text{AB}} = 16.0$ Hz, 2H, py- CH_2), 7.52 (t, 1H, py- H_β), 7.57 (d, 1H, py- H_δ), 8.02 (dt, 1H, py- H_γ), 8.70 (dd, 1H, py- H_α). HRESI(+)MS: m/z Calc. for $[\text{M}+\text{H}]^+$: 580.0910. Found: 580.0912.

Synthesis of N-(3'-Propionylnornicotinamido)-N-[2-[(triphenylmethyl)thio]ethyl]picolyamine, MEPAH-C₂CONornic-STR

In a 50 mL round bottomed flask were placed 62 mg (0.67 mmol) NaHCO₃, 100 mg (0.68 mmol) nornicotine, and 15 mL of MeCN. Water (~7 mL) was added to dissolve NaHCO₃. Then, 96 mg (0.17 mmol) N-(3'-propionyl-N-hydroxysuccinimidato)-N-[2-[(triphenylmethyl)thio]ethyl]picolyamine, dissolved in ~4 mL MeCN was added to the reaction solution. The colorless, homogeneous solution was stirred for 1 h and monitored by TLC (appears complete within 20 minutes). The MeCN (and a little H₂O) was removed *in vacuo*, and a cloudy solution with an amorphous precipitate resulted. Water (5 mL) was added, and the water-insoluble product was extracted into 6 x 10 mL CH₂Cl₂. The organic fractions were combined and washed with 4 x 50 mL H₂O. The organic layer was dried over MgSO₄ and concentrated *in vacuo* to give an off-white residue. Crude yield: 73 mg (72%). This residue was chromatographed on a 20 cm x 20 cm x 1000 μ silica plate with 10% MeOH in EtOAc as eluent. The proper fraction was scraped from the plate, washed off the silica with MeOH and concentrated *in vacuo*. Yield: 34 mg (33% overall). ¹H NMR (CD₂Cl₂, 500 MHz): δ 1.85 (m, 2H), 1.92 (m, 2H), 2.23 (m, 2H), 2.33 (m, 2H), 2.43 (m, 2H), 2.51 (m, 2H), 2.72 (m, 2H), 3.61 (s, 2H, py-CH₂), 4.97 (m, 0.5H, -NCH-(py)CH₂(pyrrolidine)), 5.09 (m, 0.5H, -NCH-(py)CH₂(pyrrolidine)) 7.11 - 7.44 (m, 18H, py-H and Tr-H), 7.59 (m, 2H, py-H), 8.41 (m, 2H, py-H), 8.46 (m, 1H, py-H). ESI(+)-MS: *m/z* 613 [M+H]⁺, 371 [M-Tr+2H]⁺, 243 [Ph₃C]⁺. HRESI(+)-MS: *m/z* Calc. for [M+H]⁺: 613.2996. Found: 613.2998.

Synthesis of *N*-(3'-Propionylornicotinamido)-*N*-(2-mercaptoethyl)picolyamine, MEPAH-C₂CONornic

To a vial containing 30 mg (0.049 mmol) *N*-(3'-propionylornicotinamido)-*N*-[2-[(triphenylmethyl)thio]ethyl]picolyamine was added 5 mL TFA. Triethylsilane was added dropwise to the resulting orange solution until color discharge was observed. A white precipitate (triphenylmethane) formed. The TFA solution was washed with 3 x 5 mL hexanes to remove the triphenylmethane. A drop of water was added to aid in separation of the layers. The resulting solution was concentrated to a pale yellow oil. This was used immediately in the next step with no further purification.

Synthesis of (*N*-(3'-Propionylornicotinamido)-*N*-(2-mercaptoethyl)picolyamino)-tricarbonylrhenium(I), Re(CO)₃(MEPA-C₂CONornic)

To a solution of 34 mg (0.044 mmol) (NEt₃)₂[ReBr₃(CO)₃] in 0.5 mL acetonitrile was added 0.25 mL NEt₃. The deprotected ligand, MEPAH-C₂CONornic, in MeCN solution was added. The resulting solution turned yellow within seconds and was stirred at room temperature for 1 hour. The MeCN and NEt₃ were then removed *in vacuo*. The resulting residue was triturated with 2 mL water to give a yellow powder. The solution was filtered, and the solid was washed with deionized water (2 x 1 mL) and *n*-hexanes (3 x 2 mL). The powder was dried in air for a short while. The precipitate was dissolved in MeCN and chromatographed on two C₁₈ reversed-phase silica plates with 2:1 MeOH:H₂O as the eluent. The material was washed off of the silica with MeOH (~60 mL), and the solution was concentrated to dryness *in vacuo* to give a solid yellow residue. Yield: 6 mg (20%). HRESI(+)-MS: *m/z* Calc. for [M+H]⁺: 641.1228. Found: 641.1210.

Synthesis of *N*-(3'-Chloropropyl)-*N*-[2-[(triphenylmethyl)thio]ethyl]picolyamine, MEPAH-C₃Cl-STr

To MEPAH-STr (0.500 g, 1.22 mmol), dissolved in 10 mL argon-purged CH₂Cl₂, was added KHCO₃ (0.611 g, 6.10 mmol) and 1-bromo-3-chloropropane (0.60 mL, 6.1 mmol). The solution was stirred and refluxed for 72 h, while monitoring the reaction progress by TLC (1:1 EtOAc/hexanes). The KHCO₃ was removed by filtration. The resulting brown solution was then chromatographed on silica (1:1 EtOAc/hexanes eluent), and the appropriate fractions were combined and concentrated to give a slightly yellow oil. Yield: 280 mg (47%). ¹H NMR (CDCl₃): δ 1.78 (p, 2H, NCH₂CH₂CH₂Cl), 2.35 (t, 2H, NCH₂CH₂S), 2.47 (m, 4H, NCH₂CH₂CH₂Cl and NCH₂CH₂S), 3.51 (t, 2H, NCH₂CH₂CH₂Cl), 3.60 (s, 2H, py-CH₂), 7.1-7.4 (m, 17H, Tr-*H* and py-*H*), 7.64 (dt, 1H, py-*H*_γ), 8.50 (d, 1H, py-*H*_α). FAB(+)-MS: *m/z* 487 [M+H]⁺, 451 [M-Cl]⁺, 243 [Ph₃C]⁺. *Anal.* Calc. for C₃₀H₃₁ClN₂S: C, 73.97; H, 6.41; N, 5.75. Found: C, 73.98; H, 6.37; N, 5.65%.

Synthesis of *N*-(3'-Morpholinopropyl)-*N*-[2-[(triphenylmethyl)thio]ethyl]picolyamine, MEPAH-C₃morph-STr

In a 100 mL three-necked round bottomed flask equipped with a condenser and a pressure-equalizing addition funnel was charged with 190 μL (2.18 mmol) morpholine, 173 mg (1.04 mmol) KI, 206 mg (2.06 mmol) KHCO₃, and 15 mL MeCN. In the addition funnel was placed 93 mg (0.19 mmol) *N*-(3'-chloropropyl)-*N*-[2-[(triphenylmethyl)thio]ethyl]picolyamine in 45 mL MeCN. The reaction pot was

brought to reflux, and the solution in the funnel was slowly dropped into the refluxing solution with vigorous stirring. After the addition, the solution was refluxed overnight. The yellow-orange solution was cooled, and the MeCN was removed in vacuo. Water (20 mL) and CH₂Cl₂ (20 mL) were added. The CH₂Cl₂ layer was removed, and another 30 mL CH₂Cl₂ was added. The organic layer was washed with 4 x 50 mL H₂O. The CH₂Cl₂ layer was dried over MgSO₄, and the CH₂Cl₂ was removed *in vacuo* after filtration. The residue was chromatographed on two silica 20 cm x 20 cm TLC plates in 10% MeOH in EtOAc. The proper fractions was scraped off of the plate, washed off the silica with MeOH, and the MeOH was removed *in vacuo* to give a yellow residue. Yield: 16 mg (16%). ¹H NMR (CD₂Cl₂, 500 MHz): δ 1.49 (p, 2H, NCH₂CH₂CH₂N-), 2.22 (t, 2H), 2.30 (m, 8H) 2.46 (m, 2H), 3.55 (s, 2H, py-CH₂), 3.58 (t, 4H, morph-H), 7.11-7.40 (m, 17H, Tr-H and py-H), 7.62 (dt, 1H, py-H_γ), 8.44 (d, 1H, py-H_α). ESI(+)-MS: *m/z* 538 [M+H]⁺, 296 [M-Tr+2H]⁺, 243 [Ph₃C]⁺.

Synthesis of *N*-(3'-Morpholinopropyl)-*N*-(2-mercaptoethyl)picolyamine, MEPAH-C₃morph

To a vial containing 12 mg (0.022 mmol) *N*-(3'-morpholinopropyl)-*N*-[2-[(triphenylmethyl)thio]ethyl]picolyamine was added 5 mL TFA. Triethylsilane was added dropwise to the resulting orange solution until color discharge was observed. A white precipitate (triphenylmethane) formed. The TFA solution was washed with 3 x 5 mL hexanes to remove the triphenylmethane. A drop of water was added to aid in separation of the layers. The resulting solution was concentrated to a pale yellow oil. This was used immediately in the next step with no further purification.

Synthesis of (*N*-(3'-Morpholinopropyl)-*N*-(2-mercaptoethyl)picolylamino)-tricarbonylrhenium(I), $\text{Re}(\text{CO})_3(\text{MEPA-C}_3\text{morph})$

To a solution of 15 mg (0.019 mmol) $(\text{NEt}_4)_2[\text{ReBr}_3(\text{CO})_3]$ in 1 mL acetonitrile was added 0.25 mL NEt_3 . The deprotected ligand, MEPAH-C₃morph in MeCN solution was added. When combined, the resulting solution turned yellow in seconds and was stirred at room temperature for 45 minutes. The MeCN and NEt_3 were then removed *in vacuo*. The resulting residue was dissolved in MeCN and chromatographed on a C₁₈ reversed-phase silica plate with 2:1 MeOH:H₂O as the eluent. A yellow band coincident with a UV-active band was scraped off of the plate. The material was washed off of the silica with MeOH, and the solution was concentrated to dryness *in vacuo* to give a solid, yellow residue. Yield: 1.7 mg (14%; slightly impure). ¹H NMR (CD_3COCD_3 , 500 MHz): δ 1.59 (m, 1H, $\text{NCH}_2\text{CH}_2\text{S}$), 2.10 (p, 2H, $-\text{NCH}_2\text{CH}_2\text{CH}_2\text{N}-$), 2.39 (m, 1H, $\text{NCH}_2\text{CH}_2\text{S}$), 2.44 (m, 6H, 4 morph-*H* and $-\text{NCH}_2\text{CH}_2\text{CH}_2\text{N}(\text{morph})$), 2.73 (m, 1H, $\text{NCH}_2\text{CH}_2\text{S}$), 3.22 (m, 1H, $\text{NCH}_2\text{CH}_2\text{S}$), 3.57 - 3.63 (m, 5H, 4 morph-*H* and $-\text{NCH}_2\text{CH}_2\text{CH}_2\text{N}(\text{morph})$), 3.84 (m, 1H, $-\text{NCH}_2\text{CH}_2\text{CH}_2\text{N}(\text{morph})$), 4.72 (AB pattern, $J_{\text{AB}} = 16.0$ Hz, 2H, py- CH_2), 7.52 (t, 1H, py- H_β), 7.59 (d, 1H, py- H_δ), 8.02 (dt, 1H, py- H_γ), 8.70 (dd, 1H, py- H_α). HRESI(+)-MS: m/z Calc. for $[\text{M}+\text{H}]^+$: 566.1118. Found: 566.1119.

X-ray Crystallography. Crystals of $\text{Re}(\text{CO})_3(\text{MEPA})$, $\text{Re}(\text{CO})_3(\text{MEPA-NEt})$, MEPAH-C₂CO₂H-STr, and $\text{Re}(\text{CO})_3(\text{MEPA-C}_2\text{COmorph})\cdot 2\text{H}_2\text{O}$ were transferred onto a microscope slide from a scintillation vial and coated with STP[®]. A crystal was selected,

mounted on a glass fiber, and optically centered. The data were collected on a Siemens platform goniometer with a CCD detector. The structures were solved by direct methods in conjunction with standard difference Fourier techniques (SHELXTL v5.1, Sheldrick, G. M. and Siemens Industrial Automation, 1997). Non-hydrogen atoms were treated anisotropically, and hydrogen atoms were placed in calculated positions ($d_{C-H} = 0.96 \text{ \AA}$), except for those of the solvated water molecules in $\text{Re}(\text{CO})_3(\text{MEPA-C2COmorph}) \cdot 2\text{H}_2\text{O}$, which were located in the difference map. A semi-empirical absorption correction from ψ scans was applied for $\text{Re}(\text{CO})_3(\text{MEPA})$, and a face-indexed absorption correction was applied for $\text{Re}(\text{CO})_3(\text{MEPA-NEt})$. The crystal of $\text{Re}(\text{CO})_3(\text{MEPA-NEt})$ was bounded by $(0,1,0)$, $(0,\bar{1},0)$, $(1,0,0)$, $(\bar{1},0,0)$, $(0,1,\bar{2})$, and $(0,\bar{1},2)$. Refinement was carried out by full-matrix least-squares on F^2 . Crystal data and structure refinement data are given in Tables 2.1 - 2.4.

Table 2.1. Crystal data and structure refinement for $\text{Re}(\text{CO})_3(\text{MEPA})$.

Empirical formula	$\text{C}_{11}\text{H}_{11}\text{N}_2\text{O}_3\text{ReS}$
Formula weight	437.48
Temperature (K)	183(2) K
Wavelength (\AA)	0.71073 \AA
Crystal system	Monoclinic
Space group	P2(1)/c
a (\AA)	20.901(17)
b (\AA)	9.101(7)
c (\AA)	14.706(12)
β ($^\circ$)	103.031(13)
Volume (\AA^3)	2725(4)
Z	8
ρ_{calc} (Mg m^{-3})	2.132
μ (mm^{-1})	9.071
F(000)	1648
Crystal dimensions (mm^3)	0.25 x 0.09 x 0.08
Theta range for data collection ($^\circ$)	2.65 to 23.28
Limiting Indices	$-22 \leq h \leq 23, -9 \leq k \leq 10, -16 \leq l \leq 14$
Reflections collected	10653
Independent reflections (R_{int})	3891 (0.0590)
Completeness to theta	99.1 %
Max. and min. transmission	0.2222 and 0.0887
Data / restraints / parameters	3891 / 0 / 326
Goodness-of-fit on F^2	1.265
Final R indices [$I > 2\sigma(I)$]	$R_1 = 0.0516, wR_2 = 0.0990$
R indices (all data)	$R_1 = 0.0621, wR_2 = 0.1024$
Extinction coefficient	0.00000(4)
Largest diff. peak and hole ($e\text{\AA}^{-3}$)	1.465 and -1.480

Table 2.2. Crystal data and structure refinement for $\text{Re}(\text{CO})_3(\text{MEPA-NEt})$.

Empirical formula	$\text{C}_{13}\text{H}_{15}\text{N}_2\text{O}_3\text{ReS}$
Formula weight	465.53
Temperature (K)	183(2) K
Wavelength (Å)	0.71073 Å
Crystal system	Monoclinic
Space group	$P2(1)/n$
a (Å)	7.2999(4)
b (Å)	14.9969(8)
c (Å)	13.5499(8)
β (°)	97.7240(10)
Volume (Å ³)	1469.93(14)
Z	4
ρ_{calc} (Mg m ⁻³)	2.104
μ (mm ⁻¹)	8.416
F(000)	888
Crystal dimensions (mm ³)	0.31 x 0.10 x 0.09
Theta range for data collection (°)	2.04 to 22.50
Limiting Indices	$-7 \leq h \leq 7, -11 \leq k \leq 16, -14 \leq l \leq 14$
Reflections collected	5514
Independent reflections (R_{int})	1921 (0.1225)
Completeness to theta = 23.25°	100.0 %
Max. and min. transmission	0.5909 and 0.2536
Data / restraints / parameters	1921 / 0 / 183
Goodness-of-fit on F^2	1.212
Final R indices [$I > 2\sigma(I)$]	$R_1 = 0.0428, wR_2 = 0.1060$
R indices (all data)	$R_1 = 0.0438, wR_2 = 0.1070$
Extinction coefficient	0.0010(3)
Largest diff. peak and hole (eÅ ⁻³)	1.755 and -2.636

Table 2.3. Crystal data and structure refinement for MEPAH-C₂CO₂H-STr.

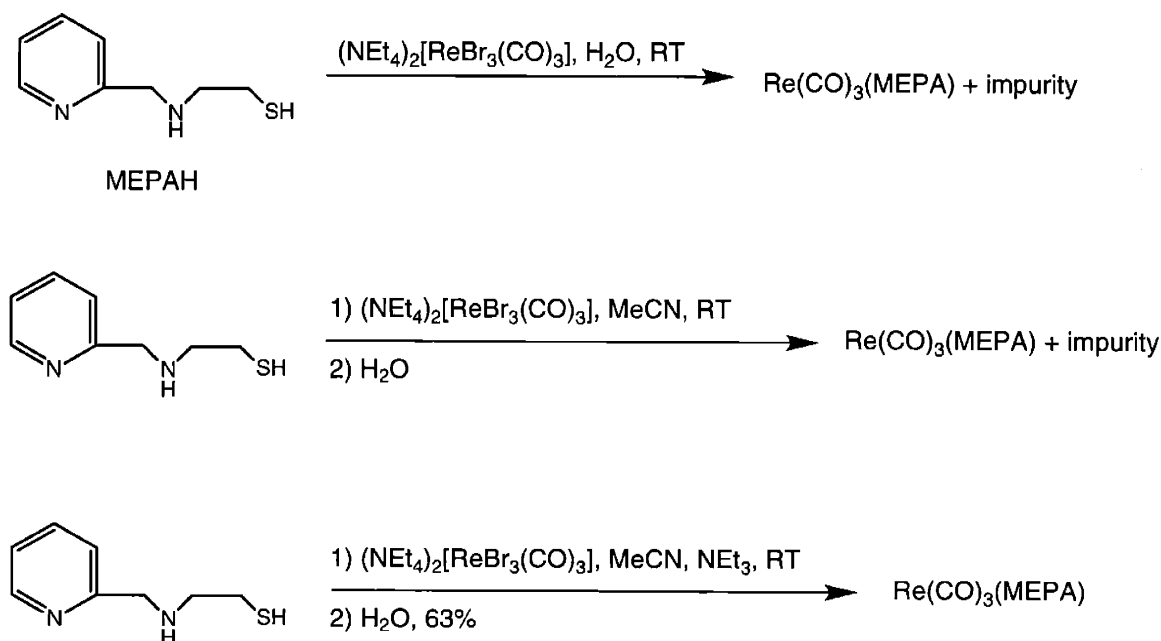
Empirical formula	C ₃₀ H ₃₀ N ₂ O ₂ S
Formula weight	482.62
Temperature (K)	183(2)
Wavelength (Å)	0.71073
Crystal system	Monoclinic
Space group	P2 ₁ /c
a (Å)	7.8561(6)
b (Å)	21.509(2)
c (Å)	15.0644(11)
β (°)	103.2710(10)
Volume (Å ³)	2477.6(3)
Z	4
ρ _{calc} (Mg m ⁻³)	1.294
μ (mm ⁻¹)	0.161
F(000)	1024
Crystal size	0.30 x 0.20 x 0.15 mm
θ range for data collection	2.35° to 23.26°
Limiting indices	-5 ≤ h ≤ 8, -23 ≤ k ≤ 23, -16 ≤ l ≤ 13
Reflections collected	9676
Independent reflections (R _{int})	3556 (0.0364)
Absorption correction	None
Data / restraints / parameters	3556 / 0 / 317
Goodness-of-fit on F ²	1.069
Final R indices [I > 2σ(I)]	R ₁ = 0.0392, wR ₂ = 0.0803
R indices (all data)	R ₁ = 0.0502, wR ₂ = 0.0840
Extinction coefficient	0.0011(5)
Largest diff. peak and hole	0.166 and -0.222 eÅ ⁻³

Table 2.4. Crystal data and structure refinement for $\text{Re}(\text{CO})_3(\text{MEPA-C}_2\text{COmorph})\cdot 2\text{H}_2\text{O}$.

Empirical formula	$\text{C}_{18}\text{H}_{26}\text{N}_3\text{O}_7\text{ReS}$
Formula weight	614.68
Temperature (K)	183(2) K
Wavelength (\AA)	0.71073 \AA
Crystal system	Triclinic
Space group	$\text{P}\bar{1}$
a (\AA)	7.6373(18)
b (\AA)	9.020(2)
c (\AA)	16.233(4)
α ($^\circ$)	85.476(4)
β ($^\circ$)	82.212(4)
γ ($^\circ$)	84.974(4)
Volume (\AA^3)	1101.2(4)
Z	2
ρ_{calc} (Mg m^{-3})	1.854
μ (mm^{-1})	5.656
F(000)	604
Crystal dimensions (mm^3)	0.13 x 0.10 x 0.08
Theta range for data collection ($^\circ$)	2.53 to 22.50
Limiting Indices	$-8 \leq h \leq 6, -9 \leq k \leq 9, -17 \leq l \leq 12$
Reflections collected	4142
Independent reflections (R_{int})	2856 (0.0300)
Completeness to theta	98.9 %
Max. and min. transmission	None
Data / restraints / parameters	2856 / 0 / 288
Goodness-of-fit on F^2	1.324
Final R indices [$I > 2\sigma(I)$]	$R_1 = 0.0656$ $wR_2 = 0.1453$
R indices (all data)	$R_1 = 0.0679, wR_2 = 0.1464$
Extinction coefficient	0.0000(7)
Largest diff. peak and hole ($\text{e}\text{\AA}^{-3}$)	2.536 and -3.784

Results and Discussion

The synthesis of $\text{Re}(\text{CO})_3(\text{MEPA})$ is very straightforward. Reaction of a 1:1 (v/v) MEPAH- NEt_3 mixture with $[\text{Re}(\text{CO})_3(\text{MeCN})_3]^+$ takes place within seconds at room temperature to give a yellow solution (Scheme 2.2). Precipitation of the neutral complex with water gives the product in good yield. It was desirable to extend this chemistry to aqueous conditions given the potential development of $^{99\text{m}}\text{Tc}$ radiopharmaceuticals from this ligand system, but all attempts to cleanly synthesize $\text{Re}(\text{CO})_3(\text{MEPA})$ in water gave a mixture of the expected product and an impurity thought to be an oligomeric species (as determined from FABMS). In fact, in the absence of base (even in MeCN; see Scheme 2.2), this impurity is observed. Any acid present (either the triqua cation or unneutralized HBr) seemed to effect this mixture.



Scheme 2.2. Synthesis of $\text{Re}(\text{CO})_3(\text{MEPA})$ including synthetic variations.

Base, however, could not be added to solutions of $[\text{Re}(\text{CO})_3(\text{H}_2\text{O})_3]^+$, as polynuclear hydrolysis products would have formed.^{16,30} The acid sensitivity can be observed by eluting a pure sample of $\text{Re}(\text{CO})_3(\text{MEPA})$ with a pH 2.25 aqueous triethylammonium phosphate (TEAP) buffer/methanol gradient on HPLC (Figure 2.5). The acid sensitivity of the rhenium species is not expected to be a problem in analogous $^{99\text{m}}\text{Tc}$ syntheses as $[\text{}^{99\text{m}}\text{Tc}(\text{CO})_3(\text{H}_2\text{O})_3]^+$ is the dominant species present in solution, even in strongly basic solutions (pH 13).^{9,24}

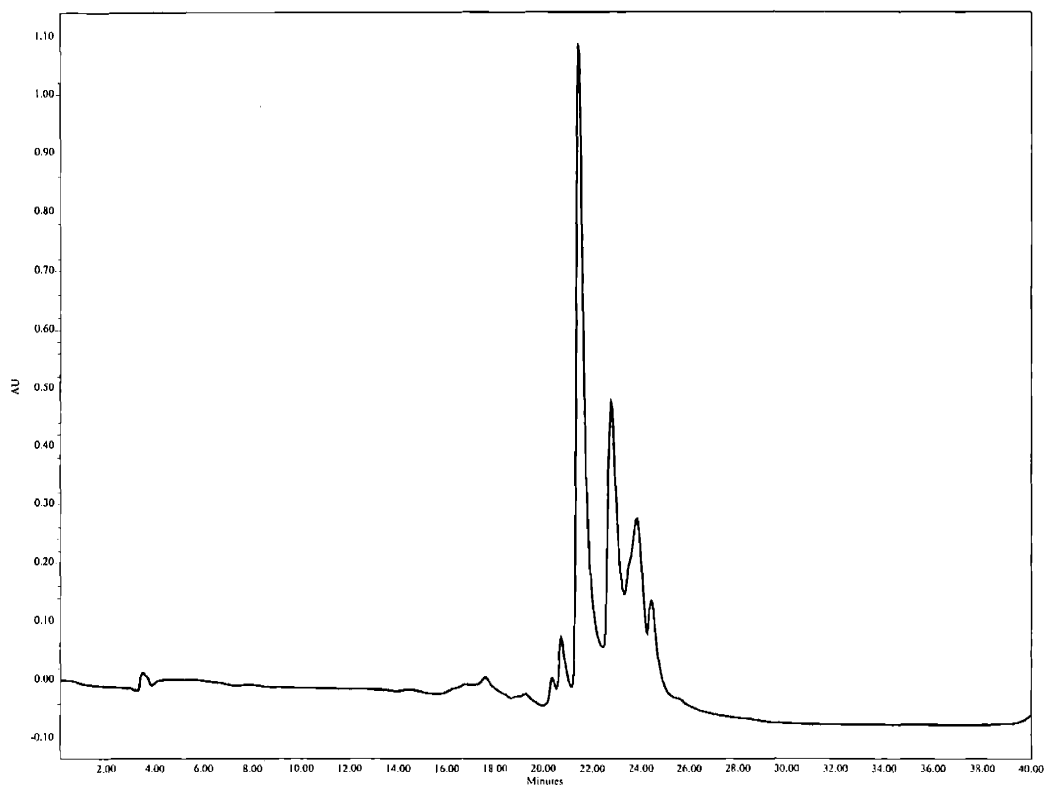


Figure 2.5. UV (280 nm) chromatogram of crystals of $\text{Re}(\text{CO})_3(\text{MEPA})$ on RP-18 HPLC with pH 2.25 TEAP buffer (A) and methanol (B) linear gradient as follows

($t/\%B$): 0/0, 5/0, 20/100, 30/100, 40/0.

The IR and ^1H NMR spectra of $\text{Re}(\text{CO})_3(\text{MEPA})$ are quite straightforward. The most notable peaks of the IR spectrum are in the $\nu(\text{CO})$ region and occur in the usual $A_1 + E$ pattern for pseudo- C_{3v} symmetry at 2000 cm^{-1} and 1874 cm^{-1} (Spectrum 2.1). The ^1H NMR spectrum (Spectrum 2.2) exhibits the expected peaks in the pyridyl region as well as more complex coupling patterns in the aliphatic region due to the hindered rotation of the coordinated ligand. An ABX pattern is noted at 4.49 ppm for the methylene protons α to the pyridine ring. In addition, an ABCD pattern is observed for the four protons on the ethylene bridge between the nitrogen and sulfur.

A stability study was conducted on the complex $\text{Re}(\text{CO})_3(\text{MEPA})$ to determine whether or not transchelation would occur in the presence of competitive ligands. In particular, glutathione is an oft-encountered thiol *in vivo*. As a model for this, $\text{Re}(\text{CO})_3(\text{MEPA})$ was stirred in CD_2Cl_2 solutions with ethanethiol (monodentate) and 1,2-ethanedithiol (bidentate). In both experiments, no transchelation was observed, even after 24 h, according to ^1H NMR spectroscopy. Though this is not an optimal model for biological conditions, it has shown $\text{Re}(\text{CO})_3(\text{MEPA})$ to be resistant to transchelation by thiols.

Crystals of $\text{Re}(\text{CO})_3(\text{MEPA})$ suitable for a single crystal X-ray diffraction study were grown by slow evaporation of a saturated acetone-water solution. Two independent molecules were observed in the asymmetric unit, but as they were nearly identical, only one is shown. The crystal structure (Figure 2.6) clearly shows the binding of the tridentate {NNS} ligand to the " $[\text{Re}(\text{CO})_3]^+$ " core. Most bond lengths and angles are

similar to those observed for other compounds of this core (Table 2.5). The Re-N(py) distances of 2.182(10) Å and 2.198(9) Å fall into the usual range.^{11,18,31-33} A notable structural characteristic is the relatively long Re-S bond length of 2.477(4) Å. It is approximately 0.2 Å longer than the corresponding Re-S bonds in related {ReON₂S₂} compounds^{2,34} but is similar to Re-S bonds in Re(I) thioether compounds.¹² A search of the literature has produced only one other example of a mononuclear Re(I) thiolate complex.³⁵

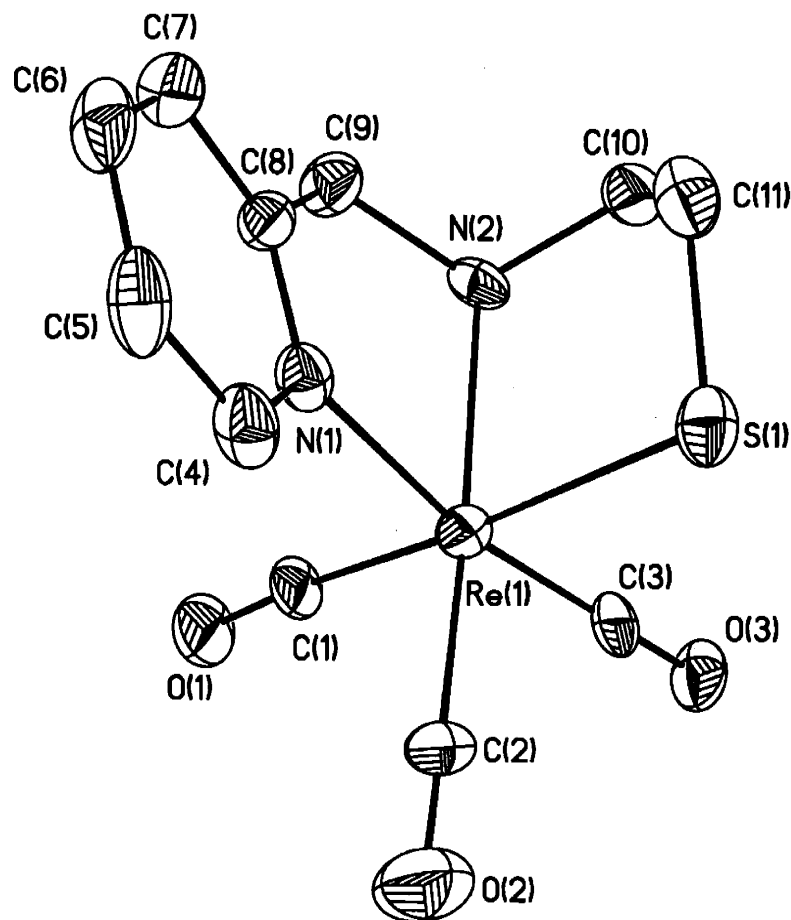
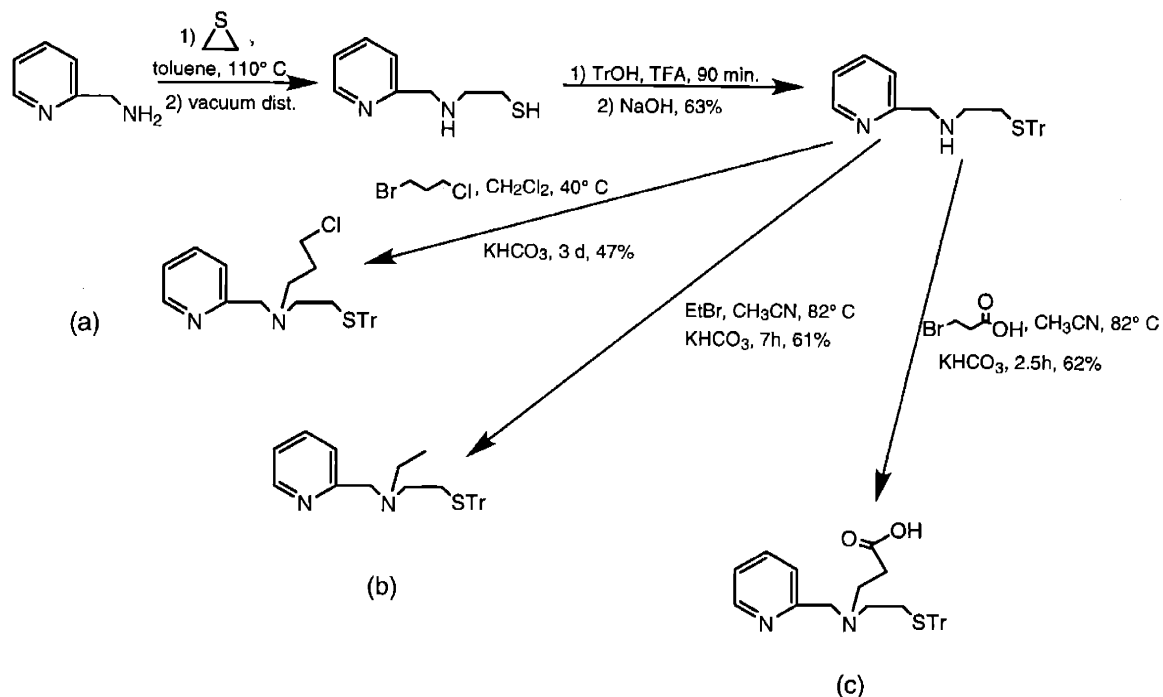


Figure 2.6. Thermal ellipsoid plot (35% probability) of Re(CO)₃(MEPA).

Table 2.5. Selected bond distances (Å) and angles (°) for Re(CO)₃(MEPA).

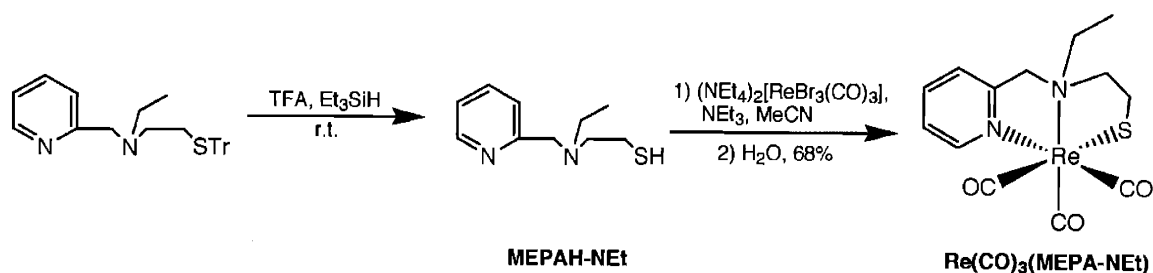
Re(1)-C(1)	1.905(13)	Re(1)-N(1)	2.182(10)
Re(1)-C(2)	1.920(14)	Re(1)-N(2)	2.204(9)
Re(1)-C(3)	1.926(15)	Re(1)-S(1)	2.477(4)
C(1)-Re(1)-C(2)	89.7(6)	C(3)-Re(1)-N(2)	97.6(5)
C(1)-Re(1)-C(3)	90.4(5)	N(1)-Re(1)-N(2)	75.2(3)
C(2)-Re(1)-C(3)	89.9(6)	C(1)-Re(1)-S(1)	175.7(4)
C(1)-Re(1)-N(1)	96.0(5)	C(2)-Re(1)-S(1)	94.6(5)
C(2)-Re(1)-N(1)	97.0(5)	C(3)-Re(1)-S(1)	90.1(4)
C(3)-Re(1)-N(1)	170.6(4)	N(1)-Re(1)-S(1)	83.0(3)
C(1)-Re(1)-N(2)	93.6(5)	N(2)-Re(1)-S(1)	82.1(3)
C(2)-Re(1)-N(2)	171.8(5)		

The synthesis of Re(CO)₃(MEPA) and confirmation of its structure led to the subsequent investigation of the derivatization of MEPAH (Scheme 2.3). Protection of the thiol of MEPAH with trifluoroacetic acid (TFA) and triphenylmethanol gave the trityl-protected thiol, MEPAH-STr, in good yield (Spectrum 2.3). A variety of molecules were reacted with MEPAH-STr to give important intermediates on the synthetic pathway to potential radiopharmaceuticals.



Scheme 2.3. Synthesis, protection, and derivatization of MEPAH.

In the presence of base, MEPAH-S-Str reacts with bromoethane to give the *N*-ethyl derivative, MEPAH-NEt-S-Str, in good yield (Scheme 2.3b and Spectrum 2.4). While the ethyl-derivatized ligand is not suitable for further reaction leading to potential bioconjugation, its synthesis demonstrates the ease of derivatization of the internal nitrogen of the ligand, as shown recently by others.³⁶ Furthermore, the deprotection of MEPAH-NEt-S-Str with TFA and Et₃SiH followed by reaction with [Re(CO)₃(MeCN)₃]⁺ in the presence of NEt₃ gave Re(CO)₃(MEPA-NEt) (Scheme 2.4). The reaction takes place quickly, indicating that derivatization has not significantly affected the affinity of the ligand for the metal center.



Scheme 2.4. Synthesis of $\text{Re}(\text{CO})_3(\text{MEPA-NEt})$.

The IR and ^1H NMR spectra of $\text{Re}(\text{CO})_3(\text{MEPA-NEt})$ are quite similar to those of $\text{Re}(\text{CO})_3(\text{MEPA})$. The same $A_1 + E$ pattern is observed in the $\nu(\text{CO})$ region with a split of the E peak (Spectrum 2.5). The ^1H NMR spectrum contains AB patterns for the methylene protons α to the pyridine (no NH to create an ABX pattern as before) as well as for the methylene protons of the pendant ethyl group at 4.66 and 3.73 ppm, respectively (Spectrum 2.6). The ethyl group AB pattern is further split by the methyl protons, causing a complex splitting pattern. Additionally, a triplet for the methyl group is observed at 1.39 ppm.

Single crystals of $\text{Re}(\text{CO})_3(\text{MEPA-NEt})$ were grown by slow evaporation of a saturated acetone-water solution. The structure of $\text{Re}(\text{CO})_3(\text{MEPA-NEt})$ has been confirmed by a single crystal X-ray diffraction study. The crystal structure (Figure 2.7 and Table 2.6) shows a general similarity of this structure to that of $\text{Re}(\text{CO})_3(\text{MEPA})$, exemplified by the similar Re-S bond length of 2.471(2) Å.

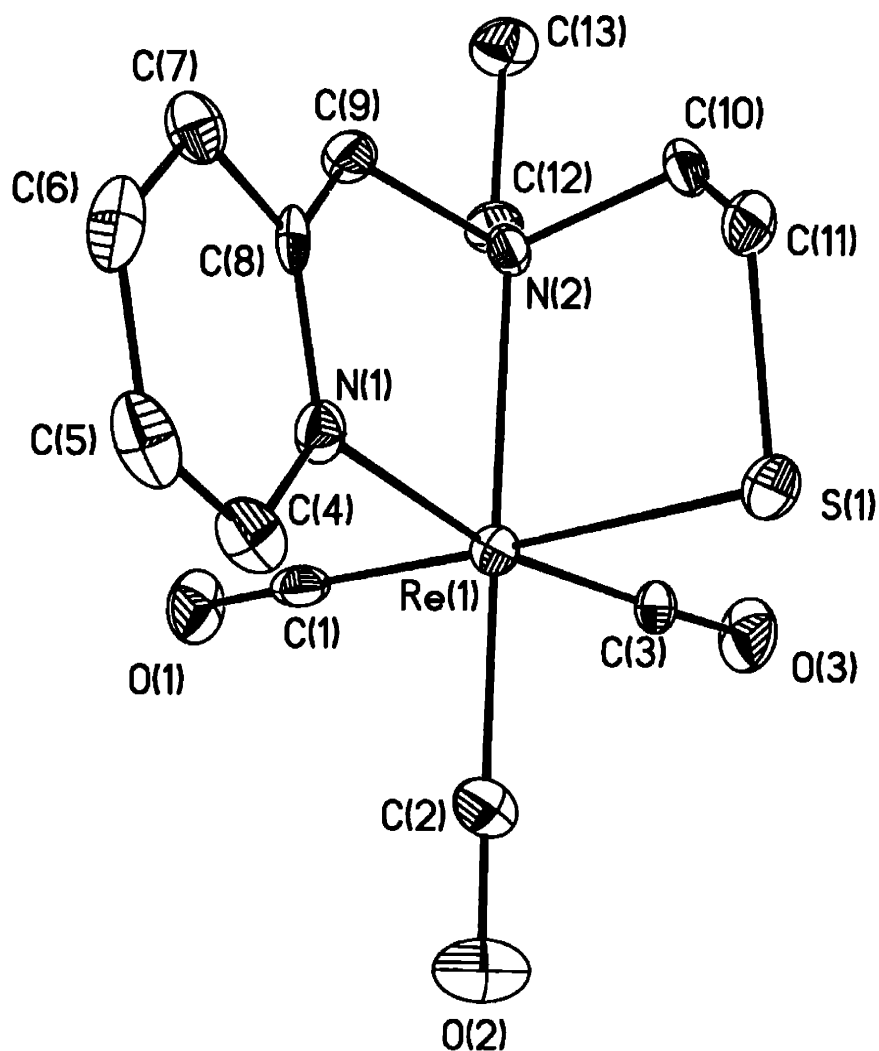


Figure 2.7. Thermal ellipsoid plot (35% probability) of $\text{Re}(\text{CO})_3(\text{MEPA-NEt})$.

Table 2.6. Selected bond distances (\AA) and angles ($^\circ$) for $\text{Re}(\text{CO})_3(\text{MEPA-NEt})$.

Re(1)-C(2)	1.907(9)	Re(1)-N(1)	2.198(7)
Re(1)-C(1)	1.925(10)	Re(1)-N(2)	2.253(7)
Re(1)-C(3)	1.926(11)	Re(1)-S(1)	2.471(2)
C(2)-Re(1)-C(1)	89.8(4)	C(1)-Re(1)-C(3)	90.5(3)
C(2)-Re(1)-C(3)	89.7(4)	C(2)-Re(1)-N(1)	98.1(3)

C(1)-Re(1)-N(1)	95.5(3)	C(2)-Re(1)-S(1)	92.1(3)
C(3)-Re(1)-N(1)	170.2(3)	C(1)-Re(1)-S(1)	178.0(2)
C(2)-Re(1)-N(2)	173.4(3)	C(3)-Re(1)-S(1)	89.8(2)
C(1)-Re(1)-N(2)	94.7(3)	N(1)-Re(1)-S(1)	83.97(18)
C(3)-Re(1)-N(2)	95.1(3)	N(2)-Re(1)-S(1)	83.4(2)
N(1)-Re(1)-N(2)	76.7(3)		

While $\text{Re}(\text{CO})_3(\text{MEPA-NEt})$ is not useful for further studies into bioconjugation, other starting points from MEPAH-STr were explored to enable linking of a biomolecule to the ligand. Two bifunctionalized haloalkanes were used.

The most successful starting point for biological work was the *N*-propionic acid derivative (Scheme 2.3c), which was obtained by refluxing MEPAH-STr with 3-bromopropionic acid in MeCN in the presence of KHCO_3 . Within 2-3 hours, the *N*-propionic acid derivative, MEPAH- $\text{C}_2\text{CO}_2\text{H-STr}$ was obtained in good yield (longer reaction times required for larger reaction scales; Spectrum 2.7). This product was easily separable from by-products (and excess starting materials) by virtue of its insolubility in MeOH, in contrast to all other reaction species (after filtration of KHCO_3). This acid group linked to MEPAH presented many possibilities, as acid groups show a varied chemistry. Since it is possible that these reaction conditions may lead to formation of pyridinium salts, it was desirable to confirm the nature of the product. Neither proton NMR spectroscopy nor FABMS could confirm this independently. However, recrystallization of the *N*-propionic acid derivative from slowly evaporating 10% MeOH in EtOAc gave colorless shards suitable for a single crystal X-ray diffraction study. The thermal ellipsoid plot of this compound is presented in Figure 2.8, and selected bond lengths and angles in Table 2.7. Bond distances and angles are consistent with accepted values, and it is clear from this study that alkylation occurs at the internal nitrogen.

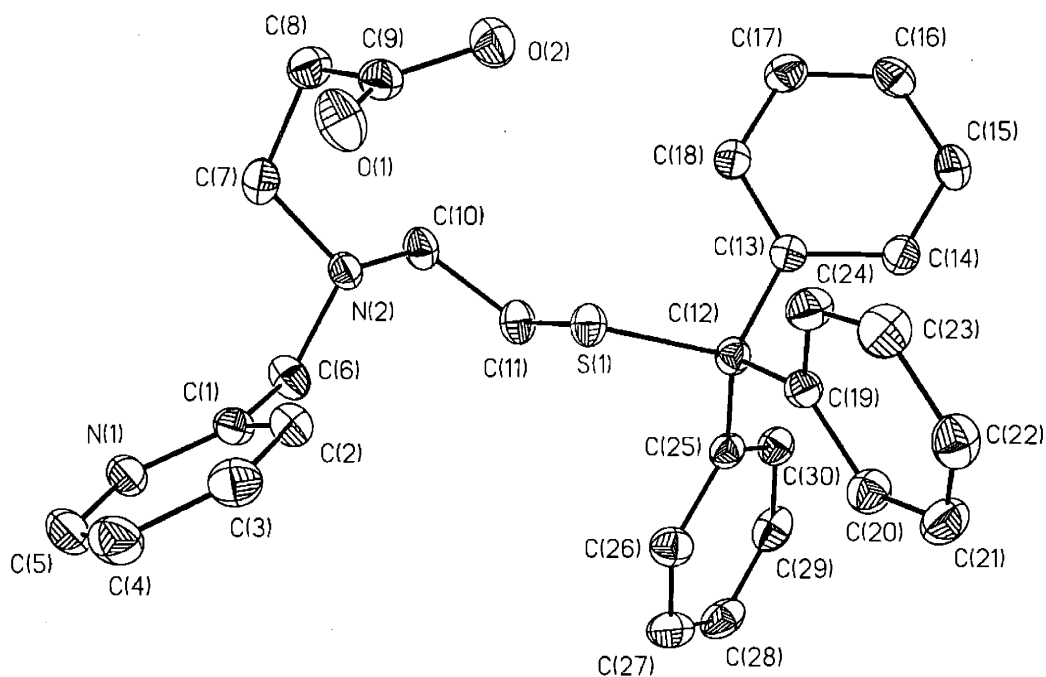


Figure 2.8. Thermal ellipsoid plot (35% probability) of *N*-propionic acid derivative of MEPAH-STr.

Table 2.7. Selected bond distances (Å) and angles (°) for *N*-propionic acid derivative of MEPAH-STr.

S(1)-C(11)	1.824(2)	S(1)-C(12)	1.859(2)
O(1)-C(9)	1.209(3)	O(2)-C(9)	1.324(3)
N(1)-C(5)	1.340(3)	N(1)-C(1)	1.343(3)
N(2)-C(7)	1.461(3)	N(2)-C(6)	1.461(3)
N(2)-C(10)	1.467(2)		
C(11)-S(1)-C(12)	102.25(9)	C(5)-N(1)-C(1)	118.2(2)
C(7)-N(2)-C(6)	109.7(2)	C(7)-N(2)-C(10)	113.4(2)
C(6)-N(2)-C(10)	111.7(2)		

Reaction of the *N*-propionic acid derivative with *N*-hydroxysuccinimide (NHS) and dicyclohexylcarbodiimide (DCC) in anhydrous THF under argon gave the activated NHS ester (Scheme 2.5). This compound was purified by column chromatography and was characterized by ¹H NMR spectroscopy (Spectrum 2.8), HRESI(+)-MS (Figure 2.9), and elemental analysis.

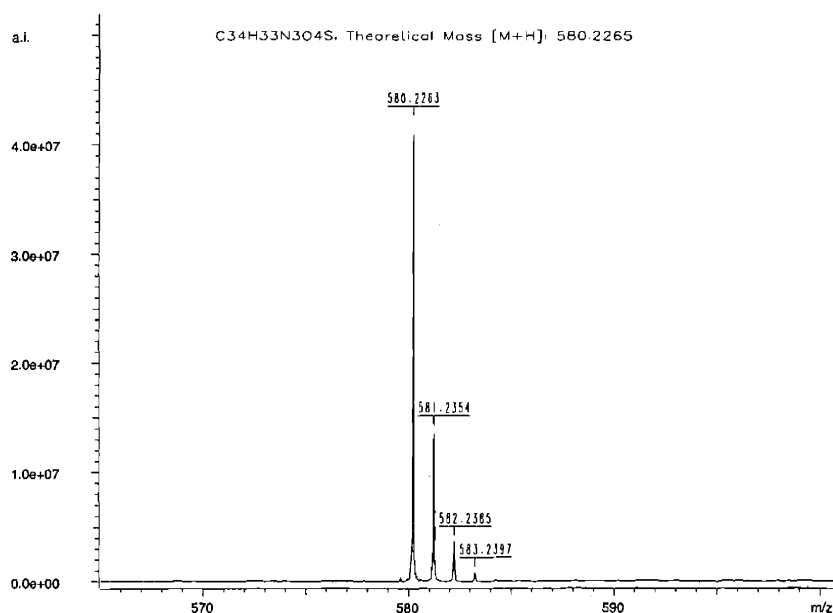
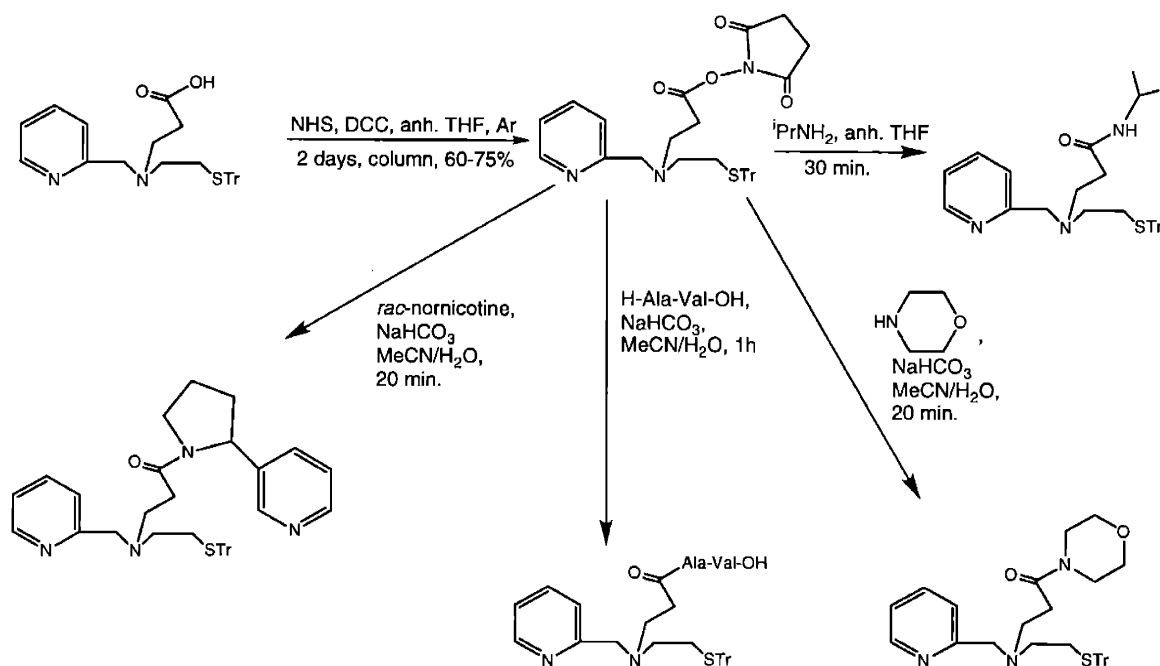


Figure 2.9. HRESI(+)-MS of NHS ester.

With the NHS ester in hand, coupling to amines to form amides was quite facile (Scheme 2.5). Reaction of *i*-PrNH₂ with the NHS ester gave the isopropylamide under anhydrous conditions. Investigation into biologically relevant amines which were not soluble in organic solvents revealed that the NHS ester did not hydrolyze to an

appreciable extent in the presence of amines in slightly basic mixed aqueous solvent systems. A 1:1 MeCN:H₂O solvent system with NaHCO₃ as a base was found to be a good system for these couplings. As a model for peptide work, the diamino acid L-alanyl-L-valine was coupled to give the expected amide (ESIMS). Reactions with other biologically relevant molecules such as morpholine and the nicotine derivative nornicotine (Figure 2.10) produced the expected amides, MEPAH-C₂COMorph-STr and MEPAH-C₂CONornic-STr, respectively. The coupled products were purified with preparative-scale TLC to ensure high purity. This was an important consideration for tracer-level work, and these ligands (Spectra 2.9 and 2.10) were used as starting points for biological studies.



Scheme 2.5. Conjugation of MEPAH-based ligand to amines to form amides.

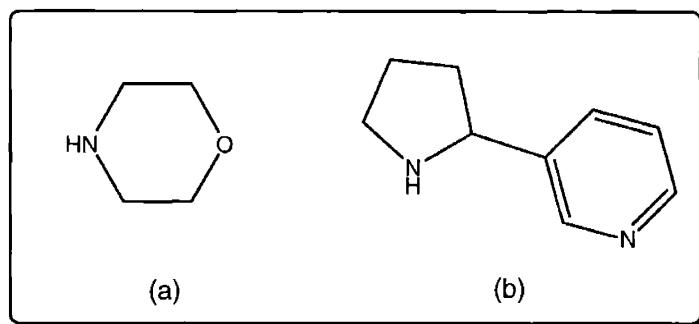
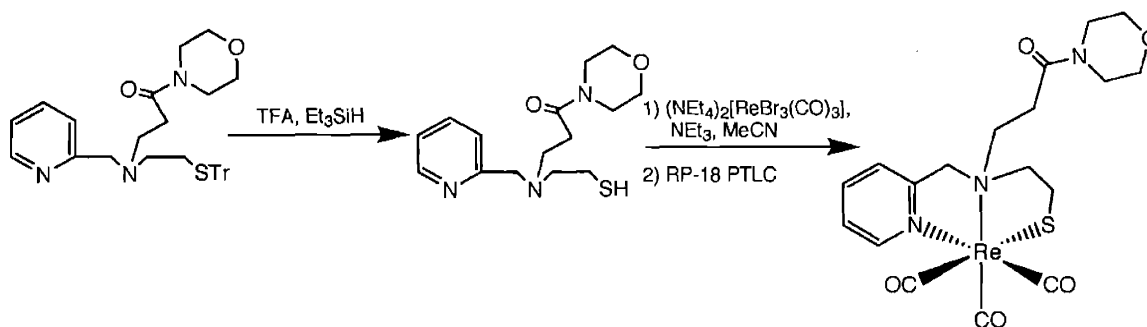


Figure 2.10. Amines whose conjugates were utilized in biological studies:

(a) morpholine and (b) nornicotine.

A sample of MEPAH-C₂COMorph-STr was deprotected with TFA-Et₃SiH. Reaction of the detritylated ligand (basified with NEt₃) with [Re(CO)₃(MeCN)₃]⁺ gave Re(CO)₃(MEPA-C₂COMorph). Reversed phase C₁₈-bound silica was used for chromatographic purification (Scheme 2.6). The ¹H NMR spectrum of this complex, a model for a radiopharmaceutical, exhibited all of the expected peaks (Spectrum 2.11) including AB coupling patterns for the py-CH₂ (4.73 ppm) methylene group and the methylene group (on the linker) α to the central nitrogen (3.99 ppm). High resolution ESI(+)-MS confirmed the presence of the complex (Figure 2.11).



Scheme 2.6. Synthesis of $\text{Re}(\text{CO})_3(\text{MEPA-C}_2\text{COMorph})$.

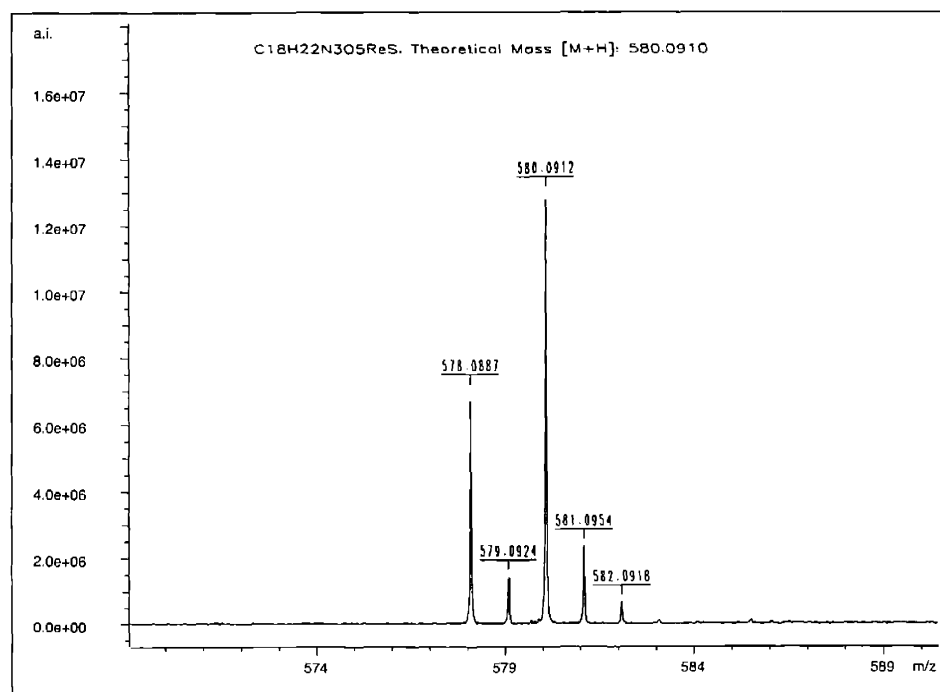


Figure 2.11. HRESI(+)-MS of $\text{Re}(\text{CO})_3(\text{MEPA-C}_2\text{COMorph})$.

Recrystallization of $\text{Re}(\text{CO})_3(\text{MEPA-C}_2\text{COMorph})$ from slowly evaporating acetone-water gave crystals of the dihydrate of this complex. In the absence of water, these pale yellow plates cracked quite readily due to desolvation. A crystal was mounted, and data was collected. Connectivity was determined and found to be consistent with the expected complex (Figure 2.12). The Re-S bond length in $\text{Re}(\text{CO})_3(\text{MEPA-C}_2\text{COMorph})\cdot 2\text{H}_2\text{O}$ is 2.457(4) Å, which is quite similar to that observed in the previously outlined examples.

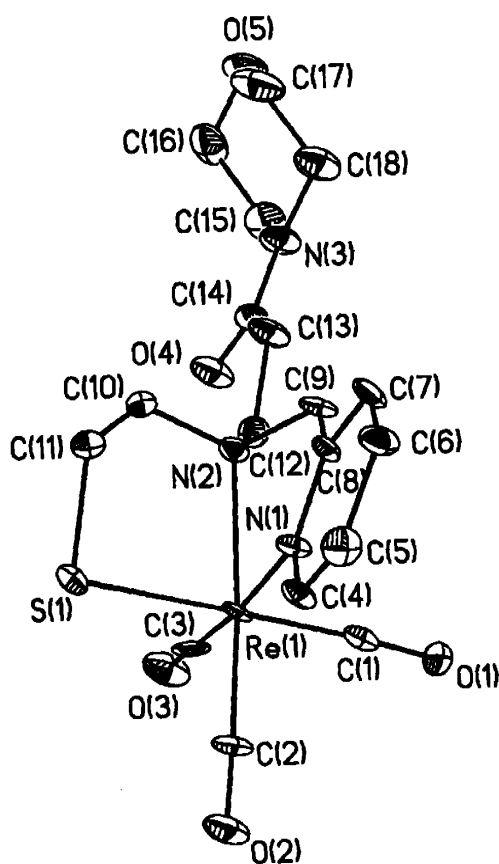


Figure 2.12. Thermal ellipsoid plot (35% probability) of $\text{Re}(\text{CO})_3(\text{MEPA-C}_2\text{COMorph})\cdot 2\text{H}_2\text{O}$ (water molecules omitted for clarity).

Table 2.8. Selected bond distances (Å) and angles (°) for $\text{Re}(\text{CO})_3(\text{MEPA-C}_2\text{COmorph})\cdot 2\text{H}_2\text{O}$.

Re(1)-C(3)	1.90(2)	Re(1)-N(1)	2.197(11)
Re(1)-C(1)	1.897(17)	Re(1)-N(2)	2.270(12)
Re(1)-C(2)	1.901(15)	Re(1)-S(1)	2.457(4)
C(3)-Re(1)-C(1)	87.0(7)	C(2)-Re(1)-N(2)	170.1(6)
C(3)-Re(1)-C(2)	90.3(6)	N(1)-Re(1)-N(2)	75.7(4)
C(1)-Re(1)-C(2)	87.6(7)	C(3)-Re(1)-S(1)	95.7(5)
C(3)-Re(1)-N(1)	173.1(5)	C(1)-Re(1)-S(1)	176.8(5)
C(1)-Re(1)-N(1)	94.0(6)	C(2)-Re(1)-S(1)	90.6(5)
C(2)-Re(1)-N(1)	96.5(6)	N(1)-Re(1)-S(1)	83.6(3)
C(3)-Re(1)-N(2)	97.4(5)	N(2)-Re(1)-S(1)	82.6(3)
C(1)-Re(1)-N(2)	98.9(5)		

A sample of MEPAH-C₂CONornic-STr was also deprotected using TFA-Et₃SiH as before to give MEPAH-C₂CONornic as a pale yellow oil. Reaction of the detritylated ligand with NEt₃-containing $[\text{Re}(\text{CO})_3(\text{MeCN})_3]^+$ gave $\text{Re}(\text{CO})_3(\text{MEPA-C}_2\text{CONornic})$ after TLC purification (Figure 2.13a). The ¹H NMR spectrum of this complex is quite complicated due to many overlapping resonances, but HRESI(+)-MS (Figure 2.13b) confirmed the synthesis of $\text{Re}(\text{CO})_3(\text{MEPA-C}_2\text{CONornic})$.

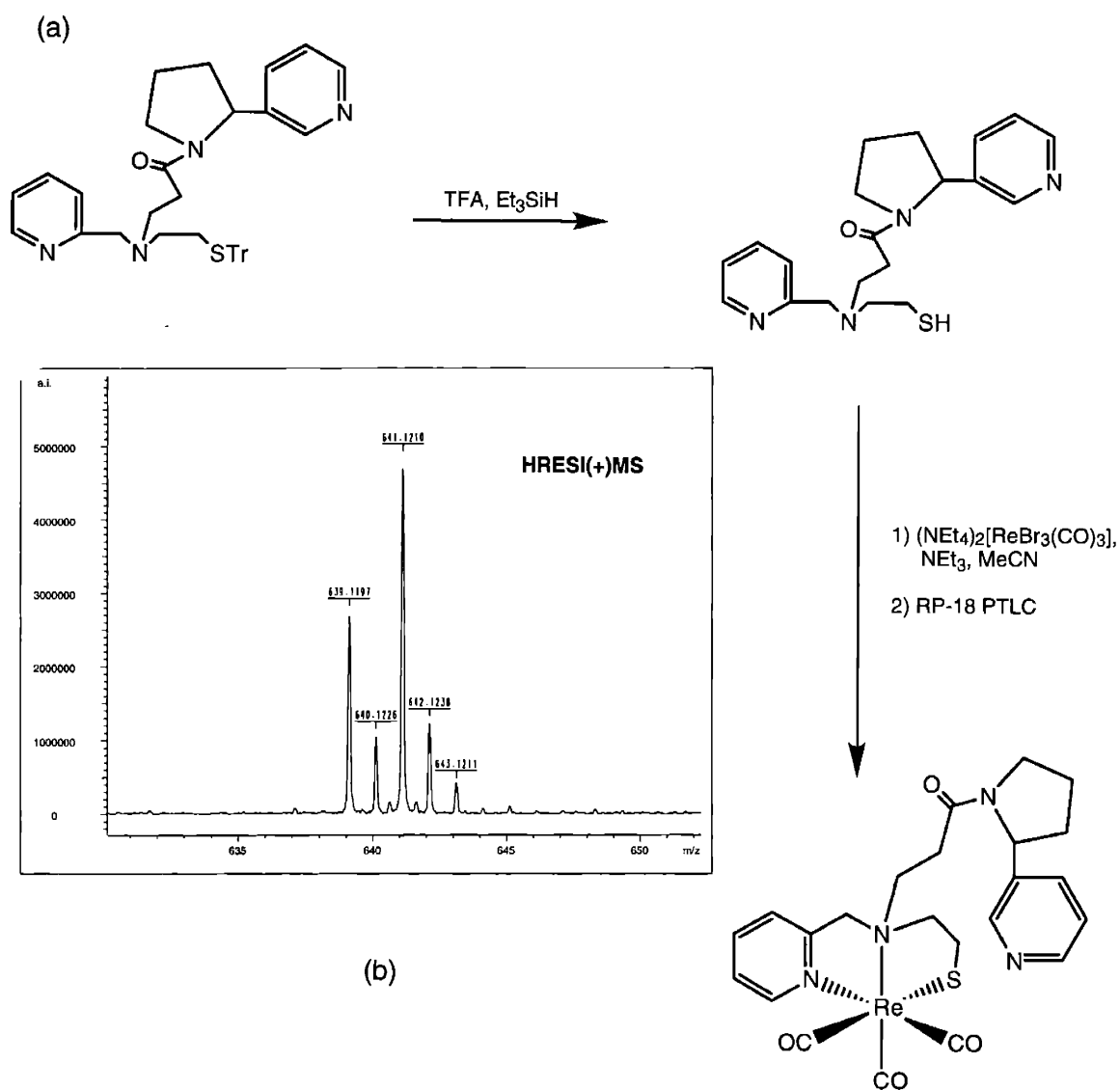


Figure 2.13. (a) Synthesis and (b) HRESI(+)-MS of $\text{Re}(\text{CO})_3(\text{MEPA-C}_2\text{CONornic})$.

The other starting point for biological work was the *N*-chloropropyl derivative, MEPAH-C₃Cl-STr, obtained from reaction of MEPAH-STr with 1-bromo-3-chloropropane (Scheme 2.3a; Spectrum 2.12). Initially, we had hoped to use MEPAH-C₃Cl-STr as a universal precursor to which several amine-containing biomolecules could be conjugated *via* nucleophilic displacement of the chloride. Similar approaches have

been reported elsewhere.^{2,37} In practice, though, this was quite challenging due to the instability of MEPAH-C₃Cl-STr under reaction conditions. Proton NMR studies showed that in a short period of time, MEPAH-C₃Cl-STr decomposed in refluxing CD₃CN, giving rise to many new peaks in the pyridyl region as well as in the rest of the spectrum. Based on successful use of chloropropyl derivatives in other work with ligands containing only aliphatic amines,^{2,37} it is supposed that the pyridine moiety is the complicating issue. However, modest yields of bioconjugated products from this route were achievable.

Biological studies with MEPAH-C₂COMorph-containing ^{99m}Tc complexes suggested that a ligand possessing an amine-linked morpholine was a desirable synthetic target. Though many problems had been encountered with MEPAH-C₃Cl-STr, modest yields of MEPAH-C₃morph-STr were achieved by slow addition of a dilute solution of MEPAH-C₃Cl-STr to a rapidly stirring, refluxing solution of morpholine in MeCN. Ten equivalents each of morpholine and base were used, as well as five equivalents of KI to assist halide displacement. Though decomposition was not halted, it was slowed significantly, and MEPAH-C₃morph-STr was obtained in 16% yield after purification by chromatography (Figure 2.14a and Spectrum 2.13).

Deprotection of MEPAH-C₃morph-STr with TFA-Et₃SiH followed by reaction with [Re(CO)₃(MeCN)₃]⁺ in basic MeCN gave a small sample of Re(CO)₃(MEPA-C₃morph) after purification on reversed phase silica (Figure 2.14a). Though recrystallization of this sample failed to yield single crystals, HRESI(+)-MS (Figure

2.14b) confirmed the presence of the expected complex. The ^1H NMR spectrum exhibited the expected peaks, although an impurity containing $(\text{NEt}_4)^+$ was also noted (no other peaks exhibited). An ESI(-)MS of the sample showed no peaks assignable to the small impurity, and the impurity did not have any effect on future studies with this complex.

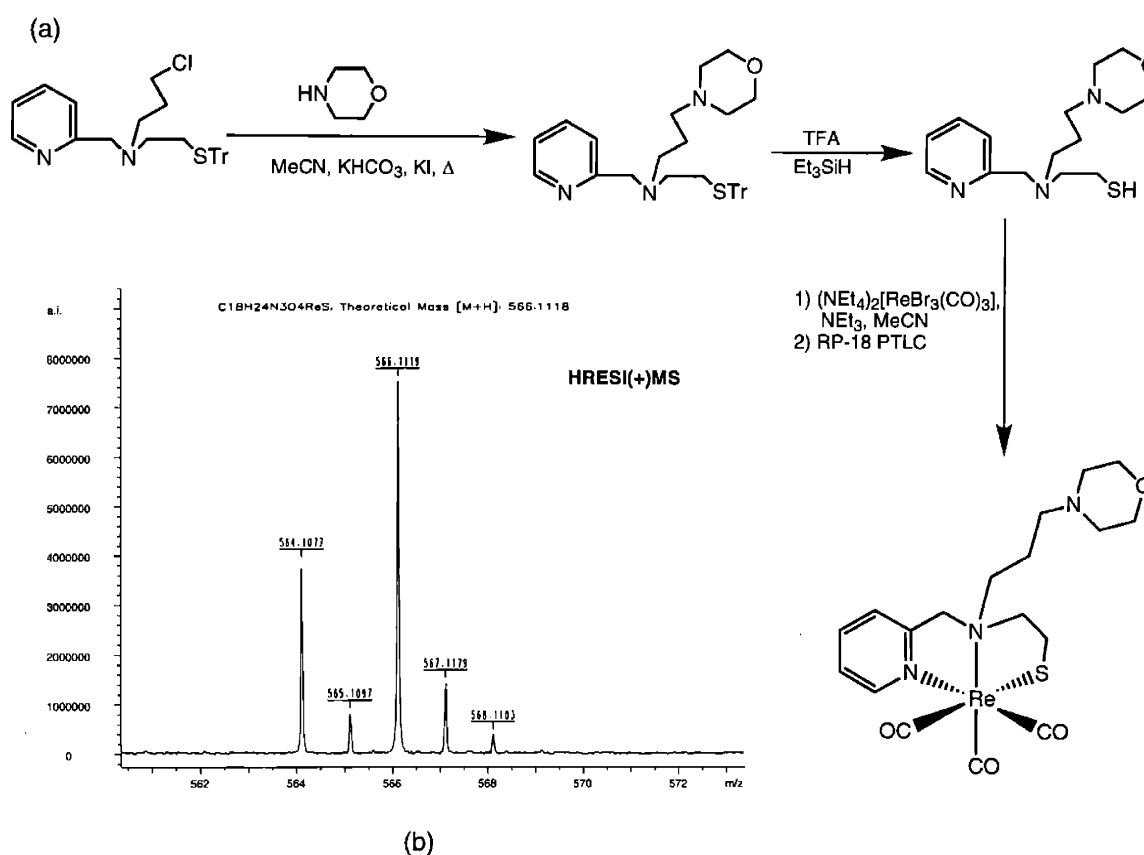


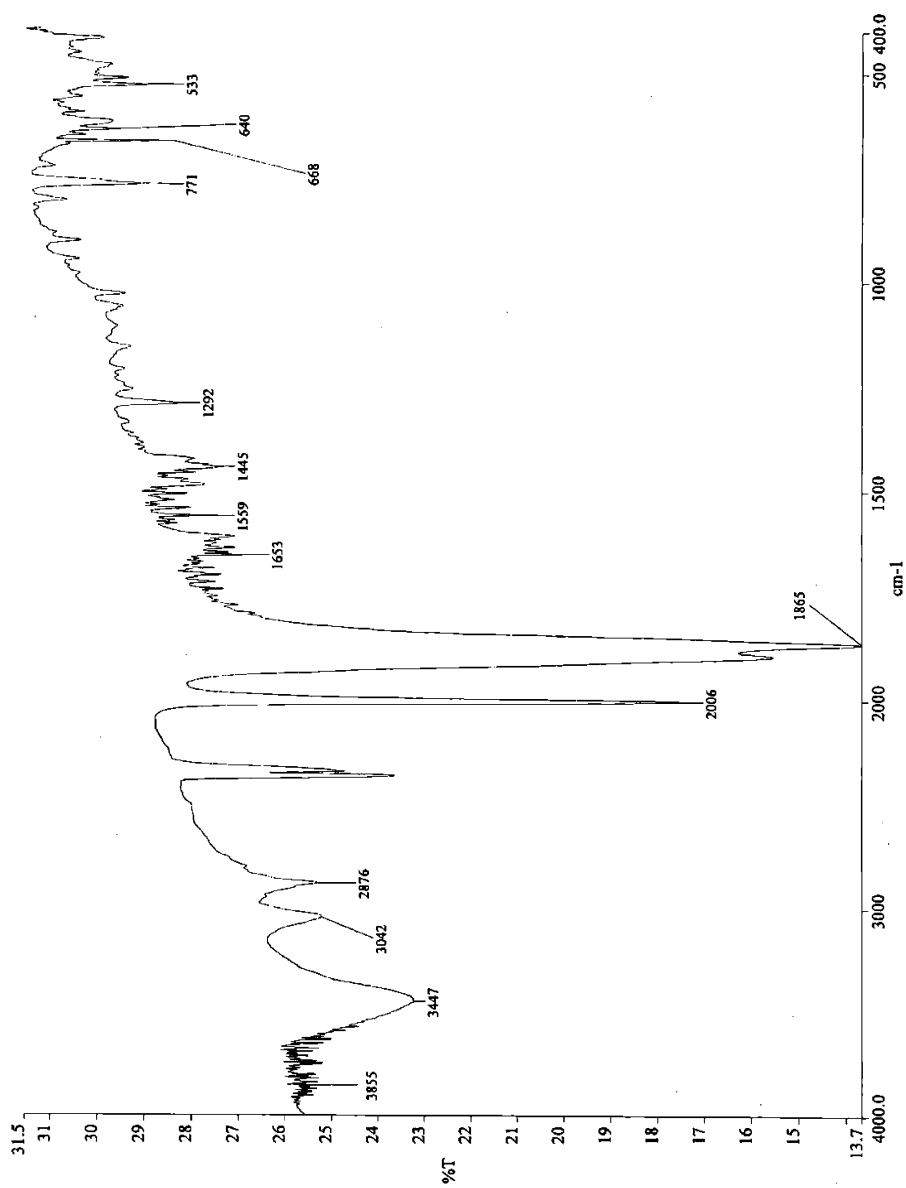
Figure 2.14. (a) Synthesis and (b) HRESI(+)-MS of $\text{Re}(\text{CO})_3(\text{MEPA-C}_3\text{morph})$.

Conclusions

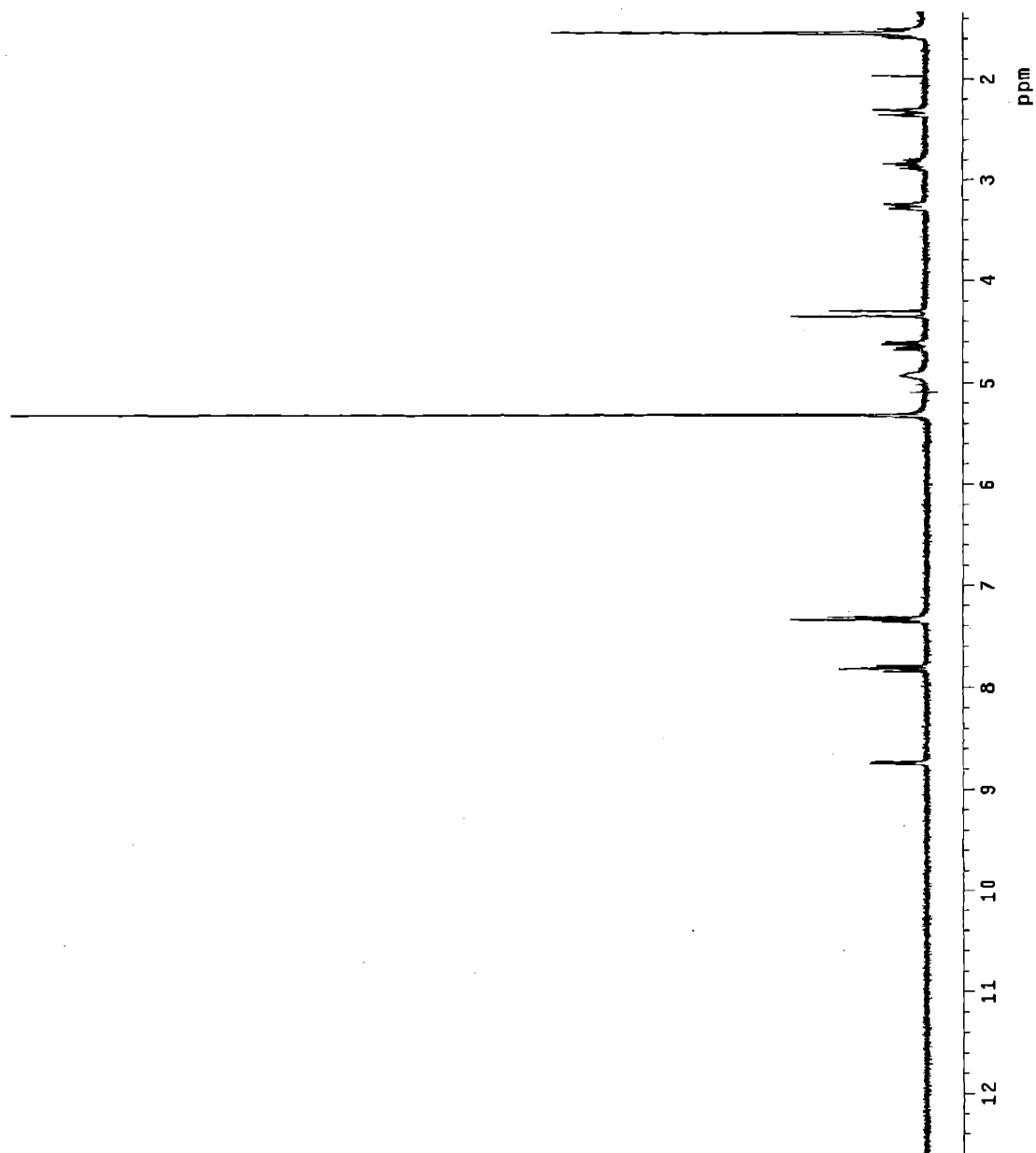
The reactivity of $[\text{Re}(\text{sol})_3(\text{CO})_3]^+$ with a variety of {NNS} ligands based on the same skeleton has been detailed. This is the first study of tricarbonylrhenium complexes of tridentate ligands possessing an aromatic N, an aliphatic N, and a thiolate S. The ligand MEPAH, which has been used previously in zinc studies, proved to be a good ligand for the "*fac*- $[\text{Re}(\text{CO})_3]^+$ " core, and in some ways, made this core look like zinc. This is supported based on Alberto's recent work which showed that the triaquatricarbonylrhenium(I) cation has a very similar lability to Zn^{2+} .²²

Derivatized MEPAH-based ligands were synthesized in a relatively facile manner and found to retain significant affinity for the metal center. Additionally, some biologically relevant rhenium complexes have been synthesized. These metal complexes exhibit properties desirable for models of radiopharmaceuticals of the conjugate design, such as a stable metal chelate, a pendant biomolecule situated well away from the metal center, and an overall neutral charge on the metal complex. Many routes of derivatization were explored; those that were pursued most vigorously were dictated primarily by the work to be presented in Chapter 3.

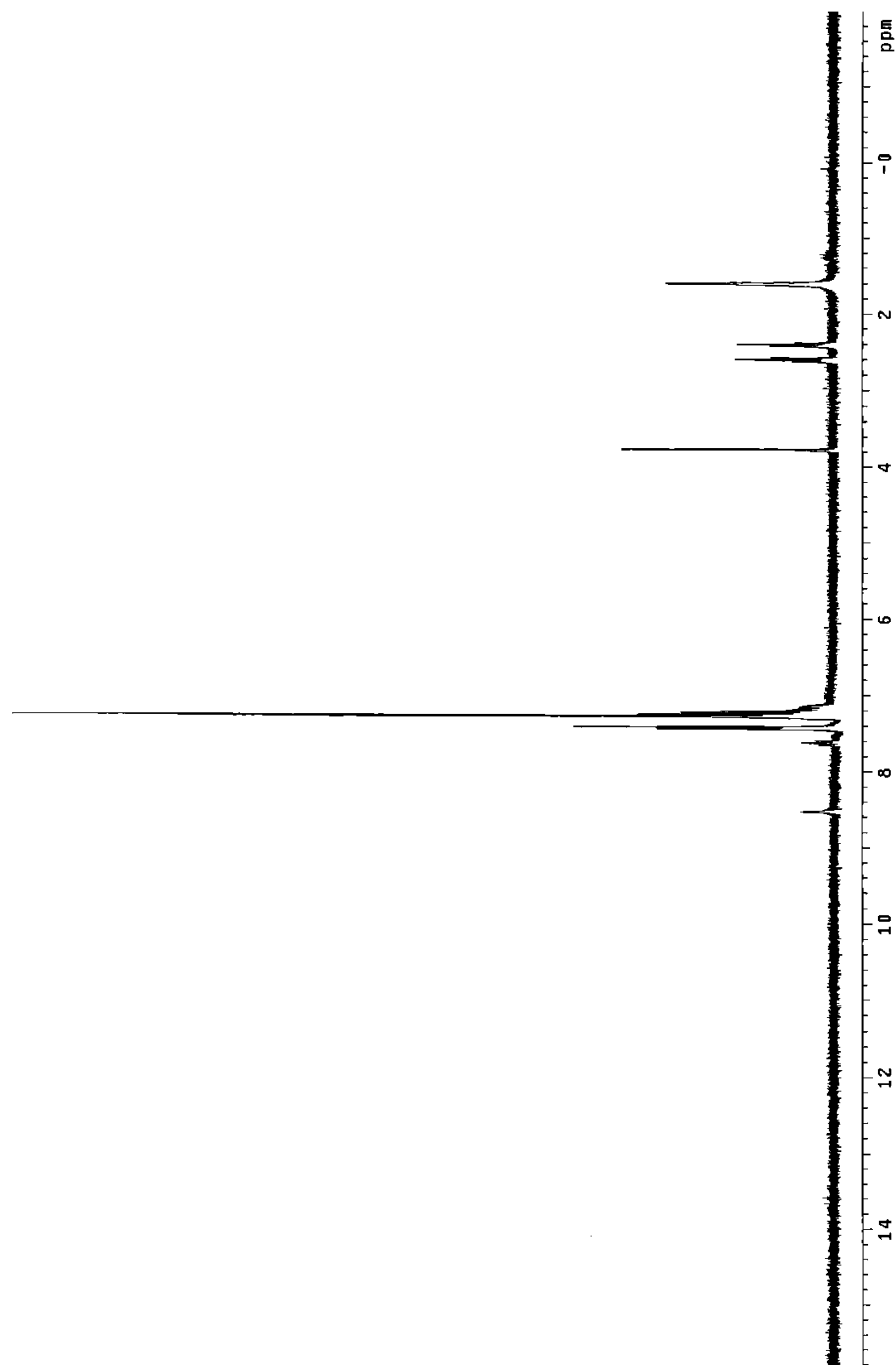
Spectrum 2.1. IR spectrum of $\text{Re}(\text{CO})_3(\text{MEPA})$.



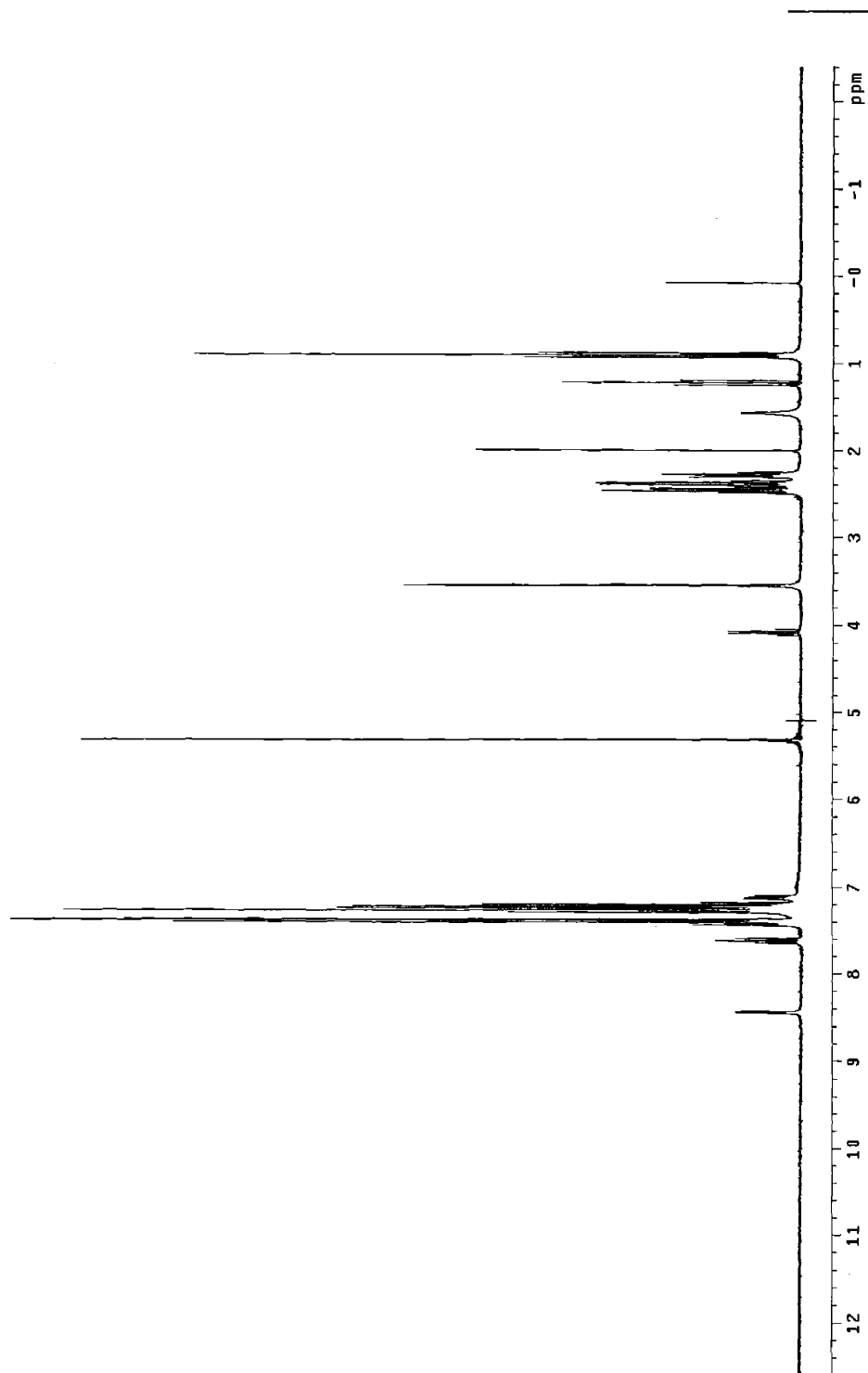
Spectrum 2.2. ^1H NMR spectrum (wet CD_2Cl_2) of $\text{Re}(\text{CO})_3(\text{MEPA})$.



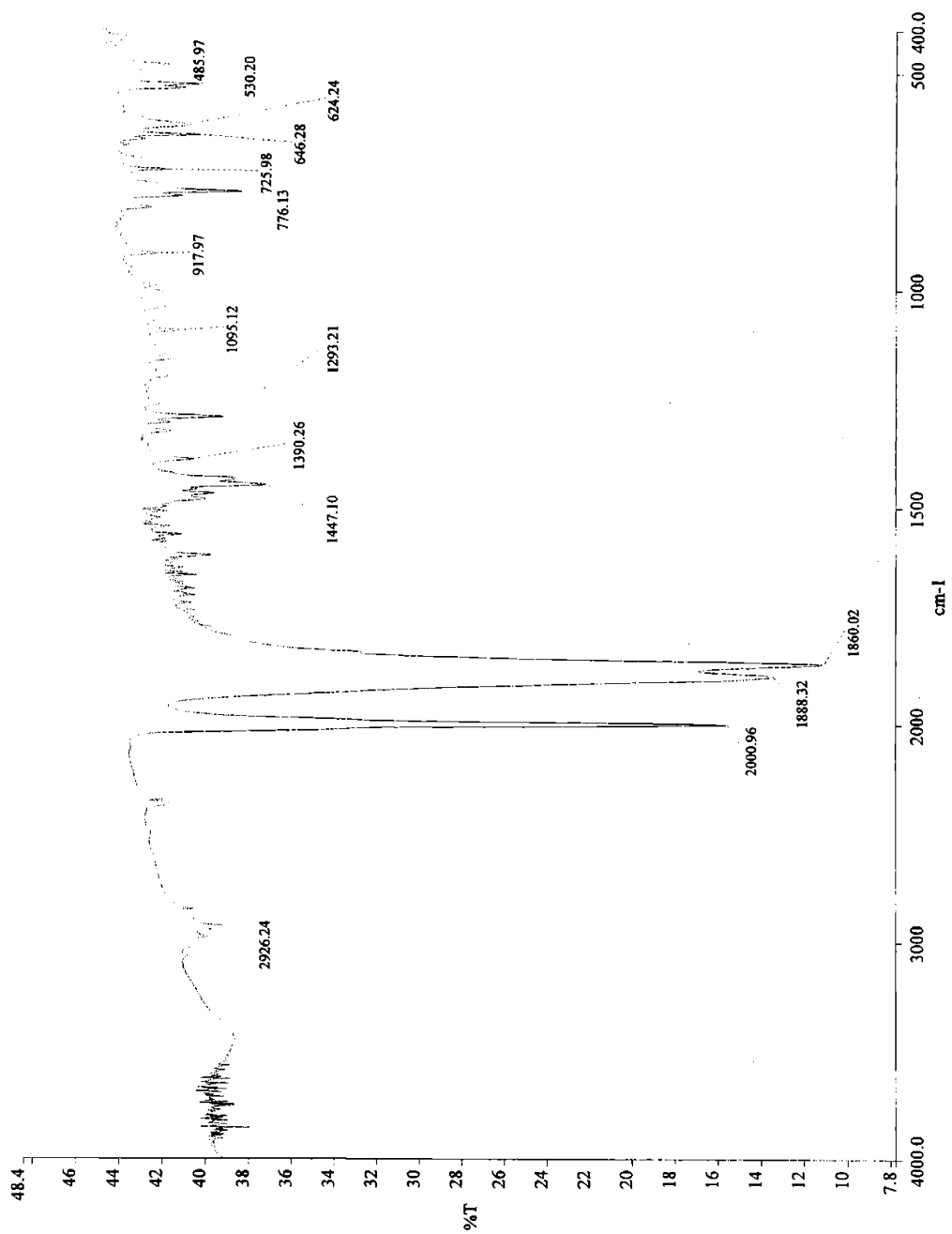
Spectrum 2.3. ^1H NMR spectrum (CDCl_3) of MEPAH-STr.



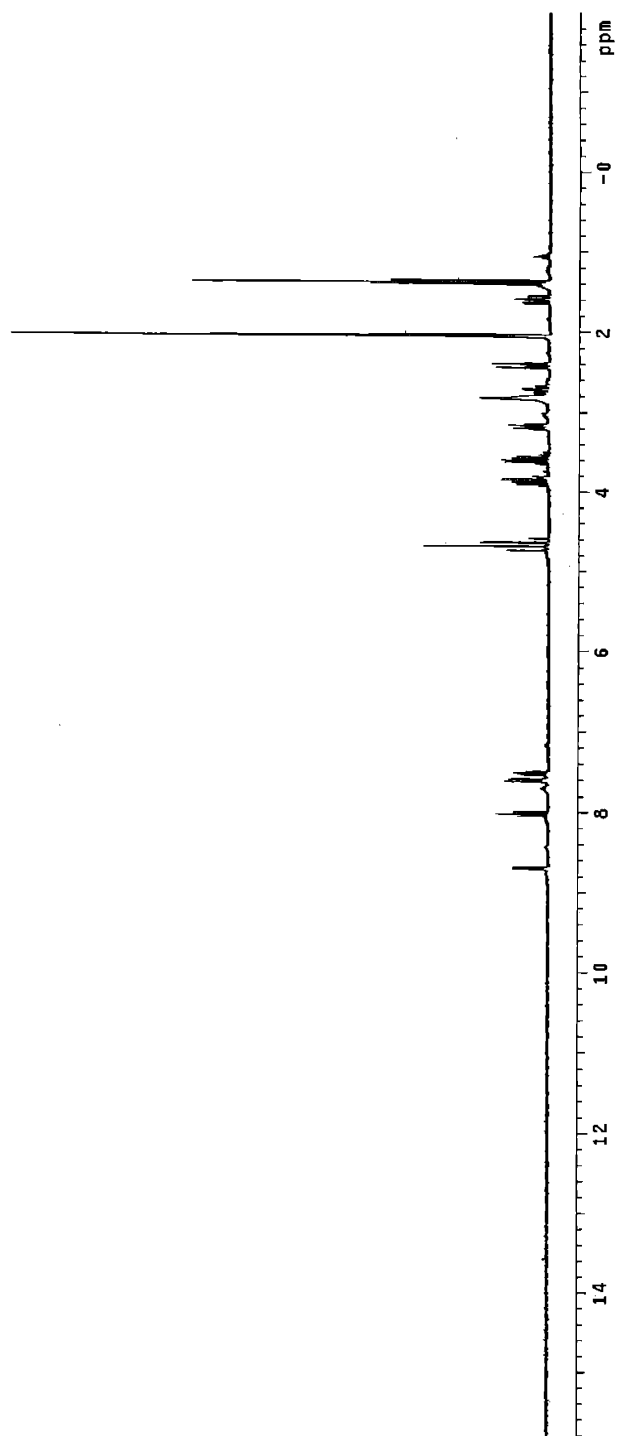
Spectrum 2.4. ^1H NMR spectrum (CD_2Cl_2) of MEPAH-NEt-STr.



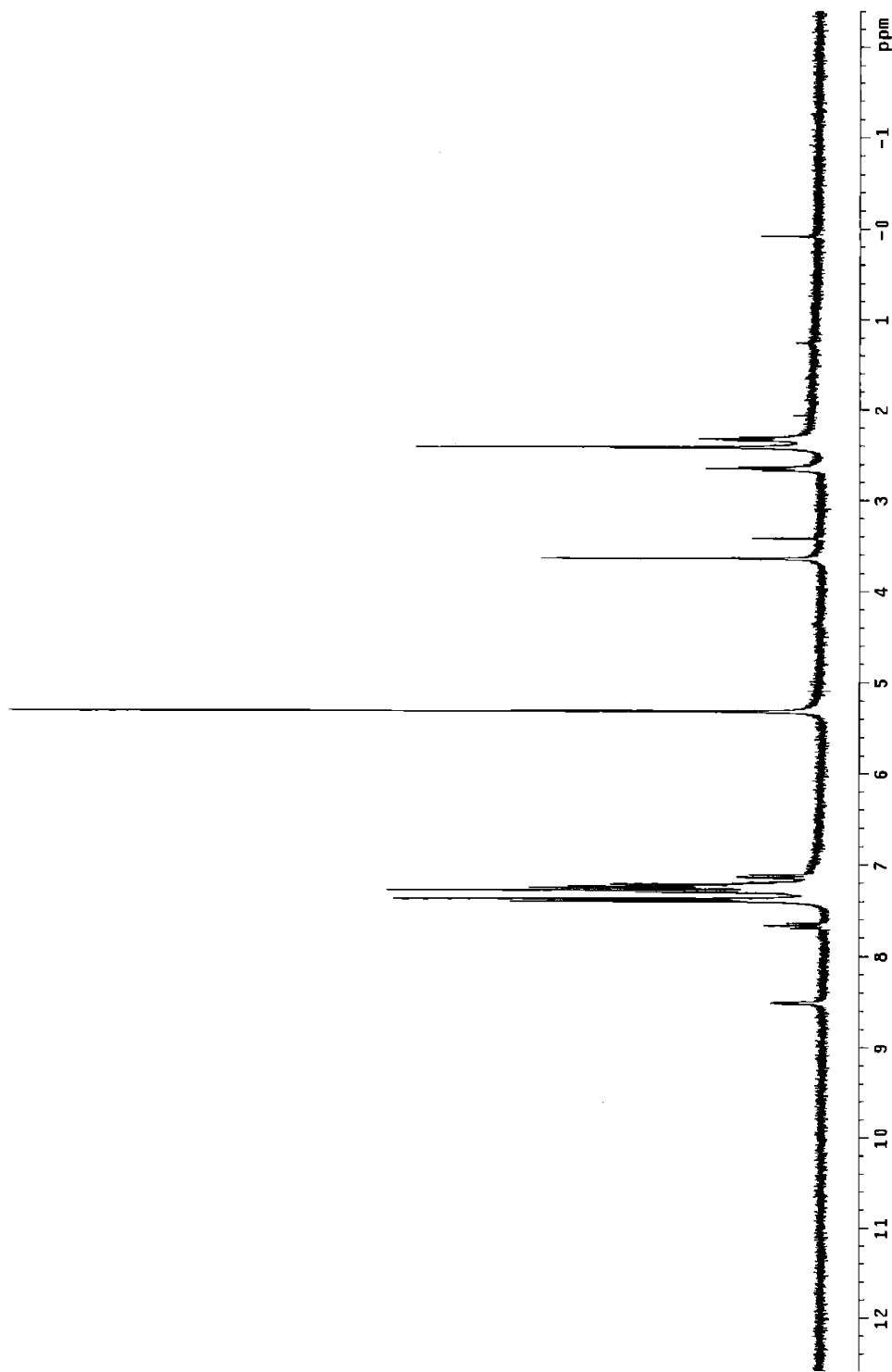
Spectrum 2.5. IR spectrum of $\text{Re}(\text{CO})_3(\text{MEPA-NEt})$.



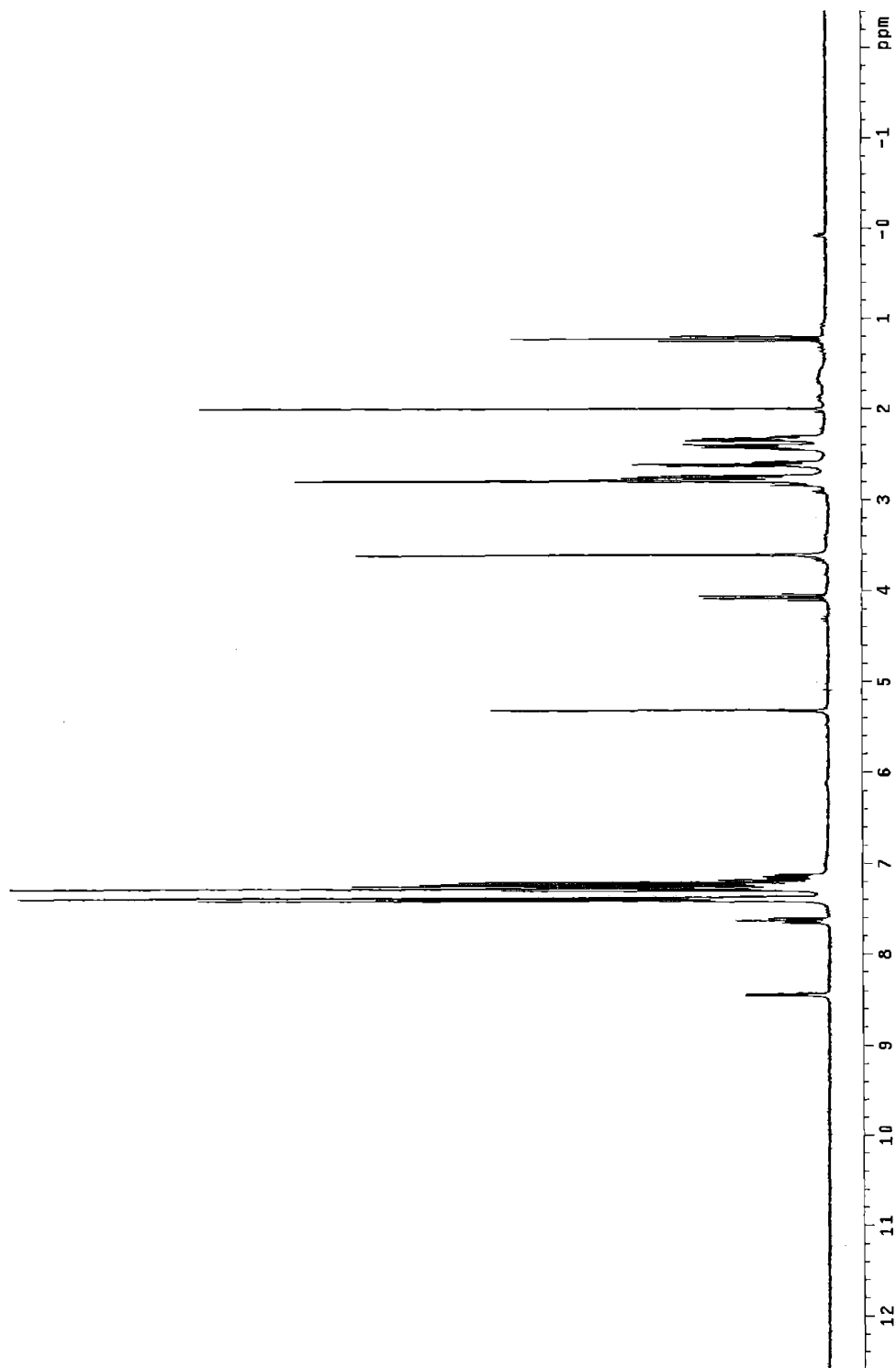
Spectrum 2.6. ^1H NMR spectrum (CD_3COCD_3) of $\text{Re}(\text{CO})_3(\text{MEPA-NEt})$.



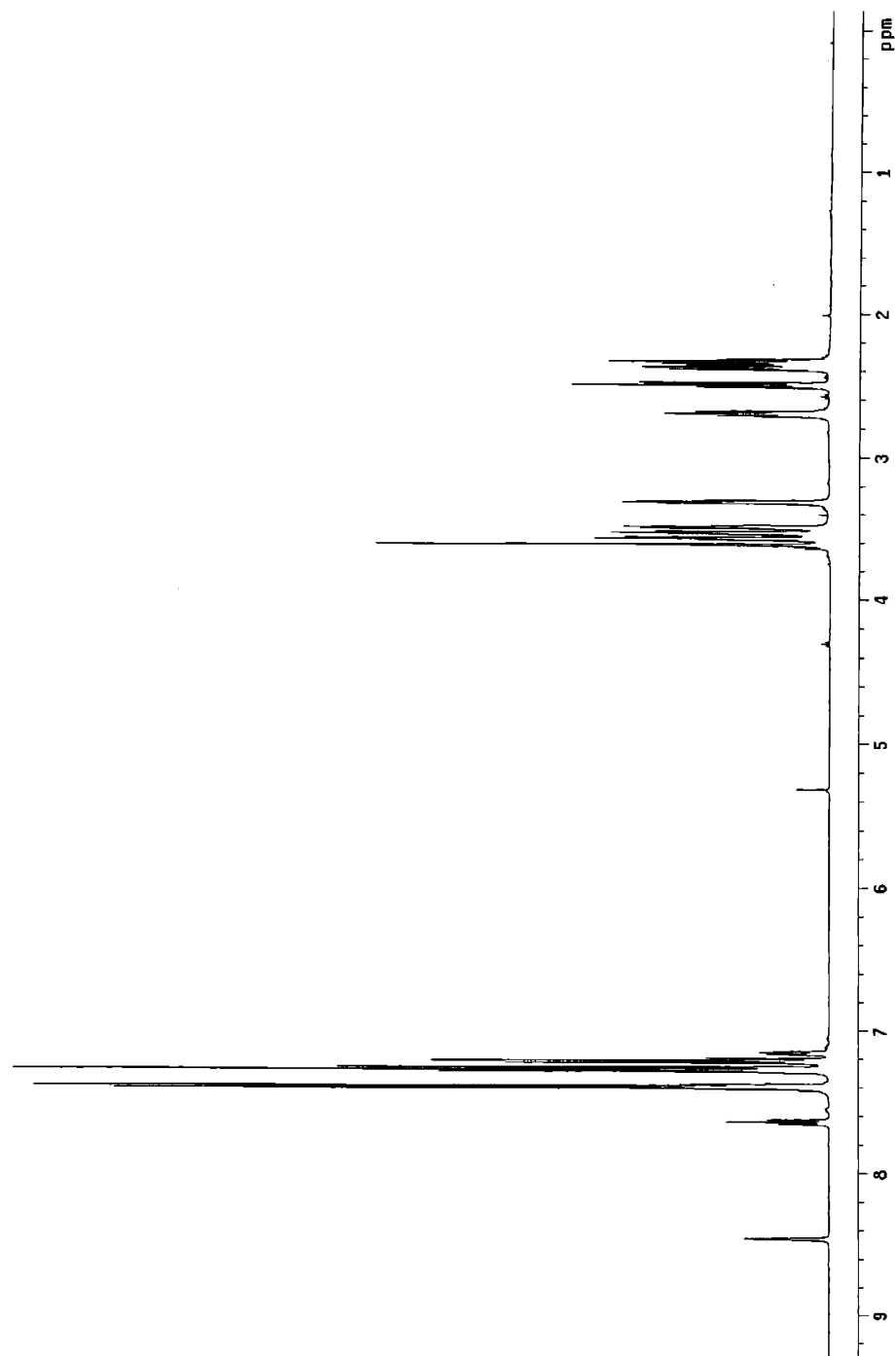
Spectrum 2.7. ^1H NMR spectrum (CD_2Cl_2) of MEPAH- $\text{C}_2\text{CO}_2\text{H}$ -STr.



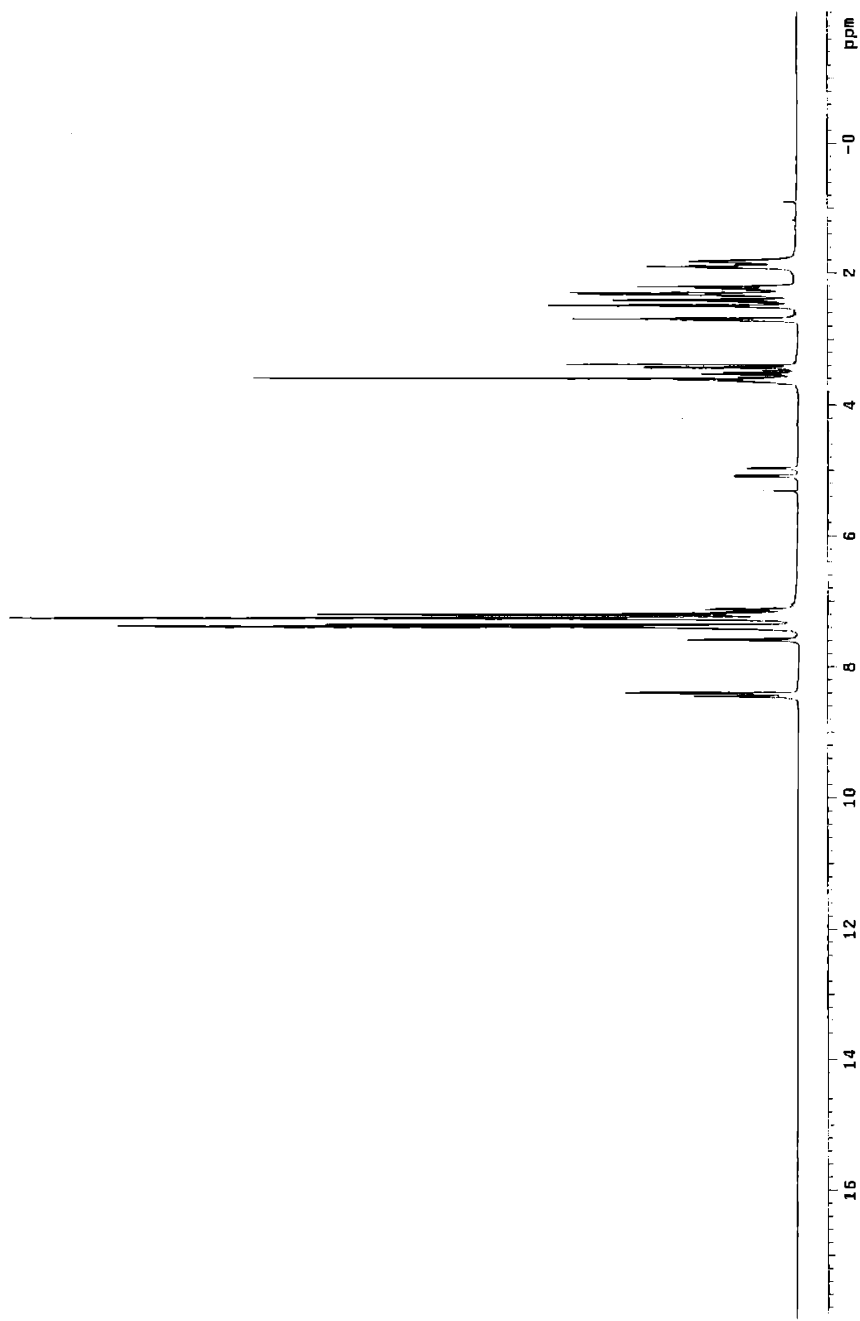
Spectrum 2.8. ^1H NMR spectrum (CD_2Cl_2 , traces EtOAc) of *N*-propionyl-NHS-MEPAH-STr.



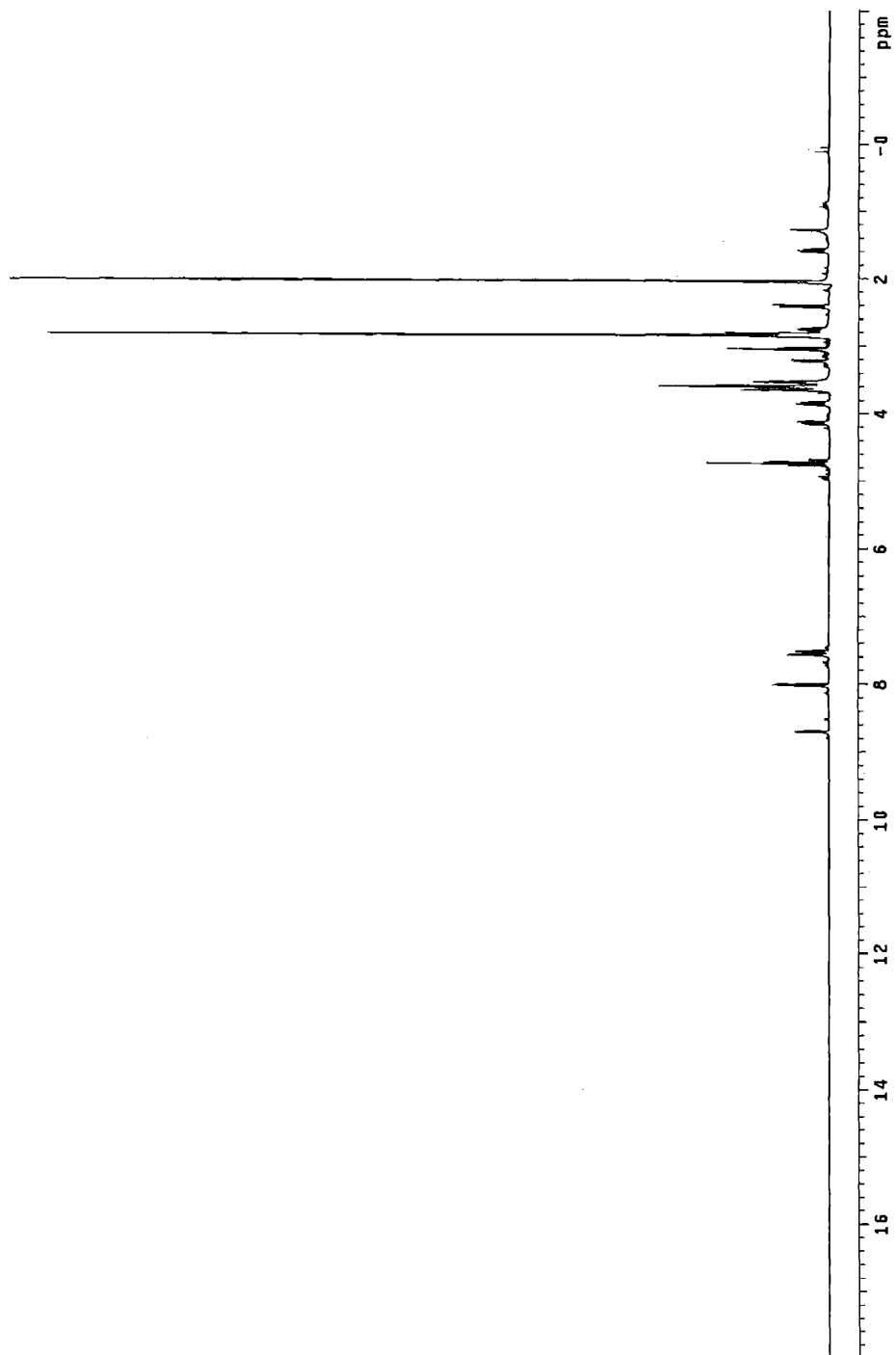
Spectrum 2.9. ^1H NMR spectrum (CD_2Cl_2) of MEPAH- $\text{C}_2\text{COmorph-Sr}$.



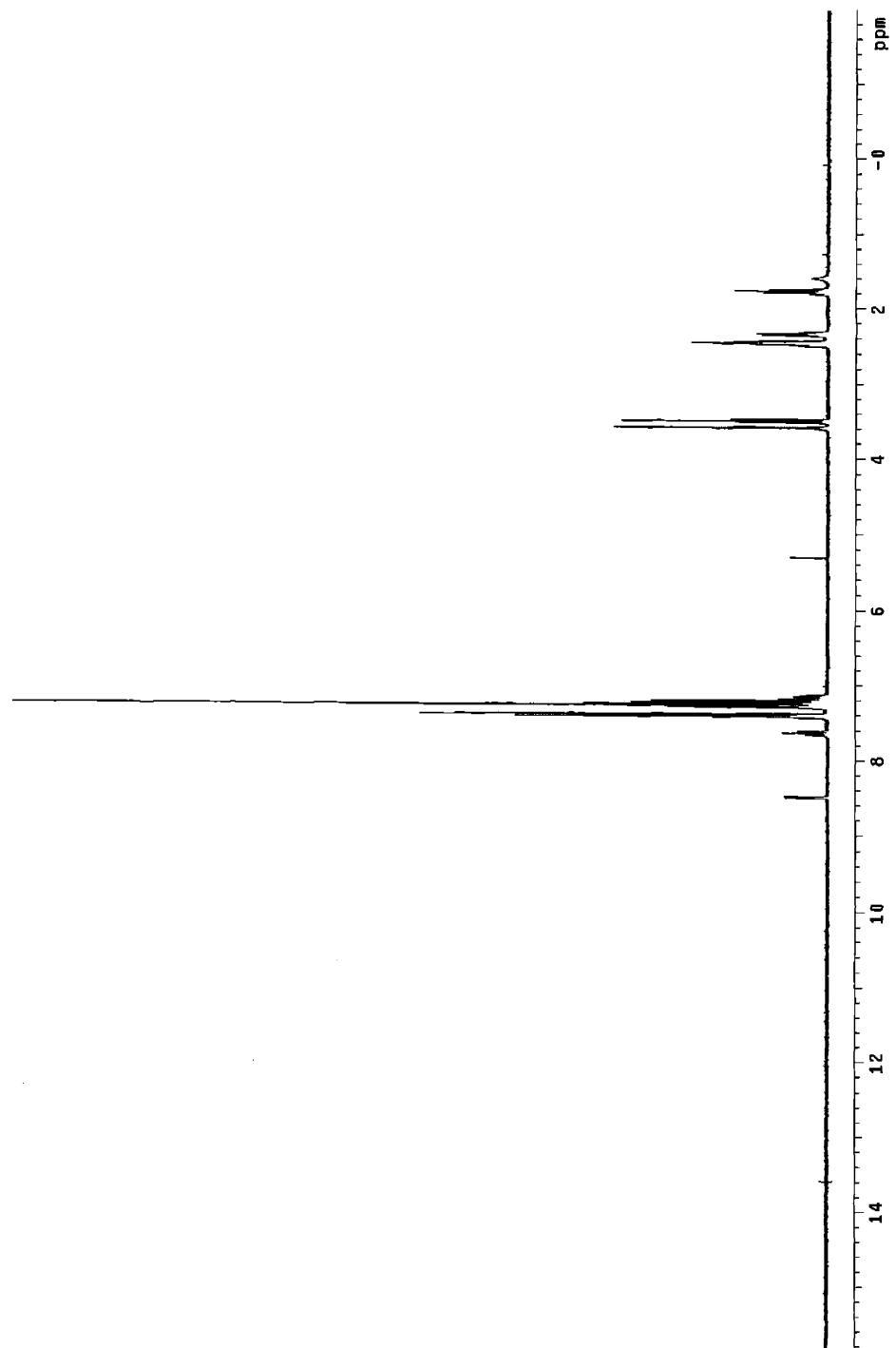
Spectrum 2.10. ^1H NMR spectrum (CD_2Cl_2) of MEPAH- $\text{C}_2\text{CONornic}$ -STr.



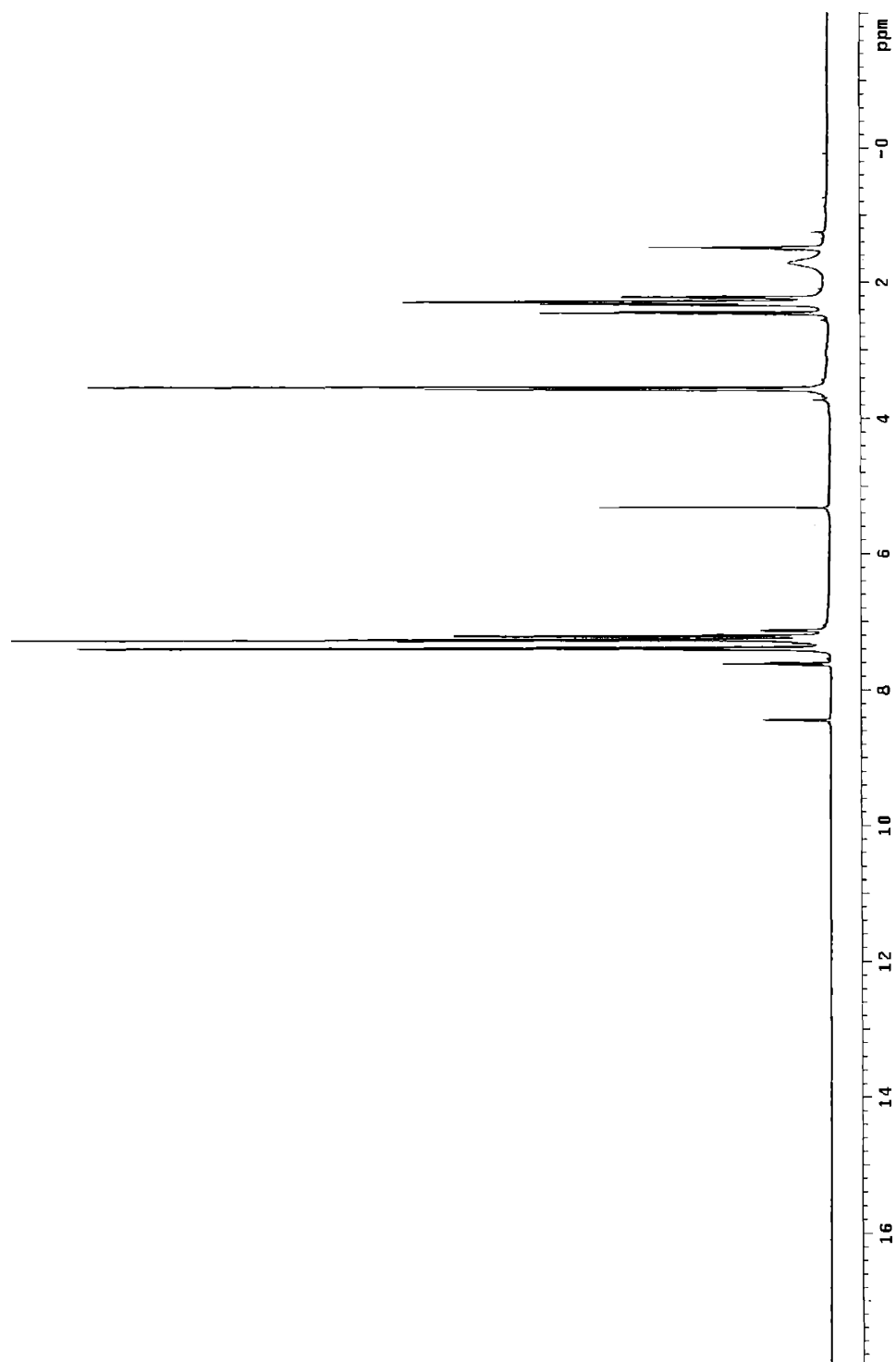
Spectrum 2.11. ^1H NMR spectrum (CD_3COCD_3) of $\text{Re}(\text{CO})_3(\text{MEPA-C}_2\text{COmorph})$.



Spectrum 2.12. ^1H NMR spectrum (CDCl_3) of MEPAH- C_3Cl -STr.



Spectrum 2.13. ^1H NMR spectrum (CD_2Cl_2) of MEPAH- C_3 morph-STr.



References

- (1) Abrams, M. J.; Davison, A.; Jones, A. G.; Costello, C. E.; Pang, H. *Inorg. Chem.* **1983**, *22*, 2798.
- (2) Meltzer, P. C.; Blundell, P.; Jones, A. G.; Mahmood, A.; Garada, B.; Zimmerman, R. E.; Davison, A.; Holman, B. L.; Madras, B. K. *J. Med. Chem.* **1997**, *40*, 1835.
- (3) Dilworth, J. R.; Parrott, S. *Chem. Soc. Rev.* **1998**, *27*, 43.
- (4) Hom, R. K.; Katzenellenbogen, J. A. *Nucl. Med. Biol.* **1997**, *24*, 485.
- (5) Chi, D. Y.; O'Neil, J. P.; Anderson, C. J.; Welch, M. J.; Katzenellenbogen, J. A. *J. Med. Chem.* **1994**, *37*, 928.
- (6) Hom, R. K.; Chi, D. Y.; Katzenellenbogen, J. A. *J. Org. Chem.* **1996**, *61*, 2624.
- (7) Johannsen, B.; Spies, H. *Top. Curr. Chem* **1996**, *176*, 77.
- (8) Alberto, R.; Schibli, R.; Egli, A.; Schubiger, P. A.; Herrmann, W. A.; Artus, G.; Abram, U.; Kaden, T. A. *J. Organomet. Chem.* **1995**, *493*, 119.
- (9) Alberto, R.; Schibli, R.; Egli, A.; Schubiger, P. A.; Abram, U.; Kaden, T. A. *J. Am. Chem. Soc.* **1998**, *120*, 7987.
- (10) Alberto, R.; Schibli, R.; Schubiger, P. A.; Abram, U.; Pietzsch, H.-J.; Johannsen, B. *J. Am. Chem. Soc.* **1999**, *121*, 6076.
- (11) Schibli, R.; Bella, R. L.; Alberto, R.; Garcia-Garayoa, E.; Ortner, K.; Abram, U.; Schubiger, P. A. *Bioconjugate Chem.* **2000**, *11*, 345.
- (12) Pietzsch, H.-J.; Gupta, A.; Reising, M.; Drews, A.; Seifert, S.; Syhre, R.; Spies, H.; Alberto, R.; Abram, U.; Schubiger, P. A.; Johannsen, B. *Bioconjugate Chem.* **2000**, *11*, 414.
- (13) Schibli, R.; Alberto, R.; Abram, U.; Abram, S.; Egli, A.; Schubiger, P. A.; Kaden, T. A. *Inorg. Chem.* **1998**, *37*, 3509.
- (14) Kramer, D. J.; Davison, A.; Jones, A. G. *Inorg. Chim. Acta* **2001**, *312*, 215.
- (15) Bernard, J.; Ortner, K.; Spingler, B.; Pietzsch, H.-J.; Alberto, R. *Inorg. Chem.* **2003**, *42*, 1014.

- (16) Alberto, R.; Egli, A.; Abram, U.; Hegetschweiler, K.; Gramlich, V.; Schubiger, P. A. *J. Chem. Soc. Dalton Trans.* **1994**, 2815.
- (17) Babich, J. W.; Coco, W. G.; Barrow, S.; Fischmann, A. J.; Femia, F. J.; Zubieta, J. *Inorg. Chim. Acta* **2000**, 309, 123.
- (18) Alberto, R.; Schibli, R.; Angst, D.; Schubiger, P. A.; Abram, U.; Abram, S.; Kaden, T. A. *Transit. Met. Chem.* **1997**, 22, 597.
- (19) Jung, C. M.; Kraus, W.; Leibnitz, P.; Pietzsch, H. J.; Kropp, J.; Spies, H. *Eur. J. Inorg. Chem.* **2002**, 1219.
- (20) Maina, T.; Tsoukalas, C.; Patsis, G.; Pirmettis, I.; Nock, B.; Papadopoulos, M.; Raptopoulou, C.; Terzis, A.; Chiotellis, E. *Polyhedron* **1999**, 18, 3545.
- (21) Maresca, K. P.; Shoup, T. M.; Femia, F. J.; Burker, M. A.; Fischmann, A.; Babich, J. W.; Zubieta, J. *Inorg. Chim. Acta* **2002**, 338, 149.
- (22) Alberto, R. Personal communication; **2002**.
- (23) Alberto, R.; Schibli, R.; Abram, U.; Egli, A.; Knapp, F. F.; Schubiger, P. A. *Radiochim. Acta* **1997**, 79, 99.
- (24) Alberto, R.; Schibli, R.; Waibel, R.; Abram, U.; Schubiger, P. A. *Coord. Chem. Rev.* **1999**, 190-192, 901.
- (25) Egli, A.; Alberto, R.; Tannahill, L.; Schibli, R.; Abram, U.; Schaffland, A.; Waibel, R.; Tourwe, D.; Jeannin, L.; Iterbeke, K.; Schubiger, P. A. *J. Nucl. Med.* **1999**, 40, 1913.
- (26) Schibli, R.; Katti, K. V.; Higginbotham, C.; Volkert, W. A.; Alberto, R. *Nucl. Med. Biol.* **1999**, 26, 711.
- (27) Schibli, R.; Schwartzbach, R.; Alberto, R.; Ortner, K.; Schmalle, H.; Dumas, C.; Egli, A.; Schubiger, P. A. *Bioconjugate Chem.* **2002**, 13, 750.
- (28) Wang, W.; Yan, Y. K.; Hor, T. S. A.; Vittal, J. J.; Wheaton, J. R.; Hall, I. H. *Polyhedron* **2002**, 21, 1991.
- (29) Brand, U.; Vahrenkamp, H. *Inorg. Chem.* **1995**, 34, 3285.
- (30) Egli, A.; Hegetschweiler, K.; Alberto, R.; Abram, U.; Schibli, R.; Hedinger, R.; Gramlich, V.; Kissner, R.; Schubiger, P. A. *Organometallics* **1997**, 16, 1833.

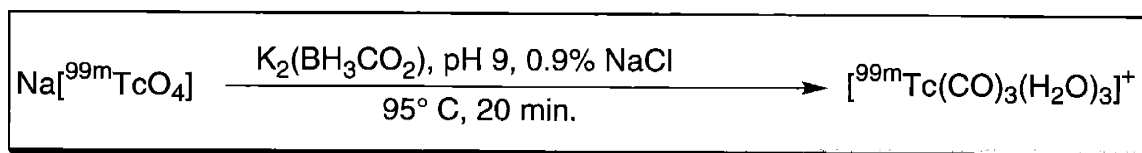
- (31) Civitello, E. R.; Dragovich, P. S.; Karpishin, T. B.; Novick, S. G.; Bierach, G.; O'Connell, J. F.; Westmoreland, T. D. *Inorg. Chem.* **1993**, *32*, 237.
- (32) Dong, Y.-B.; Yang, L.; Cheung, K.-K.; Mayr, A. *J. Organomet. Chem.* **2000**, *598*, 55.
- (33) Yam, V. W.-W.; Lau, V. C.-Y.; Cheung, K.-K. *Organometallics* **1995**, *14*, 2749.
- (34) Friebe, M.; Mahmood, A.; Bolzati, C.; Drews, A.; Johannsen, B.; Eisenhut, M.; Kramer, D.; Davison, A.; Jones, A. G. *J. Med. Chem.* **2001**, *44*, 3132.
- (35) Leung, W.-H.; Hun, T. S. M.; Fung, S.; Williams, I. D.; Wong, K.-Y. *Polyhedron* **1997**, *16*, 3641.
- (36) Wong, Y.-L.; Dilworth, J. R. *J. Chem. Soc. Dalton Trans.* **2002**, 2366.
- (37) Mahmood, A.; Friebe, M.; Eisenhut, M.; Bolzati, C.; Drews, A.; Johannsen, B.; Davison, A.; Jones, A. G. *J. Labelled Cpd. Radiopharm.* **2001**, *44*, S51.

Chapter Three

Radiopharmaceutical Application of Derivatives of *N*-(2-Mercaptoethyl)picolyamine as Ligands for the "*fac*-[^{99m}Tc(CO)₃]⁺" Core

Introduction

Alberto was able to synthesize $^{99}\text{Tc(I)}$ carbonyl starting materials using $\text{BH}_3\cdot\text{THF}$ as a non-coordinating reductant (see Chapter 1).¹ However, this work could not be easily translated to the no carrier added ($^{99\text{m}}\text{Tc}$) level since different conditions exist when working with a tracer ($<10^{-8}$ M), and the presence of aqueous solution precluded the use of borane.² Alberto found that $\text{K}_2\text{BH}_3\text{CO}_2$ was an effective reductant/CO source for $[\text{}^{99\text{m}}\text{TcO}_4]^-$ at pH 9 (Scheme 3.1). At temperatures above 85°C , potassium boranocarbonate releases CO in aqueous solution. In 15 minutes at 95°C , pertechnetate is reduced to $[\text{}^{99\text{m}}\text{Tc}(\text{CO})_3(\text{H}_2\text{O})_3]^+$ by $\text{K}_2\text{BH}_3\text{CO}_2$ in $>98\%$ radiochemical yield (r.c.y.).³ The trichloro complex is never formed in physiological saline (0.9% NaCl). The triqua complex serves as the synthon for tricarbonyl chemistry of $^{99\text{m}}\text{Tc}$.



Scheme 3.1. Synthesis of $[\text{}^{99\text{m}}\text{Tc}(\text{CO})_3(\text{H}_2\text{O})_3]^+$.

The rhenium complexes in Chapter 2 were synthesized as mimics of potential radiopharmaceuticals. Thus, MEPAH and its derivatives were investigated as ligands for the " $[\text{}^{99\text{m}}\text{Tc}(\text{CO})_3]^+$ " core. Biomolecular choice was made based on previous work,⁴⁻¹² and the biological targets are described below.

Melanoma is the cancer whose frequency is most rapidly increasing. In particular, melanoma of the skin is becoming quite common, and at least 33,000 deaths are attributable to melanoma of the skin annually.¹³ Studies by Eisenhut and co-workers have established that radioiodinated benzamides such as [¹²³I]BZA and [¹²³I]IMBA (Figure 3.1a,b) have high affinity for melanoma, and these compounds have entered phase II clinical trials for use in melanoma imaging.¹⁴⁻¹⁶

While the ¹²³I radiopharmaceuticals do provide good images of melanoma, investigations have been underway for some time into ^{99m}Tc species that have similar tumor uptake since ^{99m}Tc is more widely available than ¹²³I. Examples of some of the most successful ^{99m}Tc melanoma imaging agents are shown in Figure 3c,d. Studies of these and other ^{99m}Tc complexes have shown that the tertiary amine functionality is the most important moiety for melanoma binding.^{5,7,17} Complexes of ^{99m}Tc containing a benzamide moiety exhibit lower tumor uptake.⁴

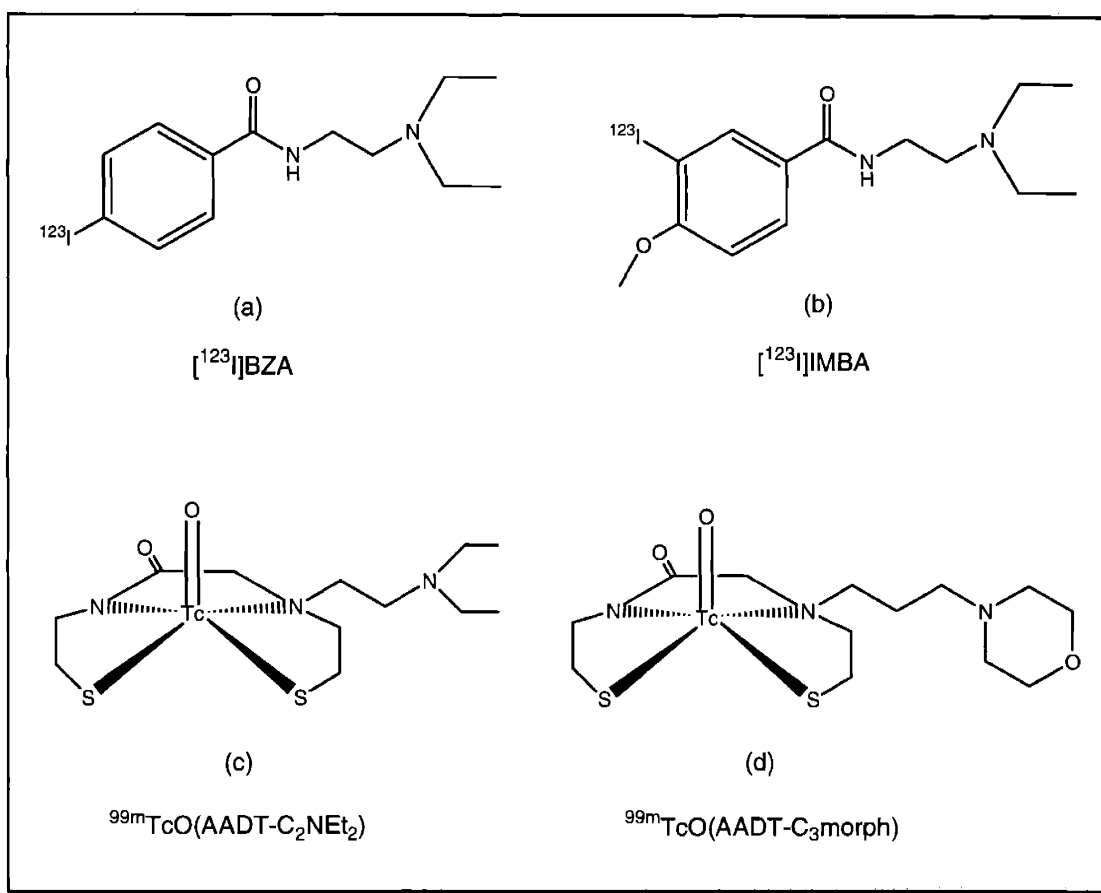


Figure 3.1. Examples of radiopharmaceuticals targeting melanoma.

The investigation of morpholine-linked MEPAH-based radiopharmaceuticals was undertaken to compare Tc(I) carbonyl compounds to higher-valent Tc(V) oxo complexes to see if lower oxidation state $^{99\text{m}}\text{Tc}$ complexes would also be viable for melanoma scintigraphy. Additionally, since both amide and amine linkages were synthesized, the importance of the tertiary amine functionality to tumor binding was evaluated.

The other biomolecule that was investigated was normicotine, which was used as an analogue to nicotine. Nicotine is a potent ligand for nicotinic acetylcholine receptors

in the brain, and has been reported as a potential treatment for Parkinson's Disease, Alzheimer's Disease, and Attention Deficit Hyperactivity Disorder.^{6,12,18,19} Radiopharmaceuticals aimed at imaging these receptors to monitor uptake changes in disease states have been synthesized, including 5-[¹²⁵I-iodo]- and [¹¹C-methyl]-nicotine.⁹⁻¹¹ These compounds have met with varying success, and the isotopes' low availability (especially ¹¹C which is cyclotron generated with $t_{1/2} = 20$ min) has led to the desire to create a ^{99m}Tc radiopharmaceutical that can image these receptors.

Thus, we have undertaken an investigation of the derivative, nornicotine (Figure 3.2), which possesses an amine proton on the pyrrolidine ring thereby allowing conjugation of the diamine to MEPAH-based ligands. The corresponding ^{99m}Tc tricarbonyl complexes were evaluated *in vivo* to determine the brain uptake of nornicotine-conjugated complexes.

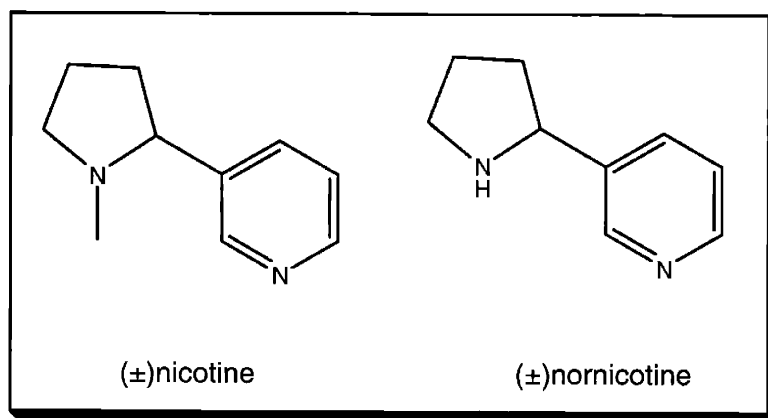


Figure 3.2. The bioactive molecule, nicotine, and its analogue, nornicotine.

Experimental

General Considerations. Trifluoroacetic acid (TFA) was distilled under nitrogen prior to use. ^{99m}Tc was obtained as $\text{Na}[^{99m}\text{TcO}_4]$ in 0.9% NaCl aqueous solution from the radiopharmacy at the Brigham & Women's Hospital, Boston, MA. $[\text{}^{99m}\text{Tc}(\text{CO})_3(\text{H}_2\text{O})_3]^+$ was synthesized as described in the literature.³ HPLC was performed on a Waters Millennium Chromatography System equipped with a 996 UV-Vis diode-array detector attached in series to a gamma detector consisting of a shielded photomultiplier powered by a Canberra voltage amplifier and connected to a ratemeter. A reversed phase C_{18} silica column (220 x 4.6 mm) equipped with a C_{18} guard (30 x 4.6 mm) was used with the following linear gradient (A: 0.005 M PBS pH 7.6; B: MeOH; gradient given in t(min)/%B: 0/5, 5/5, 35/85, 40/85, 45/98, 55/98, 65/5) at a flow rate of 1.0 mL/min. Radiochemical yields were determined by integration of the gamma chromatogram from the HPLC. Compounds prepared for radiopharmaceutical evaluation (biodistribution) were purified by preparative isolation of the appropriate peak on the HPLC.

Murine B16/F0 melanoma cells (ATCC) were grown by Dr. Zhen Cheng in T-175 flasks in 14 mL Dulbecco's Modified Eagle Medium (D-MEM; Gibco, Life Technology, Gaithersburg, MD) containing 4500 mg/L D-glucose, L-glutamine, and pyridoxine hydrochloride, 110 mg/L sodium pyruvate, 10% fetal bovine serum (FBS), 0.2% gentamicin and 0.5% penicillin–streptomycin solution. All cells were harvested from cell culture flasks by trypsinization with 1 mL trypsin–EDTA solution (0.25% trypsin, 1 mM EDTA x 4 Na) (Gibco). After being washed with 12 mL Dulbecco's Phosphate-Buffered

Saline (PBS) (Gibco), pH 7.2, the cells were counted and resuspended at a concentration of 5×10^6 cell/mL PBS.

Deprotection of Tritylated Ligands

In a typical preparation of ligands for labeling with ^{99m}Tc , 3 mg of a tritylated ligand was dissolved in 3 mL TFA to give a yellow solution. One or two drops of Et_3SiH were added, and color discharge was noted. The TFA was removed *in vacuo*. The residue was dissolved in 600 μL MeOH. This was divided into 6 test tubes. The MeOH was removed *in vacuo*, and the tubes containing deprotected ligand were stored under vacuum until they were used in labeling experiments.

General Preparation of $^{99m}\text{Tc}(\text{CO})_3(\text{MEPA-X})$ complexes

An aqueous solution of $[\text{}^{99m}\text{Tc}(\text{CO})_3(\text{H}_2\text{O})_3]^+$ (up to 50 mCi) was added to a test tube containing 0.3 mL PBS (0.005 M, pH 7.6) and ~0.25 mg of MEPAH-X (X is derivatization off of internal nitrogen). The test tube was heated in a 75°C water bath for 40 minutes. Then, the tube was centrifuged at 3400 rpm for 10 minutes to separate suspended triphenylmethane. HPLC retention times and radiochemical yields are listed below. The composition of the ^{99m}Tc complexes was confirmed by co-elution of a sample of the corresponding rhenium complex (< 1 mg in 50 μL MeOH) with the ^{99m}Tc -labeled species.

$^{99m}\text{Tc}(\text{CO})_3(\text{MEPA-C}_2\text{COmorph})$. $t_R = 30.3$ min. r.c.y.: 91%.

$^{99m}\text{Tc}(\text{CO})_3(\text{MEPA-C}_3\text{morph})$. $t_R = 34.4$ min. r.c.y.: 99%

$^{99m}\text{Tc}(\text{CO})_3(\text{MEPA-C}_2\text{CONornic})$. $t_R = 30.6$ min. r.c.y.: 91%

Animal Studies

All animal experiments were performed in compliance with the *Principles of Laboratory Animal Care* (NIH publication #85-23, revised 1985) in collaboration with Prof. Ashfaq Mahmood and Dr. Zhen Cheng. Biodistribution studies and *in vivo* tumor uptake measurements of $^{99m}\text{Tc}(\text{CO})_3(\text{MEPA-C}_2\text{COmorph})$ and $^{99m}\text{Tc}(\text{CO})_3(\text{MEPA-C}_3\text{morph})$ were performed in C57B16 mice (20 to 30 g) bearing the B16/F0 murine melanoma on the hind limb. Subcutaneous melanoma tumors (B16/F0) were obtained by an inoculation of 0.5×10^6 cells (B16/F0) (0.1 mL) subcutaneously in the left hind flank of C57B16 mice. Ten to 17 days later the animals developed palpable tumor nodules 5 to 10 mm in diameter. Biodistribution studies of $^{99m}\text{Tc}(\text{CO})_3(\text{MEPA-C}_2\text{CONornic})$ were performed in Swiss white mice (30 to 35 g). The biodistribution studies and *in vivo* tumor-uptake measurements of the ^{99m}Tc complex were carried out by tail-vein injection of 10 to 30 μCi (0.05 to 0.1 mL) of the ^{99m}Tc -labeled complexes by Ms. Alice Carmel and sacrificing the mice at the designated time post-injection. The organs and tumors were harvested and blotted dry (when appropriate), weighed, and counted in a gamma counter along with ^{99m}Tc standards of the injected dose. The results are expressed as % ID/g tissue (Tables 3.1 and 3.2).

Table 3.1. Biodistribution of $^{99m}\text{Tc}(\text{CO})_3(\text{MEPA-C}_2\text{C}_2\text{O morph})$ and $^{99m}\text{Tc}(\text{CO})_3(\text{MEPA-C}_3\text{ morph})$.

Compound	$^{99m}\text{Tc}(\text{CO})_3(\text{MEPA-C}_2\text{C}_2\text{O morph})$			$^{99m}\text{Tc}(\text{CO})_3(\text{MEPA-C}_3\text{ morph})$		
	30 minutes	1 hour		30 minutes	1 hour	2 hours
Organs						
Blood	0.54 ± 0.09%	0.31 ± 0.07%		1.89 ± 0.22%	1.43 ± 0.12%	0.92 ± 0.05%
Heart	0.22 ± 0.03%	0.13 ± 0.04%		1.02 ± 0.13%	0.77 ± 0.09%	0.42 ± 0.05%
Liver	4.25 ± 0.47%	2.83 ± 1.30%		10.71 ± 1.38%	8.62 ± 1.26%	6.94 ± 1.31%
Lungs	0.38 ± 0.06	0.27 ± 0.09%		1.93 ± 0.28%	1.43 ± 0.25%	0.90 ± 0.10%
Muscle	0.14 ± 0.04	0.09 ± 0.03%		0.44 ± 0.08%	0.32 ± 0.06%	0.25 ± 0.04
Kidneys	5.33 ± 0.94%	3.42 ± 0.34%		13.49 ± 2.76%	9.42 ± 3.34%	5.67 ± 2.72%
Spleen	0.39 ± 0.08%	0.25 ± 0.07%		1.52 ± 0.27%	1.28 ± 0.11%	1.06 ± 0.80
Brain	0.02 ± 0.00%	0.01 ± 0.01%		0.06 ± 0.01%	0.04 ± 0.01%	0.03 ± 0.00
Melanoma	0.59 ± 0.17%	0.44 ± 0.12%		1.85 ± 0.37%	1.26 ± 0.30%	1.48 ± 0.18%
Skin	2.19 ± 1.83%	0.27 ± 0.15%		0.89 ± 0.11%	0.67 ± 0.10%	0.65 ± 0.11%
Mel/Blood	1.10	1.44		0.98	0.88	1.61
Mel/Liver	0.14	0.16		0.17	0.15	0.21
Mel/Lung	1.57	1.62		0.96	0.88	1.64
Mel/Spleen	1.51	1.78		1.22	0.98	1.40
Mel/Skin	0.27	1.62		2.09	1.89	2.29

Table 3.2. Biodistribution of $^{99m}\text{Tc}(\text{CO})_3(\text{MEPA-C}_2\text{CONornic})$.

Compound	$^{99m}\text{Tc}(\text{CO})_3(\text{MEPA-C}_2\text{CONornic})$	
	30 minutes	1 hour
Organs		
Blood	0.84 ± 0.15%	0.58 ± 0.02%
Heart	0.26 ± 0.04%	0.19 ± 0.05%
Liver	7.21 ± 1.23%	6.27 ± 0.65%
Lungs	0.59 ± 0.13%	0.46 ± 0.07%
Muscle	0.20 ± 0.07%	0.13 ± 0.07%
Kidneys	4.26 ± 1.61%	2.48 ± 0.61%
Spleen	0.88 ± 0.35%	0.82 ± 0.63%
Brain	0.03 ± 0.01%	0.02 ± 0.00%
Skin	0.53 ± 0.16%	0.59 ± 0.45%

Serum Stability Studies

HPLC purified samples of $^{99m}\text{Tc}(\text{CO})_3(\text{MEPA-C}_2\text{COMorph})$ and $^{99m}\text{Tc}(\text{CO})_3(\text{MEPA-C}_2\text{CONornic})$ were incubated in calf serum at 37° C for 1 h. The solutions were then filtered through an Amicon Centricon molecular weight cutoff centrifugal filter (10 kDa cutoff) which removed all proteins >10 kDa. The columns were washed with 2 x 500 µL distilled water and recentrifuged. Activity was then monitored in the top (filtered) fraction and compared to the activity in the bottom (filtrate) fraction to determine percent serum-bound material at 1 h. Results are shown in Table 3.3.

Table 3.3. Serum stability of selected ^{99m}Tc complexes.

Compound	Percent unbound after 1 h at 37° C
$^{99m}\text{Tc}(\text{CO})_3(\text{MEPA-C}_2\text{COMorph})$	90%
$^{99m}\text{Tc}(\text{CO})_3(\text{MEPA-C}_2\text{CONornic})$	80%

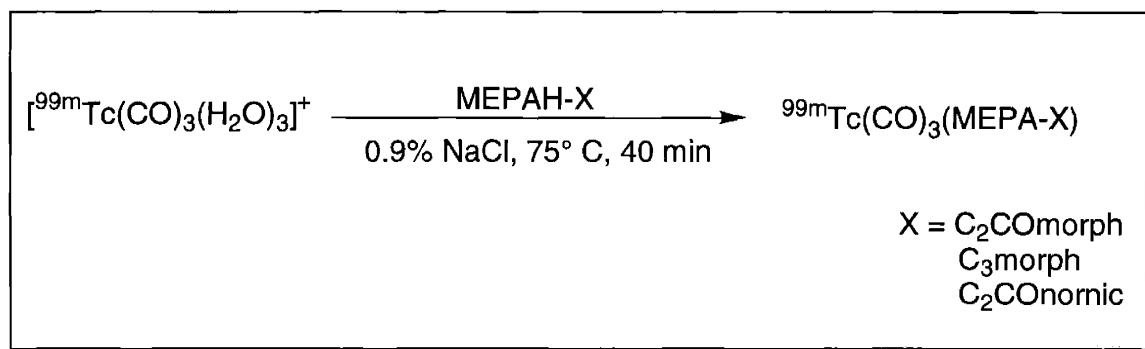
Lipophilicity Studies

An HPLC purified sample of $^{99m}\text{Tc}(\text{CO})_3(\text{MEPA-C}_2\text{CONornic})$ was dissolved in 2 mL PBS (pH 7.6) and 2 mL 1-octanol. The two layers were vortexed, allowed to settle, and centrifuged. One milliliter of the organic layer was removed and 1 mL PBS was added. The process above was repeated. The layers were separated and three 50 μL aliquots of each were placed in test tubes. These tubes were counted in a gamma counter.

$$\log D_{\text{pH } 7.6} = -0.054.$$

Results and Discussion

The syntheses of $^{99m}\text{Tc}(\text{CO})_3(\text{MEPA-X})$ compounds were accomplished by reaction of the corresponding ligands with $[\text{}^{99m}\text{Tc}(\text{CO})_3(\text{H}_2\text{O})_3]^+$ (Scheme 3.2). The fact that these compounds were synthesized in pH 9 buffer solution prevented significant decomposition from occurring after formation of the complexes (as discussed in Chapter 2). All of the compounds presented here have been synthesized in >90% radiochemical yield (r.c.y.), as determined from the integration of the γ ray HPLC chromatogram.



Scheme 3.2. Synthesis of ^{99m}Tc radiopharmaceuticals based on MEPAH.

In order to confirm the composition of the ^{99m}Tc species, it was necessary to perform co-injection experiments with the corresponding 'cold' rhenium complexes. The presence of a small amount of MeOH from the solution of the rhenium complex shifted the retention time of the ^{99m}Tc complexes slightly. One can see in Figures 3.3 - 3.5 that the compounds co-elute. The difference of time that is observed between the UV peak (first) and the γ peak (second) is due to the physical separation of the two detectors.

From this data, it is concluded that $^{99m}\text{Tc}(\text{CO})_3(\text{MEPA-C}_2\text{COmorph})$, $^{99m}\text{Tc}(\text{CO})_3(\text{MEPA-C}_3\text{morph})$, and $^{99m}\text{Tc}(\text{CO})_3(\text{MEPA-C}_2\text{CONornic})$ have been synthesized.

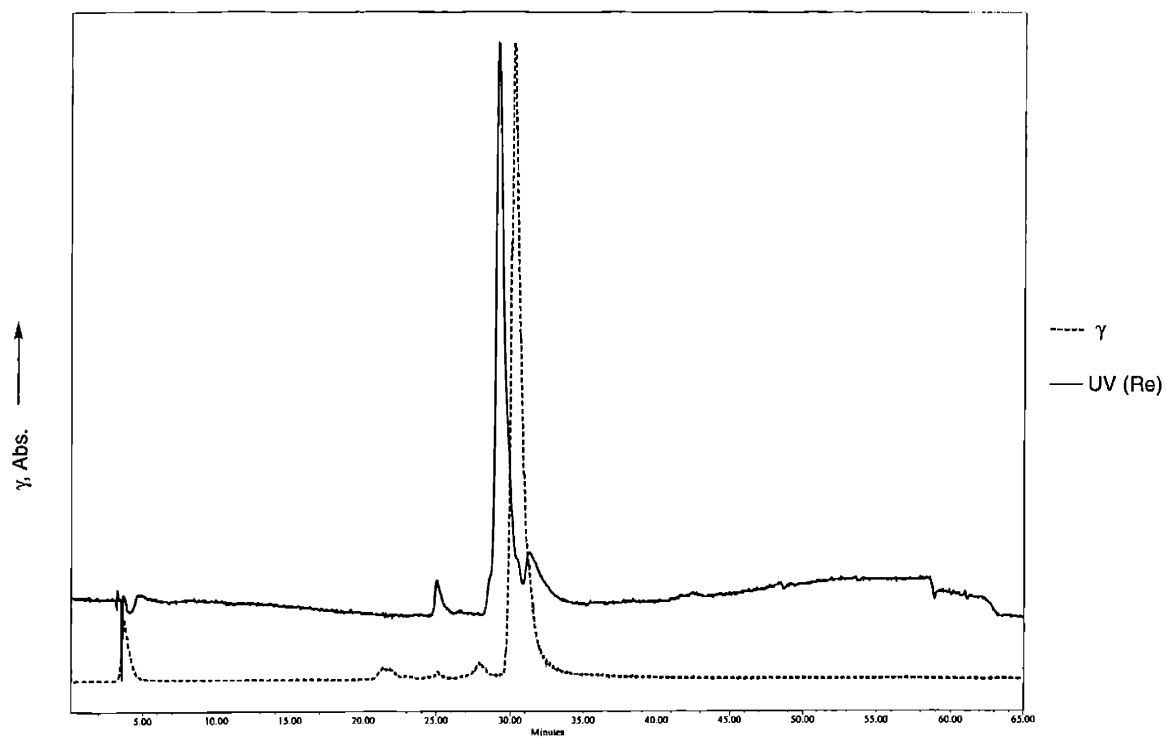


Figure 3.3. HPLC chromatogram of co-injected $^{99m}\text{Tc}/\text{Re}(\text{CO})_3(\text{MEPA-C}_2\text{COmorph})$.

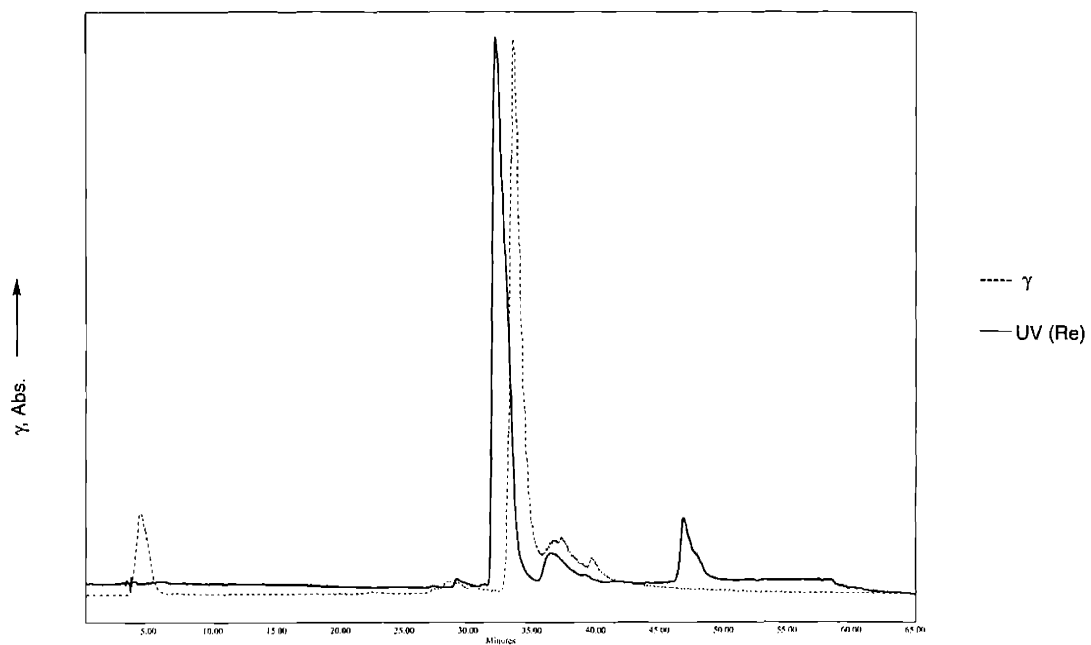


Figure 3.4. HPLC chromatogram of co-injected $^{99m}\text{Tc}/\text{Re}(\text{CO})_3(\text{MEPA}-\text{C}_3\text{morph})$.

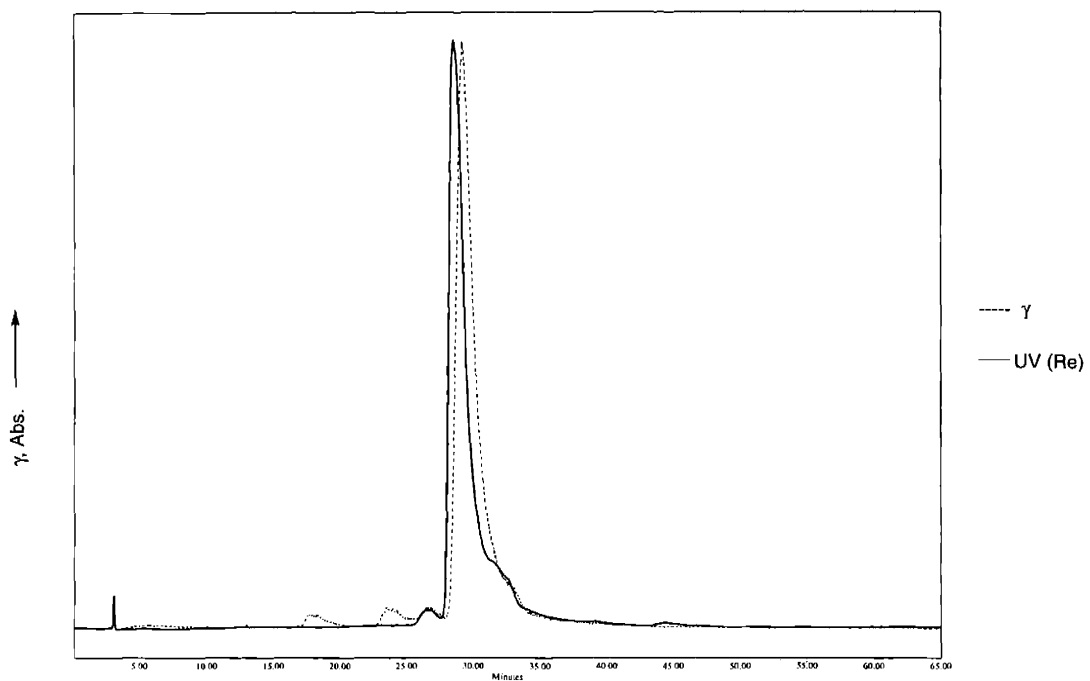


Figure 3.5. HPLC chromatogram of co-injected $^{99m}\text{Tc}/\text{Re}(\text{CO})_3(\text{MEPA}-\text{C}_2\text{CONomic})$.

One stability test prior to an *in vivo* biodistribution study was to examine the behavior of the complexes in the presence of serum proteins. Binding to serum proteins is indicative of high blood binding, which would significantly decrease the available activity for target binding. Both $^{99m}\text{Tc}(\text{CO})_3(\text{MEPA-C}_2\text{COMorph})$ and $^{99m}\text{Tc}(\text{CO})_3(\text{MEPA-C}_2\text{CONornic})$ were incubated at 37° C for 1 hour in calf serum. After filtration through a spin column, the amount of activity bound to the serum proteins was determined. In the case of $^{99m}\text{Tc}(\text{CO})_3(\text{MEPA-C}_2\text{COMorph})$, 90% of the complex remained unbound after 1 hour. The nornicotine analogue exhibited higher protein binding (~20% bound after 1 hour). The binding was not sufficiently high, though, to preclude *in vivo* animal biodistribution studies.

The first compound synthesized and evaluated for melanoma binding was $^{99m}\text{Tc}(\text{CO})_3(\text{MEPA-C}_2\text{COMorph})$. The results of the biodistribution study in C57Bl6 mice with subcutaneous melanoma are presented in Table 3.1. One can see that the ^{99m}Tc complex clears quite quickly from the body (low retained activity in all organs). Typically, the kidneys and liver possess significant activity due to the fact that they are part of the excretory pathway. Intestine and stomach activity is not reported due to the extremely high variability depending on how much fecal matter is present. From the data presented, one can conclude that $^{99m}\text{Tc}(\text{CO})_3(\text{MEPA-C}_2\text{COMorph})$ is not likely to be a successful radiopharmaceutical. Only $0.59 \pm 0.17\% \text{ID/g}$ accumulated in the tumor at 30 minutes, and it dropped to $0.44 \pm 0.12\% \text{ID/g}$ at 60 minutes. This compares rather unfavorably with $^{99m}\text{TcOAAADT-C}_3\text{morph}$ which possesses tumor uptake of $4.5\% \text{ID/g}$ at 60 minutes post-injection.⁷ Modest tumor:non-target tissue ratios were achieved, though,

with all non-excretory organs having lower uptake than the melanoma (skin value is statistically insignificant at 30 minutes). Additionally, these ratios did improve slightly at the 1 hour time point, indicating slightly more rapid washout from the background than from the tumor. Also, the tumor accumulation was non-zero; thus, an investigation into the amine derivative, $^{99m}\text{Tc}(\text{CO})_3(\text{MEPA-C}_3\text{morph})$, was undertaken.

While, unlike amides, amines have affinity for the $^{99m}\text{Tc}(\text{I})$ center, studies have shown that morpholine, in particular, has almost no affinity for the "*fac*- $[\text{M}(\text{CO})_3]^{+}$ " core ($\text{M} = \text{Tc}, \text{Re}$).²⁰ Therefore, coordination interference from morpholine was neither expected nor observed. As can be seen from the data in Table 3.1, the tumor uptake in mice is much higher (3-5 times the uptake of the amide), with uptake at 1 hour post-injection 1.3 - 2.1%ID/g, depending on the iteration. Additionally, modest to good tumor:background ratios were achieved. This compound does not possess the same degree of rapid clearance that the amide does, as can be seen by the higher activity retention in the liver and kidneys (due to increased lipophilicity), but the tumor:skin ratio, for instance, is approximately 2 at all time points. Unfortunately, excellent reproducibility of tumor uptake was not achievable with this compound. Comparing the two 1 hour experiments, all organs excepting the tumor have reproducible uptakes, within error. This could be due to some variability in the makeup of the injected tumor cells, but from both experiments, it is clear that the presence of the amine increases uptake by 200-400% in the Tc(I) system.

Initial studies with nornicotine-conjugated ^{99m}Tc complexes were carried out with the amide, $^{99m}\text{Tc}(\text{CO})_3(\text{MEPA-C}_2\text{CONornic})$. Given that significant lipophilicity is necessary to cross the blood-brain barrier (BBB), one might think that an amide is unlikely to cross, given the inherent polarity of such a compound. Indeed, this complex does not cross the BBB in any appreciable quantity (Table 3.2; max. $0.03 \pm 0.01\% \text{ID/g}$). A lipophilicity study found that $\log D_{\text{pH } 7.6}$ for this compound is -0.054, which implies significant hydrophilicity. In accordance with this property, the compound does clear very quickly, with $<1\% \text{ID/g}$ in all background tissue (excepting excretory organs). In fact, even the kidneys and liver have low activity at both 30 minutes and one hour post-injection. The poor brain uptake of this compound led to the investigation into the synthesis of the amine derivative, $^{99m}\text{Tc}(\text{CO})_3(\text{MEPA-C}_3\text{nornic})$, which would be expected to have higher lipophilicity. Studies aimed at synthesizing this potential radiopharmaceutical are detailed in Appendix B.

Conclusions

Investigations of compounds of the type $^{99m}\text{Tc}(\text{CO})_3(\text{MEPA-X})$ were carried out with the intention of creating potential radiopharmaceuticals. These complexes were evaluated both *in vitro* for serum stability, and *in vivo* for biodistribution.

The complexes $^{99m}\text{Tc}(\text{CO})_3(\text{MEPA-C}_2\text{COmorph})$ and $^{99m}\text{Tc}(\text{CO})_3(\text{MEPA-C}_3\text{morph})$ were examined for their potential use in melanoma diagnosis. The amide-linked compound, $^{99m}\text{Tc}(\text{CO})_3(\text{MEPA-C}_2\text{COmorph})$, exhibited fast clearance from background tissue but had very low uptake in melanoma. The analogous $-\text{C}_3\text{morph}$ derivative exhibited much higher tumor uptake (indicative of the importance of an amine linkage), but still well below the corresponding Tc(V) oxo complex, $^{99m}\text{TcOAADT-C}_3\text{morph}$. Additionally, although tumor:non-target tissue ratios were slightly above 1 in most cases (indicating preference of the complex for melanoma over other organs), they did not approach those of $^{99m}\text{TcOAADT-C}_3\text{morph}$, which exhibits ratios of approximately 10 (at 60 minutes post-injection).⁷

The other biomolecule of interest, nornicotine, was conjugated to the MEPAH backbone and was evaluated for brain uptake. Localization in the brain was low for the amide-linked $^{99m}\text{Tc}(\text{CO})_3(\text{MEPA-C}_2\text{CONornic})$. This was likely due to the significant hydrophilicity of the complex, an undesirable property for compounds designed to cross the BBB.

References

- (1) Alberto, R.; Schibli, R.; Egli, A.; Schubiger, P. A.; Herrmann, W. A.; Artus, G.; Abram, U.; Kaden, T. A. *J. Organomet. Chem.* **1995**, *493*, 119.
- (2) Alberto, R.; Schibli, R.; Egli, A.; Schubiger, A. P.; Abram, U.; Kaden, T. *A. J. Am. Chem. Soc.* **1998**, *120*, 7987.
- (3) Alberto, R.; Ortner, K.; Wheatley, N.; Schibli, R.; Schubiger, A. P. *J. Am. Chem. Soc.* **2001**, *123*, 3135.
- (4) Eisenhut, M.; Mohammed, A.; Mier, W.; Schönsiegel, F.; Friebe, M.; Mahmood, A.; Jones, A. G.; Haberkorn, U. *J. Med. Chem.* **2002**, *45*, 5802.
- (5) Friebe, M.; Mahmood, A.; Bolzati, C.; Drews, A.; Johannsen, B.; Eisenhut, M.; Kramer, D.; Davison, A.; Jones, A. G. *J. Med. Chem.* **2001**, *44*, 3132.
- (6) Levin, E. D.; Conners, C. K.; Sparrow, E.; Hinton, S. C.; Erhardt, D.; Meck, W. H.; Rose, J. E.; March, J. *Psychopharmacology* **1996**, *123*, 55.
- (7) Mahmood, A.; Friebe, M.; Eisenhut, M.; Bolzati, C.; Drews, A.; Johannsen, B.; Davison, A.; Jones, A. G. *J. Labelled Cpd. Radiopharm.* **2001**, *44*, S51.
- (8) Malago, E.; Mahmood, A.; Friebe, M.; Kramer, D.; Eisenhut, M.; Davison, A.; Jones, A. G. In *Technetium and Rhenium in Chemistry and Nuclear Medicine 6*, Nicolini, M. and Mazzi, U., eds., SGEEditoriali: Padova, **2002**, p. 419.
- (9) Nyback, H.; Halldin, C.; Ahlin, A.; Curvall, M.; Eriksson, L. *Psychopharmacology* **1994**, *115*, 31.
- (10) Saji, H.; Magata, Y.; Yamada, Y.; Tajima, K.; Yonekura, Y.; Konishi, J.; Ohmomo, Y.; Yokoyama, A. *Chem. Pharm. Bull.* **1992**, *40*, 734.
- (11) Saji, H.; Watanabe, A.; Magata, Y.; Ohmomo, Y.; Kiyono, Y.; Yamada, Y.; Iida, Y.; Yonekura, Y.; Konishi, J.; Yokoyama, A. *Chem. Pharm. Bull.* **1997**, *45*, 284.
- (12) White, H. K.; Levin, E. D. *Psychopharmacology* **1999**, *143*, 158.
- (13) Parkin, D. M.; Pisani, P.; Ferlay, J. *CA Cancer J. Clin.* **1999**, *49*, 33.
- (14) Eisenhut, M.; Hull, W. E.; Mohammed, A.; Mier, W.; Lay, D.; Just, W.; Gorgas, K.; Lehmann, W. D.; Haberkorn, U. *J. Med. Chem.* **2000**, *43*, 3913.
- (15) Michelot, J. M.; Moreau, M. F. C.; Veyre, A. J.; Bonafous, J. F.; Bacin, F. J.; Madelmont, J. C.; Bussiere, F.; Souteyrand, P. A.; Mauclair, L. P.; Chossat, F. M.; Papon, J. M.; Labarre, P. G.; Kauffmann, P.; Pagne, R. J. *J. Nucl. Med.* **1993**, *34*, 1260.

(16) Mohammed, A.; Nicholl, C.; Titsch, U.; Eisenhut, M. *Nucl. Med. Biol.* **1997**, *24*, 373.

(17) Friebe, M.; Mahmood, A.; Spies, H.; Berger, R.; Johannsen, B.; Mohammed, A.; Eisenhut, M.; Bolzati, C.; Davison, A.; Jones, A. G. *J. Med. Chem.* **2000**, *43*, 2745.

(18) Court, J. A.; Piggott, M. A.; Lloyd, S.; Cookson, N.; Ballard, C. G.; McKeith, I. G.; Perry, R. H.; Perry, E. K. *Neuroscience* **2000**, *98*, 79.

(19) Narahashi, T.; Fenster, C. P.; Quick, M. W.; Lester, R. A. J.; Marszalec, W.; Aistrup, G. L.; Sattelle, D. B.; Martin, B. R.; Levin, E. D. *Toxicol. Sci.* **2000**, *57*, 193.

(20) Waibel, R.; Alberto, R.; Willuda, J.; Finnern, R.; Schibli, R.; Stichelberger, A.; Egli, A.; Abram, U.; Mach, J.-P.; Plückthun, A.; Schubiger, P. A. *Nat. Biotechnol.* **1999**, *17*, 897.

Appendix A

Synthesis of Tricarbonylrhenium Complexes of Aminocarboxylate Ligands

Introduction

The versatility of the "*fac*-[Re(CO)₃]⁺" core has been demonstrated in Chapters 1 and 2. In general, the complexes synthesized were of monoanionic tridentate ligands to form neutral complexes. Another class of monoanionic tridentate ligands was investigated with respect to its reactivity with the tricarbonylrhenium(I) core, namely aminocarboxylates.

Aminocarboxylate ligands have long been used in coordination chemistry.¹ Two ligands in this wide class were investigated as precursors to some potentially biologically motivated work: ethylenediamine-*N,N'*-diacetic acid (EDDAH) and L-methionine (Figure A.1). Studies by Alberto inspired this choice of ligands. Alberto and co-workers

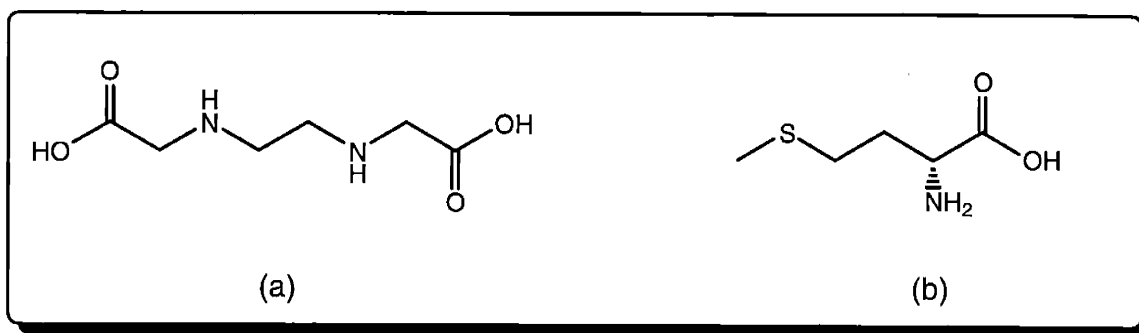


Figure A.1. The ligands (a) ethylenediamine-*N,N'*-diacetic acid and (b) L-methionine.

synthesized the compound Tc(CO)₃(PADA) (PADAH = 2-picolylamine-*N,N'*-diacetic acid; see Scheme 2.1 and Figure A.2),² which possesses an uncoordinated acid group for potential bioconjugation. The ligand EDDAH was investigated as a potentially smaller

version of PADAH, which, according to Hom and Katzenellenbogen, is an important consideration when designing radiopharmaceuticals.³ Other work by Alberto suggested that histidine-tagged peptides have high potential for use in radiopharmaceuticals since histidine binds strongly to the "[^{99m}Tc(CO)₃]" core.⁴ Through the course of his work, it was shown that methionine has good affinity for the metal center as well, but further studies were never pursued.⁵

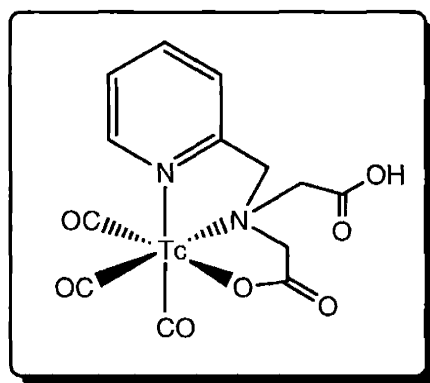


Figure A.2. Tc(CO)₃(PADA) (PADAH = picolylamine-*N,N*-diacetic acid).

Herein is described the synthesis of tricarbonylrhenium complexes of aminocarboxylate ligands. This work establishes the composition of putative ^{99m}Tc radiopharmaceuticals incorporating these ligands.

Experimental

General Considerations. All manipulations were carried out in air. All solvents and reagents were obtained commercially and used as received unless otherwise noted. $(\text{NEt}_4)_2[\text{ReBr}_3(\text{CO})_3]^6$ was prepared as described in the literature. Elemental analyses were performed by Atlantic Microlab, Inc., Norcross, GA.

Physical Measurements. Proton NMR spectra were recorded on a Varian Unity-300 (300 MHz), a Varian Mercury-300 (300 MHz), or a Varian Unity-Inova 500 (500 MHz) spectrometer. Chemical shifts were referenced to residual protons in the specified deuterated solvent. Infrared spectra were obtained on a Perkin-Elmer 2000-FTIR or Perkin-Elmer 1600-FTIR spectrometer. The fast atom bombardment mass spectra (FABMS) were recorded in a 3-nitrobenzyl alcohol matrix with a MAT 731 mass spectrometer, and the electrospray ionization mass spectra (ESIMS) were recorded on a Bruker 3T FT-MS. Mass spectra were recorded by Ms. Li Li of the MIT DCIF. Multiple masses are reported for rhenium-containing fragments to indicate the significant isotopic abundances of both ^{185}Re and ^{187}Re . Each peak was observed to have the proper relative abundances.

Synthesis of $\text{Re}(\text{CO})_3(\text{EDDA})\cdot\text{H}_2\text{O}$

To a solution of $(\text{NEt}_4)_2[\text{ReBr}_3(\text{CO})_3]$ (231 mg, 0.299 mmol) in 7 mL deionized water was added solid AgNO_3 (154 mg, 0.907 mmol). Silver bromide precipitated immediately and was removed from the solution by filtration. Solid EDDAH (53 mg,

0.30 mmol) was added to the filtrate. The EDDAH dissolved and the solution was stirred for 1-2 d. After this time, the solution was filtered through a cotton plug to remove the small amount of insoluble material. The resulting colorless solution was allowed to evaporate slowly in air. The colorless crystals that precipitated were filtered and washed with deionized water and diethyl ether. The crystals were dried in air. Yield: 49 mg (35%). These crystals were also suitable for a single crystal X-ray diffraction study. ^1H NMR (CD_3OD): δ 2.70-3.25 (ABCD pattern, 4H, $\text{NCH}_2\text{CH}_2\text{N}$), 3.46-3.66 (ABX pattern, $J_{\text{AX}} = 0$ Hz; $J_{\text{BX}} = 6.6$ Hz; $J_{\text{AB}} = 17.1$ Hz, 2H, CH_2COORe), 3.80-3.94 (ABX pattern, $J_{\text{AX}} = 8.0$ Hz; $J_{\text{BX}} = 5.0$ Hz; $J_{\text{AB}} = 17.0$ Hz, 2H, CH_2COOH), 5.2 (br s, 1H, NH), 6.7 (br s, 1H, NH). ^{13}C { ^1H } NMR (CD_3OD): δ 50.587, 54.357, 55.583, 57.953 ($-\text{CH}_2\text{NHCH}_2\text{CH}_2\text{NHCH}_2-$); 172.575, 184.389 (C=O). IR (KBr): $\nu(\text{OH})$ 3413, 3340; $\nu(\text{NH})$ 3273, 3126; $\nu(\text{CH})$ 2928; $\nu(\text{C}\equiv\text{O})$ 2020, 1919, 1901, 1880; $\nu(\text{C}=\text{O})$ 1743, 1721 cm^{-1} . FAB(+)-MS: m/z 445/447 [$\text{M}+\text{H}$] $^+$. Anal. Calc. for $\text{C}_9\text{H}_{11}\text{N}_2\text{O}_7\text{Re}\cdot\text{H}_2\text{O}$: C, 23.33; H, 2.83; N, 6.05. Found: C, 23.42; H, 2.80; N, 6.09%.

Synthesis of $\text{Re}(\text{CO})_3(\text{L-methionine})$

To a vial containing a solution of 77 mg (0.10 mmol) $(\text{NEt}_4)_2[\text{ReBr}_3(\text{CO})_3]$ in 1.5 mL deionized water, was added a solution of 60 mg (0.40 mmol) L-methionine in a small amount of deionized water. The solution was heated in a water bath to 50° C. After 50 minutes, a white solid began precipitating out of the solution. Heating was continued, and the mixture was stirred overnight. The solution was filtered. The precipitate was washed with 2 mL deionized water and 3 mL *n*-pentane, and dried in air. Yield: 19 mg (45%). ^1H NMR (CD_3OD): δ 2.12 (br s, 1H), 2.34 (m, 1H), 2.66 (m, 1H), 2.72 (s, 3H,

-SCH₃), 3.07 (br s, 1H), 3.82 (br s, 1H, -CH), 5.90 (br s, 2H, -NH₂). IR (KBr): $\nu(\text{CO})$ 2038, 1955, 1920, 1889, 1601 cm⁻¹. ESI(+)MS: m/z 418/420 [M+H]⁺. *Anal.* Calc. for C₈H₁₀NO₅ReS: C, 22.96; H, 2.41; N, 3.35; S, 7.66. Found: C, 22.98; H, 2.43; N, 3.32; S, 7.61%.

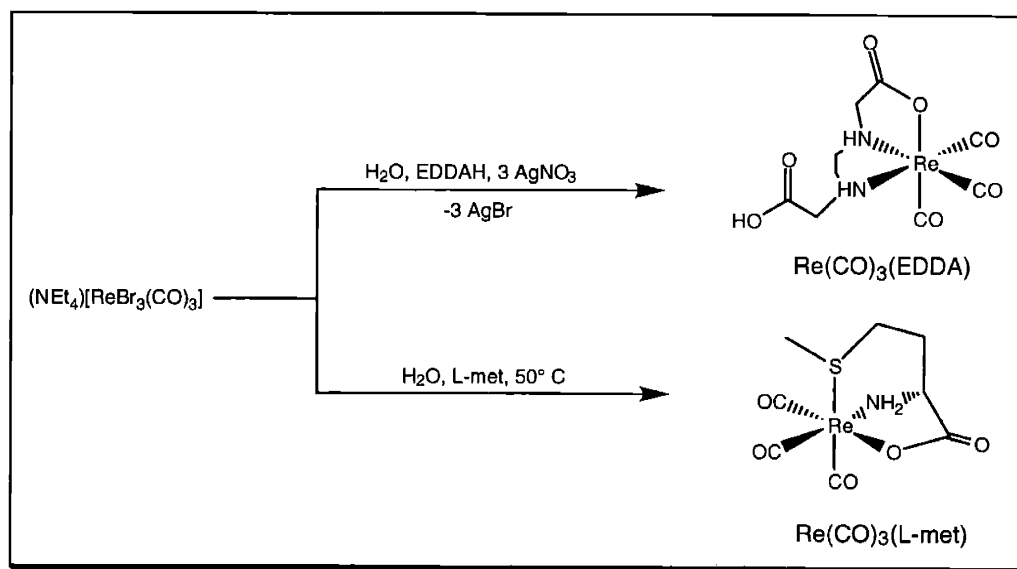
X-ray Crystallography. Crystals of Re(CO)₃(EDDA)·H₂O were transferred onto a microscope slide from a scintillation vial and coated with STP[®]. A crystal was selected, mounted on a glass fiber, and optically centered. The data were collected on a Siemens platform goniometer with a CCD detector. The structures were solved by direct methods in conjunction with standard difference Fourier techniques (SHELXTL v5.0, Sheldrick, G. M. and Siemens Industrial Automation, 1995). Non-hydrogen atoms were treated anisotropically, and hydrogen atoms were placed in calculated positions ($d_{\text{C-H}} = 0.96 \text{ \AA}$). Crystal data and structure refinement data are given in Table A.1.

Table A.1. Crystal data and structure refinement for $\text{Re}(\text{CO})_3(\text{EDDA})\cdot\text{H}_2\text{O}$.

Empirical formula	$\text{C}_9\text{H}_{13}\text{N}_2\text{O}_8\text{Re}$
Formula weight	463.41
Temperature (K)	177(2) K
Wavelength (\AA)	0.71073 \AA
Crystal system	Triclinic
Space group	$\text{P}\bar{1}$
a (\AA)	7.793(2)
b (\AA)	10.494(4)
c (\AA)	16.408(4)
α ($^\circ$)	88.63(2)
β ($^\circ$)	82.05(2)
γ ($^\circ$)	87.44(3)
Volume (\AA^3)	1327.4(7)
Z	4
ρ_{calc} (Mg m^{-3})	2.229
μ (mm^{-1})	9.184
F(000)	840
Crystal dimensions (mm^3)	0.3 x 0.3 x 0.1
Theta range for data collection ($^\circ$)	1.25 to 23.25
Limiting Indices	$-7 \leq h \leq 8, -11 \leq k \leq 11, -18 \leq l \leq 16$
Reflections collected	5495
Independent reflections (R_{int})	3739 (0.0744)
Data / restraints / parameters	3739 / 0 / 364
Goodness-of-fit on F^2	1.215
Final R indices [$I > 2\sigma(I)$]	$R_1 = 0.0425, wR_2 = 0.1224$
R indices (all data)	$R_1 = 0.0438, wR_2 = 0.1280$
Extinction coefficient	0.0061(6)
Largest diff. peak and hole ($\text{e}\text{\AA}^{-3}$)	2.259 and -3.289

Results and Discussion

Reaction of EDDAH and L-methionine with $[\text{Re}(\text{CO})_3(\text{H}_2\text{O})_3]^+$ proceeds in air to give the two expected complexes, $\text{Re}(\text{CO})_3(\text{EDDA})$ and $\text{Re}(\text{CO})_3(\text{L-met})$ (Scheme A.1). Since neither of these ligands possesses a functional group that has a high affinity for the Re(I) center, the complexation is rather slow, and in the case of $\text{Re}(\text{CO})_3(\text{L-met})$, requires some heating.



Scheme A.1. Synthesis of $\text{Re}(\text{CO})_3(\text{EDDA})$ and $\text{Re}(\text{CO})_3(\text{L-met})$.

The precipitation of $\text{Re}(\text{CO})_3(\text{EDDA})$ affords the complex as a monohydrate directly as colorless plates. A single crystal X-ray diffraction study has given a crystal structure of the complex (Figure A.3). The bond distances and angles are within accepted ranges for compounds of the "*fac*- $[\text{Re}(\text{CO})_3]^+$ " core.^{2,7,8} The uncoordinated carboxylic acid group can be assigned as protonated, as the C(4)-O(5) bond distance of 1.311(12) Å is longer than the carbonyl C(4)-O(4) bond distance of 1.214(13) Å. This makes sense

based on the fact that as the complex is formed, one equivalent of HNO_3 is released. As the solution reduces in volume, the mother liquor becomes quite acidic, approaching pH 1.

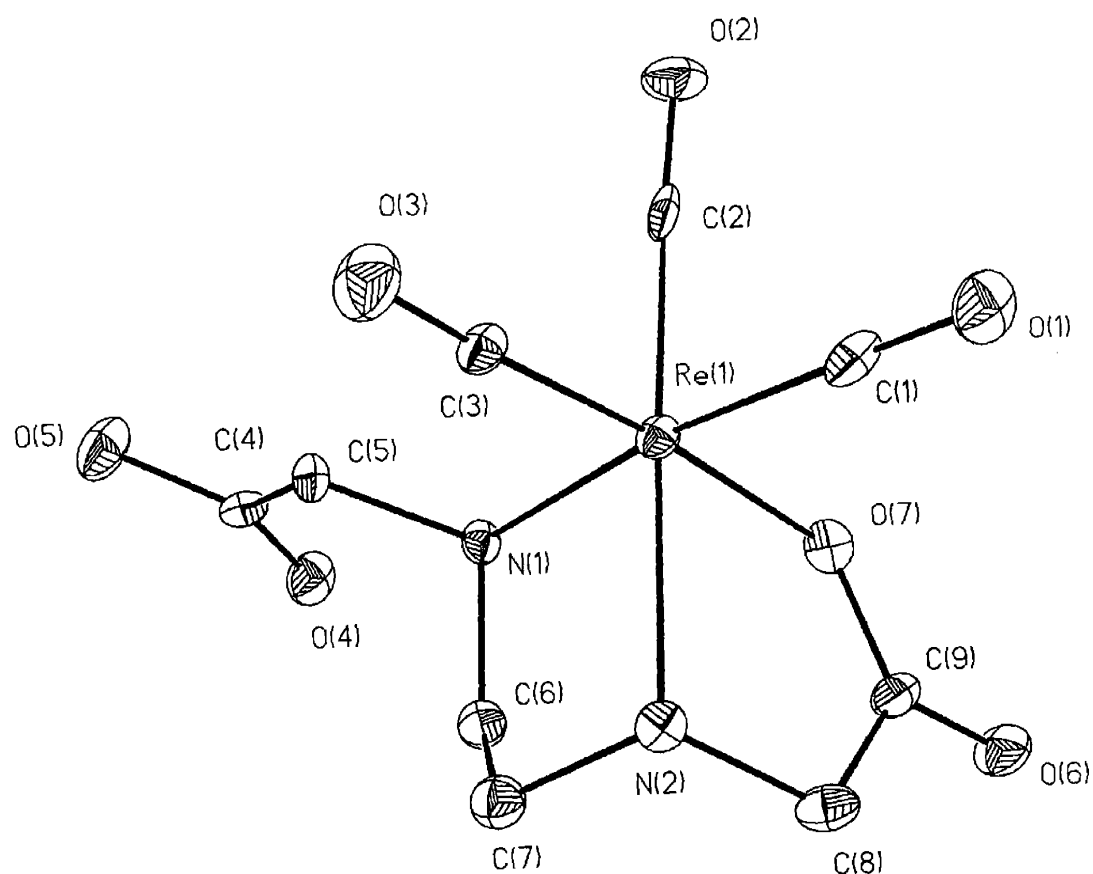


Figure A.3. Thermal ellipsoid plot (35% probability) of $\text{Re}(\text{CO})_3(\text{EDDA}) \cdot \text{H}_2\text{O}$ (water molecule omitted for clarity).

The complex $\text{Re}(\text{CO})_3(\text{EDDA})$ has also been characterized by IR and ^1H NMR spectroscopies, mass spectrometry, and elemental analysis. The IR spectrum shows the expected $A_1 + E \nu(\text{C}\equiv\text{O})$ pattern, as well as $\nu(\text{C}=\text{O})$ stretches for the two acetate groups. The ^1H NMR exhibits the expected broad singlets for the two amine protons, two ABX

patterns for the methylene protons on the acetate groups, and an ABCD pattern for the ethylene bridge. The FAB(+) mass spectrum exhibits a peak for the parent ion.

The complex $\text{Re}(\text{CO})_3(\text{L-met})$ was isolated as a white powder in moderate yield. The complex has been previously reported, but no experimental details were given, and it was characterized only by mass spectrometry.⁹ Unfortunately, all attempts to recrystallize $\text{Re}(\text{CO})_3(\text{L-met})$ gave only microcrystalline powders. However, satisfactory analyses and spectroscopies were obtained (*vide supra*). $\text{Re}(\text{CO})_3(\text{L-met})$ can be considered a starting point for synthesis of radiopharmaceuticals containing methionine-tagged bioactive peptides. Alberto has made great use of histidine as a ligand and tag for peptides by *N*-acetylation, followed by linking to a peptide on a solid-phase synthesizer. As previously mentioned, studies have shown that histidine does have higher affinity for the "*fac*-[^{99m}Tc(CO)₃]⁺" core than methionine. However, radiopharmaceuticals designed with a methionine tag will likely have different chemical properties, pharmacokinetics, and biodistribution due to the difference of the ligand environment.

Conclusions

Herein are described the syntheses of tricarbonylrhenium complexes of the aminocarboxylate ligands, ethylenediamine-*N,N'*-diacetic acid and L-methionine. The expected complexes, $\text{Re}(\text{CO})_3(\text{EDDA})$ and $\text{Re}(\text{CO})_3(\text{L-met})$, in which the coordinated carboxylic acid group has deprotonated, are formed. These complexes can be considered frameworks for new radiopharmaceuticals based on the *fac*- $[\text{}^{99\text{m}}\text{Tc}(\text{CO})_3]^+$ core.

References

- (1) McLendon, G.; Motekaitis, R. J.; Martell, A. E. *Inorg. Chem.* **1975**, *14*, 1993.
- (2) Alberto, R.; Schibli, R.; Egli, A.; Schubiger, A. P.; Abram, U.; Kaden, T. *A. J. Am. Chem. Soc.* **1998**, *120*, 7987.
- (3) Hom, R. K.; Katzenellenbogen, J. A. *Nucl. Med. Biol.* **1997**, *24*, 485.
- (4) Waibel, R.; Alberto, R.; Willuda, J.; Finnern, R.; Schibli, R.; Stichelberger, A.; Egli, A.; Abram, U.; Mach, J.-P.; Plückthun, A.; Schubiger, P. A. *Nat. Biotechnol.* **1999**, *17*, 897.
- (5) Egli, A.; Alberto, R.; Tannahill, L.; Schibli, R.; Abram, U.; Schaffland, A.; Tourwé, D.; Schubiger, P. A. in: *Technetium, Rhenium, and Other Metals in Chemistry and Nuclear Medicine 5*; SGEEditoriali: Padova, 1999, p. 507.
- (6) Alberto, R.; Egli, A.; Abram, U.; Hegetschweiler, K.; Gramlich, V.; Schubiger, P. A. *J. Chem. Soc. Dalton Trans.* **1994**, 2815.
- (7) Pietzsch, H.-J.; Gupta, A.; Reisgys, M.; Drews, A.; Seifert, S.; Syhre, R.; Spies, H.; Alberto, R.; Abram, U.; Schubiger, P. A.; Johannsen, B. *Bioconjugate Chem.* **2000**, *11*, 414.
- (8) Schibli, R.; Bella, R. L.; Alberto, R.; Garcia-Garayoa, E.; Ortner, K.; Abram, U.; Schubiger, P. A. *Bioconjugate Chem.* **2000**, *11*, 345.
- (9) Berger, R.; Schaffland, A.; Spies, H. *Forschungszent. Rossendorf* **1998**, *FZR-200*, 126.

Appendix B

Synthesis and Bioevaluation of Rhenium and Technetium Complexes of a Nor nicotine Conjugate

Introduction

As discussed in Chapter 3, the amine-linked nornicotine derivative, MEPAH-C₃nornic-STr, was a desirable synthetic target since the resulting putative ^{99m}Tc radiopharmaceutical, ^{99m}Tc(CO)₃(MEPA-C₃nornic), was expected to possess more lipophilicity than the amide-linked ^{99m}Tc(CO)₃(MEPA-C₂CONornic). The amide-linked complex exhibited almost no brain uptake, and it was hoped that the -C₃nornic derivative would penetrate the blood-brain barrier to a greater extent. Herein is presented synthetic and biological work aimed at determining the brain uptake of this amine derivative of nornicotine.

Experimental

General Considerations. All manipulations were carried out in air unless otherwise noted. All solvents and reagents were obtained commercially and used as received unless otherwise noted. $(\text{NEt}_4)_2[\text{ReBr}_3(\text{CO})_3]^1$ was prepared as described in the literature. $^{99\text{m}}\text{Tc}$ was obtained as $\text{Na}[^{99\text{m}}\text{TcO}_4]$ in 0.9% NaCl aqueous solution from the radiopharmacy at the Brigham & Women's Hospital, Boston, MA. $[^{99\text{m}}\text{Tc}(\text{CO})_3(\text{H}_2\text{O})_3]^+$ was synthesized as described in the literature.² Normal phase preparative scale silica TLC plates were purchased from Analtech (20 cm x 20 cm x 1000 μ), and C_{18} reversed-phase silica TLC plates were purchased from Whatman (20 cm x 20 cm x 1000 μ).

Physical Measurements. Proton NMR spectra were recorded on a Varian Unity-300 (300 MHz), a Varian Mercury-300 (300 MHz), or a Varian Unity-Inova 500 (500 MHz) spectrometer. Chemical shifts were referenced to residual protons in the specified deuterated solvent. The electrospray ionization mass spectra (ESIMS) were recorded on a Bruker 3T FT-MS by Ms. Li Li of the MIT DCIF. HPLC was performed on a Waters Millennium Chromatography System equipped with a 996 UV-Vis diode-array detector attached in series to a gamma detector consisting of a shielded photomultiplier powered by a Canberra voltage amplifier and connected to a ratemeter. A reversed phase C_{18} silica column (220 x 4.6 mm) equipped with a C_{18} guard (30 x 4.6 mm) was used with the following linear gradient (A: 0.005 M PBS pH 7.6; B: MeOH; gradient given in t(min)/%B: 0/5, 5/5, 35/85, 40/85, 45/98, 55/98, 65/5) at a flow rate of 1.0 mL/min. Radiochemical yields were determined by integration of the gamma chromatogram from

the HPLC. Compounds prepared for biodistribution were purified by preparative isolation of the appropriate peak on the HPLC.

Synthesis of *N*-(3'-Nornicotinopropyl)-*N*-[2-[(triphenylmethyl)thio]ethyl]picolyamine, MEPAH-C₃nornic-STr

To a 50 mL Schlenk flask was placed 56 mg (0.091 mmol) MEPAH-C₂CONornic-STr, and an Ar atmosphere was set. By cannula, 10 mL anhydrous CH₂Cl₂ was transferred to the flask; the MEPAH-C₂CONornic-STr dissolved. The reaction vessel was cooled to 0°, and then 0.30 mL (0.30 mmol) of 1 M diisobutylaluminum hydride (DIBAL) was added *via* syringe. The solution turned slightly yellow, and it was stirred at room temperature for 45 minutes. Methanol (5 mL) and H₂O (~1 mL) were added to quench the remaining DIBAL. The solvents were removed *in vacuo*. The residue was reconstituted with 10 mL CH₂Cl₂ and 10 mL H₂O. The CH₂Cl₂ layer was collected. The aqueous layer was extracted with 5 x 10 mL CH₂Cl₂. The organic fractions were combined, dried over MgSO₄, and concentrated *in vacuo*. The crude, yellow residue was purified by preparative-scale TLC (1:1 MeOH:EtOAc eluent). The product was washed off of the silica with MeOH (50 mL), and the solvent was removed *in vacuo* to give the product as a faintly yellow residue. Yield: 13 mg (24%). ¹H NMR (CD₂Cl₂, 500 MHz): δ 1.45 (p, 2H, NCH₂CH₂CH₂N-), 1.98 (p, 2H), 2.18 (m, 6H), 2.38 (m, 5H) 3.19 (t, 2H), 3.49 (s, 2H, py-CH₂), 7.1-7.4 (m, 19H, Tr-*H* and py-*H*), 7.59 (m, 2H, py-*H*), 8.43 (m, 2H, py-*H*). HRESI(+)-MS: *m/z* Calc. for [M+H]⁺: 599.3203. Found: 599.3208.

Synthesis of *N*-(3'-Nornicotinopropyl)-*N*-(2-mercaptoethyl)picolyamine, MEPAH-C₃nornic

To a vial containing 12 mg (0.020 mmol) *N*-(3'-nornicotinopropyl)-*N*-[2-[(triphenylmethyl)thio]ethyl]picolyamine was added 5 mL TFA. Triethylsilane was added dropwise to the resulting yellow-orange solution until color discharge was observed. The TFA solution was washed with 3 x 5 mL hexanes to remove the triphenylmethane. A drop of water was added to aid in separation of the layers. The resulting solution was concentrated to a pale yellow oil. This was used immediately in the next step with no further purification.

Synthesis of (*N*-(3'-Nornicotinopropyl)-*N*-(2-mercaptoethyl)picolyamino)-tricarbonylrhenium(I), Re(CO)₃(MEPA-C₃nornic)

To a solution of 10 mg (0.013 mmol) (NEt₄)₂[ReBr₃(CO)₃] in 1 mL acetonitrile. was added the deprotected ligand, MEPAH-C₃nornic, in 0.25 mL MeCN and 0.25 NEt₃. The resulting solution turned yellow in seconds and was stirred at room temperature for 45 minutes. The MeCN and NEt₃ were then removed *in vacuo*. The resulting residue was dissolved in MeCN and chromatographed on a C₁₈ reversed-phase silica plate with 2:1 MeOH:H₂O as the eluent. A yellow band coincident with a UV active band was scraped off of the plate (R_f ~ 0.1). The material was washed off of the silica with MeOH, and the solution was concentrated to dryness *in vacuo* to give a solid, yellow residue. Yield: 1.5 mg (15%; slightly impure). HRESI(+)-MS: *m/z* Calc. for [M+H]⁺: 627.1435. Found: 627.1440.

Deprotection of MEPAH-C₃nornic-STr for Labeling Experiments

The protected ligand, MEPAH-C₃nornic-STr (1 mg), was dissolved in 3 mL TFA to give a yellow solution. Two drops of Et₃SiH were added, and color discharge was noted. The TFA was removed *in vacuo*. The residue was dissolved in 600 μL MeOH. This was divided into 2 test tubes. The MeOH was removed *in vacuo*, and the tubes containing MEPAH-C₃nornic were stored under vacuum until they were used in labeling experiments.

Synthesis of Tentatively Formulated ^{99m}Tc(CO)₃(MEPA-C₃nornic)

An aqueous solution of [^{99m}Tc(CO)₃(H₂O)₃]⁺ (up to 50 mCi) was added to a test tube containing 0.3 mL PBS (0.005 M, pH 7.6) and ~0.25 mg of MEPAH-C₃nornic. The test tube was heated in a 75° C water bath for 40 minutes. Then, the tube was centrifuged at 3400 rpm for 10 minutes to separate suspended triphenylmethane. $t_R = 33.6$ min.; radiochemical yield: 28-40%. The composition of the ^{99m}Tc complex was confirmed by co-elution of a sample of Re(CO)₃(MEPA-C₃nornic) (< 1 mg in 50 μL MeOH) with the ^{99m}Tc-labeled species.

Animal Studies

All animal experiments were performed in compliance with the *Principles of Laboratory Animal Care* (NIH publication #85-23, revised 1985) in conjunction with Prof. Ashfaq Mahmood and Dr. Zhen Cheng. Biodistribution studies and *in vivo* tumor uptake measurements of ^{99m}Tc(CO)₃(MEPA-C₃nornic) were performed in Swiss white mice (20 to 30 g). The biodistribution studies of the ^{99m}Tc complex were carried out by

tail-vein injection of 10 to 15 μCi (0.05 to 0.1 mL) of the labeled complex by Ms. Alice Carmel and sacrificing the mice at the designated time post-injection. The organs were harvested and blotted dry (when appropriate), weighed, and counted in a gamma counter along with $^{99\text{m}}\text{Tc}$ standards of the injected dose. The results are expressed as % ID/g tissue (Table B.1).

Table B.1. Biodistribution of $^{99\text{m}}\text{Tc}(\text{CO})_3(\text{MEPA-C}_3\text{normic})$.

Compound	$^{99\text{m}}\text{Tc}(\text{CO})_3(\text{MEPA-C}_3\text{normic})$	
Time	30 minutes	1 hour
Organs		
Blood	$2.18 \pm 0.36\%$	$1.60 \pm 0.26\%$
Heart	$0.84 \pm 0.19\%$	$0.60 \pm 0.15\%$
Liver	$18.91 \pm 2.28\%$	$16.55 \pm 2.40\%$
Lungs	$2.39 \pm 0.64\%$	$1.72 \pm 0.42\%$
Muscle	$0.47 \pm 0.08\%$	$0.31 \pm 0.05\%$
Kidneys	$5.13 \pm 0.76\%$	$4.52 \pm 0.71\%$
Spleen	$2.86 \pm 1.65\%$	$2.52 \pm 0.84\%$
Brain	$0.08 \pm 0.02\%$	$0.06 \pm 0.01\%$
Skin	$1.14 \pm 0.14\%$	$0.99 \pm 0.38\%$

Lipophilicity Studies

An HPLC purified sample of $^{99\text{m}}\text{Tc}(\text{CO})_3(\text{MEPA-C}_2\text{CONornic})$ was dissolved in 2 mL PBS (pH 7.6) and 2 mL 1-octanol. The two layers were vortexed, allowed to settle, and centrifuged. One milliliter of the organic layer was removed and 1 mL PBS was added. The process above was repeated. The layers were separated and three 50 μL aliquots of each were placed in test tubes. These tubes were counted in a gamma counter. $\log D_{\text{pH } 7.6} = 0.80$.

Results and Discussion

Reaction of the amide, MEPAH-C₂CONornic-STr, with diisobutylaluminum hydride (DIBAL) in anhydrous CH₂Cl₂ gave the amine derivative, MEPAH-C₃nornic-STr, in modest yield after chromatographic purification (Figure B.1a). The use of MEPAH-C₃Cl-STr as a starting material proved to be unsuccessful, even when using the conditions developed for the synthesis of MEPAH-C₃morph-STr (see Chapter 2). Additionally, DIBAL was chosen as a reducing agent due to the expectation that it would not cleave the trityl protecting group (unlike other reductants such as BH₃·THF).^{3,4}

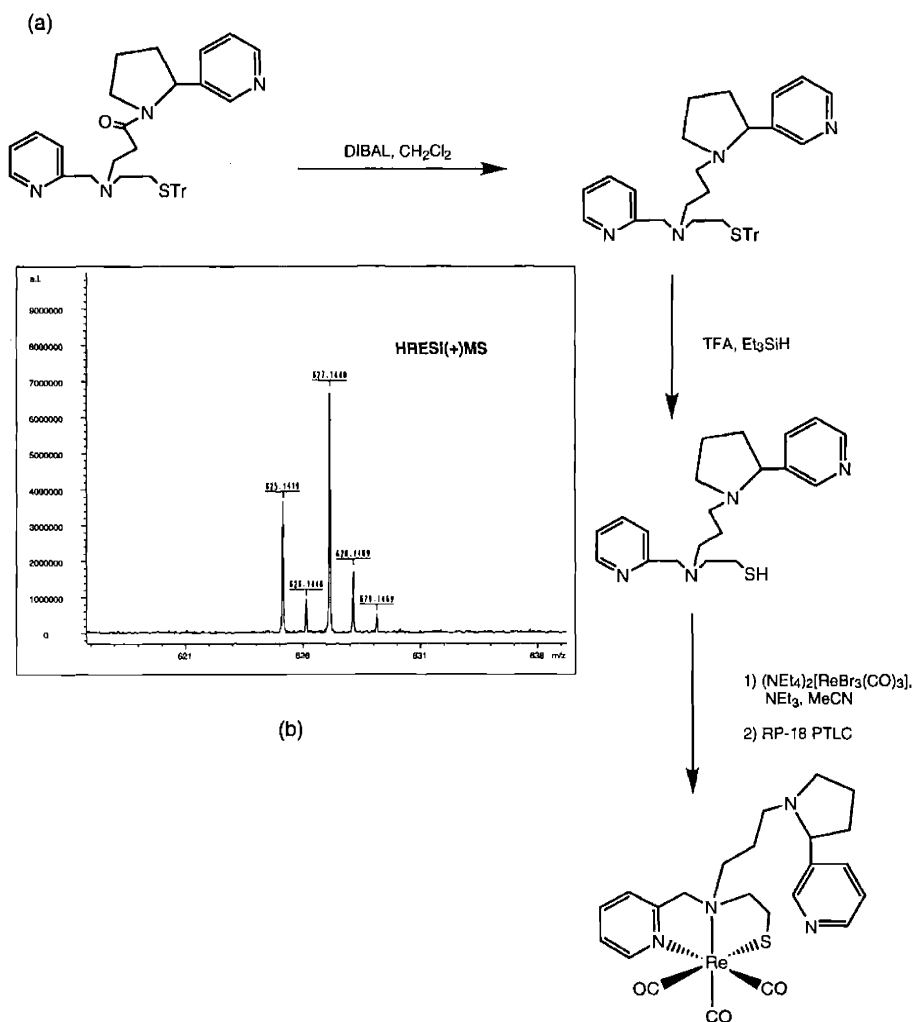


Figure B.1. (a) Synthesis and (b) HRESI(+)-MS of Re(CO)₃(MEPA-C₃nornic).

The protected amine was detritylated with TFA-Et₃SiH, reacted with [Re(CO)₃(MeCN)₃]⁺ in the presence of NEt₃, and chromatographed on RP-18 reversed phase silica to give a sample of Re(CO)₃(MEPA-C₃nornic) (Figure B.1a). This complex was characterized by HRESI(+)-MS (Figure B.1b). Additionally, an impurity containing (NEt₄)⁺ was present. A ¹H NMR spectrum also exhibited ethyl peaks consistent with an ionic impurity containing (NEt₄)⁺. The remainder of the spectrum is complicated due to overlapping resonances and, perhaps, the anionic impurity. However, due to the fact that the complex was formed, ^{99m}Tc complex synthesis and biodistribution studies were pursued.

Reaction of MEPAH-C₃nornic with [^{99m}Tc(CO)₃(H₂O)₃]⁺ did not give a clean product. Figure B.2 shows the results of a co-injection experiment of the ^{99m}Tc product mixture and the somewhat impure Re(CO)₃(MEPA-C₃nornic). The chemistry appears to be different at the tracer level, as a more hydrophilic product (t_R ~ 25 min) is formed in addition to the co-eluted peak at t_R = 33 min (in 28% r.c.y.). Although this compound is only tentatively formulated as ^{99m}Tc(CO)₃(MEPA-C₃nornic), *in vivo* biodistribution and lipophilicity studies were carried out.

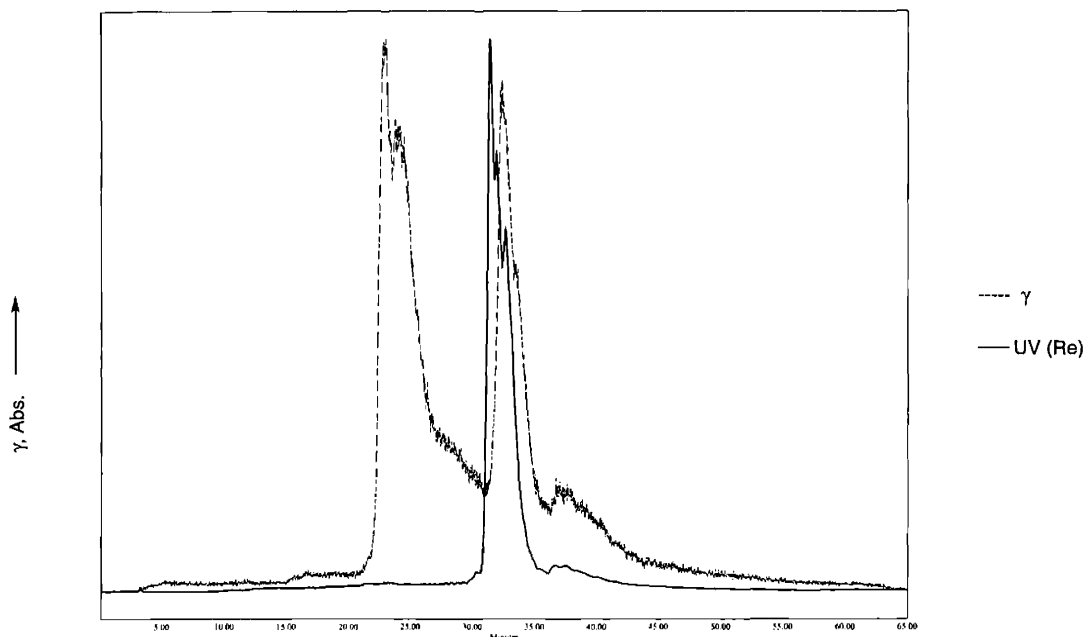


Figure B.2. HPLC chromatogram of co-injected $^{99m}\text{Tc}/\text{Re}(\text{CO})_3(\text{MEPA}-\text{C}_3\text{normic})$.

Using the same animal model as for $^{99m}\text{Tc}(\text{CO})_3(\text{MEPA}-\text{C}_2\text{CONornic})$ (see Chapter 3), an HPLC purified sample of $^{99m}\text{Tc}(\text{CO})_3(\text{MEPA}-\text{C}_3\text{normic})$ was injected into Swiss white mice. As can be seen in Table B.1, brain uptake was still quite low (only $0.08 \pm 0.02\%$ ID/g at 30 minutes post-injection) despite the presence of an amine linkage, but it was significantly greater than the uptake of its amide counterpart. A lipophilicity study confirmed that the compound is significantly more lipophilic than $^{99m}\text{Tc}(\text{CO})_3(\text{MEPA}-\text{C}_2\text{CONornic})$ ($\log D_{\text{pH } 7.6} = 0.80$ compared with -0.054 for the amide). For comparison, brain imaging agents such as TRODAT-1⁵ show slightly higher uptake at 60 minutes (0.12% ID/g as compared to 0.06% ID/g in $^{99m}\text{Tc}(\text{CO})_3(\text{MEPA}-\text{C}_3\text{normic})$). The lipophilicity of TRODAT-1, however, is much higher, with a $\log D_{\text{pH } 7.0}$ of 2.36, a desirable characteristic for radiopharmaceuticals designed to cross the blood-brain barrier.

Conclusions

The synthesis of an amine-linked nornicotine conjugate, MEPAH-C₃nornic, and its tricarbonylrhenium and tricarbonyltechnetium complexes, has been described. While the syntheses of the metal complexes are not entirely clean, a product formulated as ^{99m}Tc(CO)₃(MEPA-C₃nornic) has been evaluated as a potential brain imaging agent. Initial *in vivo* studies in Swiss white mice have shown that significantly more activity is taken up by the brain (0.08% ID/g at 30 minutes post-injection) with this complex as compared to the amide-linked ^{99m}Tc(CO)₃(MEPA-C₂CONornic) (0.03% ID/g at 30 minutes post-injection). Although the uptake is still relatively low, these results are promising, and further investigations into this system are warranted.

References

- (1) Alberto, R.; Egli, A.; Abram, U.; Hegetschweiler, K.; Gramlich, V.; Schubiger, P. A. *J. Chem. Soc. Dalton Trans.* **1994**, 2815.
- (2) Alberto, R.; Ortner, K.; Wheatley, N.; Schibli, R.; Schubiger, A. P. *J. Am. Chem. Soc.* **2001**, *123*, 3135.
- (3) Sadighi, J. P. Personal communication; **2003**.
- (4) Kocienski, P. J. *Protecting Groups*; G. Thieme: Stuttgart; New York, 1994.
- (5) Meegalla, S. K.; Plössl, K.; Kung, M.-P.; Chumpradit, S.; Stevenson, D. A.; Kushner, S. A.; McElgin, W. T.; Mozley, D.; Kung, H. F. *J. Med. Chem.* **1997**, *40*, 9.

Appendix C

X-ray Crystallographic Data

Compound C.1. Full thermal ellipsoid plot of $\text{Tc}(\text{CO})_3(\text{L}_{\text{OEt}})$.

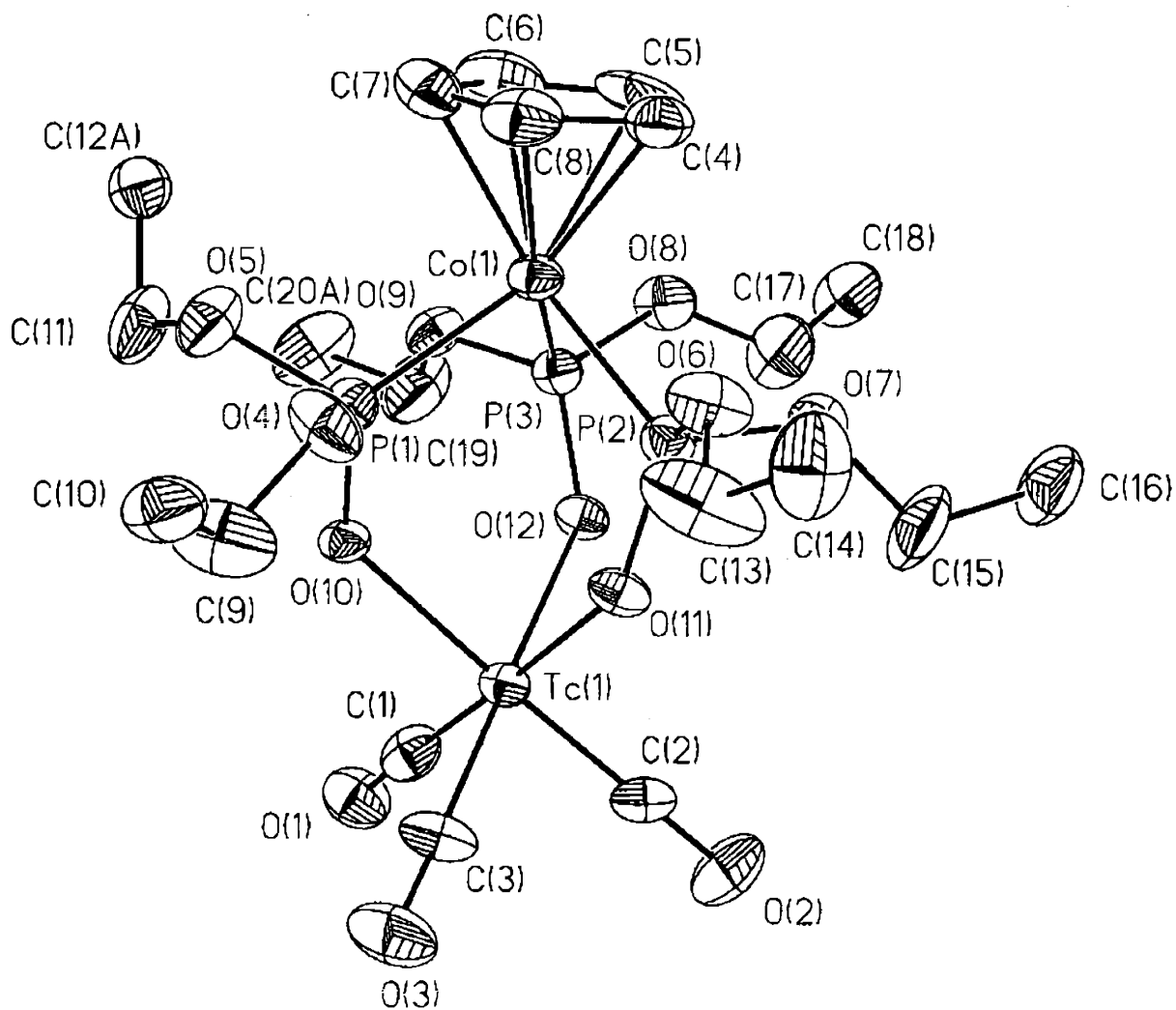


Table C.1.1. Atomic coordinates ($\times 10^4$) and equivalent isotropic displacement parameters ($\text{\AA}^2 \times 10^3$) for $\text{Tc}(\text{CO})_3(\text{L}_{\text{OEt}})$. $U(\text{eq})$ is defined as one third of the trace of the orthogonalized U^{ij} tensor.

	x	y	z	U(eq)
Tc(1)	1459(1)	1059(1)	2583(1)	33(1)
Co(1)	-1734(1)	1989(1)	2574(1)	35(1)
P(1)	-1115(3)	1160(2)	3564(2)	38(1)
P(2)	-99(3)	2541(2)	2779(2)	38(1)
P(3)	-1056(3)	1395(2)	1373(2)	34(1)
O(1)	2097(8)	-442(5)	1965(6)	64(3)
O(2)	3543(8)	1560(6)	1516(7)	79(3)
O(3)	3132(9)	836(6)	4325(7)	83(3)
O(4)	-907(7)	1523(4)	4611(5)	59(3)
O(5)	-2112(7)	606(5)	3832(6)	63(3)
O(6)	-233(7)	3161(4)	3561(6)	62(3)
O(7)	68(7)	3003(5)	1818(6)	58(2)
O(8)	-1440(7)	1739(5)	351(5)	55(2)
O(9)	-1752(6)	660(4)	1283(5)	44(2)
O(10)	-75 (6)	727(4)	3310(5)	35(2)
O(11)	974(6)	2124(4)	3042(5)	38(2)
O(12)	231(6)	1266(4)	1367(5)	36(2)
C(1)	1828(11)	143(8)	2211(9)	49(4)
C(2)	2744(11)	1369(7)	1926(9)	47(3)
C(3)	2500(11)	928(7)	3655(10)	55(4)
C(4)	-2584(10)	2950(7)	2568(12)	53(4)
C(5)	-3000(14)	2558(13)	1752(11)	85(6)
C(6)	-3459 (13)	1929(10)	2109(15)	73(5)
C(7)	-3398(12)	1949(8)	3098(15)	72(5)
C(8)	-2846(11)	2565(9)	3398(10)	58(4)
C(9)	-252(13)	1159(9)	5376(9)	84(5)
C(10)	-516(11)	1426(8)	6303(9)	68(4)
C(11)	-2361(13)	-66(7)	3416(11)	73(5)
C(12A)	-3538(42)	-24(25)	3004(45)	58(13)
C(12B)	-3704(63)	-247(35)	3340(58)	109(24)
C(13)	510(15)	3298(10)	4336(11)	99(6)
C(14)	486(14)	4032(8)	4682(10)	84(5)
C(15)	1125(14)	3289(11)	1572(12)	113(7)
C(16)	1075(12)	3774(9)	771(10)	85(5)
C(17)	-757 (14)	2101(11)	-243(11)	109(7)
C(18)	-1148(11)	2245(8)	-1209(9)	72(4)
C(19)	-1409(14)	103(10)	637(13)	89(5)
C(20A)	-2074(32)	-535(25)	588(32)	89(16)
C(20B)	-1495(108)	-542(35)	783(58)	144(50)

Table C.1.2. Bond lengths [\AA] and angles [$^\circ$] for $\text{Tc}(\text{CO})_3(\text{L}_{\text{OEt}})$.

Tc(1)-C(1)	1.84(2)	Tc(1)-C(2)	1.869(14)
Tc(1)-C(3)	1.877(14)	Tc(1)-O(11)	2.168(7)
Tc(1)-O(10)	2.170(6)	Tc(1)-O(12)	2.178(6)
Co(1)-C(4)	2.046(12)	Co(1)-C(8)	2.060(12)
Co(1)-C(6)	2.07(2)	Co(1)-C(7)	2.09(2)
Co(1)-C(5)	2.096(13)	Co(1)-P(2)	2.160(3)
Co(1)-P(1)	2.163(3)	Co(1)-P(3)	2.170(3)
P(1)-O(10)	1.504(7)	P(1)-O(4)	1.604(8)
P(1)-O(5)	1.605(9)	P(2)-O(11)	1.496(7)
P(2)-O(6)	1.594(8)	P(2)-O(7)	1.599(8)
P(3)-O(12)	1.508(7)	P(3)-O(9)	1.593(8)
P(3)-O(8)	1.592(8)	O(1)-C(1)	1.189(14)
O(2)-C(2)	1.162(13)	O(3)-C(3)	1.162(13)
O(4)-C(9)	1.44(2)	O(5)-C(11)	1.40(2)
O(6)-C(13)	1.36(2)	O(7)-C(15)	1.39(2)
O(8)-C(17)	1.35(2)	O(9)-C(19)	1.44(2)
C(4)-C(8)	1.40(2)	C(4)-C(5)	1.41(2)
C(5)-C(6)	1.39(2)	C(6)-C(7)	1.36(2)
C(7)-C(8)	1.37(2)	C(9)-C(10)	1.42(2)
C(11)-C(12A)	1.45(6)	C(13)-C(14)	1.45(2)
C(15)-C(16)	1.43(2)	C(17)-C(18)	1.41(2)
C(19)-C(20A)	1.42(4)		
C(1)-Tc(1)-C(2)	87.3(5)	C(1)-Tc(1)-C(3)	87.1(5)
C(2)-Tc(1)-C(3)	85.8(6)	C(1)-Tc(1)-O(11)	178.1(4)
C(2)-Tc(1)-O(11)	94.6(4)	C(3)-Tc(1)-O(11)	93.1(4)
C(1)-Tc(1)-O(10)	94.0(4)	C(2)-Tc(1)-O(10)	177.8(4)
C(3)-Tc(1)-O(10)	96.1(4)	O(11)-Tc(1)-O(10)	84.2(3)
C(1)-Tc(1)-O(12)	95.9(4)	C(2)-Tc(1)-O(12)	94.4(4)
C(3)-Tc(1)-O(12)	177.0(4)	O(11)-Tc(1)-O(12)	83.9(2)
O(10)-Tc(1)-O(12)	83.6(3)	C(4)-Co(1)-C(8)	39.8(5)
C(4)-Co(1)-C(6)	65.8(6)	C(8)-Co(1)-C(6)	65.2(5)
C(4)-Co(1)-C(7)	65.3(5)	C(8)-Co(1)-C(7)	38.5(5)
C(6)-Co(1)-C(7)	38.2(6)	C(4)-Co(1)-C(5)	39.7(6)
C(8)-Co(1)-C(5)	66.1(5)	C(6)-Co(1)-C(5)	39.0(6)
C(7)-Co(1)-C(5)	64.8(6)	C(4)-Co(1)-P(2)	90.0(4)
C(8)-Co(1)-P(2)	104.1(5)	C(6)-Co(1)-P(2)	153.0(6)
C(7)-Co(1)-P(2)	141.9(6)	C(5)-Co(1)-P(2)	114.4(7)
C(4)-Co(1)-P(1)	140.8(5)	C(8)-Co(1)-P(1)	102.8(4)
C(6)-Co(1)-P(1)	116.2(6)	C(7)-Co(1)-P(1)	92.3(4)
C(5)-Co(1)-P(1)	154.8(6)	P(2)-Co(1)-P(1)	89.89(13)
C(4)-Co(1)-P(3)	129.5(5)	C(8)-Co(1)-P(3)	161.1(4)
C(6)-Co(1)-P(3)	96.6(5)	C(7)-Co(1)-P(3)	128.2(6)
C(5)-Co(1)-P(3)	96.6(5)	P(2)-Co(1)-P(3)	89.82(13)

P(1)-Co(1)-P(3)	89.69(12)	O(10)-P(1)-O(4)	110.5(4)
O(10)-P(1)-O(5)	107.5(5)	O(4)-P(1)-O(5)	98.2(5)
O(10) -P(1) -Co(1)	118.8(3)	O(4) -P(1) -Co(1)	107.2(3)
O(5)-P(1)-Co(1)	112.7(4)	O(11)-P(2)-O(6)	108.7(4)
O(11)-P(2)-O(7)	110.5(4)	O(6)-P(2)-O(7)	100.9(5)
O(11)-P(2)-Co(1)	119.6(3)	O(6)-P(2)-Co(1)	108.8(3)
O(7)-P(2)-Co(1)	106.8(3)	O(12)-P(3)-O(9)	110.9(4)
O(12)-P(3)-O(8)	107.0(4)	O(9)-P(3)-O(8)	99.2(5)
O(12)-P(3)-Co(1)	118.6(3)	O(9)-P(3)-Co(1)	107.4(3)
O(8)-P(3)-Co(1)	111.9(3)	C(9)-O(4)-P(1)	120.7(8)
C(11)-O(5)-P(1)	128.0(8)	C(13)-O(6)-P(2)	126.1(9)
C(15)-O(7)-P(2)	123.5(8)	C(17)-O(8)-P(3)	126.4(8)
C(19)-O(9)-P(3)	121.2(8)	P(1)-O(10)-Tc(1)	129.4(4)
P(2)-O(11) -Tc(1)	129.1(4)	P(3)-O(12)-Tc(1)	129.1(4)
O(1)-C(1) -Tc(1)	178.2(11)	O(2)-C(2)-Tc(1)	179.7(12)
O(3)-C(3)-Tc(1)	178.7(13)	C(8)-C(4)-C(5)	108.0(13)
C(8)-C(4)-Co(1)	70.7(7)	C(5)-C(4)-Co(1)	72.1(8)
C(6)-C(5)-C(4)	106.2(13)	C(6)-C(5)-Co(1)	69.4(8)
C(4)-C(5)-Co(1)	68.2(7)	C(7)-C(6)-C(5)	109(2)
C(7)-C(6)-Co(1)	71.7(9)	C(5)-C(6)-Co(1)	71.6(9)
C(6)-C(7)-C(8)	109.1(14)	C(6)-C(7)-Co(1)	70.1(9)
C(8)-C(7)-Co(1)	69.6(8)	C(7)-C(8)-C(4)	107.4(12)
C(7)-C(8)-Co(1)	71.9(8)	C(4)-C(8)-Co(1)	69.6(7)
C(10)-C(9)-O(4)	111.4(11)	O(5)-C(11)-C(12A)	106(2)
O(6)-C(13)-C(14)	114.4(13)	O(7)-C(15)-C(16)	115.4(13)
O(8)-C(17)-C(18)	119.9(13)	C(20A)-C(19)-O(9)	118(2)

Table C.1.3. Anisotropic displacement parameters ($\text{\AA}^2 \times 10^3$) for $\text{Tc}(\text{CO})_3(\text{L}_{\text{OEt}})$. The anisotropic displacement factor exponent takes the form: $-2\pi^2[h^2a^{*2}U^{11} + \dots + 2hk a^* b^* U^{12}]$

	U^{11}	U^{22}	U^{33}	U^{23}	U^{13}	U^{12}
Tc(1)	31(1)	42(1)	28(1)	-1(1)	1(1)	6(1)
Co(1)	31(1)	44(1)	31(1)	-3(1)	2(1)	6(1)
P(1)	42(2)	42(2)	30(2)	0(2)	7(2)	4(2)
P(2)	37(2)	38(2)	39(2)	0(2)	-4(2)	1(2)
P(3)	34(2)	45(2)	22(2)	0(2)	-1(1)	1(2)
O(1)	69(7)	65(7)	58(6)	-5(6)	4(5)	17(6)
O(2)	57(7)	106(9)	78(7)	-4(6)	33(6)	-17(6)
O(3)	74(7)	110(9)	60(7)	4(6)	-31(6)	17(6)
O(4)	83(7)	67(6)	29(5)	2(5)	1(4)	28(5)
O(5)	58(6)	58(7)	76(6)	-9(5)	26(5)	-10(5)
O(6)	59(6)	47(6)	77(7)	-31(5)	-23(5)	9(5)
O(7)	50(6)	66(6)	58(6)	17(5)	-6(4)	-2(5)
O(8)	50(5)	86(7)	28(5)	10(5)	3(4)	8(5)
O(9)	37(5)	47(5)	48(5)	-15(4)	10(4)	-3(4)
O(10)	28(4)	49(5)	28(4)	3(4)	6(3)	7(4)
O(11)	38(5)	47(5)	29(4)	-4(4)	-14(3)	6(4)
O(12)	37(5)	44(5)	27(4)	-2(4)	-9(3)	3(4)
C(1)	43(8)	68(11)	37(8)	-8(7)	10(6)	-6(8)
C(2)	32(8)	56(9)	52(9)	-8(7)	-2(7)	8(7)
C(3)	46(9)	65(10)	53(9)	-11(7)	-17(7)	21(7)
C(4)	38(8)	49(9)	71(11)	-4(9)	3(8)	7(7)
C(5)	64(11)	150(18)	42(11)	37(13)	7(8)	69(12)
C(6)	65(11)	83(14)	70(13)	-26(11)	-7(9)	26(10)
C(7)	59(10)	48(11)	111(17)	13(10)	7(10)	17(8)
C(8)	51(9)	85(12)	38(9)	-11(9)	10(7)	22(9)
C(9)	91(12)	123(14)	37(9)	-32(10)	-9(8)	38(11)
C(10)	49(9)	112(13)	43(9)	7(9)	1(7)	8(8)
C(11)	78(13)	44(10)	99(12)	-6(9)	38(10)	-17(9)
C(12A)	23(24)	22(25)	131(44)	7(21)	34(23)	-31(19)
C(12B)	73(31)	91(51)	166(62)	-8(38)	51(34)	-70(32)
C(13)	120(15)	117(15)	56(10)	-42(10)	-37(10)	56(12)
C(14)	114(14)	71(12)	64(10)	-12(9)	-4(9)	-28(10)
C(15)	76(13)	153(18)	109(14)	77(14)	-10(10)	-59(12)
C(16)	73(11)	113(14)	69(10)	36(10)	4(8)	-34(10)
C(17)	78(12)	169(19)	77(12)	77(13)	-35(10)	-33(12)
C(18)	61(10)	112(13)	42(9)	6(9)	-2(7)	-19(9)
C(19)	77(12)	89(16)	106(14)	-9(13)	34(10)	-13(11)
C(20A)	77(19)	100(37)	88(25)	-49(20)	7(17)	-34(19)
C(20B)	354(151)	0(36)	90(57)	4(30)	129(79)	-76(56)

Table C.1.4. Hydrogen coordinates ($\times 10^4$) and isotropic displacement parameters ($\text{\AA}^2 \times 10^3$) for $\text{Tc}(\text{CO})_3(\text{L}_{\text{OEt}})$.

	x	y	z	U(eq)
H(4A)	-2215(10)	3434(7)	2557(12)	64
H(5A)	-2971(14)	2703(13)	1056(11)	102
H(6A)	-3816(13)	1535(10)	1705(15)	87
H(7A)	-3693(12)	1570(8)	3534(15)	87
H(8A)	-2694(11)	2722(9)	4086(10)	69
H(9A)	-427(13)	640(9)	5345(9)	101
H(9B)	585(13)	1222(9)	5281(9)	101
H(10A)	-57(11)	1169(8)	6807(9)	102
H(10B)	-1341(11)	1357(8)	6403(9)	102
H(10C)	-331(11)	1938(8)	6339(9)	102
H(11A)	-2295(13)	-446(7)	3915(11)	87
H(11B)	-1816(13)	-174(7)	2903(11)	87
H(12A)	-3754(42)	-483(25)	2702(45)	87
H(12B)	-3590(42)	356(25)	2513(45)	87
H(12C)	-4066(42)	84(25)	3520(45)	87
H(13A)	1306(15)	3183(10)	4154(11)	119
H(13B)	319(15)	2975(10)	4875(11)	119
H(14A)	1041(14)	4087(8)	5237(10)	125
H(14B)	-293(14)	4148(8)	4882(10)	125
H(14C)	695(14)	4357(8)	4160(10)	125
H(15A)	1648(14)	2889(11)	1419(12)	136
H(15B)	1473(14)	3541(11)	2146(12)	136
H(16A)	1856(12)	3946(9)	653(10)	128
H(16B)	579(12)	4181(9)	919(10)	128
H(16C)	755(12)	3527(9)	190(10)	128
H(17A)	-22(14)	1832(11)	-270(11)	131
H(17B)	-569(14)	2567(11)	70(11)	131
H(18A)	-551(11)	2511(8)	-1539(9)	108
H(18B)	-1858(11)	2533(8)	-1208(9)	108
H(18C)	-1308(11)	1793(8)	-1550(9)	108
H(19A)	-1409(14)	308(10)	-26(13)	107
H(19B)	-600(14)	-29(10)	824(13)	107
H(20A)	-1749(32)	-864(25)	119(32)	133
H(20B)	-2875(32)	-420(25)	383(32)	133
H(20C)	-2056(32)	-762(25)	1230(32)	133

Compound C.2. Full thermal ellipsoid plot of $\text{Re}(\text{CO})_3(\text{L}_{\text{OEt}})$.

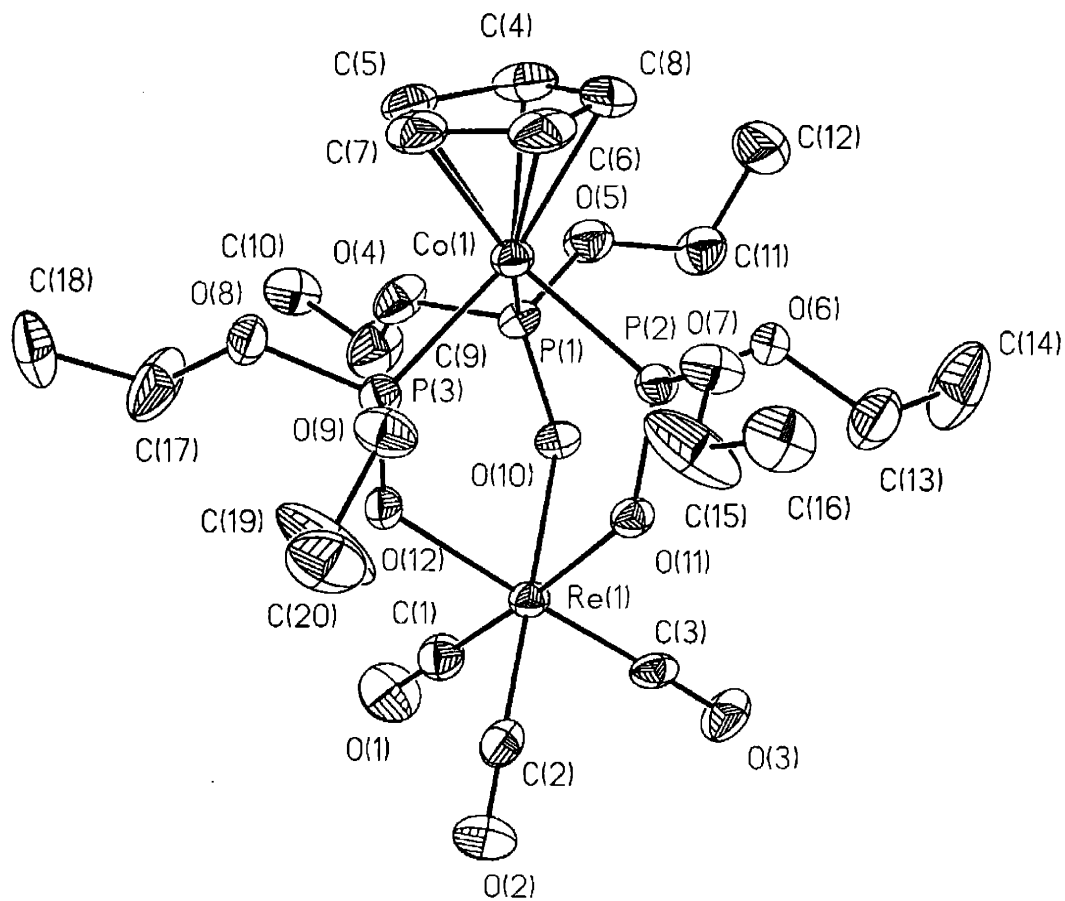


Table C.2.1. Atomic coordinates ($\times 10^4$) and equivalent isotropic displacement parameters ($\text{\AA}^2 \times 10^3$) for $\text{Re}(\text{CO})_3(\text{L}_{\text{OEt}})$. $U(\text{eq})$ is defined as one third of the trace of the orthogonalized U^{ij} tensor.

	x	y	z	U(eq)
Re(1)	6465(1)	1054(1)	2590(1)	32(1)
Co(1)	3231(1)	1978(1)	2594(1)	32(1)
P(1)	3870(2)	1150(1)	3584(1)	34(1)
P(2)	3912(2)	1390(1)	1390(1)	33(1)
P(3)	4859(2)	2539(1)	2794(1)	36(1)
O(11)	5210(4)	1258(2)	1400(3)	33(1)
O(7)	3539(4)	1739(3)	359(3)	48(1)
O(10)	4935(4)	719(2)	3315(3)	34(1)
O(6)	3238(4)	639(2)	1296(3)	40(1)
O(5)	2907(4)	582(3)	3881(4)	51(1)
O(4)	4097(4)	1515(3)	4625(3)	52(1)
O(12)	5954(4)	2109(2)	3055(3)	36(1)
O(8)	4758(4)	3147(3)	3605(4)	53(1)
O(9)	5029(4)	2999(3)	1829(4)	50(1)
O(3)	7117(5)	-457(3)	1947(4)	59(2)
O(1)	8155(5)	826(4)	4342(4)	75(2)
O(2)	8553(5)	1587(3)	1507(4)	70(2)
C(7)	2368(6)	2953(4)	2576(7)	53(2)
C(5)	2143(6)	2575(5)	3427(6)	50(2)
C(8)	1478(6)	1911(5)	2141(8)	62(2)
C(11)	2636(7)	-86(4)	3419(6)	56(2)
C(4)	1580(7)	1933(5)	3141(7)	57(2)
C(9)	4756(9)	1150(6)	5388(6)	75(3)
C(10)	4494(7)	1420(5)	6339(5)	59(2)
C(6)	1989(7)	2544(5)	1782(6)	58(2)
C(16)	3823(7)	2246(5)	-1189(5)	62(2)
C(15)	4216(8)	2136(7)	-227(7)	101(4)
C(13)	3602(9)	110(5)	610(7)	77(3)
C(17)	5503(9)	3290(6)	4383(7)	94(4)
C(3)	6854(6)	115(5)	2184(5)	40(2)
C(2)	7752(7)	1386(4)	1918(5)	41(2)
C(1)	7501(7)	910(4)	3680(6)	47(2)
C(20)	6060(8)	3770(5)	786(7)	74(3)
C(18)	5484(9)	4040(5)	4685(6)	75(3)
C(19)	6096(8)	3310(7)	1621(8)	107(5)
C(14)	3057(12)	-530(5)	612(8)	111(5)
C(12)	1412(8)	-105(6)	3080(9)	97(4)

Table C.2.2. Bond lengths [\AA] and angles [$^\circ$] for $\text{Re}(\text{CO})_3(\text{L}_{\text{OEt}})$.

Re(1)-C(2)	1.887(8)	Re(1)-C(1)	1.889(8)
Re(1)-C(3)	1.893(8)	Re(1)-O(12)	2.155(4)
Re(1)-O(10)	2.157(4)	Re(1)-O(11)	2.162(4)
Co(1)-C(6)	2.061(8)	Co(1)-C(5)	2.061(7)
Co(1)-C(7)	2.067(7)	Co(1)-C(4)	2.079(7)
Co(1)-C(8)	2.086(8)	Co(1)-P(3)	2.152(2)
Co(1)-P(1)	2.160~2)	Co(1)-P(2)	2.162(2)
P(1)-O(10)	1.525(4)	P(1)-O(4)	1.593(5)
P(1)-O(5)	1.599(5)	P(2)-O(11)	1.513(4)
P(2)-O(7)	1.598(5)	P(2)-O(6)	1.601(5)
P(3)-O(12)	1.521(5)	P(3)-O(8)	1.597(5)
P(3)-O(9)	1.597(5)	O(7)-C(15)	1.364(9)
O(6)-C(13)	1.438(9)	O(5)-C(11)	1.423(9)
O(4)-C(9)	1.434(9)	O(8)-C(17)	1.363(10)
O(9)-C(19)	1.400(9)	O(3)-C(3)	1.157(8)
O(1)-C(1)	1.163(9)	O(2)-C(2)	1.165(8)
C(7)-C(6)	1.383(11)	C(7)-C(5)	1.400(11)
C(5)-C(4)	1.405(11)	C(8)-C(4)	1.375(12)
C(8)-C(6)	1.416(12)	C(11)-C(12)	1.463(12)
C(9)-C(10)	1.446(10)	C(16)-C(15)	1.392(11)
C(13)-C(14)	1.347(12)	C(17)-C(18)	1.457(13)
C(20)-C(19)	1.430(12)		
C(2)-Re(1)-C(1)	87.3(3)	C(2)-Re(1)-C(3)	87.5(3)
C(1)-Re(1)-C(3)	87.3(3)	C(2)-Re(1)-O(12)	94.5(2)
C(1)-Re(1)-O(12)	93.7(3)	C(3)-Re(1)-O(12)	177.8(2)
C(2)-Re(1)-O(10)	176.8(2)	C(1)-Re(1)-O(10)	95.2(3)
C(3)-Re(1)-O(10)	94.6(2)	O(12)-Re(1)-O(10)	83.4(2)
C(2)-Re(1)-O(11)	94.8(2)	C(1)-Re(1)-O(11)	176.4(2)
C(3)-Re(1)-O(11)	95.7(2)	O(12)-Re(1)-O(11)	83.3(2)
O(10)-Re(1)-O(11)	82.5(2)	C(6)-Co(1)-C(5)	66.5(3)
C(6)-Co(1)-C(7)	39.1(3)	C(5)-Co(1)-C(7)	39.6(3)
C(6)-Co(1)-C(4)	66.1(4)	C(5)-Co(1)-C(4)	39.7(3)
C(7)-Co(1)-C(4)	66.0(3)	C(6)-Co(1)-C(8)	39.9(3)
C(5)-Co(1)-C(8)	66.0(3)	C(7)-Co(1)-C(8)	65.9(3)
C(4)-Co(1)-C(8)	38.5(3)	C(6)-Co(1)-P(3)	113.5(3)
C(5)-Co(1)-P(3)	102.5(2)	C(7)-Co(1)-P(3)	89.5(2)
C(4)-Co(1)-P(3)	141.2(3)	C(8)-Co(1)-P(3)	153.0(3)
C(6)-Co(1)-P(1)	155.8(3)	C(5)-Co(1)-P(1)	103.4(2)
C(7)-Co(1)-P(1)	141.4(3)	C(4)-Co(1)-P(1)	91.9(3)
C(8)-Co(1)-P(1)	116.2(3)	P(3)-Co(1)-P(1)	89.82(8)
C(6)-Co(1)-P(2)	96.4(2)	C(5)-Co(1)-P(2)	161.8(2)
C(7)-Co(1)-P(2)	128.8(3)	C(4)-Co(1)-P(2)	128.9(3)
C(8)-Co(1)-P(2)	97.1(3)	P(3)-Co(1)-P(2)	89.81(7)

P(1)-Co(1)-P(2)	89.80(7)	O(10)-P(1)-O(4)	110.1(3)
O(10)-P(1)-O(5)	106.8(3)	O(4)-P(1)-O(5)	98.0(3)
O(10)-P(1)-Co(1)	118.4(2)	O(4)-P(1)-Co(1)	107.3(2)
O(5)-P(1)-Co(1)	114.3(2)	O(11)-P(2)-O(7)	107.3(2)
O(11)-P(2)-O(6)	109.5(3)	O(7)-P(2)-O(6)	100.1(3)
O(11)-P(2)-Co(1)	118.0(2)	O(7)-P(2)-Co(1)	112.4(2)
O(6)-P(2)-Co(1)	108.1(2)	O(12)-P(3)-O(8)	107.1(3)
O(12)-P(3)-O(9)	110.1(3)	O(8)-P(3)-O(9)	102.4(3)
O(12)-P(3)-Co(1)	118.9(2)	O(8)-P(3)-Co(1)	109.9(2)
O(9)-P(3)-Co(1)	107.1(2)	P(2)-O(11)-Re(1)	131.2(2)
C(15)-O(7)-P(2)	127.3(5)	P(1)-O(10)-Re(1)	130.1(3)
C(13)-O(6)-P(2)	119.6(5)	C(11)-O(5)-P(1)	127.1(5)
C(9)-O(4)-P(1)	120.8(5)	P(3)-O(12)-Re(1)	130.0(3)
C(17)-O(8)-P(3)	128.4(5)	C(19)-O(9)-P(3)	122.3(5)
C(6)-C(7)-C(5)	108.6(8)	C(6)-C(7)-Co(1)	70.2(4)
C(5)-C(7)-Co(1)	70.0(4)	C(7)-C(5)-C(4)	107.1(7)
C(7)-C(5)-Co(1)	70.4(4)	C(4)-C(5)-Co(1)	70.8(4)
C(4)-C(8)-C(6)	107.9(8)	C(4)-C(8)-Co(1)	70.4(5)
C(6)-C(8)-Co(1)	69.1(5)	O(5)-C(11)-C(12)	110.4(7)
C(8)-C(4)-C(5)	108.7(8)	C(8)-C(4)-Co(1)	71.0(5)
C(5)-C(4)-Co(1)	69.5(4)	O(4)-C(9)-C(10)	111.7(7)
C(7)-C(6)-C(8)	107.6(8)	C(7)-C(6)-Co(1)	70.7(4)
C(8)-C(6)-Co(1)	71.0(5)	O(7)-C(15)-C(16)	118.1(8)
C(14)-C(13)-O(6)	116.9(8)	O(8)-C(17)-C(18)	113.0(8)
O(3)-C(3)-Re(1)	178.4(6)	O(2)-C(2)-Re(1)	179.4(7)
O(1)-C(1)-Re(1)	178.8(7)	O(9)-C(19)-C(20)	114.8(8)

Table C.2.3. Anisotropic displacement parameters ($\text{\AA}^2 \times 10^3$) for $\text{Re}(\text{CO})_3(\text{L}_{\text{OEt}})$. The anisotropic displacement factor exponent takes the form: $-2\pi^2[h^2 a^{*2} U^{11} + \dots + 2 h k a^* b^* U^{12}]$

	U^{11}	U^{22}	U^{33}	U^{23}	U^{13}	U^{12}
Re(1)	27(1)	37(1)	31(1)	-2(1)	0(1)	5(1)
Co(1)	28(1)	36(1)	33(1)	-2(1)	1(1)	6(1)
P(1)	34(1)	37(1)	33(1)	-2(1)	8(1)	4(1)
P(2)	29(1)	41(1)	28(1)	-1(1)	-1(1)	1(1)
P(3)	34(1)	34(1)	40(1)	-4(1)	-2(1)	2(1)
O(11)	31(2)	42(3)	26(2)	-1(2)	2(2)	6(2)
O(7)	38(3)	72(4)	34(3)	18(3)	0(2)	4(3)
O(10)	35(3)	36(3)	31(3)	7(2)	7(2)	5(2)
O(6)	33(3)	41(3)	44(3)	-13(2)	2(2)	0(2)
O(5)	46(3)	47(3)	61(3)	-3(3)	16(3)	-1(3)
O(4)	64(3)	60(4)	32(3)	0(2)	1(2)	25(3)
O(12)	33(3)	36(3)	37(3)	-9(2)	-4(2)	2(2)
O(8)	44(3)	46(3)	66(4)	-26(3)	-13(3)	12(3)
O(9)	39(3)	49(3)	63(3)	17(3)	4(2)	-3(2)
O(3)	67(4)	43(3)	67(4)	-12(3)	7(3)	19(3)
O(1)	60(4)	100(5)	63(4)	7(4)	-31(3)	18(4)
O(2)	46(3)	85(5)	81(4)	-6(4)	27~3)	-15(3)
C(7)	39(4)	35(5)	85(7)	6(5)	9(4)	13(4)
C(5)	37(4)	62(6)	51(5)	-8(4)	6(4)	20(4)
C(8)	31(4)	65(6)	88(7)	-18(6)	-7(4)	13(4)
C(11)	58(5)	40(5)	72(6)	0(4)	16(4)	0(4)
C(4)	38(5)	56(6)	80(7)	10(5)	18(4)	14(4)
C(9)	83(7)	100(8)	42(5)	-12(5)	-7(5)	24(6)
C(10)	50(5)	89(7)	39(5)	11(4)	2(4)	4(5)
C(6)	43(5)	79(7)	52(5)	4(5)	-7(4)	34(5)
C(16)	60(5)	91(7)	35(5)	19(5)	2(4)	-2(5)
C(15)	58(6)	165(12)	78(7)	63(7)	-22(5)	-42(7)
C(13)	86(7)	64(7)	84(7)	-30(6)	36(6)	-19(6)
C(17)	108(8)	101(9)	67(6)	-49(6)	-41(6)	54(7)
C(3)	30(4)	66(6)	24(4)	1(4)	6(3)	7(4)
C(2)	45(5)	43(4)	35(4)	-7(4)	-1(4)	10(4)
C(1)	46(5)	45(5)	50(5)	-2(4)	-1(4)	6(4)
C(20)	63(6)	89(8)	73(6)	16(6)	25(5)	-16(5)
C(18)	90(7)	69(7)	65(6)	-19(5)	-12(5)	-35(6)
C(19)	60(6)	150(11)	108(8)	75(8)	-26(6)	-57(7)
C(14)	179(13)	58(7)	99(9)	-28(6)	53(9)	-29(8)
C(12)	55(6)	79(8)	157(11)	-39(8)	10(6)	-14(5)

Table C.2.4. Hydrogen coordinates ($\times 10^4$) and isotropic displacement parameters ($\text{\AA}^2 \times 10^3$) for $\text{Re}(\text{CO})_3(\text{L}_{\text{OEt}})$.

	x	y	z	U(eq)
H(7A)	2735(6)	3427(4)	2547(7)	63
H(5A)	2308(6)	2739(5)	4097(6)	60
H(8A)	1115(6)	1526(5)	1746(8)	74
H(11A)	2793(7)	-476(4)	3875(6)	67
H(11B)	3124(7)	-153(4)	2870(6)	67
H(4A)	1302(7)	1564(5)	3582(7)	69
H(9A)	5579(9)	1212(6)	5291(6)	90
H(9B)	4585(9)	640(6)	5355(6)	90
H(10A)	4949(7)	1165(5)	6830(5)	89
H(10B)	3682(7)	1351(5)	6442(5)	89
H(10C)	4676(7)	1923(5)	6378(5)	89
H(6A)	2029(7)	2681(5)	1095(6)	70
H(16A)	4379(7)	2532(5)	-1517(5)	93
H(16B)	3089(7)	2492(5)	-1202(5)	93
H(16C)	3730(7)	1790(5)	-1512(5)	93
H(15A)	4972(8)	1906(7)	-235(7)	121
H(15B)	4333(8)	2604(7)	74(7)	121
H(13A)	3500(9)	313(5)	-39(7)	92
H(13B)	4428(9)	26(5)	733(7)	92
H(17A)	6287(9)	3164(6)	4216(7)	112
H(17B)	5299(9)	2990(6)	4926(7)	112
H(20A)	6823(8)	3960(5)	696(7)	111
H(20B)	5529(8)	4159(5)	884(7)	111
H(20C)	5804(8)	3501(5)	220(7)	111
H(18A)	6022(9)	4110(5)	5232(6)	113
H(18B)	4714(9)	4166(5)	4865(6)	113
H(18C)	5702(9)	4340(5)	4155(6)	113
H(19A)	6652(8)	2928(7)	1521(8)	128
H(19B)	6377(8)	3585(7)	2183(8)	128
H(14A)	3370(12)	-837(5)	128(8)	166
H(14B)	2240(12)	-461(5)	468(8)	166
H(14C)	3171(12)	-749(5)	1242(8)	166
H(12A)	1242(8)	-558(6)	2771(9)	146
H(12B)	1260(8)	278(6)	2622(9)	146
H(12C)	930(8)	-45(6)	3626(9)	146

Compound C.3. Thermal ellipsoid plot of $(\text{NEt}_4)[\text{Re}_2(\text{CO})_6(\mu\text{-pz})_2(\mu\text{-OMe})]$ showing the tetraethylammonium cation and both molecules of the asymmetric unit.

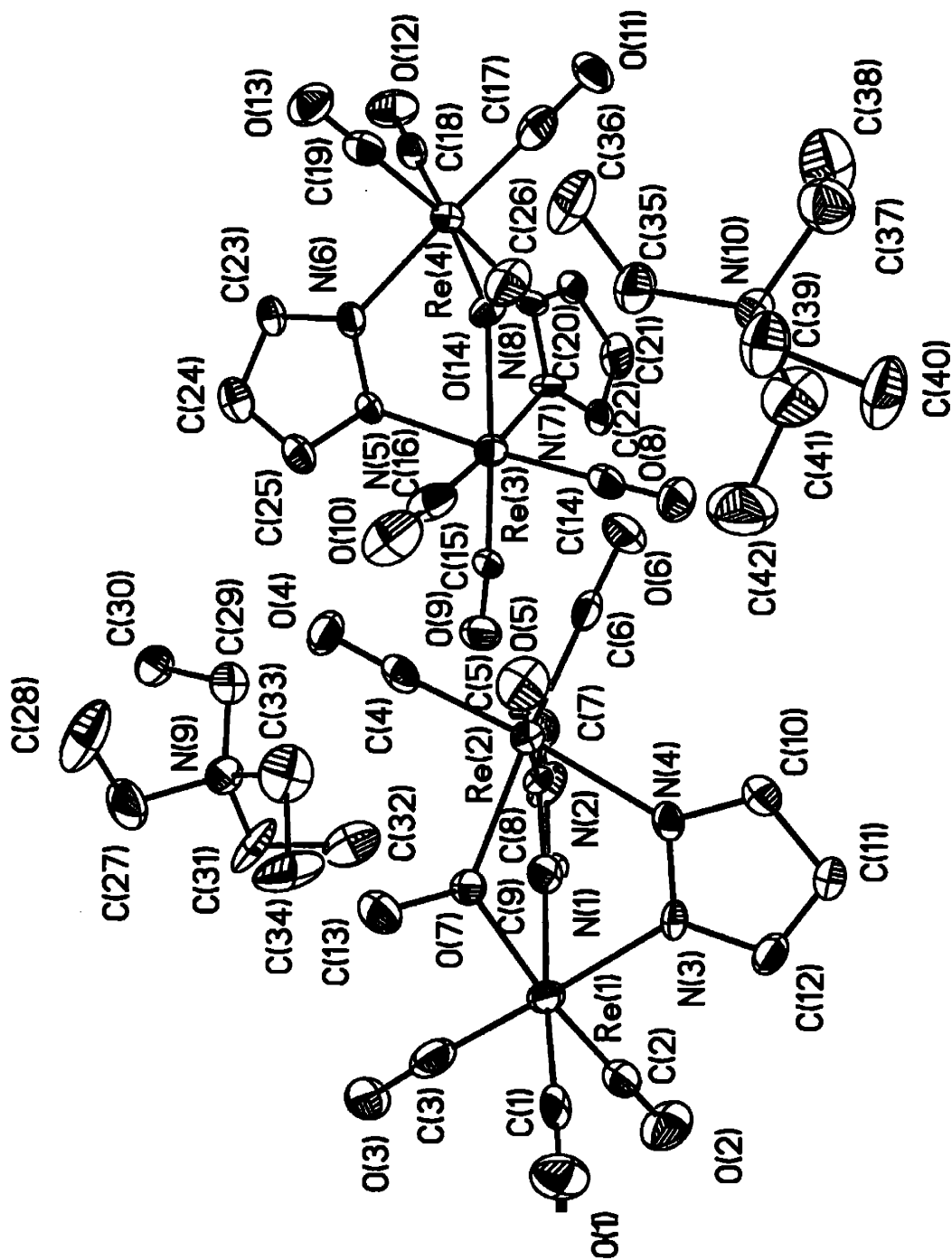


Table C.3.1. Atomic coordinates ($\times 10^4$) and equivalent isotropic displacement parameters ($\text{\AA}^2 \times 10^3$) for $(\text{NEt}_4)[\text{Re}_2(\text{CO})_6(\mu\text{-pz})_2(\mu\text{-OMe})]$. $U(\text{eq})$ is defined as one third of the trace of the orthogonalized U^{ij} tensor.

	x	y	z	U(eq)
Re(1)	4319(1)	765(1)	1582(1)	35(1)
Re(2)	3587(1)	3304(1)	1552(1)	32(1)
Re(3)	8707(1)	6020(1)	1022(1)	34(1)
Re(4)	9175(1)	8506(1)	788(1)	35(1)
O(1)	2126(10)	-603(6)	1787(3)	66(3)
O(2)	6369(11)	-674(7)	1921(3)	72(3)
O(3)	4388(10)	-380(6)	884(2)	59(3)
O(4)	3130(9)	4234(6)	811(2)	53(3)
O(5)	790(10)	3940(6)	1729(2)	55(3)
O(6)	4673(10)	5233(6)	1832(2)	66(3)
O(7)	3076(7)	1895(5)	1372(2)	31(2)
O(8)	8443(10)	5536(6)	1807(2)	60(3)
O(9)	9807(9)	4027(6)	906(2)	55(2)
O(10)	5957(10)	5110(8)	831(3)	94(4)
O(11)	9371(9)	10029(6)	1383(2)	66(3)
O(12)	10986(10)	9829(6)	395(3)	72(3)
O(13)	6782(10)	9559(6)	401(2)	64(3)
O(14)	8059(8)	7471(5)	1050(2)	38(2)
N(1)	5836(10)	1811(7)	1469(2)	36(2)
N(2)	5540(10)	2764(6)	1458(2)	29(2)
N(3)	4243(10)	1596(7)	2062(2)	37(3)
N(4)	3957(9)	2552(7)	2051(2)	31(2)
N(5)	8921(9)	6456(6)	480(2)	33(2)
N(6)	9011(9)	7399(7)	388(2)	36(3)
N(7)	10643(9)	6736(6)	1125(2)	31(2)
N(8)	10818(10)	7641(6)	1039(2)	33(2)
N(9)	6407(11)	2580(7)	97(2)	45(3)
N(10)	891(10)	7231(6)	2492(2)	36(3)
C(1)	2938(13)	-86(9)	1715(3)	37(3)
C(2)	5572(16)	-133(9)	1793(3)	52(4)
C(3)	4346(14)	77(9)	1145(4)	56(4)
C(4)	3266(11)	3867(8)	1090(3)	37(3)
C(5)	1839(14)	3714(8)	1658(3)	37(3)
C(6)	4233(12)	4493(9)	1724(3)	36(3)
C(7)	6685(15)	3211(10)	1391(3)	50(4)
C(8)	7684(14)	2566(10)	1344(3)	51(4)
C(9)	7085(14)	1700(9)	1394(3)	49(4)
C(10)	3922(11)	2839(8)	2389(3)	37(3)
C(11)	4147(13)	2085(9)	2622(3)	48(4)
C(12)	4324(12)	1327(9)	2408(3)	45(3)

C(13)	1912(12)	1723(8)	1133(3)	47(3)
C(14)	8585(13)	5711(8)	1513(3)	43(3)
C(15)	9405(14)	4798(9)	964(3)	46(4)
C(16)	6959(16)	5474(9)	911(4)	61(4)
C(17)	9322(13)	9458(10)	1156(4)	53(4)
C(18)	10317(13)	9310(9)	539(3)	42(3)
C(19)	7659(14)	9162(9)	552(4)	48(4)
C(20)	12108(13)	7867(8)	1127(3)	40(3)
C(21)	12762(14)	7105(10)	1289(3)	54(4)
C(22)	11792(12)	640g(9)	1276(3)	37(3)
C(23)	9036(11)	7440(9)	32(3)	35(3)
C(24)	8919(13)	6523(10)	-112(3)	56(4)
C(25)	8868(12)	5948(9)	175(3)	45(3)
C(26)	6884(14)	7712(9)	1217(3)	63(4)
C(27)	5471(16)	2297(11)	-222(4)	87(6)
C(28)	4372(16)	3052(13)	-280(4)	105(7)
C(29)	7113(16)	3505(10)	44(4)	77(5)
C(30)	7621(13)	3632(9)	-335(3)	51(4)
C(31)	7483(14)	1766(11)	122(4)	75(5)
C(32)	8431(15)	1762(10)	463(4)	76(5)
C(33)	5737(16)	2678(11)	420(4)	83(5)
C(34)	4878(17)	1766(9)	513(4)	90(6)
C(35)	759(14)	7412(9)	2099(3)	51(4)
C(36)	-355(14)	8103(10)	1953(3)	70(5)
C(37)	1274(15)	8134(10)	2702(4)	66(4)
C(38)	2563(16)	8568(12)	2645(4)	83(5)
C(39)	445(14)	6893(10)	2595(3)	63(4)
C(40)	450(16)	6504(11)	2968(3)	77(5)
C(41)	1969(15)	6500(10)	2574(4)	75(5)
C(42)	1766(17)	5515(10)	2414(4)	99(6)

Table C.3.2. Bond lengths [\AA] and angles [$^\circ$] for $(\text{NEt}_4)[\text{Re}_2(\text{CO})_6(\mu\text{-pz})_2(\mu\text{-OMe})]$.

Re(1)-C(2)	1.899(16)	O(14)-C(26)	1.428(13)
Re(1)-C(3)	1.912(15)	N(1)-C(9)	1.319(14)
Re(1)-C(1)	1.930(14)	N(1)-N(2)	1.367(11)
Re(1)-O(7)	2.121(7)	N(2)-C(7)	1.352(14)
Re(1)-N(3)	2.159(8)	N(3)-C(12)	1.351(13)
Re(1)-N(1)	2.182(9)	N(3)-N(4)	1.370(12)
Re(2)-C(6)	1.881(13)	N(4)-C(10)	1.340(12)
Re(2)-C(4)	1.911(13)	N(5)-C(25)	1.350(13)
Re(2)-C(5)	1.921(15)	N(5)-N(6)	1.371(11)
Re(2)-O(7)	2.134(7)	N(6)-C(23)	1.345(12)
Re(2)-N(2)	2.158(9)	N(7)-C(22)	1.318(13)
Re(2)-N(4)	2.160(9)	N(7)-N(8)	1.324(11)
Re(3)-C(15)	1.870(13)	N(8)-C(20)	1.342(14)
Re(3)-C(14)	1.917(13)	N(9)-C(33)	1.452(15)
Re(3)-C(16)	1.922(16)	N(9)-C(29)	1.498(15)
Re(3)-O(14)	2.140(7)	N(9)-C(27)	1.507(16)
Re(3)-N(5)	2.164(9)	N(9)-C(31)	1.567(16)
Re(3)-N(7)	2.186(9)	N(10)-C(35)	1.498(13)
Re(4)-C(18)	1.914(14)	N(10)-C(41)	1.500(15)
Re(4)-C(19)	1.920(15)	N(10)-C(39)	1.505(15)
Re(4)-C(17)	1.920(15)	N(10)-C(37)	1.521(14)
Re(4)-O(14)	2.129(7)	C(7)-C(8)	1.373(17)
Re(4)-N(6)	2.159(9)	C(8)-C(9)	1.375(16)
Re(4)-N(8)	2.188(9)	C(10)-C(11)	1.379(14)
O(1)-C(1)	1.141(14)	C(11)-C(12)	1.355(15)
O(2)-C(2)	1.171(15)	C(20)-C(21)	1.365(15)
O(3)-C(3)	1.177(14)	C(21)-C(22)	1.374(16)
O(4)-C(4)	1.167(12)	C(23)-C(24)	1.395(15)
O(5)-C(5)	1.154(14)	C(24)-C(25)	1.353(16)
O(6)-C(6)	1.184(13)	C(27)-C(28)	1.528(19)
O(7)-C(13)	1.426(12)	C(29)-C(30)	1.573(17)
O(8)-C(14)	1.154(13)	C(31)-C(32)	1.527(18)
O(9)-C(15)	1.181(13)	C(33)-C(34)	1.598(18)
O(10)-C(16)	1.141(15)	C(35)-C(36)	1.541(16)
O(11)-C(17)	1.171(14)	C(37)-C(38)	1.462(18)
O(12)-C(18)	1.157(14)	C(39)-C(40)	1.507(15)
O(13)-C(19)	1.146(14)	C(41)-C(42)	1.510(18)
C(2)-Re(1)-C(3)	88.0(5)	C(3)-Re(1)-O(7)	96.3(4)
C(2)-Re(1)-C(1)	86.8(5)	C(1)-Re(1)-O(7)	98.5(4)
C(3)-Re(1)-C(1)	88.9(5)	C(2)-Re(1)-N(3)	94.6(4)
C(2)-Re(1)-O(7)	173.2(4)	C(3)-Re(1)-N(3)	177.4(5)

C(1)-Re(1)-N(3)	91.9(4)	O(14)-Re(4)-N(6)	80.0(3)
O(7)-Re(1)-N(3)	81.1(3)	C(18)-Re(4)-N(8)	94.4(4)
C(2)-Re(1)-N(1)	94.7(5)	C(19)-Re(4)-N(8)	175.0(4)
C(3)-Re(1)-N(1)	95.9(4)	C(17)-Re(4)-N(8)	93.9(4)
C(1)-Re(1)-N(1)	175.0(4)	O(14)-Re(4)-N(8)	80.2(3)
O(7)-Re(1)-N(1)	79.7(3)	N(6)-Re(4)-N(8)	84.8(3)
N(3)-Re(1)-N(1)	83.2(3)	C(13)-O(7)-Re(1)	121.8(6)
C(6)-Re(2)-C(4)	88.4(4)	C(13)-O(7)-Re(2)	121.0(6)
C(6)-Re(2)-C(5)	87.4(5)	Re(1)-O(7)-Re(2)	117.2(3)
C(4)-Re(2)-C(5)	89.2(5)	C(26)-O(14)-Re(4)	122.4(7)
C(6)-Re(2)-O(7)	173.5(4)	C(26)-O(14)-Re(3)	120.8(7)
C(4)-Re(2)-O(7)	94.5(4)	Re(4)-O(14)-Re(3)	116.7(4)
C(5)-Re(2)-O(7)	98.4(4)	C(9)-N(1)-N(2)	108.5(9)
C(6)-Re(2)-N(2)	94.5(4)	C(9)-N(1)-Re(1)	130.9~8)
C(4)-Re(2)-N(2)	94.2(4)	N(2)-N(1)-Re(1)	120.5(7)
C(5)-Re(2)-N(2)	176.1(4)	C(7)-N(2)-N(1)	105.8(10)
O(7)-Re(2)-N(2)	79.5(3)	C(7)-N(2)-Re(2)	131.8(9)
C(6)-Re(2)-N(4)	96.0(4)	N(1)-N(2)-Re(2)	122.4(7)
C(4)-Re(2)-N(4)	175.1(4)	C(12)-N(3)-N(4)	107.1(9)
C(5)-Re(2)-N(4)	92.8(4)	C(12)-N(3)-Re(1)	130.9(9)
O(7)-Re(2)-N(4)	80.9(3)	N(4)-N(3)-Re(1)	121.7(6)
N(2)-Re(2)-N(4)	83.6(3)	C(10)-N(4)-N(3)	106.8(9)
C(15)-Re(3)-C(14)	88.0(5)	C(10)-N(4)-Re(2)	131.7(8)
C(15)-Re(3)-C(16)	87.3(6)	N(3)-N(4)-Re(2)	121.4(7)
C(14)-Re(3)-C(16)	89.0(6)	C(25)-N(5)-N(6)	106.8(9)
C(15)-Re(3)-O(14)	173.8(4)	C(25)-N(5)-Re(3)	131.1(8)
C(14)-Re(3)-O(14)	96.9(4)	N(6)-N(5)-Re(3)	121.8(7)
C(16)-Re(3)-O(14)	96.5(4)	C(23)-N(6)-N(5)	107.6(9)
C(15)-Re(3)-N(5)	94.4(4)	C(23)-N(6)-Re(4)	131.2(8)
C(14)-Re(3)-N(5)	176.0(4)	N(5)-N(6)-Re(4)	121.1(7)
C(16)-Re(3)-N(5)	94.3(5)	C(22)-N(7)-N(8)	107.9(9)
O(14)-Re(3)-N(5)	80.5(3)	C(22)-N(7)-Re(3)	130.0(8)
C(15)-Re(3)-N(7)	96.0(5)	N(8)-N(7)-Re(3)	122.1(7)
C(14)-Re(3)-N(7)	94.0(4)	N(7)-N(8)-C(20)	108.2(9)
C(16)-Re(3)-N(7)	175.6(4)	N(7)-N(8)-Re(4)	121.6(7)
O(14)-Re(3)-N(7)	79.9(3)	C(20)-N(8)-Re(4)	130.2(8)
N(5)-Re(3)-N(7)	82.7(3)	C(33)-N(9)-C(29)	107.0(11)
C(18)-Re(4)-C(19)	88.6(5)	C(33)-N(9)-C(27)	113.1(12)
C(18)-Re(4)-C(17)	86.4(5)	C(29)-N(9)-C(27)	112.9(10)
C(19)-Re(4)-C(17)	90.3(5)	C(33)-N(9)-C(31)	112.8(10)
C(18)-Re(4)-O(14)	173.0(4)	C(29)-N(9)-C(31)	107.8(11)
C(19)-Re(4)-O(14)	96.5(4)	C(27)-N(9)-C(31)	103.2(10)
C(17)-Re(4)-O(14)	98.4(4)	C(35)-N(10)-C(41)	108.3(10)
C(18)-Re(4)-N(6)	95.1(4)	C(35)-N(10)-C(39)	108.1(9)
C(19)-Re(4)-N(6)	90.9(4)	C(41)-N(10)-C(39)	111.9(10)
C(17)-Re(4)-N(6)	178.1(4)	C(35)-N(10)-C(37)	111.6(9)

C(41)-N(10)-C(37)	108.7(11)
C(39)-N(10)-C(37)	108.3(10)
O(1)-C(1)-Re(1)	178.4(10)
O(2)-C(2)-Re(1)	178.3(13)
O(3)-C(3)-Re(1)	177.0(11)
O(4)-C(4)-Re(2)	176.6(10)
O(5)-C(5)-Re(2)	178.0(10)
O(6)-C(6)-Re(2)	178.3(11)
N(2)-C(7)-C(8)	111.2(12)
C(7)-C(8)-C(9)	103.3(12)
N(1)-C(9)-C(8)	111.1(12)
N(4)-C(10)-C(11)	110.9(10)
C(12)-C(11)-C(10)	104.1(10)
N(3)-C(12)-C(11)	111.0(11)
O(8)-C(14)-Re(3)	176.5(12)
O(9)-C(15)-Re(3)	175.8(11)
O(10)-C(16)-Re(3)	175.8(15)
O(11)-C(17)-Re(4)	177.7(13)
O(12)-C(18)-Re(4)	177.1(12)
O(13)-C(19)-Re(4)	177.3(13)
N(8)-C(20)-C(21)	109.7(11)
C(20)-C(21)-C(22)	103.3(12)
N(7)-C(22)-C(21)	110.8(11)
N(6)-C(23)-C(24)	109.8(11)
C(25)-C(24)-C(23)	104.3(11)
N(5)-C(25)-C(24)	111.4(11)
N(9)-C(27)-C(28)	108.5(12)
N(9)-C(29)-C(30)	114.6(10)
C(32)-C(31)-N(9)	115.1(13)
N(9)-C(33)-C(34)	114.3(12)
N(10)-C(35)-C(36)	117.0(10)
C(38)-C(37)-N(10)	116.9(12)
N(10)-C(39)-C(40)	115.8(11)
N(10)-C(41)-C(42)	118.3(13)

Table C.3.3. Anisotropic displacement parameters ($\text{\AA}^2 \times 10^3$) for $(\text{NEt}_4)[\text{Re}_2(\text{CO})_6(\mu\text{-pz})_2(\mu\text{-OMe})]$. The anisotropic displacement factor exponent takes the form: $-2\pi^2[h^2a^*U^{11} + \dots + 2hk a^* b^* U^{12}]$

	U^{11}	U^{22}	U^{33}	U^{23}	U^{13}	U^{12}
Re(1)	45(1)	28(1)	35(1)	2(1)	8(1)	1(1)
Re(2)	37(1)	28(1)	31(1)	1(1)	0(1)	1(1)
Re(3)	35(1)	32(1)	36(1)	2(1)	4(1)	4(1)
Re(4)	39(1)	28(1)	36(1)	-1(1)	2(1)	0(1)
O(1)	63(8)	57(7)	81(7)	1(5)	21(6)	-20(5)
O(2)	89(9)	56(7)	72(7)	11(5)	12(6)	33(6)
O(3)	97(9)	44(6)	41(6)	-11(5)	24(5)	0(5)
O(4)	61(7)	52(6)	41(5)	18(5)	-12(5)	-13(5)
O(5)	46(7)	63(6)	59(6)	2(5)	16(5)	15(5)
O(6)	88(8)	42(6)	61(6)	-17(5)	-26(6)	0(5)
O(7)	27(5)	30(4)	34(4)	1(4)	0(4)	1(4)
O(8)	77(8)	62(6)	40(6)	10(5)	10(5)	-11(5)
O(9)	72(7)	39(6)	55(6)	-2(5)	11(5)	-7(5)
O(10)	43(7)	93(8)	139(10)	46(7)	-30(7)	-34(6)
O(11)	68(8)	59(6)	67(7)	-32(5)	-24(6)	29(5)
O(12)	80(9)	45(6)	93(8)	16(5)	21(6)	-18(6)
O(13)	54(7)	56(6)	78(7)	14(5)	-13(6)	7(5)
O(14)	42(6)	36(5)	39(5)	11(4)	9(4)	3(4)
N(1)	40(7)	42(7)	28(6)	-3(5)	13(5)	-3(5)
N(2)	42(7)	22(6)	23(5)	5(4)	1(5)	-2(5)
N(3)	58(8)	40(6)	14(5)	0(5)	3(5)	0(5)
N(4)	26(6)	40(6)	27(6)	-2(5)	4(4)	-10(5)
N(5)	37(7)	31(6)	29(6)	4(5)	-6(5)	-7(5)
N(6)	39(7)	41(6)	28(6)	-1(5)	-3(5)	-8(5)
N(7)	32(7)	16(5)	46(6)	0(4)	3(5)	0(5)
N(8)	36(7)	20(6)	41(6)	4(4)	~5(5)	4(5)
N(9)	58(8)	47(7)	32(6)	7(5)	16(6)	-13(6)
N(10)	42(7)	34(6)	32(6)	5(5)	-1(5)	0(5)
C(1)	54(10)	41(8)	17(6)	-11(6)	9(6)	14(7)
C(2)	77(12)	42(9)	38(8)	4(7)	4(8)	-19(8)
C(3)	71(11)	44(9)	54(10)	20(7)	11(8)	4(8)
C(4)	25(8)	36(7)	47(8)	-12(6)	-12(6)	1(6)
C(5)	61(10)	26(7)	21(7)	14(5)	-7(7)	-16(7)
C(6)	42(9)	42(8)	23(7)	7(6)	0(6)	11(6)
C(7)	60(11)	50(9)	38(8)	6(7)	-8(7)	-30(8)
C(8)	42(10)	64(10)	47(9)	21(8)	8(7)	3(8)
C(9)	54(10)	48(9)	46(8)	14(7)	12(7)	10(8)
C(10)	33(8)	39(8)	38(8)-	-7(6)	1(6)	3(6)
C(11)	71(11)	45(9)	25(7)	4(7)	-3(7)	0(7)
C(12)	53(10)	48(9)	32(8)	15(7)	-4(6)	-9(7)

C(13)	44(9)	45(8)	52(8)	-9(7)	-2(7)	-6(7)
C(14)	46(9)	35(8)	45(8)	-8(7)	-1(7)	-12(6)
C(15)	75(11)	28(8)	34(8)	0(6)	-10(7)	-16(7)
C(16)	52(11)	45(9)	84(11)	21(8)	0(9)	8(8)
C(17)	31(9)	65(10)	61(10)	16(8)	-11(7)	7(7)
C(18)	39(9)	44(8)	40(8)	-7(7)	-14(6)	-2(7)
C(19)	50(10)	35(8)	58(9)	-6(7)	4(8)	-7(7)
C(20)	42(9)	37(8)	39(8)	-1(6)	-12(7)	-16(7)
C(21)	32(9)	78(11)	48(9)	-3(8)	-13(7)	10(8)
C(22)	33(8)	43(8)	32(7)	-1(6)	-10(6)	2(7)
C(23)	28(8)	54(8)	25(7)	4(6)	7(6)	-6(6)
C(24)	59(11)	68(10)	40(8)	-11(8)	6(7)	-3(8)
C(25)	41(9)	48(8)	45(8)	-11(7)	-6(7)	-8(7)
C(26)	63(11)	72(10)	58(9)	9(8)	18(8)	33(9)
C(27)	84(14)	75(12)	90(12)	-17(9)	-53(11)	7(10)
C(28)	59(13)	159(17)	94(13)	68(13)	-15(10)	7(12)
C(29)	106(14)	55(10)	63(10)	1(8)	-31(10)	-2(9)
C(30)	64(11)	55(9)	38(8)	9(7)	16(7)	-8(7)
C(31)	48(10)	102(13)	74(11)	68(10)	-5(8)	1(9)
C(32)	58(12)	69(11)	104(13)	24(9)	23(10)	12(8)
C(33)	67(13)	103(14)	81(12)	6(10)	25(10)	-3(10)
C(34)	136(17)	49(10)	100(12)	27(9)	89(12)	9(10)
C(35)	66(11)	57(9)	32(8)	6(7)	11(7)	2(8)
C(36)	65(12)	84(11)	56(9)	32(8)	-14(8)	-1(9)
C(37)	66(12)	63(10)	67(10)	4(8)	4(9)	-10(8)
C(38)	77(13)	112(14)	62(10)	-1(9)	19(9)	43(11)
C(39)	55(11)	87(11)	46(9)	8(8)	7(8)	-6(8)
C(40)	92(14)	102(13)	37(8)	20(8)	5(8)	-9(10)
C(41)	61(12)	79(12)	89(12)	5(10)	24(9)	36(9)
C(42)	109(16)	60(12)	123(15)	-9(11)	-18(12)	22(10)

Table C.3.4. Hydrogen coordinates ($\times 10^4$) and isotropic displacement parameters ($\text{\AA}^2 \times 10^3$) for $(\text{NEt}_4)[\text{Re}_2(\text{CO})_6(\mu\text{-pz})_2(\mu\text{-OMe})]$.

	x	y	z	U(eq)
H(7A)	6783	3870	1378	60
H(8A)	8556	2686	1291	61
H(9A)	7506	1112	1377	59
H(10A)	3767	3464	2458	44
H(11A)	4172	2093	2869	57
H(12A)	4481	706	2488	54
H(13A)	1841	1052	1082	71
H(13B)	1981	2069	916	71
H(13C)	1131	1931	1241	71
H(20A)	12497	8453	1085	48
H(21A)	13650	7067	1385	64
H(22A)	11929	5791	1362	44
H(23A)	9120	7996	99	42
H(24A)	8884	6347	-350	67
H(25A)	8804	5286	163	54
H(26A)	6746	8390	1205	95
H(26B)	6994	7516	1462	95
H(26C)	6123	7393	1098	95
H(27A)	5076	1679	-181	104
H(27B)	5960	2252	-431	104
H(28A)	3768	2882	-482	158
H(28B)	4770	3661	-320	158
H(28C)	3888	3088	-72	158
H(29A)	7875	3552	222	93
H(29B)	6508	4025	85	93
H(30A)	8055	4241	-348	77
H(30B)	6873	3601	-514	77
H(30C)	8246	3133	-376	77
H(31A)	7023	1156	101	90
H(31B)	8012	1823	-80	90
H(32A)	9057	1245	455	114
H(32B)	7924	1682	665	114
H(32C)	8910	2356	484	114
H(33A)	5149	3228	396	99
H(33B)	6407	2800	618	99
H(34A)	4464	1884	729	135
H(34B)	5455	1220	545	135
H(34C)	4197	1647	322	135
H(35A)	609	6804	1979	62
H(35B)	1608	7658	2035	62
H(36A)	-333	8171	1700	105

H(36B)	-216	8715	2065	105
H(36C)	-1211	7855	2002	105
H(37A)	578	8605	2645	79
H(37B)	1277	7987	2954	79
H(38A)	2690	9134	2788	124
H(38B)	2573	8733	2398	124
H(38C)	3271	8123	2711	124
H(39A)	-775	6401	2429	75
H(39B)	-1070	7423	2568	75
H(40A)	-1342	6306	3007	115
H(40B)	-158	6991	3137	115
H(40C)	145	5967	2997	115
H(41A)	2103	6428	2831	90
H(41B)	2794	6755	2497	90
H(42A)	2535	5127	2484	149
H(42B)	1650	5564	2159	149
H(42C)	983	5230	2498	149

Table C.4.1. Atomic coordinates ($\times 10^4$) and equivalent isotropic displacement parameters ($\text{\AA}^2 \times 10^3$) for $(\text{NEt}_4)[\text{Re}_2(\text{CO})_6(\mu\text{-pz})_2(\mu\text{-OH})]\cdot(\text{CH}_3)_2\text{CO}\cdot 0.5\text{H}_2\text{O}$. $U(\text{eq})$ is defined as one third of the trace of the orthogonalized U^{ij} tensor.

	x	y	z	U(eq)
Re(1)	3295(1)	1085(1)	2840(1)	29(1)
O(1)	3915(4)	-71(6)	724(7)	62(2)
O(2)	2318(4)	706(7)	3159(7)	69(2)
O(3)	4219(4)	-144(6)	4490(7)	64(2)
O(4)	3831(4)	2500	2707(8)	30(2)
O(5)	5016(5)	2500	1347(13)	79(4)
O(6)	5751(14)	2500	7540(30)	93(9)
N(1)	2619(3)	1965(6)	1733(7)	31(2)
N(2)	2874(3)	1973(5)	4301(6)	25(2)
N(3)	4486(7)	2500	7562(14)	100(8)
C(1)	3674(5)	387(8)	1506(9)	43(2)
C(2)	2698(5)	-60(8)	3028(8)	42(2)
C(3)	3873(5)	344(8)	3878(9)	46(3)
C(4)	2175(4)	1647(8)	939(9)	41(2)
C(5)	1887(7)	2500	413(15)	51(4)
C(6)	2604(4)	1641(8)	5314(8)	33(2)
C(7)	2442(6)	2500	6000(12)	34(3)
C(8)	4862(10)	1610(30)	7950(15)	178(15)
C(9)	4449(15)	420(30)	7730(20)	191(16)
C(10)	3825(6)	2500	8105(13)	42(3)
C(11)	3781(8)	2500	9427(15)	65(5)
C(12)	4391(12)	2500	6210(20)	190(20)
C(13)	4690(40)	2500	5540(40)	350(50)
C(14)	6165(7)	2500	1216(17)	72(6)
C(15)	5524(10)	2500	1734(19)	123(12)
C(16)	5510(30)	2500	3010(60)	380(60)

Table C.4.2. Bond lengths [Å] and angles [°] for (NEt₄)[Re₂(CO)₆(μ-pz)₂-(μ-OH)]·(CH₃)₂CO·0.5H₂O.

Re(1)-C(1)	1.907(10)	N(2)-N(2)#1	1.353(13)
Re(1)-C(3)	1.909(11)	N(3)-C(8)	1.44(2)
Re(1)-C(2)	1.918(11)	N(3)-C(8)#1	1.44(2)
Re(1)-O(4)	2.126(4)	N(3)-C(10)	1.48(2)
Re(1)-N(1)	2.171(7)	N(3)-C(12)	1.53(3)
Re(1)-N(2)	2.172(7)	C(4)-C(5)	1.375(13)
O(1)-C(1)	1.164(12)	C(5)-C(4)#1	1.375(13)
O(2)-C(2)	1.144(12)	C(6)-C(7)	1.385(12)
O(3)-C(3)	1.166(12)	C(7)-C(6)#1	1.385(12)
O(4)-Re(1)#1	2.126(4)	C(8)-C(9)	1.76(4)
O(5)-C(15)	1.12(2)	C(10)-C(11)	1.48(2)
N(1)-C(4)	1.333(12)	C(12)-C(13)	0.97(7)
N(1)-N(1)#1	1.373(14)	C(14)-C(15)	1.43(3)
N(2)-C(6)	1.332(11)	C(15)-C(16)	1.43(7)
C(1)-Re(1)-C(3)	89.7(4)	C(10)-N(3)-C(12)	107.0(14)
C(1)-Re(1)-C(2)	89.0(4)	O(1)-C(1)-Re(1)	177.1(9)
C(3)-Re(1)-C(2)	86.7(5)	O(2)-C(2)-Re(1)	176.4(9)
C(1)-Re(1)-O(4)	98.0(4)	O(3)-C(3)-Re(1)	177.3(10)
C(3)-Re(1)-O(4)	98.7(4)	N(1)-C(4)-C(5)	109.4(9)
C(2)-Re(1)-O(4)	171.2(3)	C(4)-C(5)-C(4)#1	105.5(12)
C(1)-Re(1)-N(1)	93.0(3)	N(2)-C(6)-C(7)	108.5(9)
C(3)-Re(1)-N(1)	177.3(3)	C(6)-C(7)-C(6)#1	105.7(12)
C(2)-Re(1)-N(1)	93.5(4)	N(3)-C(8)-C(9)	113.2(16)
O(4)-Re(1)-N(1)	80.8(3)	N(3)-C(10)-C(11)	117.8(13)
C(1)-Re(1)-N(2)	176.3(4)	C(13)-C(12)-N(3)	133(4)
C(3)-Re(1)-N(2)	92.6(3)	O(5)-C(15)-C(16)	112(3)
C(2)-Re(1)-N(2)	94.0(3)	O(5)-C(15)-C(14)	133(2)
O(4)-Re(1)-N(2)	78.9(3)	C(16)-C(15)-C(14)	115(3)
N(1)-Re(1)-N(2)	84.7(3)		
Re(1)-O(4)-Re(1)#1	117.5(4)		
C(4)-N(1)-N(1)#1	107.8(6)		
C(4)-N(1)-Re(1)	130.7(6)		
N(1)#1-N(1)-Re(1)	121.40(19)		
C(6)-N(2)-N(2)#1	108.7(5)		
C(6)-N(2)-Re(1)	129.6(6)		
N(2)#1-N(2)-Re(1)	121.69(17)		
C(8)-N(3)-C(8)#1	105(3)		
C(8)-N(3)-C(10)	111.0(12)		
C(8)#1-N(3)-C(10)	111.0(12)		
C(8)-N(3)-C(12)	111.5(12)		
C(8)#1-N(3)-C(12)	111.5(12)		

Symmetry transformations used to generate equivalent atoms:
#1 $x, -y+1/2, z$

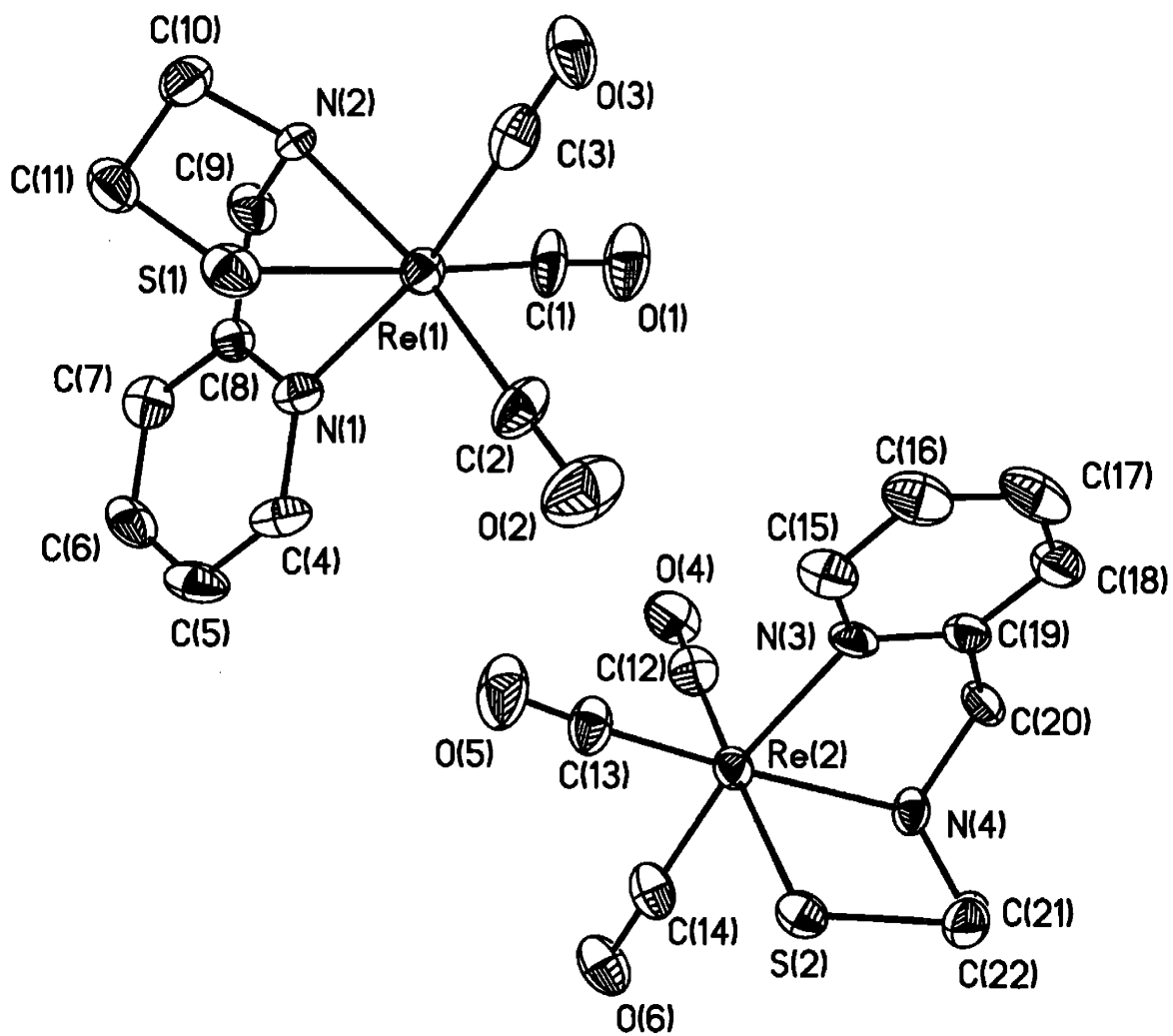
Table C.4.3. Anisotropic displacement parameters ($\text{\AA}^2 \times 10^3$) for $(\text{NEt}_4)[\text{Re}_2(\text{CO})_6(\mu\text{-pz})_2(\mu\text{-OH})] \cdot (\text{CH}_3)_2\text{CO} \cdot 0.5\text{H}_2\text{O}$. The anisotropic displacement factor exponent takes the form: $-2\pi^2 [h^2 a^{*2} U^{11} + \dots + 2 h k a^* b^* U^{12}]$

	U^{11}	U^{22}	U^{33}	U^{23}	U^{13}	U^{12}
Re(1)	26(1)	28(1)	34(1)	-1(1)	4(1)	3(1)
O(1)	77(5)	51(5)	57(5)	-13(4)	19(4)	14(4)
O(2)	101(7)	46(5)	60(5)	-2(4)	6(5)	-43(5)
O(3)	69(5)	62(5)	62(5)	15(4)	-4(4)	34(4)
O(4)	27(4)	21(4)	42(5)	0	2(4)	0
O(5)	30(6)	107(11)	101(10)	0	8(6)	0
N(1)	30(4)	27(4)	35(4)	-2(3)	-1(3)	-3(3)
N(2)	16(3)	26(3)	33(4)	-1(3)	4(3)	1(3)
N(3)	28(7)	230(30)	44(8)	0	4(6)	0
C(1)	48(6)	50(6)	32(5)	3(5)	-2(5)	1(5)
C(2)	62(6)	33(6)	31(5)	-1(4)	7(5)	3(5)
C(3)	48(6)	47(6)	42(6)	-8(5)	7(5)	9(5)
C(4)	35(5)	49(6)	38(5)	-7(5)	-2(4)	-10(5)
C(5)	41(8)	55(10)	56(10)	0	-22(7)	0
C(6)	25(4)	37(5)	39(5)	6(4)	4(4)	3(4)
C(7)	28(6)	47(8)	28(7)	0	7(5)	0
C(8)	92(13)	380(40)	65(11)	21(16)	8(9)	160(20)
C(9)	180(30)	230(40)	160(30)	-20(20)	-10(20)	140(30)
C(10)	32(7)	49(9)	44(8)	0	8(6)	0
C(11)	50(9)	88(13)	58(11)	0	31(8)	0
C(12)	46(12)	490(80)	47(15)	0	26(12)	0
C(13)	580(130)	350(80)	130(40)	0	-220(70)	0
C(14)	24(8)	120(17)	72(12)	0	1(8)	0
C(15)	44(12)	280(40)	40(11)	0	0(9)	0
C(16)	130(40)	700(200)	280(80)	0	50(50)	0

Table C.4.4. Hydrogen coordinates ($\times 10^4$) and isotropic displacement parameters ($\text{\AA}^2 \times 10^3$) for $(\text{NEt}_4)[\text{Re}_2(\text{CO})_6(\mu\text{-pz})_2(\mu\text{-OH})] \cdot (\text{CH}_3)_2\text{CO} \cdot 0.5\text{H}_2\text{O}$.

	x	y	z	U(eq)
H(4)	2075	957	768	49
H(5)	1565	2500	-176	61
H(6)	2535	949	5524	40
H(7)	2262	2500	6762	41
H(8A)	4964	1686	8791	214
H(8B)	5274	1591	7516	214
H(9A)	4057	408	8208	286
H(9B)	4730	-147	7969	286
H(9C)	4336	344	6907	286
H(10A)	3592	1892	7814	50
H(10B)	3592	3108	7814	50
H(11A)	3376	2180	9669	98
H(11B)	3794	3204	9715	98
H(11C)	4143	2117	9754	98
H(12A)	4114	1899	6061	232
H(12B)	4114	3101	6061	232
H(13A)	4486	2198	4856	529
H(13B)	5076	2100	5745	529
H(13C)	4822	3202	5362	529
H(14A)	6313	1795	1119	108
H(14B)	6463	2867	1730	108
H(14C)	6151	2837	453	108

Compound C.5. Thermal ellipsoid plot of both molecules of $\text{Re}(\text{CO})_3(\text{MEPA})$ in the asymmetric unit.





Room 14-0551
77 Massachusetts Avenue
Cambridge, MA 02139
Ph: 617.253.5668 Fax: 617.253.1690
Email: docs@mit.edu
<http://libraries.mit.edu/docs>

DISCLAIMER OF QUALITY

Due to the condition of the original material, there are unavoidable flaws in this reproduction. We have made every effort possible to provide you with the best copy available. If you are dissatisfied with this product and find it unusable, please contact Document Services as soon as possible.

Thank you.

*Due to a typographical error
every page hereon is numbered as
pg. 192 ?/?*

Table C.5.1. Atomic coordinates ($\times 10^4$) and equivalent isotropic displacement parameters ($\text{\AA}^2 \times 10^3$) for $\text{Re}(\text{CO})_3(\text{MEPA})$. $U(\text{eq})$ is defined as one third of the trace of the orthogonalized U^{ij} tensor.

	x	y	z	U(eq)
Re(1)	1006(1)	4341(1)	3426(1)	32(1)
Re(2)	4039(1)	6028(1)	6485(1)	33(1)
S(1)	723(2)	2083(4)	2481(2)	43(1)
S(2)	4277(2)	3754(4)	7429(2)	40(1)
O(1)	1318(5)	7219(12)	4518(7)	68(3)
O(2)	1799(6)	2761(14)	5143(8)	86(4)
O(3)	-240(5)	3987(10)	4178(6)	52(3)
O(4)	3808(5)	8964(12)	5441(7)	63(3)
O(5)	3348(5)	4327(15)	4744(7)	85(4)
O(6)	5359(5)	5761(11)	5925(7)	60(3)
N(1)	1787(5)	4495(10)	2665(7)	34(2)
N(2)	544(4)	5401(11)	2092(6)	32(2)
N(3)	3168(4)	6128(11)	7089(7)	36(2)
N(4)	4414(S)	7068(11)	7887(6)	35(2)
C(1)	1195(7)	6161(16)	4070(9)	49(4)
C(2)	1506(7)	3330(17)	4500(9)	51(4)
C(3)	225(7)	4119(13)	3902(9)	43(3)
C(4)	2341(6)	3699(14)	2873(10)	44(3)
C(5)	2797(6)	3753(15)	2322(11)	51(4)
C(6)	2677(6)	4610(16)	1543(10)	50(4)
C(7)	2118(6)	5421(14)	1328(9)	45(3)
C(8)	1680(6)	5344(12)	1919(8)	32(3)
C(9)	1058(6)	6169(14)	1699(9)	43(3)
C(10)	130(6)	4395(14)	1408(9)	44(3)
C(11)	491(6)	2967(15)	1338(9)	48(4)
C(12)	3888(6)	7858(16)	5823(10)	45(3)
C(13)	3638(7)	4981(16)	5397(9)	48(3)
C(14)	4854(7)	5878(14)	6137(9)	45(3)
C(15)	2626(6)	5315(15)	6801(10)	49(4)
C(16)	2127(7)	5270(17)	7272(11)	58(4)
C(17)	2199(7)	6122(17)	8048(12)	63(4)
C(18)	2742(6)	6952(16)	8355(10)	50(4)
C(19)	3233(6)	6979(13)	7872(9)	38(3)
C(20)	3851(6)	7837(14)	8146(9)	41(3)
C(21)	4766(6)	6063(15)	8588(9)	44(3)
C(22)	4412(6)	4605(14)	8588(9)	43(3)

Table C.5.2. Bond lengths [\AA] and angles [$^\circ$] for $\text{Re}(\text{CO})_3(\text{MEPA})$.

Re(1)-C(1)	1.905(13)	N(1)-C(8)	1.319(14)
Re(1)-C(2)	1.920(14)	N(1)-C(4)	1.341(15)
Re(1)-C(3)	1.926(15)	N(2)-C(10)	1.486(15)
Re(1)-N(1)	2.182(10)	N(2)-C(9)	1.502(15)
Re(1)-N(2)	2.204(9)	N(3)-C(15)	1.341(16)
Re(1)-S(1)	2.477(4)	N(3)-C(19)	1.368(15)
Re(2)-C(13)	1.888(14)	N(4)-C(21)	1.448(15)
Re(2)-C(14)	1.892(14)	N(4)-C(20)	1.490(14)
Re(2)-C(12)	1.919(16)	C(4)-C(5)	1.383(19)
Re(2)-N(3)	2.198(9)	C(5)-C(6)	1.362(19)
Re(2)-N(4)	2.243(9)	C(6)-C(7)	1.357(18)
Re(2)-S(2)	2.479(4)	C(7)-C(8)	1.399(17)
S(1)-C(11)	1.827(14)	C(8)-C(9)	1.474(17)
S(2)-C(22)	1.835(13)	C(10)-C(11)	1.518(18)
O(1)-C(1)	1.162(15)	C(15)-C(16)	1.377(19)
O(2)-C(2)	1.131(15)	C(16)-C(17)	1.36(2)
O(3)-C(3)	1.141(15)	C(17)-C(18)	1.354(19)
O(4)-C(12)	1.147(16)	C(18)-C(19)	1.374(17)
O(5)-C(13)	1.176(15)	C(19)-C(20)	1.486(17)
O(6)-C(14)	1.171(15)	C(21)-C(22)	1.519(18)
C(1)-Re(1)-C(2)	89.7(6)	C(13)-Re(2)-N(4)	171.2(4)
C(1)-Re(1)-C(3)	90.4(5)	C(14)-Re(2)-N(4)	97.4(5)
C(2)-Re(1)-C(3)	89.9(6)	C(12)-Re(2)-N(4)	94.8(5)
C(1)-Re(1)-N(1)	96.0(5)	N(3)-Re(2)-N(4)	76.2(4)
C(2)-Re(1)-N(1)	97.0(5)	C(13)-Re(2)-S(2)	92.8(4)
C(3)-Re(1)-N(1)	170.6(4)	C(14)-Re(2)-S(2)	90.7(4)
C(1)-Re(1)-N(2)	93.6(5)	C(12)-Re(2)-S(2)	176.2(4)
C(2)-Re(1)-N(2)	171.8(5)	N(3)-Re(2)-S(2)	83.6(3)
C(3)-Re(1)-N(2)	97.6(5)	N(4)-Re(2)-S(2)	81.6(3)
N(1)-Re(1)-N(2)	75.2(3)	C(11)-S(1)-Re(1)	97.5(4)
C(1)-Re(1)-S(1)	175.7(4)	C(22)-S(2)-Re(2)	97.9(4)
C(2)-Re(1)-S(1)	94.6(5)	C(8)-N(1)-C(4)	118.8(11)
C(3)-Re(1)-S(1)	90.1(4)	C(8)-N(1)-Re(1)	117.3(8)
N(1)-Re(1)-S(1)	83.0(3)	C(4)-N(1)-Re(1)	123.7(8)
N(2)-Re(1)-S(1)	82.1(3)	C(10)-N(2)-C(9)	112.6(9)
C(13)-Re(2)-C(14)	89.3(6)	C(10)-N(2)-Re(1)	113.9(7)
C(13)-Re(2)-C(12)	91.0(6)	C(9)-N(2)-Re(1)	109.8(7)
C(14)-Re(2)-C(12)	88.9(5)	C(15)-N(3)-C(19)	119.6(10)
C(13)-Re(2)-N(3)	96.6(5)	C(15)-N(3)-Re(2)	124.6(9)
C(14)-Re(2)-N(3)	172.0(5)	C(19)-N(3)-Re(2)	115.4(8)
C(12)-Re(2)-N(3)	96.5(5)	C(21)-N(4)-C(20)	114.7(10)

C(21)-N(4)-Re(2)	113.8(7)
C(20)-N(4)-Re(2)	107.5(7)
O(1)-C(1)-Re(1)	175.4(12)
O(2)-C(2)-Re(1)	178.5(15)
O(3)-C(3)-Re(1)	179.5(11)
N(1)-C(4)-C(5)	121.4(13)
C(6)-C(5)-C(4)	119.5(12)
C(7)-C(6)-C(5)	119.6(13)
C(6)-C(7)-C(8)	118.5(13)
N(1)-C(8)-C(7)	122.3(11)
N(1)-C(8)-C(9)	117.2(10)
C(7)-C(8)-C(9)	120.4(11)
C(8)-C(9)-N(2)	110.5(10)
N(2)-C(10)-C(11)	110.5(10)
C(10)-C(11)-S(1)	110.4(9)
O(4)-C(12)-Re(2)	178.5(13)
O(5)-C(13)-Re(2)	175.2(12)
O(6)-C(14)-Re(2)	178.9(12)
N(3)-C(15)-C(16)	122.7(14)
C(17)-C(16)-C(15)	116.9(14)
C(18)-C(17)-C(16)	121.7(13)
C(17)-C(18)-C(19)	120.3(14)
N(3)-C(19)-C(18)	118.8(12)
N(3)-C(19)-C(20)	116.2(10)
C(18)-C(19)-C(20)	125.0(12)
C(19)-C(20)-N(4)	111.8(10)
N(4)-C(21)-C(22)	112.5(10)
C(21)-C(22)-S(2)	109.9(8)

Table C.5.3. Anisotropic displacement parameters ($\text{\AA}^2 \times 10^3$) for $\text{Re}(\text{CO})_3(\text{MEPA})$. The anisotropic displacement factor exponent takes the form: $-2\pi^2 [h^2 a^{*2} U^{11} + \dots + 2 h k a^* b^* U^{12}]$

	U^{11}	U^{22}	U^{33}	U^{23}	U^{13}	U^{12}
Re(1)	32(1)	36(1)	29(1)	2(1)	8(1)	-3(1)
Re(2)	29(1)	42(1)	32(1)	-2(1)	11(1)	-2(1)
S(1)	33(2)	43(2)	56(2)	-7(2)	14(2)	-6(2)
S(2)	33(2)	41(2)	48(v)	-1(2)	13(2)	0(1)
O(1)	86(8)	75(7)	46(6)	-24(6)	19(5)	-39(6)
O(2)	77(8)	107(10)	69(8)	41(7)	5(6)	-1(7)
O(3)	60(6)	57(6)	49(6)	-17(5)	32(5)	-24(5)
O(4)	72(7)	58(7)	68(7)	20(6)	34(6)	16(6)
O(5)	57(7)	140(11)	55(7)	-39(7)	10(5)	-33(7)
O(6)	53(6)	69(7)	70(7)	6(5)	39(5)	-8(5)
N(1)	29(6)	30(5)	40(6)	0(5)	1(5)	0(5)
N(2)	25(5)	45(6)	23(5)	-2(4)	-1(4)	7(5)
N(3)	19(5)	46(6)	46(6)	3(5)	12(4)	4(5)
N(4)	33(6)	44(6)	27(5)	-10(5)	6(4)	-10(5)
C(1)	59(9)	61(9)	30(7)	-22(7)	15(6)	-31(8)
C(2)	49(9)	71(10)	31(8)	16(7)	2(6)	-12(8)
C(3)	57(9)	28(7)	39(8)	-11(6)	1(7)	-17(7)
C(4)	30(7)	38(8)	58(9)	6(6)	-4(6)	2(6)
C(5)	22(7)	43(8)	85(11)	-9(8)	8(7)	0(6)
C(6)	30(8)	60(9)	65(10)	-20(8)	25(7)	-10(7)
C(7)	46(9)	42(8)	47(8)	0(6)	11(7)	-6(7)
C(8)	32(7)	32(7)	32(7)	0(5)	10(5)	-2(6)
C(9)	41(8)	48(8)	44(8)	-2(6)	19(6)	-5(7)
C(10)	36(7)	56(9)	37(7)	1(6)	3(6)	-6(6)
C(11)	36(7)	57(9)	56(9)	-20(7)	19(6)	-7(7)
C(12)	30(7)	53(9)	54(9)	9(7)	13(6)	-20(7)
C(13)	45(8)	67(9)	34(8)	-3(7)	15(6)	-15(7)
C(14)	53(9)	36(7)	50(8)	-10(6)	22(7)	-10(7)
C(15)	39(8)	45(8)	64(10)	-2(7)	14(7)	2(7)
C(16)	39(8)	56(9)	83(12)	7(9)	23(8)	-4(7)
C(17)	41(9)	65(10)	94(13)	9(10)	43(9)	-3(8)
C(18)	40(8)	61(9)	52(9)	8(7)	19(7)	10(7)
C(19)	36(7)	37(7)	41(8)	5(6)	11(6)	12(6)
C(20)	37(7)	47(8)	43(8)	-10(6)	18(6)	5(6)
C(21)	39(7)	61(9)	32(7)	-3(7)	8(6)	-4(7)
C(22)	41(8)	56(9)	35(7)	9(6)	11(6)	3(7)

Table C.5.4. Hydrogen coordinates ($\times 10^4$) and isotropic displacement parameters ($\text{\AA}^2 \times 10^3$) for $\text{Re}(\text{CO})_3(\text{MEPA})$.

	x	y	z	U(eq)
H(2)	273	6110	2226	39
H(4)	4706	7774	7810	42
H(4A)	2420	3098	3398	53
H(5)	3182	3208	2483	61
H(6)	2975	4639	1161	60
H(7)	2028	6015	800	54
H(9A)	907	6260	1028	51
H(9B)	1129	7151	1960	51
H(10A)	19	4864	800	S3
H(10B)	-275	4189	1600	53
H(11A)	882	3165	1107	58
H(11B)	211	2312	901	58
H(15)	2585	4757	6261	59
H(16)	1757	4685	7069	69
H(17)	1867	6135	8376	75
H(18)	2784	7506	8897	60
H(20A)	3951	8000	8815	50
H(20B)	3791	8789	7841	50
H(21A)	4822	6514	9199	53
H(21B)	5199	5885	8476	53
H(22A)	3993	4763	8753	52
H(22B)	4672	3954	9050	52

Table C.6.1. Atomic coordinates ($\times 10^4$) and equivalent isotropic displacement parameters ($\text{\AA}^2 \times 10^3$) for $\text{Re}(\text{CO})_3(\text{MEPA-NEt})$. $U(\text{eq})$ is defined as one third of the trace of the orthogonalized U^{ij} tensor.

	x	y	z	$U(\text{eq})$
Re(1)	1610(1)	1939(1)	8013(1)	22(1)
S(1)	4726(3)	2414(2)	8769(2)	30(1)
O(1)	-2323(8)	1408(5)	7101(5)	39(2)
O(2)	3243(11)	488(6)	6786(6)	66(2)
O(3)	1796(10)	3299(5)	6325(5)	43(2)
N(1)	1633(9)	1175(4)	9399(5)	23(2)
N(2)	672(10)	2943(4)	9075(6)	20(2)
C(1)	-853(13)	1595(6)	7455(6)	26(2)
C(2)	2598(13)	1040(6)	7240(7)	32(2)
C(3)	1713(11)	2779(7)	6946(7)	28(2)
C(4)	2452(11)	362(6)	9573(7)	31(2)
C(5)	2655(11)	-35(6)	10502(7)	34(2)
C(6)	2003(12)	403(7)	11271(7)	34(2)
C(7)	1173(11)	1228(6)	11099(6)	28(2)
C(8)	992(10)	1603(6)	10148(6)	20(2)
C(9)	-61(11)	2445(6)	9885(6)	27(2)
C(10)	2226(11)	3536(6)	9487(6)	25(2)
C(11)	3998(12)	3031(5)	9813(7)	28(2)
C(12)	-868(11)	3504(6)	8543(6)	26(2)
C(13)	-1634(12)	4226(6)	9148(7)	34(2)

Table C.6.2. Bond lengths [\AA] and angles [$^\circ$] for $\text{Re}(\text{CO})_3(\text{MEPA-NEt})$.

Re(1)-C(2)	1.907(9)	N(1)-C(4)	1.365(11)
Re(1)-C(1)	1.925(10)	N(2)-C(9)	1.486(11)
Re(1)-C(3)	1.926(11)	N(2)-C(10)	1.490(11)
Re(1)-N(1)	2.198(7)	N(2)-C(12)	1.508(11)
Re(1)-N(2)	2.253(7)	C(4)-C(5)	1.383(13)
Re(1)-S(1)	2.471(2)	C(5)-C(6)	1.369(13)
S(1)-C(11)	1.828(9)	C(6)-C(7)	1.384(13)
O(1)-C(1)	1.150(11)	C(7)-C(8)	1.396(12)
O(2)-C(2)	1.167(12)	C(8)-C(9)	1.497(13)
O(3)-C(3)	1.154(12)	C(10)-C(11)	1.513(12)
N(1)-C(8)	1.337(11)	C(12)-C(13)	1.510(12)

C(2)-Re(1)-C(1)	89.8(4)	C(5)-C(6)-C(7)	119.3(8)
C(2)-Re(1)-C(3)	89.7(4)	C(6)-C(7)-C(8)	120.0(8)
C(1)-Re(1)-C(3)	90.5(3)	N(1)-C(8)-C(7)	120.6(8)
C(2)-Re(1)-N(1)	98.1(3)	N(1)-C(8)-C(9)	116.4(7)
C(1)-Re(1)-N(1)	95.5(3)	C(7)-C(8)-C(9)	122.8(8)
C(3)-Re(1)-N(1)	170.2(3)	N(2)-C(9)-C(8)	112.1 (6)
C(2)-Re(1)-N(2)	173.4(3)	N(2)-C(10)-C(11)	112.9(7)
C(1)-Re(1)-N(2)	94.7(3)	C(10)-C(11)-S(1)	110.7(6)
C(3)-Re(1)-N(2)	95.1(3)	N(2)-C(12)-C(13)	116.5(7)
N(1)-Re(1)-N(2)	76.7(3)		
C(2)-Re(1)-S(1)	92.1(3)		
C(1)-Re(1)-S(1)	178.0(2)		
C(3)-Re(1)-S(1)	89.8(2)		
N(1)-Re(1)-S(1)	83.97(18)		
N(2)-Re(1)-S(1)	83.4(2)		
C(11)-S(1)-Re(1)	96.9(3)		
C(8)-N(1)-C(4)	119.2(8)		
C(8)-N(1)-Re(1)	115.8(5)		
C(4)-N(1)-Re(1)	124.5(6)		
C(9)-N(2)-C(10)	110.8(7)		
C(9)-N(2)-C(12)	108.3(7)		
C(10)-N(2)-C(12)	109.1(6)		
C(9)-N(2)-Re(1)	107.9(5)		
C(10)-N(2)-Re(1)	110.9(5)		
C(12)-N(2)-Re(1)	109.8(5)		
O(1)-C(1)-Re(1)	178.0(7)		
O(2)-C(2)-Re(1)	178.2(9)		
O(3)-C(3)-Re(1)	178.1(8)		
N(1)-C(4)-C(5)	122.1(9)		
C(6)-C(5)-C(4)	118.8(8)		

Table C.6.3. Anisotropic displacement parameters ($\text{\AA}^2 \times 10^3$) for $\text{Re}(\text{CO})_3(\text{MEPA-NEt})$.
 The anisotropic displacement factor exponent takes the form: $-2\pi^2 [h^2 a^{*2} U^{11} + \dots + 2 h k a^* b^* U^{12}]$

	U^{11}	U^{22}	U^{33}	U^{23}	U^{13}	U^{12}
Re(1)	19(1)	22(1)	24(1)	-3(1)	5(1)	-2(1)
S(1)	17(1)	36(1)	37(1)	-5(1)	6(1)	-1(1)
O(1)	23(3)	53(4)	38(4)	0(3)	-3(3)	-11(3)
O(2)	81(6)	58(5)	66(5)	-25(5)	31(4)	1(5)
O(3)	52(5)	47(4)	31(4)	11(4)	10(3)	-15(4)
N(1)	17(4)	23(4)	31(4)	1(3)	5(3)	-1(3)
N(2)	17(4)	15(3)	29(4)	-4(3)	5(3)	-2(3)
C(1)	39(6)	22(4)	18(4)	-3(4)	11(4)	2(4)
C(2)	37(5)	25(5)	34(5)	-5(4)	6(4)	-2(4)
C(3)	13(4)	35(5)	36(5)	-13(5)	7(4)	-10(4)
C(4)	23(8)	23(5)	44(5)	-1(4)	-3(4)	5(4)
C(5)	21(5)	17(4)	61(6)	7(4)	-7(4)	4(4)
C(6)	26(5)	43(6)	32(5)	15(5)	-1(4)	-12(4)
C(7)	22(4)	29(5)	31(5)	-3(4)	-3(3)	-7(4)
C(8)	13(4)	21(4)	26(5)	6(4)	0(3)	-9(4)
C(9)	22(4)	35(5)	24(4)	-7(4)	7(3)	-6(4)
C(10)	20(4)	23(5)	34(5)	-8(4)	4(3)	-8(4)
C(11)	15(5)	32(5)	37(6)	-4(4)	6(4)	-2(3)
C(12)	26(5)	26(5)	25(4)	1(4)	5(3)	6(4)
C(13)	27(5)	37(5)	40(5)	-5(5)	6(4)	10(4)

Table C.6.4. Hydrogen coordinates ($\times 10^4$) and isotropic displacement parameters ($\text{\AA}^2 \times 10^3$) for $\text{Re}(\text{CO})_3(\text{MEPA-NEt})$.

	x	y	z	U(eq)
H(4)	2896	58	9037	37
H(5)	3236	-600	10606	41
H(6)	2120	143	11916	41
H(7)	725	1539	11629	34
H(9A)	-1377	2299	9674	32
H(9B)	9	2829	10484	32
H(10A)	1868	3866	10065	30
H(10B)	2449	3979	8974	30
H(11A)	3806	2611	10353	33
H(11B)	4982	3456	10077	33
H(12A)	-1896	3102	8282	31
H(12B)	-413	3788	7962	31
H(13A)	-1906	3975	9781	52
H(13B)	-2772	4465	8776	52
H(13C)	-722	4705	9281	52

Table C.7.1. Atomic coordinates ($\times 10^4$) and equivalent isotropic displacement parameters ($\text{\AA}^2 \times 10^3$) for MEPAH-C₂CO₂H-Str. U(eq) is defined as one third of the trace of the orthogonalized U^{ij} tensor.

	x	y	z	U(eq)
S(1)	4176(1)	3869(1)	2055(1)	32(1)
O(1)	3591(2)	2198(1)	362(1)	51(1)
O(2)	5806(2)	2359(1)	1570(1)	45(1)
N(1)	-2494(2)	2909(1)	416(1)	36(1)
N(2)	1690(2)	2797(1)	1966(1)	29(1)
C(1)	-802(3)	3063(1)	709(1)	34(1)
C(2)	213(3)	3229(1)	109(2)	37(1)
C(3)	-537(3)	3252(1)	-810(2)	43(1)
C(4)	-2285(3)	3105(1)	-1114(2)	46(1)
C(5)	-3203(3)	2936(1)	-481(2)	44(1)
C(6)	-67(3)	3063(1)	1727(1)	38(1)
C(7)	1594(3)	2125(1)	1821(2)	36(1)
C(8)	3344(3)	1830(1)	1826(2)	40(1)
C(9)	4237(3)	2147(1)	1168(2)	37(1)
C(10)	2625(3)	2975(1)	2890(1)	35(1)
C(11)	3089(3)	3661(1)	2961(1)	35(1)
C(12)	5580(3)	4532(1)	2568(1)	29(1)
C(13)	7241(3)	4307(1)	3265(1)	28(1)
C(14)	8627(3)	4719(1)	3538(1)	34(1)
C(15)	10168(3)	4543(1)	4133(1)	38(1)
C(16)	10357(3)	3943(1)	4475(1)	38(1)
C(17)	9010(3)	3529(1)	4210(2)	40(1)
C(18)	7469(3)	3707(1)	3606(1)	35(1)
C(19)	6204(3)	4818(1)	1756(1)	28(1)
C(20)	6028(3)	5441(1)	1527(2)	38(1)
C(21)	6683(3)	5676(1)	814(2)	43(1)
C(22)	7522(3)	5294(1)	322(2)	42(1)
C(23)	7694(3)	4674(1)	538(2)	44(1)
C(24)	7048(3)	4438(1)	1245(2)	38(1)
C(25)	4478(3)	4997(1)	2972(1)	30(1)
C(26)	2866(3)	5194(1)	2443(2)	38(1)
C(27)	1876(3)	5636(1)	2766(2)	45(1)
C(28)	2460(3)	5894(1)	3619(2)	46(1)
C(29)	4025(3)	5697(1)	4155(2)	42(1)
C(30)	5029(3)	5250(1)	3838(1)	34(1)

Table C.7.2. Bond lengths [Å] and angles [°] for MEPAH-C₂CO₂H-STr.

S(1)-C(11)	1.824(2)	S(1)-C(12)	1.859(2)
O(1)-C(9)	1.209(3)	O(2)-C(9)	1.324(3)
N(1)-C(5)	1.340(3)	N(1)-C(1)	1.343(3)
N(2)-C(7)	1.461(3)	N(2)-C(6)	1.461(3)
N(2)-C(10)	1.467(2)	C(1)-C(2)	1.382(3)
C(1)-C(6)	1.509(3)	C(2)-C(3)	1.376(3)
C(3)-C(4)	1.381(3)	C(4)-C(5)	1.370(3)
C(7)-C(8)	1.513(3)	C(8)-C(9)	1.503(3)
C(10)-C(11)	1.518(3)	C(12)-C(25)	1.537(3)
C(12)-C(19)	1.545(3)	C(12)-C(13)	1.553(3)
C(13)-C(18)	1.385(3)	C(13)-C(14)	1.392(3)
C(14)-C(15)	1.384(3)	C(15)-C(16)	1.384(3)
C(16)-C(17)	1.370(3)	C(17)-C(18)	1.391(3)
C(19)-C(20)	1.383(3)	C(19)-C(24)	1.391(3)
C(20)-C(21)	1.389(3)	C(21)-C(22)	1.371(3)
C(22)-C(23)	1.372(3)	C(23)-C(24)	1.378(3)
C(25)-C(30)	1.387(3)	C(25)-C(26)	1.398(3)
C(26)-C(27)	1.386(3)	C(27)-C(28)	1.378(3)
C(28)-C(29)	1.374(3)	C(29)-C(30)	1.396(3)
C(11)-S(1)-C(12)	102.25(9)	C(5)-N(1)-C(1)	118.2(2)
C(7)-N(2)-C(6)	109.7(2)	C(7)-N(2)-C(10)	113.4(2)
C(6)-N(2)-C(10)	111.7(2)	N(1)-C(1)-C(2)	121.7(2)
N(1)-C(1)-C(6)	116.9(2)	C(2)-C(1)-C(6)	121.4(2)
C(3)-C(2)-C(1)	119.3(2)	C(2)-C(3)-C(4)	119.3(2)
C(5)-C(4)-C(3)	118.2(2)	N(1)-C(5)-C(4)	123.4(2)
N(2)-C(6)-C(1)	111.7(2)	N(2)-C(7)-C(8)	113.5(2)
C(9)-C(8)-C(7)	111.6(2)	O(1)-C(9)-O(2)	124.1(2)
O(1)-C(9)-C(8)	123.5(2)	O(2)-C(9)-C(8)	112.4(2)
N(2)-C(10)-C(11)	112.4(2)	C(10)-C(11)-S(1)	109.3(2)
C(25)-C(12)-C(19)	111.4(2)	C(25)-C(12)-C(13)	113.4(2)
C(19)-C(12)-C(13)	106.8(2)	C(25)-C(12)-S(1)	109.21(13)
C(19)-C(12)-S(1)	104.02(13)	C(13)-C(12)-S(1)	111.60(13)
C(18)-C(13)-C(14)	117.3(2)	C(18)-C(13)-C(12)	123.9(2)
C(14)-C(13)-C(12)	118.7(2)	C(15)-C(14)-C(13)	121.7(2)
C(16)-C(15)-C(14)	120.0(2)	C(17)-C(16)-C(15)	119.2(2)
C(16)-C(17)-C(18)	120.7(2)	C(13)-C(18)-C(17)	121.2(2)
C(20)-C(19)-C(24)	117.6(2)	C(20)-C(19)-C(12)	123.5(2)
C(24)-C(19)-C(12)	118.9(2)	C(19)-C(20)-C(21)	120.8(2)
C(22)-C(21)-C(20)	120.6(2)	C(21)-C(22)-C(23)	119.2(2)
C(22)-C(23)-C(24)	120.5(2)	C(23)-C(24)-C(19)	121.3(2)
C(30)-C(25)-C(26)	117.6(2)	C(30)-C(25)-C(12)	123.0(2)
C(26)-C(25)-C(12)	119.4(2)	C(27)-C(26)-C(25)	121.1(2)

C(28)-C(27)-C(26) 120.7(2)
C(28)-C(29)-C(30) 120.7(2)

C(29)-C(28)-C(27) 119.1(2)
C(25)-C(30)-C(29) 120.9(2)

Table C.7.3. Anisotropic displacement parameters ($\text{\AA}^2 \times 10^3$) for MEPAH-C₂CO₂H-STr. The anisotropic displacement factor exponent takes the form: $-2\pi^2 [h^2 a^{*2} U^{11} + \dots + 2 h k a^* b^* U^{12}]$

	U ¹¹	U ²²	U ³³	U ²³	U ¹³	U ¹²
S(1)	33(1)	33(1)	30(1)	-5(1)	7(1)	-6(1)
O(1)	41(1)	73(1)	37(1)	-2(1)	5(1)	-7(1)
O(2)	37(1)	48(1)	47(1)	0(1)	4(1)	-3(1)
N(1)	29(1)	38(1)	39(1)	-7(1)	1(1)	3(1)
N(2)	24(1)	32(1)	29(1)	-1(1)	3(1)	-2(1)
C(1)	30(1)	32(1)	37(1)	-3(1)	3(1)	5(1)
C(2)	32(1)	38(1)	39(1)	1(1)	3(1)	0(1)
C(3)	48(2)	42(1)	39(1)	5(1)	9(1)	4(1)
C(4)	49(2)	50(2)	35(1)	2(1)	-2(1)	7(1)
C(5)	31(1)	48(2)	47(2)	-9(1)	-4(1)	6(1)
C(6)	29(1)	50(1)	36(1)	-7(1)	7(1)	1(1)
C(7)	38(1)	35(1)	34(1)	0(1)	6(1)	-8(1)
C(8)	42(1)	33(1)	42(1)	2(1)	5(1)	2(1)
C(9)	32(1)	36(1)	41(2)	-5(1)	7(1)	5(1)
C(10)	31(1)	41(1)	29(1)	1(1)	2(1)	-6(1)
C(11)	35(1)	41(1)	30(1)	-6(1)	7(1)	-7(1)
C(12)	30(1)	28(1)	29(1)	-2(1)	5(1)	-2(1)
C(13)	30(1)	29(1)	26(1)	-2(1)	8(1)	0(1)
C(14)	35(1)	32(1)	35(1)	1(1)	7(1)	-3(1)
C(15)	32(1)	45(2)	35(1)	-2(1)	4(1)	-7(1)
C(16)	31(1)	50(2)	32(1)	5(1)	4(1)	5(1)
C(17)	44(2)	33(1)	42(1)	7(1)	9(1)	4(1)
C(18)	34(1)	33(1)	39(1)	1(1)	6(1)	-2(1)
C(19)	28(1)	29(1)	26(1)	-1(1)	2(1)	0(1)
C(20)	41(1)	34(1)	40(1)	-2(1)	13(1)	0(1)
C(21)	50(2)	33(1)	47(1)	9(1)	14(1)	0(1)
C(22)	44(1)	50(2)	36(1)	5(1)	15(1)	-5(1)
C(23)	50(2)	46(2)	42(1)	-3(1)	23(1)	2(1)
C(24)	42(1)	33(1)	40(1)	2(1)	14(1)	3(1)
C(25)	33(1)	26(1)	32(1)	3(1)	11(1)	-1(1)
C(26)	40(1)	40(1)	36(1)	4(1)	11(1)	4(1)
C(27)	44(2)	42(1)	53(2)	15(1)	19(1)	13(1)
C(28)	57(2)	30(1)	61(2)	4(1)	34(1)	8(1)
C(29)	57(2)	34(1)	42(1)	-7(1)	24(1)	-5(1)
C(30)	37(1)	32(1)	34(1)	0(1)	12(1)	-2(1)

Table C.7.4. Hydrogen coordinates ($\times 10^4$) and isotropic displacement parameters ($\text{\AA}^2 \times 10^3$) for MEPAH-C₂CO₂H-STr.

	x	y	z	U(eq)
H(2B)	6260(2)	2532(1)	1181(1)	68
H(2A)	1415(3)	3327(1)	329(2)	45
H(3A)	140(3)	3368(1)	-1231(2)	52
H(4A)	-2837(3)	3122(1)	-1744(2)	56
H(5A)	-4404(3)	2832(1)	-690(2)	53
H(6A)	-29(3)	3495(1)	1957(1)	46
H(6B)	-848(3)	2820(1)	2026(1)	46
H(7A)	779(3)	2038(1)	1228(2)	44
H(7B)	1106(3)	1931(1)	2304(2)	44
H(8A)	4102(3)	1855(1)	2449(2)	48
H(8B)	3170(3)	1385(1)	1661(2)	48
H(10A)	3711(3)	2726(1)	3067(1)	41
H(10B)	1887(3)	2877(1)	3323(1)	41
H(11A)	3873(3)	3749(1)	3563(1)	42
H(11B)	2014(3)	3913(1)	2905(1)	42
H(14A)	8513(3)	5133(1)	3310(1)	41
H(15A)	11096(3)	4833(1)	4307(1)	45
H(16A)	11408(3)	3820(1)	4888(1)	46
H(17A)	9130(3)	3117(1)	4442(2)	48
H(18A)	6557(3)	3412(1)	3424(1)	42
H(20A)	5453(3)	5712(1)	1862(2)	45
H(21A)	6548(3)	6105(1)	664(2)	52
H(22A)	7978(3)	5457(1)	-162(2)	51
H(23A)	8263(3)	4405(1)	197(2)	53
H(24A)	7183(3)	4008(1)	1387(2)	45
H(26A)	2444(3)	5022(1)	1852(2)	46
H(27A)	783(3)	5763(1)	2396(2)	54
H(28A)	1790(3)	6204(1)	3833(2)	55
H(29A)	4429(3)	5867(1)	4748(2)	51
H(30A)	6104(3)	5117(1)	4219(1)	41

Table C.8.1. Atomic coordinates ($\times 10^4$) and equivalent isotropic displacement parameters ($\text{\AA}^2 \times 10^3$) for $\text{Re}(\text{CO})_3(\text{MEPA-C}_2\text{COmorph})\cdot 2\text{H}_2\text{O}$. $U(\text{eq})$ is defined as one third of the trace of the orthogonalized U^{ij} tensor.

	x	y	z	$U(\text{eq})$
Re(1)	1478(1)	3115(1)	1278(1)	19(1)
S(1)	-64(5)	1691(5)	2471(3)	35(1)
O(1)	3393(15)	4708(13)	-301(7)	35(3)
O(2)	-1085(16)	2190(14)	160(8)	44(3)
O(3)	-793(16)	6072(14)	1531(8)	48(3)
O(4)	3582(16)	7638(14)	3069(8)	49(3)
O(5)	8259(18)	7634(17)	4720(9)	60(4)
O(6)	1720(20)	8400(20)	4605(11)	70(5)
O(7)	6940(20)	2707(18)	3969(10)	66(4)
N(1)	3312(15)	1098(13)	1202(7)	22(3)
N(2)	3377(16)	3394(13)	2206(7)	23(3)
N(3)	6439(19)	7256(16)	3359(9)	41(4)
C(1)	2690(20)	4115(17)	326(11)	27(4)
C(2)	-90(20)	2528(18)	569(10)	32(4)
C(3)	60(20)	4930(20)	1440(10)	35(4)
C(4)	3014(19)	-178(16)	892(9)	24(3)
C(5)	4220(20)	-1404(18)	842(10)	32(4)
C(6)	5820(20)	-1316(18)	1141(10)	31(4)
C(7)	6148(19)	-23(18)	1482(10)	30(4)
C(8)	4859(19)	1157(17)	1507(9)	23(3)
C(9)	5125(19)	2614(16)	1841(10)	26(4)
C(10)	2770(20)	2759(19)	3045(9)	32(4)
C(11)	1790(20)	1346(19)	3069(10)	34(4)
C(12)	3680(20)	5035(18)	2255(10)	31(4)
C(13)	5170(20)	5266(19)	2750(12)	39(4)
C(14)	4980(20)	6831(18)	3064(10)	31(4)
C(15)	6400(30)	8750(20)	3702(12)	50(5)
C(16)	6640(30)	8530(30)	4608(13)	59(6)
C(17)	8240(30)	6230(30)	4389(16)	73(7)
C(18)	8050(30)	6350(20)	3485(13)	52(5)

Table C.8.2. Bond lengths [Å] and angles [°] for Re(CO)₃(MEPA-C₂COmorph)·2H₂O.

Re(1)-C(3)	1.90(2)	N(2)-C(9)	1.522(19)
Re(1)-C(1)	1.897(17)	N(2)-C(12)	1.53(2)
Re(1)-C(2)	1.901(15)	N(3)-C(14)	1.36(2)
Re(1)-N(1)	2.197(11)	N(3)-C(18)	1.44(2)
Re(1)-N(2)	2.270(12)	N(3)-C(15)	1.50(2)
Re(1)-S(1)	2.457(4)	C(4)-C(5)	1.38(2)
S(1)-C(11)	1.818(16)	C(5)-C(6)	1.39(2)
O(1)-C(1)	1.194(19)	C(6)-C(7)	1.38(2)
O(2)-C(2)	1.150(18)	C(7)-C(8)	1.38(2)
O(3)-C(3)	1.18(2)	C(8)-C(9)	1.50(2)
O(4)-C(14)	1.24(2)	C(10)-C(11)	1.53(2)
O(5)-C(17)	1.41(3)	C(12)-C(13)	1.52(2)
O(5)-C(16)	1.44(3)	C(13)-C(14)	1.53(2)
N(1)-C(4)	1.341(18)	C(15)-C(16)	1.50(3)
N(1)-C(8)	1.348(18)	C(17)-C(18)	1.49(3)
N(2)-C(10)	1.465(19)		
C(3)-Re(1)-C(1)	87.0(7)	C(14)-N(3)-C(18)	127.5(15)
C(3)-Re(1)-C(2)	90.3(6)	C(14)-N(3)-C(15)	120.4(15)
C(1)-Re(1)-C(2)	87.6(7)	C(18)-N(3)-C(15)	111.7(14)
C(3)-Re(1)-N(1)	173.1(5)	O(1)-C(1)-Re(1)	176.3(13)
C(1)-Re(1)-N(1)	94.0(6)	O(2)-C(2)-Re(1)	177.6(15)
C(2)-Re(1)-N(1)	96.5(6)	O(3)-C(3)-Re(1)	178.3(16)
C(3)-Re(1)-N(2)	97.4~5)	N(1)-C(4)-C(5)	123.6(14)
C(1)-Re(1)-N(2)	98.9(5)	C(4)-C(5)-C(6)	118.0(14)
C(2)-Re(1)-N(2)	170.1(6)	C(7)-C(6)-C(5)	119.5(15)
N(1)-Re(1)-N(2)	75.7(4)	C(6)-C(7)-C(8)	118.7(14)
C(3)-Re(1)-S(1)	95.7(5)	N(1)-C(8)-C(7)	122.4(14)
C(1)-Re(1)-S(1)	176.8(5)	N(1)-C(8)-C(9)	115.5(13)
C(2)-Re(1)-S(1)	90.6(5)	C(7)-C(8)-C(9)	122.1(13)
N(1)-Re(1)-S(1)	83.6(3)	C(8)-C(9)-N(2)	111.7(12)
N(2)-Re(1)-S(1)	82.6(3)	N(2)-C(10)-C(11)	114.8(13)
C(11)-S(1)-Re(1)	97.1(5)	C(10)-C(11)-S(1)	110.1(11)
C(17)-O(5)-C(16)	109.7(14)	C(13)-C(12)-N(2)	113.3(13)
C(4)-N(1)-C(8)	117.8(12)	C(12)-C(13)-C(14)	111.3(14)
C(4)-N(1)-Re(1)	125.8(9)	O(4)-C(14)-N(3)	122.6(15)
C(8)-N(1)-Re(1)	116.4(9)	O(4)-C(14)-C(13)	121.8(14)
C(10)-N(2)-C(9)	111.7(12)	N(3)-C(14)-C(13)	115.5(15)
C(10)-N(2)-C(12)	108.9(11)	N(3)-C(15)-C(16)	108.6(17)
C(9)-N(2)-C(12)	107.6(11)	O(5)-C(16)-C(15)	110.9(16)
C(10)-N(2)-Re(1)	112.7(9)	O(5)-C(17)-C(18)	113.2(19)
C(9)-N(2)-Re(1)	104.5(8)	N(3)-C(18)-C(17)	108.7(17)
C(12)-N(2)-Re(1)	111.3(9)		

Table C.8.3. Anisotropic displacement parameters ($\text{\AA}^2 \times 10^3$) for $\text{Re}(\text{CO})_3(\text{MEPA}-\text{C}_2\text{COmorph})\cdot 2\text{H}_2\text{O}$. The anisotropic displacement factor exponent takes the form: $-2\pi^2[h^2a^{*2}U^{11} + \dots + 2hk a^* b^* U^{12}]$

	U^{11}	U^{22}	U^{33}	U^{23}	U^{13}	U^{12}
Re(1)	8(1)	24(1)	28(1)	-7(1)	-8(1)	-3(1)
S(1)	18(2)	53(3)	34(2)	-1(2)	-5(2)	-14(2)
O(1)	32(7)	46(7)	26(6)	2(5)	-1(5)	-10(6)
O(2)	30(7)	52(8)	56(8)	-13(6)	-20(6)	-11(6)
O(3)	32(7)	43(8)	72(9)	-27(7)	-18(6)	14(6)
O(4)	30(7)	54(8)	67(9)	-23(7)	-18(6)	1(6)
O(5)	45(9)	84(11)	61(9)	-22(8)	-30(7)	-14(8)
O(6)	59(10)	105(14)	53(10)	-22(9)	-13(8)	-28(10)
O(7)	49(9)	92(12)	53(9)	14(8)	-9(8)	14(8)
N(1)	16(7)	24(7)	29(7)	-9(6)	-11(5)	4(5)
N(2)	17(7)	29(7)	25(7)	-12(6)	-5(5)	-1(5)
N(3)	36(9)	45(9)	50(9)	-20(7)	-21(7)	-6(7)
C(1)	16(8)	29(9)	40(11)	-6(8)	-11(8)	0(7)
C(2)	23(9)	39(10)	38(10)	-8(8)	-21(8)	-1(8)
C(3)	36(10)	49(12)	29(9)	6(8)	-26(8)	-19(9)
C(4)	15(8)	25(9)	34(9)	-12(7)	-6(6)	-7(7)
C(5)	37(10)	27(9)	34(10)	-11(7)	-5(8)	2(8)
C(6)	21(9)	36(10)	36(10)	-6(8)	-12(7)	7(7)
C(7)	10(8)	43(10)	38(10)	-12(8)	4(7)	-3(7)
C(8)	11(8)	32(9)	28(9)	3(7)	-4(6)	-9(7)
C(9)	18(8)	27(9)	38(9)	-9(7)	-18(7)	0(7)
C(10)	26(9)	51(11)	20(8)	-1(7)	-7(7)	-9(8)
C(11)	27(9)	47(11)	27(9)	6(8)	-10(7)	-1(8)
C(12)	29(9)	37(10)	27(9)	-7(7)	-3(7)	4(8)
C(13)	27(9)	39(10)	59(12)	-16(9)	-19(8)	-6(8)
C(14)	29(10)	37(10)	32(9)	-15(7)	-9(7)	-7(8)
C(15)	55(13)	47(12)	57(13)	-23(10)	-14(10)	-19(10)
C(16)	41(12)	81(16)	61(14)	-30(12)	-4(10)	-22(11)
C(17)	50(14)	84(18)	95(19)	0(14)	-43(13)	-11(12)
C(18)	41(12)	53(12)	70(14)	-21(11)	-25(10)	-2(10)

Table C.8.4. Hydrogen coordinates ($\times 10^4$) and isotropic displacement parameters ($\text{\AA}^2 \times 10^3$) for $\text{Re}(\text{CO})_3(\text{MEPA-C}_2\text{COmorph})\cdot 2\text{H}_2\text{O}$.

	x	y	z	U(eq)
H(61)	2200(300)	8200(300)	4080(160)	70(80)
H(60)	1300(400)	7500(300)	4520(170)	100(100)
H(70)	7470(160)	2420(130)	4520(80)	0(30)
H(71)	8000(300)	2410(190)	3440(110)	50(50)
H(4)	1907	-239	695	28
H(5)	3966	-2283	610	39
H(6)	6693	-2138	1112	37
H(7)	7234	53	1694	36
H(9A)	5706	3270	1387	31
H(9B)	5921	2431	2278	31
H(10A)	1977	3522	3345	38
H(10B)	3814	2530	3348	38
H(11A)	1359	1032	3654	41
H(11B)	2618	531	2834	41
H(12A)	3948	5494	1683	37
H(12B)	2567	5555	2515	37
H(13A)	6320	5115	2393	47
H(13B)	5159	4518	3230	47
H(15A)	5255	9324	3637	60
H(15B)	7364	9320	3394	60
H(16A)	6660	9509	4837	71
H(16B)	5618	8027	4918	71
H(17A)	7240	5706	4697	88
H(17B)	9349	5628	4475	88
H(18A)	9083	6812	3162	63
H(18B)	8002	5345	3289	63

Compound C.9. Thermal ellipsoid plot of $\text{Re}(\text{CO})_3(\text{EDDA})\cdot\text{H}_2\text{O}$ showing both molecules of the asymmetric unit and solvated water molecules.

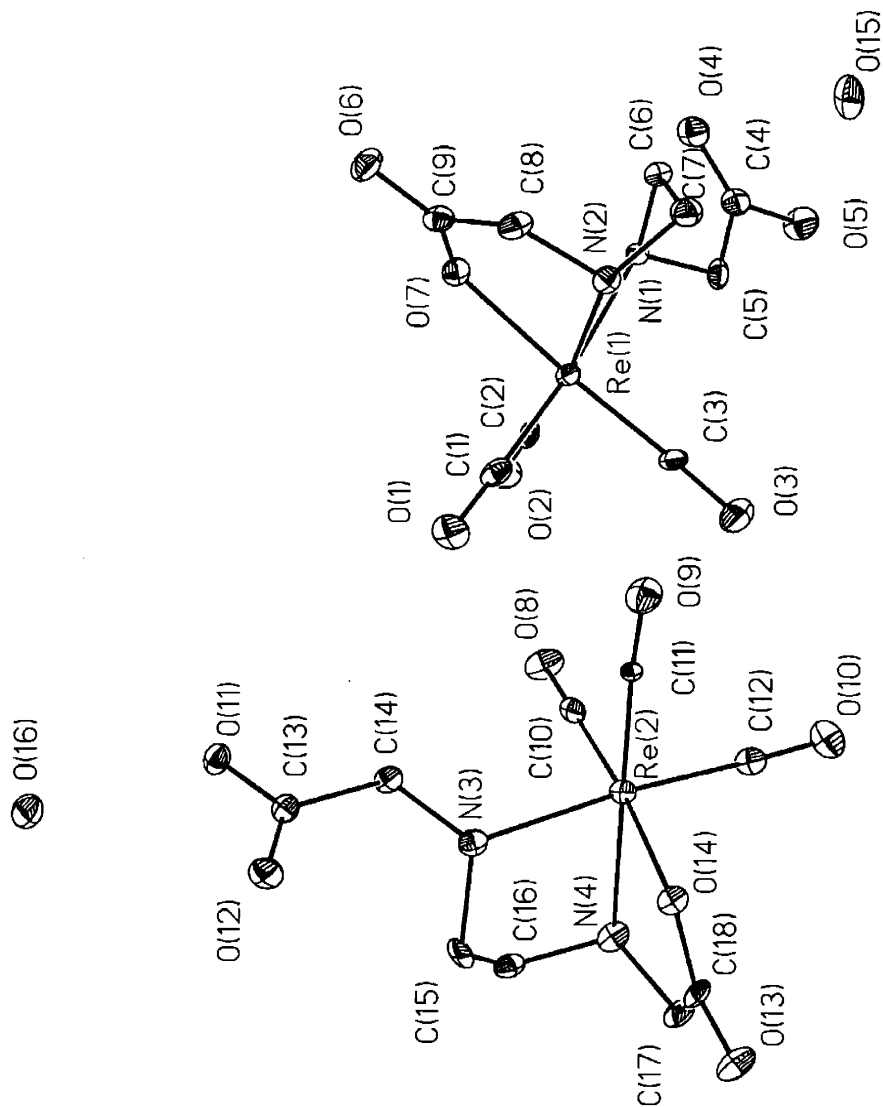


Table C.9.1. Atomic coordinates ($\times 10^4$) and equivalent isotropic displacement parameters ($\text{\AA}^2 \times 10^3$) for $\text{Re}(\text{CO})_3(\text{EDDA})\cdot\text{H}_2\text{O}$. $U(\text{eq})$ is defined as one third of the trace of the orthogonalized U^{ij} tensor

	x	y	z	U(eq)
Re(1)	4546(1)	808(1)	1607(1)	16(1)
Re(2)	206(1)	2433(1)	4707(1)	15(1)
N(3)	-1768(10)	3813(7)	4287(5)	19(2)
O(11)	-3737(9)	4388(6)	2414(4)	24(2)
O(10)	2819(9)	593(7)	5404(5)	32(2)
N(4)	-2120(10)	1912(7)	5567(5)	21(2)
O(9)	3429(10)	3458(7)	3660(4)	32(2)
O(12)	-3814(9)	5683(6)	3495(4)	26(2)
C(16)	-3677(12)	2402(9)	5205(6)	21(2)
C(13)	-3299(12)	4707(8)	3131(6)	19(2)
O(8)	100(10)	506(6)	3339(4)	31(2)
C(14)	-2120(13)	3660(8)	3430(6)	20(2)
C(15)	-3413(12)	3760(8)	4901(6)	20(2)
C(11)	2179(11)	3113(8)	4036(5)	14(2)
C(17)	-2019(13)	2440(9)	6395(6)	24(2)
C(10)	144(12)	1229(9)	3853(6)	21(2)
C(12)	1797(12)	1295(8)	5155(6)	20(2)
O(14)	32(8)	3807(5)	5661(4)	18(1)
O(13)	-1023(10)	4302(7)	6937(4)	28(2)
C(18)	-950(12)	3611(8)	6345(5)	18(2)
O(1)	1598(10)	2781(6)	2150(5)	32(2)
N(2)	6657(10)	2172(7)	1401(5)	19(2)
O(2)	1684(9)	-1125(7)	1640(5)	34(2)
N(1)	6772(9)	-454(7)	1076(5)	18(2)
C(9)	5458(12)	2360(8)	63(6)	22(2)
C(8)	6472(13)	2997(9)	660(6)	25(2)
C(2)	2811(13)	-430(9)	1619(6)	22(2)
C(3)	4618(12)	416(9)	2731(6)	20(2)
C(6)	8281(12)	317(9)	783(6)	23(2)
C(7)	8331(13)	1439(10)	1341(6)	26(2)
C(1)	2704(14)	2047(9)	1953(6)	23(2)
O(7)	4669(8)	1330(6)	336(4)	22(1)
O(6)	5404(9)	2803(7)	-629(4)	31(2)
O(4)	8833(10)	-2485(7)	327(5)	31(2)
O(3)	4588(10)	183(8)	3441(5)	39(2)
C(5)	7283(12)	-1575(9)	1567(6)	23(2)
C(4)	8353(13)	-2587(9)	1061(6)	24(2)
O(5)	8720(11)	-3590(7)	1507(5)	38(2)
O(16)	-6371(9)	5421(7)	1796(4)	31(2)
O(15)	11014(12)	-5248(7)	721(5)	46(2)

Table C.9.2. Bond lengths [\AA] and angles [$^\circ$] for $\text{Re}(\text{CO})_3(\text{EDDA})\cdot\text{H}_2\text{O}$.

Re(1)-C(3)	1.888(9)	Re(1)-C(2)	1.914(10)
Re(1)-C(1)	1.928(10)	Re(1)-O(7)	2.134(6)
Re(1)-N(2)	2.214(7)	Re(1)-N(1)	2.226(7)
Re(2)-C(12)	1.893(9)	Re(2)-C(10)	1.916(10)
Re(2)-C(11)	1.918(9)	Re(2)-O(14)	2.140(6)
Re(2)-N(4)	2.219(8)	Re(2)-N(3)	2.233(8)
N(3)-C(14)	1.483(12)	N(3)-C(15)	1.519(12)
O(11)-C(13)	1.324(12)	O(10)-C(12)	1.169(12)
N(4)-C(16)	1.490(12)	N(4)-C(17)	1.492(12)
O(9)-C(11)	1.147(11)	O(12)-C(13)	1.222(12)
C(16)-C(15)	1.512(13)	C(13)-C(14)	1.517(13)
O(8)-C(10)	1.153(12)	C(17)-C(18)	1.509(13)
O(14)-C(18)	1.287(11)	O(13)-C(18)	1.219(11)
O(1)-C(1)	1.147(12)	N(2)-C(7)	1.478(13)
N(2)-C(8)	1.495(12)	O(2)-C(2)	1.163(12)
N(1)-C(6)	1.476(12)	N(1)-C(5)	1.481(12)
C(9)-O(6)	1.222(12)	C(9)-O(7)	1.307(11)
C(9)-C(8)	1.524(13)	C(3)-O(3)	1.181(12)
C(6)-C(7)	1.514(14)	O(4)-C(4)	1.214(13)
C(5)-C(4)	1.511(14)	C(4)-O(5)	1.311(12)
C(3)-Re(1)-C(2)	88.2(4)	C(3)-Re(1)-C(1)	87.6(4)
C(2)-Re(1)-C(1)	87.8(4)	C(3)-Re(1)-O(7)	175.1(3)
C(2)-Re(1)-O(7)	96.5(3)	C(1)-Re(1)-O(7)	93.8(3)
C(3)-Re(1)-N(2)	99.2(3)	C(2)-Re(1)-N(2)	171.6(3)
C(1)-Re(1)-N(2)	96.5(3)	O(7)-Re(1)-N(2)	76.0(3)
C(3)-Re(1)-N(1)	98.4(3)	C(2)-Re(1)-N(1)	96.3(3)
C(1)-Re(1)-N(1)	172.7(3)	O(7)-Re(1)-N(1)	79.8(3)
N(2)-Re(1)-N(1)	78.7(3)	C(12)-Re(2)-C(10)	88.0(4)
C(12)-Re(2)-C(11)	86.6(4)	C(10)-Re(2)-C(11)	86.9(4)
C(12)-Re(2)-O(14)	95.9(3)	C(10)-Re(2)-O(14)	174.9(3)
C(11)-Re(2)-O(14)	96.5(3)	C(12)-Re(2)-N(4)	96.6(3)
C(10)-Re(2)-N(4)	100.5(3)	C(11)-Re(2)-N(4)	171.9(3)
O(14)-Re(2)-N(4)	75.8(2)	C(12)-Re(2)-N(3)	175.2(3)
C(10)-Re(2)-N(3)	95.8(3)	C(11)-Re(2)-N(3)	96.5(3)
O(14)-Re(2)-N(3)	80.1(3)	N(4)-Re(2)-N(3)	79.8(3)
C(14)-N(3)-C(15)	111.8(7)	C(14)-N(3)-Re(2)	115.6(6)
C(15)-N(3)-Re(2)	108.2(5)	C(16)-N(4)-C(17)	113.1(7)
C(16)-N(4)-Re(2)	107.7(5)	C(17)-N(4)-Re(2)	109.4(5)
N(4)-C(16)-C(15)	109.4(7)	O(12)-C(13)-O(11)	124.4(8)
O(12)-C(13)-C(14)	126.1(8)	O(11)-C(13)-C(14)	109.4(8)
N(3)-C(14)-C(13)	114.2(7)	C(16)-C(15)-N(3)	109.7(7)
O(9)-C(11)-Re(2)	175.3(8)	N(4)-C(17)-C(18)	112.3(7)
O(8)-C(10)-Re(2)	179.7(8)	O(10)-C(12)-Re(2)	177.5(8)

C(18)-O(14)-Re(2)	119.6(5)	O(13)-C(18)-O(14)	123.3(8)
O(13)-C(18)-C(17)	120.3(8)	O(14)-C(18)-C(17)	116.3(7)
C(7)-N(2)-C(8)	113.4(7)	C(7)-N(2)-Re(1)	108.2(6)
C(8)-N(2)-Re(1)	110.4(5)	C(6)-N(1)-C(5)	111.0(7)
C(6)-N(1)-Re(1)	110.0(6)	C(5)-N(1)-Re(1)	118.5(6)
O(6)-C(9)-O(7)	122.9(8)	O(6)-C(9)-C(8)	120.9(8)
O(7)-C(9)-C(8)	116.2(8)	N(2)-C(8)-C(9)	111.9(7)
O(2)-C(2)-Re(1)	175.9(8)	O(3)-C(3)-Re(1)	177.1(8)
N(1)-C(6)-C(7)	110.2(8)	N(2)-C(7)-C(6)	109.1(8)
O(1)-C(1)-Re(1)	179.1(9)	C(9)-O(7)-Re(1)	119.2(6)
N(1)-C(5)-C(4)	113.7(8)	O(4)-C(4)-O(5)	123.6(10)
O(4)-C(4)-C(5)	124.2(9)	O(5)-C(4)-C(5)	112.2(9)

Table C.9.3. Anisotropic displacement parameters ($\text{\AA}^2 \times 10^3$) for $\text{Re}(\text{CO})_3(\text{EDDA}) \cdot \text{H}_2\text{O}$. The anisotropic displacement factor exponent takes the form: $-2\pi^2 [h^2 a^{*2} U^{11} + \dots + 2 h k a^* b^* U^{12}]$

	U^{11}	U^{22}	U^{33}	U^{23}	U^{13}	U^{12}
Re(1)	19(1)	16(1)	14(1)	0(1)	0(1)	0(1)
Re(2)	18(1)	10(1)	18(1)	1(1)	0(1)	-1(1)
N(3)	21(4)	18(4)	18(4)	-3(3)	-2(3)	-3(3)
O(11)	34(4)	19(3)	19(3)	-2(3)	-7(3)	6(3)
O(10)	30(4)	21(4)	46(5)	3(3)	-7(3)	-1(3)
N(4)	32(5)	9(4)	21(4)	3(3)	-1(3)	-6(3)
O(9)	33(4)	33(4)	30(4)	8(3)	-2(3)	-11(3)
O(12)	32(4)	16(4)	27(4)	-6(3)	-1(3)	5(3)
C(16)	21(5)	27(5)	16(5)	-3(4)	1(4)	-8(4)
C(13)	21(5)	15(5)	19(5)	3(4)	-2(4)	-3(4)
O(8)	47(5)	18(4)	27(4)	-8(3)	2(3)	-5(3)
C(14)	30(5)	11(4)	18(5)	-1(4)	0(4)	5(4)
C(15)	19(5)	13(4)	29(5)	-9(4)	-7(4)	9(4)
C(11)	10(4)	19(5)	11(4)	4(3)	1(4)	0(4)
C(17)	35(6)	22(5)	14(5)	7(4)	0(4)	0(4)
C(10)	20(5)	16(5)	24(5)	11(4)	3(4)	7(4)
C(12)	27(5)	10(4)	22(5)	0(4)	0(4)	1(4)
O(14)	24(3)	12(3)	18(3)	-1(2)	-2(3)	-3(3)
O(13)	44(4)	25(4)	16(4)	-3(3)	-3(3)	-9(3)
C(18)	29(5)	15(4)	10(5)	3(4)	-3(4)	0(4)
O(1)	38(4)	18(4)	37(4)	-7(3)	-1(3)	7(3)
N(2)	23(4)	17(4)	17(4)	-5(3)	-2(3)	0(3)
O(2)	28(4)	32(4)	41(4)	4(3)	-3(3)	-15(3)
N(1)	16(4)	21(4)	15(4)	1(3)	0(3)	4(3)
C(9)	23(5)	17(5)	23(5)	2(4)	2(4)	-1(4)
C(8)	29(5)	26(5)	19(5)	-1(4)	1(4)	-9(4)
C(2)	28(5)	20(5)	16(5)	8(4)	-4(4)	8(4)
C(3)	22(5)	20(5)	16(5)	2(4)	5(4)	4(4)
C(6)	21(5)	28(5)	18(5)	2(4)	1(4)	0(4)
C(7)	25(5)	27(5)	26(5)	2(4)	-1(4)	-1(4)
C(1)	35(6)	16(5)	17(5)	3(4)	1(4)	-2(4)
O(7)	26(4)	22(3)	18(3)	-7(3)	-3(3)	2(3)
O(6)	35(4)	35(4)	23(4)	11(3)	-5(3)	-9(3)
O(4)	31(4)	24(4)	35(5)	1(3)	1(3)	8(3)
O(3)	45(5)	46(5)	25(4)	6(3)	-3(3)	3(4)
C(5)	22(5)	25(5)	24(5)	7(4)	-10(4)	-1(4)
C(4)	23(5)	21(5)	29(6)	6(4)	-2(4)	-8(4)
O(5)	48(5)	26(4)	38(4)	9(3)	0(4)	9(3)
O(16)	32(4)	32(4)	28(4)	8(3)	-3(3)	-2(3)
O(15)	57(5)	31(4)	52(5)	-10(4)	-24(4)	22(4)

Table C.9.4. Hydrogen coordinates ($\times 10^4$) and isotropic displacement parameters ($\text{\AA}^2 \times 10^3$) for $\text{Re}(\text{CO})_3(\text{EDDA})\cdot\text{H}_2\text{O}$.

	x	y	z	U(eq)
H(3A)	-1347(10)	4623(7)	4316(5)	23
H(11)	-4205(141)	5025(31)	2199(34)	36
H(4A)	-2143(10)	1027(7)	5613(5)	25
H(16A)	-4717(12)	2372(9)	5625(6)	26
H(16B)	-3861(12)	1860(9)	4741(6)	26
H(14A)	-2655(13)	2830(8)	3391(6)	24
H(14B)	-1003(13)	3638(8)	3060(6)	24
H(15A)	-3322(12)	4314(8)	5372(6)	24
H(15B)	-4420(12)	4077(8)	4636(6)	24
H(17A)	-1503(13)	1777(9)	6737(6)	29
H(17B)	-3206(13)	2660(9)	6667(6)	29
H(2A)	6566(10)	2693(7)	1857(5)	23
H(1A)	6437(9)	-787(7)	604(5)	21
H(8A)	7638(13)	3189(9)	375(6)	30
H(8B)	5869(13)	3815(9)	838(6)	30
H(6A)	8206(12)	630(9)	215(6)	27
H(6B)	9362(12)	-219(9)	776(6)	27
H(7A)	8543(13)	1130(10)	1895(6)	32
H(7B)	9286(13)	1993(10)	1116(6)	32
H(4)	9922(10)	-2533(125)	240(8)	47
H(5A)	6222(12)	-1960(9)	1853(6)	28
H(5B)	7955(12)	-1285(9)	1992(6)	28

Acknowledgments

First, and foremost, I must thank my thesis supervisor, Professor Alan Davison. He has been a wonderful advisor. Alan gives his students a great deal of intellectual freedom, and he aims to teach his students, by his hands-off approach, how to go about solving a research problem. That being said, Alan's great wealth of empirical knowledge is always available in case things are not going well. I have been honored to be Alan's last graduate student; he has been a great mentor for many students over the past 40 years.

The Davison Group, of course, has been an important part of my graduate experience. Professor Terry Nicholson has been the only research associate in the group during my entire tenure at MIT. Over the last 1 1/2 years, he has been the only other member of the group. Our conversations about varied topics, ranging from technetium chemistry to the perennial futility of the Rangers, Knicks, and Mets, have been extremely valuable for me during the last five years. Co-graduate students, Dr. Evan Freiberg and Dr. Ann Shellenbarger-Jones, were invaluable resources early in my graduate career and have remained in close contact with the group. I also thank Allison Kelsey and Gabriella Browne for help with administrative issues during my time in the group.

The Jones Group, our collaborating group at Harvard Medical School, has been an integral part of my graduate experience. All of the biological work was performed there. Professor Alun Jones has been a very good resource talking about the chemistry/biology interface, and in helping me acclimate to the medical school environment. A huge thank you goes to Professor Ashfaq Mahmood, who showed me the ropes in the lab at HMS. Without him, the ^{99m}Tc chemistry and biology presented here would not have been possible. Dr. Zhen Cheng has been an incredible help to me during my time at HMS. He grew the tumor cells, helped inject them into the mice, and performed dissections along with Ash (as I am way too squeamish to deal with all of the blood). With time, I got better (I was able to weigh and sacrifice the animals), but Zhen and Ash always did the dirty work, and for that I am extremely grateful. Special thanks also go to Ms. Alice Carmel who performed all of the tail vein injections of purified ^{99m}Tc compounds.

Members of the Schrock Group have been very welcoming to me, especially since Dr. Freiberg graduated in 2001 (leaving me as the only graduate student in the Davison Group). Professor Dick Schrock has been very gracious and has included me (and my wife) in many group activities, including a ski trip to Talbot House in South Pomfret, Vermont, this past winter. Particular thanks go to Dr. Parisa Mehrkhodavandi and Sarah Dolman for helping with thesis revisions, and to Sarah Aeilts and Peter Tsang for being good friends.

I want to take this opportunity to thank my thesis chair, Professor Joseph Sadighi, for reading my thesis and for taking the time each year to have an in-depth conversation with me about my research. His vast knowledge of organic synthesis was very important in steering my research, and I much appreciate his time. I also acknowledge Professor Kit Cummins, the third member of my committee, for taking time out of his busy schedule to read this thesis.

The research of Professor Roger Alberto has laid the groundwork for much new chemistry. I thank him for his help with syntheses of his starting materials and for interesting conversations at various times during my graduate career.

Mass spectrometry was an important part of the characterization of many of the compounds reported here. All of these spectra were obtained by Ms. Li Li of the MIT Department of Chemistry Instrumentation Facility (DCIF). Li Li obtained spectra with very short turn-around time, and this was very helpful for furthering my research at a good pace. Dr. Mark Wall, head of the DCIF, Dr. David Bray, and Dr. Jeff Simpson (former head of the DCIF) were all very helpful in case any problems arose regarding NMR studies. Dr. Bill Davis has been a tremendous help with crystallographic problems. Though I was trained to mount crystals and solve structures, sometimes problems do arise, and Bill's great skills helped me conquer some of the non-routine issues that I encountered throughout my studies.

Our contacts at the Radiation Protection Office, Mitch Galanek, Kristina White, and Steve Greenlaw, have all been helpful in keeping the 'hot lab' at MIT (where all ^{99}Tc work is done) in working order. A special thank you goes to Mr. Greenlaw, who performed weekly inspections in the lab. His work is greatly appreciated.

My teachers were very important to the development of my love for mathematics and science. I acknowledge Professor Bruce M. Foxman, who was an integral part of my undergraduate experience at Brandeis University. Special thanks also go to Mr. Gary Kulik, Mrs. Glynis Nau-Ritter, Mrs. Joan Beckerman, Mrs. Edna Zemanian, Professor Albert Carlson, and the late Mrs. Fran Greenspan for their support and encouragement.

I would be remiss if I did not thank my most important support staff, my family. My parents, David and Hilary, have always been there with much love and support. Especially at the beginning of my MIT experience, their discussions with me helped me to persevere through what was a very difficult adjustment to life in the MIT society. I also acknowledge my grandfather, Jack Berger, who always imparts words of love and wisdom, my grandmother, Margaret Kramer, my brother and sister, Ari and Alizah, and my brother's fiancée, Gabby Lann, the newest 'addition' to the family. My wife Allison's family has also been an important part of my support system, as they live in Sharon, MA, and have served as the nearby parental home. Allison's parents, Gerry and Rita Katz, and her grandmother, Beatrice Mazer, are very caring and loving people. Allison's sister, Lauren Katz, has also been a pleasure to be around as she has meandered up and down the East Coast over the last few years. I also thank Scott Schneider and Jeff Levine, two wonderful friends, and my most common phone calls (both to and from). Especially over the last 18 months or so, when I was often lonely in the office, it was great to have someone to talk to. Lastly, and most importantly, I thank my better half, my wife, Allison. She has endured the graduate experience through me and with me, and at times has probably felt that she, too, was a graduate student. It is desirable to leave work at the office, but invariably, the day's frustrations come home with you, and I thank her for putting up with that. I love you very much.

Biographical Note

The author was born on Sunday, February 13, 1977, at 7:05 AM, at St. Charles Hospital in Port Jefferson, NY. His interest in chemistry was started when his parents bought him a chemistry set as a gift. Some years later, in 1994, he graduated as valedictorian of his class at Mount Sinai High School, Mount Sinai, NY. He had the opportunity to perform some research at SUNY Stony Brook's Marine Science Research Center under Professor Robert Aller as part of a summer research program coordinated by Mrs. Edna Zemanian and Mrs. Melanie Jacobs Krieger. This research dealt with the redox cycle of manganese (the member of the Group 7 triad not discussed in this thesis) in Long Island Sound seawater, and won fourth prize at the International Science and Engineering Fair in Birmingham, Alabama, in 1994. Daniel attended Brandeis University, where he met his wife, Allison, and graduated in 1998, *summa cum laude* with Highest Honors in Chemistry. He had a very enjoyable time in the labs of Professor Bruce Foxman, where he completed a senior thesis. He came to MIT in the fall of 1998. Daniel's avid outside interests include vocal performance, tropical meteorology, hockey, and computer flight and sports simulation.

CURRICULUM VITAE

Name: Daniel Joshua Kramer
Date of Birth: February 13, 1977
Place of Birth: Port Jefferson, New York

Education:

1998 B.A. Brandeis University, Waltham, MA; Chemistry
2003 Ph.D. Massachusetts Institute of Technology, Cambridge, MA; Inorganic Chemistry

PUBLICATIONS

- (1) D. J. Kramer, A. Davison, A. G. Jones, W. M. Davis. "N-(2-Mercaptoethyl)-picolylamine as a Diaminomonothiolate Ligand for the "fac-[Re(CO)₃]" Core." *Inorganic Chemistry*, **2002**, *41*, 6181-6183.
- (2) D. J. Kramer, A. Davison, A. G. Jones, W. M. Davis. "N-(2-Mercaptoethyl)-picolylamine: a Diaminomonothiolate Ligand for the "fac-[Re(CO)₃]" Core." In *Technetium and Rhenium in Chemistry and Nuclear Medicine 6*, Nicolini, M. and Mazzi, U., eds., SGEEditoriali: Padova, **2002**, 43-48.
- (3) T. Nicholson, D. J. Kramer, A. Davison, A. G. Jones. "Technetium Organohydrazide Chemistry." In *Technetium and Rhenium in Chemistry and Nuclear Medicine 6*, Nicolini, M. and Mazzi, U., eds., SGEEditoriali: Padova, **2002**, 63-68
- (4) D. J. Kramer, A. Davison, A. G. Jones. "Reactions of Tris(solvento)-tricarbonyltechnetium(I) and Tris(solvento)tricarbonylrhenium(I) with Tripodal Ligands." In *Technetium and Rhenium in Chemistry and Nuclear Medicine 6*, Nicolini, M. and Mazzi, U., eds., SGEEditoriali: Padova, **2002**, 107-109.
- (5) E. Malago, A. Mahmood, M. Friebe, D. Kramer, M. Eisenhut, A. Davison, A. G. Jones. "Differential *in vivo* Behavior of Tc(V)oxo N₂S₂ Complexes with Melanoma Affinity." In *Technetium and Rhenium in Chemistry and Nuclear Medicine 6*, Nicolini, M. and Mazzi, U., eds., SGEEditoriali: Padova, **2002**, 419-421.
- (6) D. J. Kramer, A. Davison, A. G. Jones. "Structural Models for [M(CO)₃(H₂O)₃]⁺ (M= Tc, Re): Fully Aqueous Synthesis of Technetium and Rhenium Tricarbonyl Complexes of Tripodal Oxygen Donor Ligands." *Inorganica Chimica Acta* **2001**, *312*, 215-220.
- (7) T. Nicholson, D. J. Kramer, A. Davison, A. G. Jones. "Synthesis and Characterization of a Technetium Nitrido Dimer." *Inorganica Chimica Acta* **2001**, *316*, 110-112.
- (8) M. Friebe, A. Mahmood, C. Bolzati, A. Drews, B. Johannsen, M. Eisenhut, D. Kramer, A. Davison, A. G. Jones. "[^{99m}Tc]Oxotechnetium(V) Complexes of Amine-Amide-Dithiol Chelates with Dialkylaminoalkyl Substituents as Potential Diagnostic Probes for Malignant Melanoma." *Journal of Medicinal Chemistry* **2001**, *44*, 3132-3140